

**SYNTHETIC TRANSFORMATIONS OF PHYTOCHEMICALS  
FROM *ZINGIBER ZERUMBET* (L.) SMITH AND SYNTHESIS OF  
CARBOHYDRATE APPENDED ALKYLIDENE  
CYCLOPENTENES AS BIOACTIVE ANALOGUES**

THESIS SUBMITTED TO  
**THE UNIVERSITY OF KERALA**  
IN PARTIAL FULFILLMENT OF THE REQUIREMENTS  
FOR THE DEGREE OF  
**DOCTOR OF PHILOSOPHY**  
IN CHEMISTRY  
UNDER THE FACULTY OF SCIENCE

BY  
**AJISH K. R.**

ORGANIC CHEMISTRY SECTION  
NATIONAL INSTITUTE FOR INTERDISCIPLINARY SCIENCE AND TECHNOLOGY (CSIR)  
THIRUVANANTHAPURAM-695 019  
KERALA, INDIA

2014

*.....To My Family*

## **DECLARATION**

I hereby declare that the Ph.D. thesis entitled “**SYNTHETIC TRANSFORMATIONS OF PHYTOCHEMICALS FROM *ZINGIBER ZERUMBET* (L.) SMITH AND SYNTHESIS OF CARBOHYDRATE APPENDED ALKYLIDENE CYCLOPENTENES AS BIOACTIVE ANALOGUES**” is an independent work carried out by me and it has not been submitted anywhere else for any other degree, diploma or title.

**Ajish K. R.**

Trivandrum  
May, 2014

**NATIONAL INSTITUTE FOR INTERDISCIPLINARY SCIENCE & TECHNOLOGY**

**Council of Scientific & Industrial Research**

**GOVERNMENT OF INDIA**  
Trivandrum-695 019, India



**Dr. K. V. Radhakrishnan**  
Organic Chemistry Section  
Chemical Sciences and Technology Division

Telephone: 91-471-2515420  
Fax: 91-471-2491712

---

---

**CERTIFICATE**

*This is to certify that the work embodied in the thesis entitled “**SYNTHETIC TRANSFORMATIONS OF PHYTOCHEMICALS FROM ZINGIBER ZERUMBET (L.) SMITH AND SYNTHESIS OF CARBOHYDRATE APPENDED ALKYLIDENE CYCLOPENTENES AS BIOACTIVE ANALOGUES**” has been carried out by **Mr. Ajish K. R.** under my supervision and guidance at the Organic Chemistry Section of National Institute for Interdisciplinary Science and Technology (CSIR), Trivandrum and the same has not been submitted elsewhere for any other degree.*

**K. V. Radhakrishnan**  
(Thesis Supervisor)

Trivandrum

May, 2014

---

**Email: [radhu2005@gmail.com](mailto:radhu2005@gmail.com)**

---



## *ACKNOWLEDGEMENTS*

It is with great respect and immense pleasure that I express my deep sense of gratitude to my mentor and research supervisor **Dr. K. V. Radhakrishnan** for his constant encouragement and intellectual inspiration during the course of my doctoral studies.

I am grateful to Dr. Suresh Das, Director, National Institute for Interdisciplinary Science and Technology, for providing all the laboratory facilities to carry out this work.

My sincere thanks are also due to

- Dr. G. Vijay Nair for his inspiration and constructive criticism
- Dr. K. R. Gopidas and Dr. D. Ramaiah present and former Head, Chemicals Sciences and Technology Division for their support
- Dr. Mangalam S. Nair, Dr. Jayalekshmy A., Dr. Luxmi Varma R., Dr. Kaustabh Kumar Maiti and Dr. Sasidhar B.S., Scientists, Organic Chemistry Section for their support and suggestions
- Dr. K. G. Raghu (Agro Processing and Natural Product Division) for biological studies
- Dr. Kana M. Sureshan and Mr. Alex Andrews (IISER, Trivandrum) for single crystal X-ray analysis
- Ms. Remya Ramesh, Mr. Parthiban V., Ms. Shanubi K., Ms. Dhanya B. P. for their assistance in conducting some of the experiments reported in this thesis
- Ms. Priya Rani M for her great care, support and helps at all stages of my research
- Mrs. S. Viji and Ms. Aathira S. for HRMS and elemental analysis, Mrs. Saumini Mathew, Mr. Adarsh, Mr. Preethanuj P., Mr. Vipin, Mr. Arun Thomas, Mr. Saran and Mr. Shyam for recording NMR spectra
- Ms. Vineetha V.P., Ms. Antu Antony, Ms. Riya P., Ms. Priya Rani and Mr. Prathapan for their help in conducting biological assays
- Dr. Nayana Joseph, Ms. Joshni John, Dr. Jubi John, Dr. Rani Rajan, Dr. Jinesh M. Kuthanapillil, Dr. Sholly Clair George, Dr. Sreeja Tulasi, Dr. Praveen L., Dr.

Suchithra Madhavan, Dr. K. Selvakumar and Dr. Smitha Mohanlal, for their help and cooperation during various stages of my doctoral studies

- Mr. Praveen Prakash, Mr. Albish K. Paul, Mr. Sarath Chand S., Mr. Sajin Francis K. and Mr. Ashwani Kumar for their great support and also for making my stay at Trivandrum a very pleasant and memorable one
- Ms. Jijy E. and Ms Anupriya S. for their love, care, help and support
- Mr. Baiju T. V, Ms. Jisha Babu, Mr. Sinu C. R., Dr. Rony Rajan Paul, Ms. Anu Jose, Ms. Parvathy R. for their camaraderie and support
- My Juniors; Ms. Shimi M., Ms. Saranya S., Ms. Maya R. J., Ms. Dhanya S. R., Mr. Mineesh E. G., Ms. Santhini P. V., Mr. Ajesh Vijayan, Ms. Aparna P. S., Ms. Remya Raj, Ms. Athira Krishna, Mr. Santhi Maniganda, Mr. Sasikumar, Ms. Prabha B., Ms. Greeshma G., Ms. Sreedevi P., Ms. Seetha Lakshmi K. C., Ms. Padmaja D. V. M., Ms. Nisha N., Ms. Jyothi B. Nair, Mr. Jayakrishnan and Mr. Jagadeesh K., for their care, support and friendship during my stay at NIIST
- All my teachers from Mar Athanasius College, CMS College and UCTE who bestowed their knowledge upon me and for encouraging me to take up a career in chemistry
- Dr. A. Maria Starwin for his guidance, help and encouragement in qualifying the CSIR-UGC-NET exam
- Mr. Eldhose K. V. and Mr. Kuttan P.P., for their friendship and support
- Mr. Jacob, Mr. Jomi Jose, Mr. Suresh V. N., Mr. Bipin, Mr. Rakesh, Mr. Saji and Mr. Bijoy, my postgraduate classmates for their companionship and support
- All members of church at Balaramapuram for their care and prayer during my stay at Trivandrum
- All my friends at NIIST
- CSIR, New Delhi for financial assistance

Words are inadequate to express my feelings for my parents, sister, brother, friends and teachers for all the encouragement and support throughout my career

Above all, I bow before the Almighty for all his blessings

**Ajish K. R.**

# CONTENTS

Declaration	i
Certificate	ii
Acknowledgements	iii
List of Tables	x
List of Figures	xi
Abbreviations	xv
Preface	xvii

## CHAPTER 1

<b>Natural Products and their Analogues in Drug Discovery</b>	<b>1-24</b>
1.1 Introduction	1
1.2 Classification of natural products (NPs)	1
1.2.1. Classification based on source/origin	1
1.2.1.1. Plant derived natural products	2
1.2.1.2. Microbial world derived natural products	3
1.2.1.3. Marine world derived natural products	5
1.2.1.4. Animal derived natural products	6
1.2.2. Classification based on chemical structure	7
1.2.2.1. Flavonoids	8
1.2.2.2. Terpenoids (Terpenes)	9
1.2.2.3. Glycosides	11
1.3 Nature as source of new drug compounds	12
1.4 Important natural product derived drugs	13
1.5 Approaches in natural product drug discovery	16
1.5.1. The holistic approach	17
1.5.2. The reductionist approach	18
1.6 Importance of synthetic methodologies in modern drug discovery	19
1.6.1. Camptothecin and its derivatives	19

1.6.2. Podophyllotoxin and its derivatives	20
1.6.3. Penicillin and its derivatives	21
1.6.4. Semisynthesis of paclitaxel from 10-deacetylbaocatin III	22
1.7. Conclusion and present work	23
<b>CHAPTER 2</b>	
<b>Isolation, Characterization and Biological Evaluation of Phytochemicals from <i>Zingiber zerumbet</i> (L.) Smith</b>	<b>25-66</b>
2.1 <i>Zingiber zerumbet</i> Smith: An Overview	25
2.2 Various names of <i>Zingiber zerumbet</i>	26
2.3 Scientific classification	27
2.4 Distribution	27
2.5 Phytochemical investigation of <i>Zingiber zerumbet</i>	28
2.5.1. Phytochemistry of leaf and rhizome essential oil	28
2.5.2. Phytochemicals from the rhizomes of <i>Zingiber zerumbet</i>	30
2.6 Multipotential bioactivities of <i>Zingiber zerumbet</i>	32
2.6.1. Biological properties of extracts of <i>Z. zerumbet</i>	32
2.6.2. Biological properties of compounds of <i>Z. zerumbet</i>	33
2.7 Objective of the present work	35
2.8 Results and discussion	36
2.8.1. Identification of compounds <b>1-7</b>	36
2.8.1.1. Identification of compound <b>1</b>	36
2.8.1.2. Identification of compound <b>2</b>	38
2.8.1.3. Identification of compound <b>3</b>	39
2.8.1.4. Identification of compound <b>4</b>	41
2.8.1.5. Identification of compound <b>5</b>	44
2.8.1.6. Identification of compound <b>6</b>	46
2.8.1.7. Identification of compound <b>7</b>	48
2.8.2. Synthesis and characterization of compound <b>8</b> (Afzelin)	50
2.9 Biological evaluation of compounds	53
2.9.1. $\alpha$ -Glucosidase enzyme inhibition properties	53

2.9.2. Anti-glycation properties	55
2.9.3. Aldose reductase enzyme inhibition studies	56
2.10. Conclusion	58
2.11. Experimental details	58
2.12. Spectral details of compounds <b>1-8</b>	59
2.13. Procedures for various biological assays	65
2.13.1. Procedure for $\alpha$ -glucosidase inhibition assay	65
2.13.2. Procedure for aldose reductase inhibition assay	65
2.13.3. Procedure for anti-glycation activity assay	66

### **CHAPTER 3**

#### **Synthesis and Biological Evaluation of Novel Derivatives of Zerumbone**

##### **PART A**

#### **Transition Metal Catalyzed Regio- and Diastereoselective 1,4-Conjugate Addition of Zerumbone Using Boronic Acids: A Simple Route toward Novel Zerumbone Derivatives** **67-99**

3.1	Introduction	67
3.2	Reactions of zerumbone: An overview	68
	3.2.1. Cyclization reaction	68
	3.2.2. Reduction reaction	70
	3.2.3. Ring expansion reaction	71
	3.2.4. Epoxidation reaction	71
	3.2.5. Ring opening reaction	72
	3.2.6. 1,4-Conjugate addition reaction	72
3.3	Rhodium catalyzed 1,4-conjugate addition reactions using boronic acids	73
3.4	Palladium catalyzed 1,4-conjugate addition reactions	76
3.5	Objective of the present work	78
3.6	Results and discussion	78
3.7	Mechanistic pathway	86
3.8	Biological evaluation of 1,4-adducts	87
	3.8.1. Anti-bacterial properties	87

3.8.2. $\alpha$ -Glucosidase enzyme inhibition properties	87
3.9 Conclusion	87
3.10 Experimental section	88

## CHAPTER 3

### Synthesis and Biological Evaluation of Novel Derivatives of Zerumbone

#### Part B

#### Synthesis of Novel Zerumbone Derivatives *via* Regio- and Stereoselective Palladium Catalyzed Decarboxylative Coupling Reactions: A New Class of $\alpha$ -Glucosidase Inhibitors 100-123

3.11 Introduction	100
3.12 Heck reaction	100
3.12.1. Oxidative Heck coupling reaction	101
3.12.2. Decarboxylative coupling reaction- An oxidative Heck reaction	102
3.13 Objective of the present study	104
3.14 Results and discussion	104
3.15 Mechanism	111
3.16 Synthetic utility of decarboxylative coupled product	111
3.17 Biological evaluation of compounds <b>78-84</b>	113
3.17.1. $\alpha$ -Glucosidase inhibition assay of compounds <b>78-84</b>	113
3.18 Conclusion	114
3.19 Experimental methods	115

## CHAPTER 4

### Synthesis and Biological Evaluation of Carbohydrate Appended Alkylidene Cyclopentenes 124-157

4.1 Introduction	124
4.2 Glycosides in medicine: Role of glycosidic residue in biological activity	124
4.3 Click chemistry in drug designing	126
4.4 Palladium catalyzed ring-opening reaction of fulvene derived bicyclic	129

hydrazines	
4.5 Objective of the present work	131
4.6 Results and discussion	131
4.7 Biological evaluation of glycohybrids	139
4.7.1. $\alpha$ -Amylase and $\alpha$ -glucosidase inhibition assay	139
4.7.2. Anti-glycation inhibition assay	141
4.7.3. Cytotoxicity studies (MTT assay)	142
4.8 Conclusion	142
4.8 Experimental section	143
<b>Bibliography and References</b>	158
<b>Summary</b>	172
<b>List of Publications</b>	175

## List of Tables

1.1	Classification of terpenoids	10
1.2	List of natural product derived modern drugs	13
2.1	Different names of <i>Zingiber zerumbet</i>	26
2.2	Scientific classification of <i>Zingiber zerumbet</i>	27
2.3	Essential oil components of leaf and rhizome	28
2.4	Biological properties various extracts of rhizomes of <i>Z. zerumbet</i>	32
2.5	IC <sub>50</sub> values of compounds <b>1-8</b> against $\alpha$ -glucosidase enzyme	54
2.6	IC <sub>50</sub> values of compounds <b>1-8</b> against aldose reductase enzyme	57
3.1	Optimization studies for palladium catalyzed 1,4-conjugate addition	82
3.2	Optimization studies for rhodium-catalyzed 1,4-conjugate addition	84
3.3	Generality of rhodium-catalyzed 1,4-conjugate addition	85
3.4	Optimization studies of palladium catalyzed decarboxylative coupling reaction of aryl carboxylic acids with zerumbone <b>1</b>	109
3.5	Palladium catalyzed decarboxylative coupling of various carboxylic acids	110
3.6	IC <sub>50</sub> values of compounds <b>78-84</b> against $\alpha$ -glucosidase enzyme	114
4.1	Palladium catalyzed synthesis of azido alkylidene cyclopentenes	134
4.2	Propargyl glycosides	135
4.3	Novel Glycohybrids	139
4.4	IC <sub>50</sub> values of compounds <b>22a, 22c, 22e</b> and <b>22f</b> against $\alpha$ -glucosidase enzyme	140
4.5	IC <sub>50</sub> values of compounds <b>22a, 22c, 22e</b> and <b>22f</b> against glycation reaction	142
4.6	MTT assay results of compound <b>22f</b>	142



## List of Figures

1.1	Pacific yew	2
1.2	World market for drugs from plant sources	2
1.3	Paclitaxel (Taxol <sup>®</sup> ) <b>1</b> and artemisinin <b>2</b>	3
1.4	<i>Penicillium chrysogenum</i>	3
1.5	Structure of asperlicin <b>3</b> , lovastatin <b>4</b> and ciclosporin <b>5</b>	4
1.6	A sea sponge	5
1.7	Spongouridine <b>6</b> , spongothymidine <b>7</b> and discodermolide <b>8</b>	6
1.8	Ecuadorian poison frog	6
1.9	Epibatidine <b>9</b> , cilazapril <b>10</b> and captopril <b>11</b>	7
1.10	Basic flavonoid structure	8
1.11	Chemical structures of the flavonoid family	9
1.12	(a) Parsley leaves-source of flavones (b) Blueberries-source of dietary anthocyanidins	9
1.13	Structures of different terpenoids	11
1.14	Glycosides	12
1.15	All new chemical entities from 1981- 2002	12
1.16	Structures of some drugs	16
1.17	History of drug development since ancient times	17
1.18	Scheme of present-day drug development	18
1.19	Clinical phases of drug development, which might be applied for traditional medicines	18
1.20	Camptothecin <b>12</b> and its derivatives <b>13</b> and <b>14</b>	20
1.21	Podophyllotoxin <b>15</b> and its derivatives ( <b>16</b> and <b>17</b> )	21
1.22	Structures of compounds <b>18-22</b>	22

1.23	10-deacetylbaccatin III <b>23</b>	23
2.1	<i>Zingiber zerumbet</i> Smith	26
2.2	Selected compounds isolated from <i>Z. zerumbet</i> Smith	31
2.3	$\alpha$ -Humulene <b>1</b>	36
2.4	$^1\text{H}$ NMR of compound <b>1</b> ( $\alpha$ -humulene)	37
2.5	$^{13}\text{C}$ NMR of compound <b>1</b> ( $\alpha$ -humulene)	37
2.6	Mass spectrum of compound <b>1</b> ( $\alpha$ -humulene)	37
2.7	Zerumbone <b>2</b>	38
2.8	$^1\text{H}$ NMR of compound <b>2</b> (zerumbone)	38
2.9	$^{13}\text{C}$ NMR of compound <b>2</b> (zerumbone)	39
2.10	Mass spectrum of compound <b>2</b> (zerumbone)	39
2.11	Zerumbol <b>3</b>	40
2.12	$^1\text{H}$ NMR of compound <b>3</b> (zerumbol)	40
2.13	$^{13}\text{C}$ NMR of compound <b>3</b> (zerumbol)	41
2.14	Mass spectrum of compound <b>3</b> (zerumbol)	41
2.15	Zerumbone epoxide <b>4</b>	42
2.16	$^1\text{H}$ NMR of compound <b>4</b> (zerumbone epoxide)	42
2.17	$^{13}\text{C}$ NMR of compound <b>4</b> (zerumbone epoxide)	43
2.18	Mass spectrum of compound <b>4</b> (zerumbone epoxide)	43
2.19	Single crystal X-ray structure of zerumbone epoxide	44
2.20	Kaempferol <b>5</b>	44
2.21	$^1\text{H}$ NMR of compound <b>5</b> (kaempferol)	45
2.22	$^{13}\text{C}$ NMR of compound <b>5</b> (kaempferol)	45
2.23	Mass spectrum of compound <b>5</b> (kaempferol)	46

2.24	Kaempferol-3- <i>O</i> -methylether <b>6</b>	46
2.25	<sup>1</sup> H NMR of compound <b>6</b> (kaempferol-3- <i>O</i> -methylether)	47
2.26	<sup>13</sup> C NMR of compound <b>6</b> (kaempferol-3- <i>O</i> -methylether)	47
2.27	Mass spectrum of compound <b>6</b> (kaempferol-3- <i>O</i> -methylether)	48
2.28	3'',4''- <i>O</i> -Diacetyl afzelin <b>7</b>	48
2.29	<sup>1</sup> H NMR of compound <b>7</b> (3'',4''- <i>O</i> -diacetylafzelin)	49
2.30	<sup>13</sup> C NMR of compound <b>7</b> (3'',4''- <i>O</i> -diacetylafzelin)	50
2.31	Mass spectrum of compound <b>7</b> (3'',4''- <i>O</i> -diacetylafzelin)	50
2.32	Afzelin <b>8</b>	51
2.33	<sup>1</sup> H NMR of compound <b>8</b> (afzelin)	52
2.34	<sup>13</sup> C NMR of compound <b>8</b> (afzelin)	52
2.35	Mass spectrum of compound <b>8</b> (afzelin)	53
2.36	Glycation inhibition of compounds <b>1-8</b> at 100μM concentration	55
2.37	Percentage of inhibition of protein glycation reaction by (a) compound <b>1</b> (b) compound <b>5</b> (c) compound <b>6</b> (d) compound <b>7</b>	56
2.38	Aldose reductase inhibition of compounds <b>1-3</b> and <b>5-8</b> with varying concentrations	57
3.1	Zerumbone <b>1</b>	67
3.2	X-ray structure of zerumbone	68
3.3	<sup>1</sup> H NMR spectrum of compound <b>48</b>	80
3.4	<sup>13</sup> C NMR of compound <b>48</b>	80
3.5	Mass spectra of compound <b>48</b>	81
3.6	Single crystal X-ray structure (ORTEP representation) of product <b>48</b>	81
3.7	<sup>1</sup> H NMR spectrum of compound <b>78</b>	106
3.8	<sup>13</sup> C NMR spectrum of compound <b>78</b>	106

3.9	Mass spectra of compound <b>78</b>	107
3.10	Single crystal X-ray structure (ORTEP representation) of product <b>78</b>	107
3.11	Conformational change from zerumbone <b>1</b> to compound <b>78</b>	108
3.12	<sup>1</sup> H NMR spectrum of compound <b>87</b>	112
3.13	<sup>13</sup> C NMR spectrum of compound <b>87</b>	113
3.14	$\alpha$ -Glucosidase enzyme inhibition properties of compounds <b>78-84</b> , zerumbone and acarbose (standard) with varying concentration	113
4.1	(a) Ribavirin <b>1</b> -antiviral drug (b) Salicin <b>2</b> -anti-inflammatory agent (c) Oleandrin <b>3</b> -cardiac glycoside	125
4.2	Cis-platin derivative <b>4</b>	126
4.3	HIV-I protease inhibitor <b>5</b>	128
4.4	(a) Bitertanol <b>6</b> - broad spectrum fungicide (b) an analgesic <b>7</b>	128
4.5	A new PTP1B inhibitor <b>8</b>	129
4.6	(a) Streptazon <b>11</b> (b) Prostaglandin E1 <b>12</b>	131
4.7	<sup>1</sup> H NMR spectrum of compound <b>17a</b>	133
4.8	<sup>13</sup> C NMR spectrum of compound <b>17a</b>	133
4.9	<sup>1</sup> H NMR of compound <b>21a</b>	136
4.10	<sup>13</sup> C NMR of compound <b>21a</b>	137
4.11	<sup>1</sup> H NMR of compound <b>22a</b>	138
4.12	<sup>13</sup> C NMR of compound <b>22a</b>	138
4.13	$\alpha$ -Glucosidase inhibition of compounds <b>22a</b> , <b>22c</b> , <b>22e</b> and <b>22f</b> with varying concentrations	140
4.14	Glycation inhibition of compounds <b>22a</b> , <b>22c</b> , <b>22e</b> and <b>22f</b> with varying concentrations	141

## ABBREVIATIONS

Ac	: acetyl	DMF	: dimethyl formamide
Ar	: aryl	DMSO	: dimethyl sulphoxide
aq	: aqueous	dppb	: bis(diphenylphosphino)butane
acac	: acetylacetonate	dppe	: bis(diphenylphosphino)ethane
atm	: atmosphere	dppf	: bis(diphenylphosphino)ferrocene
BINAP	: 2,2'-bis(diphenylphosphino)-1,1' binaphthyl	E	: electrophile
Bn	: benzyl	EI	: electron impact
<sup>t</sup> Bu	: tertiary butyl	ESI	: electrospray ionization
BTMAC	: benzyltrimethylammonium chloride	Et	: ethyl
calcd	: calculated	equiv.	: equivalent
cod	: 1,5-cyclooctadiene	FAB	: fast atom bombardment
coe	: cyclooctene	h	: hour
cm	: centimeter	HRMS	: high resolution mass spectra
Cpd	: cyclopentadiene	Hz	: hertz
d	: doublet	IR	: infrared
dba	: dibenzylidene acetone	<i>J</i>	: coupling constant
dd	: doublet of a doublet	LA	: Lewis acid
ddd	: doublet of double doublet	LAH	: lithium aluminum hydride
br.d	: broad doublet	LRMS	: low resolution mass spectra
br.s	: broad singlet	m	: multiplet
DCM	: dichloromethane	mCPBA	: meta-chloroperoxybenzoic acid
DEAD	: diethyl azodicarboxylate	Me	: methyl
		mg	: milligram

DIPEA	: diisopropylethyl amine	MHz	: mega hertz
Mp	: melting point	mL	: millilitre
MS	: mass spectroscopy	TFA	: trifluoroacetic acid
MTT	: 3-(4,5-dimethylthiazol-2-yl)-2,5-diphenyltetrazolium bromide	THF	: tetrahydrofuran
NMR	: nuclear magnetic resonance	TLC	: thin layer chromatography
Nu	: nucleophile	TMS	: trimethyl silyl
<i>o</i>	: ortho	<i>tert</i>	: tertiary
<i>p</i>	: para	UV	: ultra violet
Ph	: phenyl	$\mu\text{M}$	: micro molar
Pt	: platinum		
q	: quartet		
R <sub>f</sub>	: retention factor		
rt	: room temperature		
Rh	: rhodium		
s	: singlet		
SD	: standard deviation		
t	: triplet		
TBAF	: tetrabutylammonium fluoride		

## PREFACE

Natural products have been the single most productive source of leads for the development of drugs. Of the 877 small new molecules introduced in drug discovery between 1981 and 2002, roughly half (49%) were natural products, semi synthetic natural products, analogues, or synthetic compounds based on NP pharmacophores. Furthermore, over a 100 natural-product-derived compounds are currently undergoing clinical trials and at least a 100 similar projects are in preclinical development. Inspired by these facts about natural products, we decided to invest our time on isolation, characterization and biological evaluation of phytochemicals from a plant *viz Zingiber zerumbet* (L.) Smith.

As mentioned earlier, natural products as such find use as drugs in modern era of chemotherapy. However, its use is limited because of many reasons. One of the most important reasons is the solubility of the natural products. The bioactives, which have potent activity under *in vitro* condition sometime, show poor or no activity under *in vivo* conditions due to the poor water solubility or lipophilicity. Other reasons include the limited availability from the natural source, poor/moderate activity, lack of chiral centres, adverse side effects, need of high dosage, very high cost of production *etc.* Hence, it is very important to develop novel and stereoselective methodologies to synthesize new and potent analogues. The investigations along this line form the focal theme of this thesis entitled **“SYNTHETIC TRANSFORMATIONS OF PHYTOCHEMICALS FROM *ZINGIBER ZERUMBET* (L.) SMITH AND SYNTHESIS OF CARBOHYDRATE APPENDED ALKYLIDENE CYCLOPENTENES AS BIOACTIVE ANALOGUES”**.

The thesis is divided into four chapters. Relevant references are given at the end of the thesis. An overview of importance of the natural products and their analogues in modern drug discovery is presented in the first chapter of the thesis. The definition of the present research problem is also incorporated in this chapter.

Second chapter presents the results of our investigations on the isolation, characterization and biological evaluation of phytochemicals from *Zingiber zerumbet* (L.)

Smith. Seven phytochemicals were isolated from the dried rhizomes of *Zingiber zerumbet* and one natural product was synthesized by alkaline hydrolysis. All the eight compounds were screened against  $\alpha$ -glucosidase enzyme, aldose reductase enzyme and protein glycation reaction inhibition assays. Kaempferol and kaempferol-3-*O*-methylether were found to be potent  $\alpha$ -glucosidase, aldose reductase as well as protein glycation inhibitors.

The third chapter comprises of two parts *viz* part A and part B, and explain our efforts toward the synthetic transformations of bioactive zerumbone by transition metal catalyzed reactions. An efficient method for the synthesis of novel zerumbone derivatives *via* palladium and rhodium catalyzed regio- and diastereoselective 1,4-conjugate addition using boronic acids is described in part A. Part B of chapter 3 deals with the synthesis of novel zerumbone derivatives *via* a regioselective palladium catalyzed decarboxylative coupling reaction with arene carboxylic acids. Preliminary *in vitro* analysis revealed that most of the newly synthesised derivatives are potent  $\alpha$ -glucosidase enzyme inhibitors.

A new and efficient route towards the synthesis of glycohybrids having an alkylidene cyclopentene moiety with triazole ring as a linker is explained in the final chapter of the thesis. The developed protocol involves a palladium-catalyzed ring opening reaction and click chemistry as the key steps. Out of the six compounds synthesized, four were screened against  $\alpha$ -glucosidase,  $\alpha$ -amylase and protein glycation reaction inhibition assays. It is noteworthy that four compounds were found to be non-cytotoxic against H9c2 cardiac myoblast cell lines by MTT assay.

It may be mentioned that each chapter of the thesis is presented as an independent unit and therefore the structural formulae, schemes and figures are numbered chapter wise.

A summary of the work is given towards the end of the thesis.



## Natural Products and their Analogues in Drug Discovery

---

### 1.1. Introduction

Natural products (NPs) are chemical compounds or substances produced by living organisms that usually possess pharmacological or biological activities. NPs are secondary metabolites of natural origin. NPs represent a rich source of new molecules with pharmacological or biological properties, which are lead compounds for the development of new drugs. Many well-known drugs listed in the modern pharmacopoeia have their origin in nature. The inspiration for drug discovery since the inception of penicillin till date can be mainly attributed to natural products [Hanson 2003].

Before going into the details of the importance of NPs and its synthetic analogues in the modern drug discovery, a brief account on the classification of NPs based on its origin and chemical structure is included.

### 1.2. Classification of natural products (NPs)

Thousands of simple to complex and diverse NPs are reported and is being reported in the literature, which in turn makes it difficult to systematically classify them in a standard way. Among the various approaches developed so far, the two important and widely accepted ways of classification are; (i) classification based on source/origin and (ii) classification based on chemical structure [Alexander *et al.* 2003].

#### 1.2.1. Classification based on source/origin

Based on the source or origin, the whole family of NPs can be categorized into the following groups.

- Plant derived NPs
- Microbial world derived NPs
- Marine world derived NPs
- Animal derived NPs

### 1.2.1.1. Plant derived natural products



**Figure 1.1.** Pacific yew

Plants have been well documented for their medicinal uses for years. They have evolved and adapted over millions of years to withstand bacteria, insects, fungi and weather to produce unique, structurally diverse secondary metabolites. An important medicinal plant *viz* Pacific yew, source of paclitaxel, is shown in figure 1.1. To date, 35,000- 70,000 plants have been screened for their pharmacological use [Koehn and Carter 2005]. A graphical representation of their contribution to the world market for herbal medicines is shown in figure 1.2.

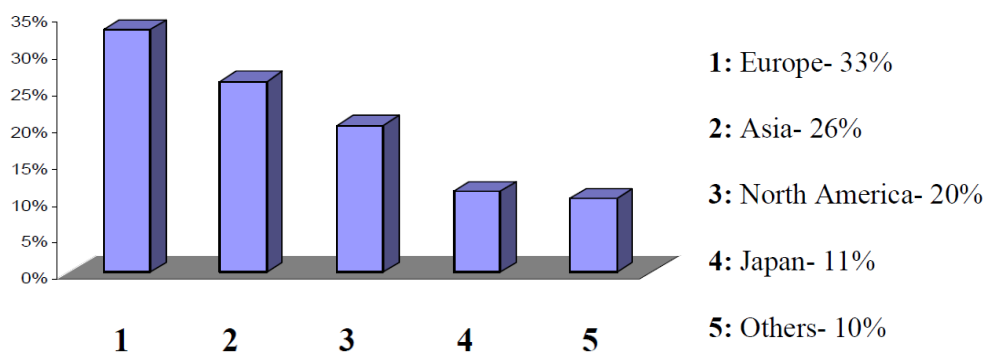


**Figure 1.2.** World market for drugs from plant sources

**Source:** *Environmental Health Perspectives* **1999**, 107, 783-789

Plants have been a rich source of simple to complex lead molecules. According to the World Health Organization (WHO), 80% of people still rely on plant-based traditional

medicines for primary healthcare and 80% of 122 plant-derived drugs were related to their original ethnopharmacological purpose [WHO News 2002]. Hence, modern drug design and discovery cannot ignore the remarkable contribution extended by the plant based natural entities. Many of such NPs were found useful as drugs for the treatment of various fatal diseases. Two important plant derived molecules *viz* paclitaxel (Taxol<sup>®</sup>) **1** and artemisinin **2** have found its use as drugs for cancer and malaria respectively (Figure 1.3).

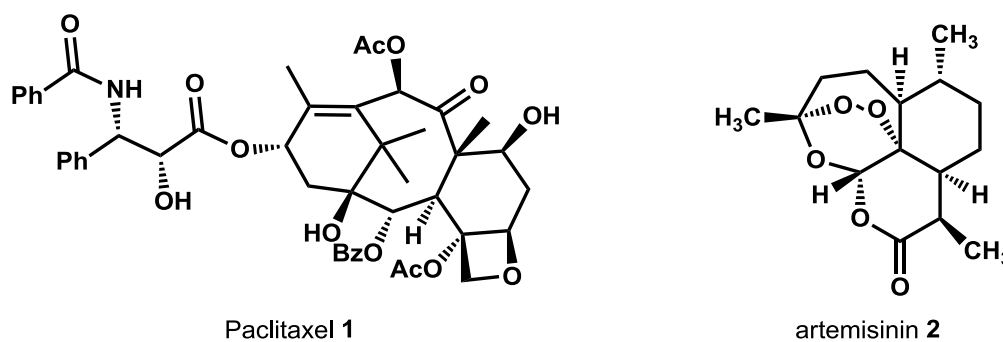


**Figure 1.3.** Paclitaxel (Taxol<sup>®</sup>) **1** and artemisinin **2**

Terpenoids, phytosterols, alkaloids, phenols and polyphenols are the main classes of compounds found in plants. As most of these molecules are structurally very complex and stereochemically rigid, its synthesis remains as a challenge.

#### 1.2.1.2. Microbial world derived natural products



**Figure 1.4.** *Penicillium chrysogenum*

Wide varieties of microorganisms such as bacteria and fungi have contributed a significant number of lead molecules to drug discovery and its development. However, these organisms were not explored until the discovery of penicillin by Alexander Fleming in 1928. An important fungus *Penicillium chrysogenum*, source of penicillin is shown in figure 1.4. Since the inception of penicillin, a large number of marine and terrestrial microorganisms have been studied and screened for new drug candidates. Most of the drugs developed from microorganisms are used as anti-microbial agents. However, a few possess other medicinal applications. For example asperlicin **3**, isolated from fungus acts as a novel antagonist of peptide hormone *viz* cholecystokinin (CCK) which is involved in the control of appetite. Also, lovastatin **4** is used for cholesterol lowering and ciclosporin **5** is used in suppressing the immune response after the transplantation surgeries (Figure 1.5) [Chin *et al.* 2006].

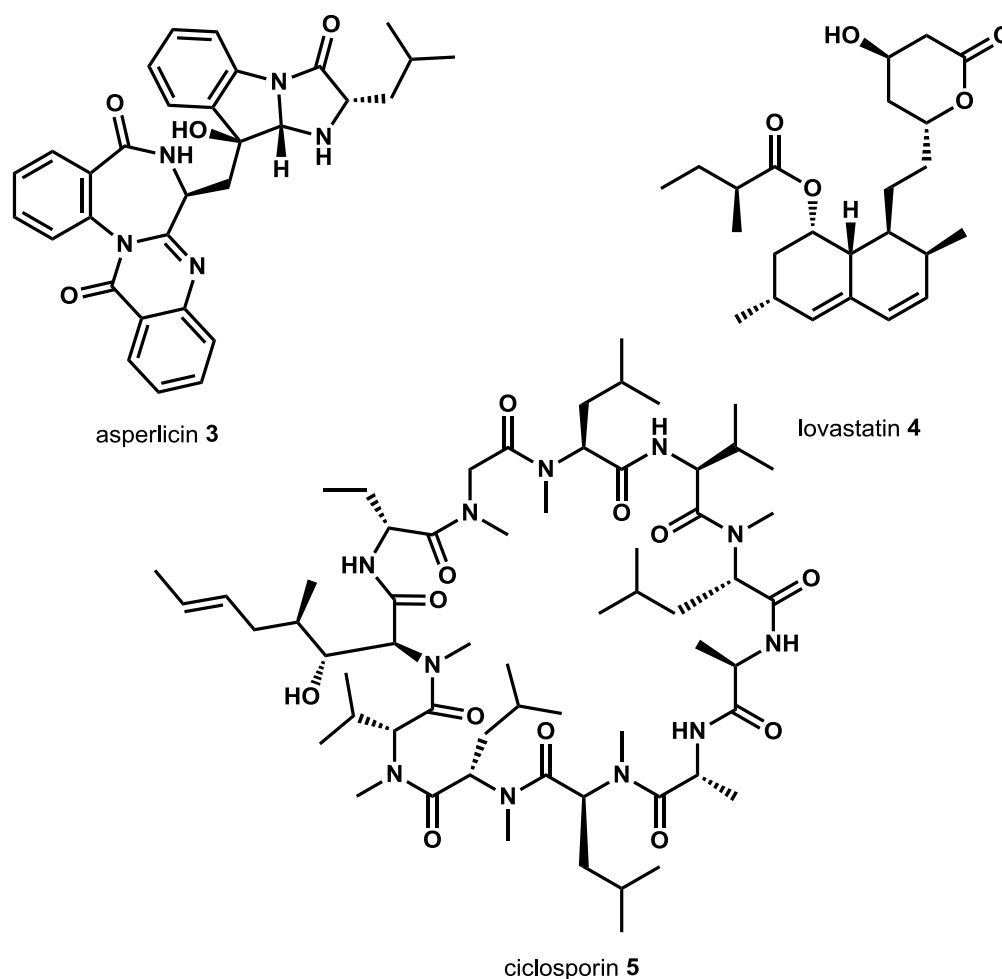


**Figure 1.5.** Structures of asperlicin **3**, lovastatin **4** and ciclosporin **5**

### 1.2.1.3. Marine world derived natural products



**Figure 1.6.** A sea sponge

The sea contains many untapped sources of molecules with promising activities due to the extensive varieties of marine species. The census shows that over 6000 potentially new species are available in the sea. It points to the fact that the marine environment represents a largely unexploited reservoir of many unknown natural compounds, which in turn needs to be evaluated for their potential medicinal applications [Haefner 2003]. An example for marine world derived natural product source namely sea sponge is shown in figure 1.6.

In recent years, there has been a great interest in finding lead compounds from marine sources. Various molecules isolated from coral, sponges, fish and marine microorganisms are reported to have anti-inflammatory, anti-viral and anti-cancer activities. Spongouridine **6** and spongothymidine **7** were isolated from Caribbean sponge (*Cryptotheca crypta*) in the 1950s, the first two compounds from marine sources. These compounds are nucleotides and show great potential as anti-cancer and anti-viral agents. Another example is discodermolide **8**, isolated from the marine sponge *Discodermia dissoluta*, which has a similar mode of action to that of paclitaxel and possesses strong antitumor activity (Figure 1.7). It also exhibits better water solubility as compared to paclitaxel.

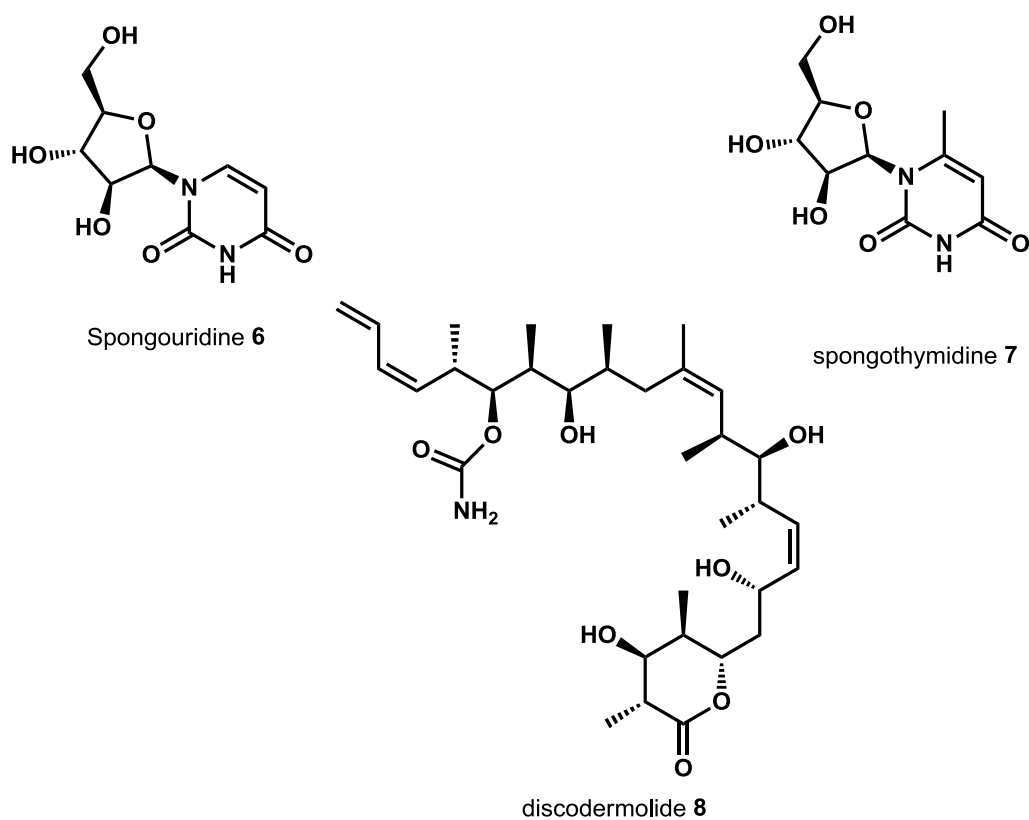


**Figure 1.7.** Spongouridine 6, spongothymidine 7 and discodermolide 8

#### 1.2.1.4. Animal derived natural products



**Figure 1.8.** Ecuadorian poison frog

Animals are also good sources for compounds that can be used as drugs. For example, a series of antibiotic peptides were extracted from the skin of the African clawed frog and epibatidine **9** was obtained from the skin of an Ecuadorian poison frog (Figure 1.8), which is ten times more potent than morphine [Spande *et al.* 1992]. It is documented in

the literature that venoms and toxins have played an important role in the drug discovery for a number of diseases. For instance, cilazapril **10** and captopril **11**, two effective drugs against hypertension were developed from a natural product called teprotide isolated from a Brazilian viper (Figure 1.9). [Blood pressure <http://www.medicinenet.com/captopril/article.htm>].

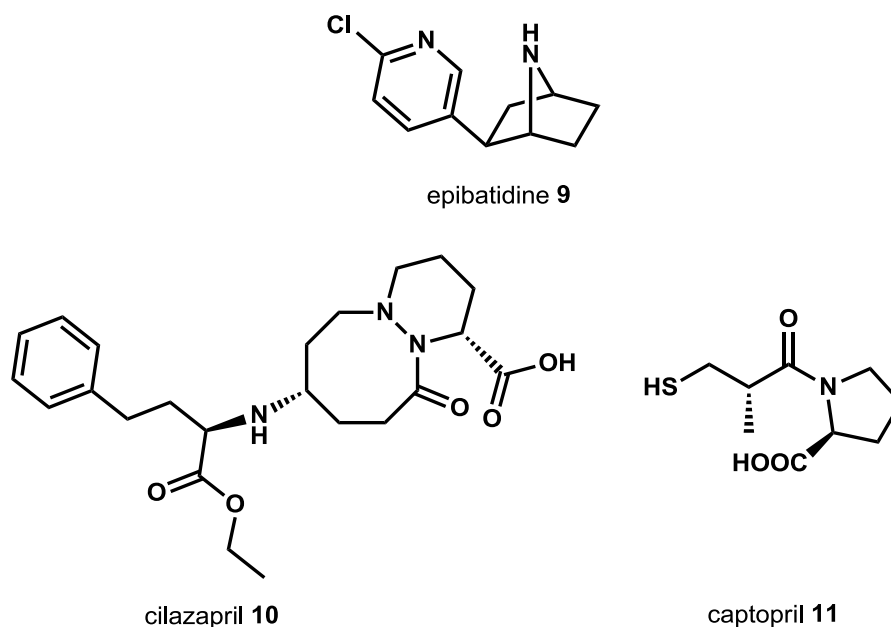


**Figure 1.9.** Epibatidine **9**, cilazapril **10** and captopril **11**

### 1.2.2. Classification based on chemical structure

Due to biological and geographical diversity, natural products show a great deal of chemical diversity. Many of the natural products have complex molecular structures, with cyclic semi-rigid scaffolds, several chiral centers, more than five H-bond donors, more than ten H-bond acceptors, more than five rotatable C-C bonds and a large polar surface area. Moreover, large number of secondary metabolites contains heteroatoms such as nitrogen and oxygen in plenty. All these facts about the natural products make it necessary to classify them into various sub-classes according to the chemical characteristics for a better and clear understanding. A list that comprises the main classes of compounds is given below.

- Aliphatic natural products
- Polyketides
- Oxygen heterocycles
- Simple aromatic natural products
- Benzofuranoids
- Benzopyranoids
- **Flavonoids**
- Tannins
- Polycyclic aromatic natural products
- **Terpenoids**
- Steroids
- Alkaloids
- Specialized amino acids and peptides
- **Glycosides**
- Polypyrroles
- Lignans

Among the various classes of compounds, a detailed account of flavonoids, terpenoids and glycosides are given in the following sections.

#### 1.2.2.1. Flavonoids

Flavonoids are a group of polyphenolic plant secondary metabolites which possess an array of pharmacological activities. They are synthesized by the phenylpropanoid metabolic pathway in which the amino acid phenylalanine is used to produce 4-coumaroyl-CoA. This can be combined with malonyl-CoA to yield the true backbone of flavonoids [Colerige *et al.* 1980; Bors *et al.* 1990].

The flavonoid compounds possess a common phenylbenzopyran moiety. They are mainly divided into six sub-classes based on the connection position of **B** and **C** rings as well as the degree of saturation, oxidation and hydroxylation of the **C** ring as flavonols, flavones, flavanones, flavan-3-ols, isoflavones and anthocyanidines [Graf 2005]. The basic structure with the numbering system and structures of different flavonoids are shown in figure 1.10 and figure 1.11 respectively.

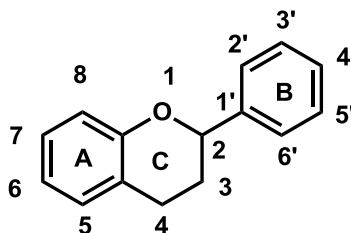


**Figure 1.10.** Basic flavonoid structure.



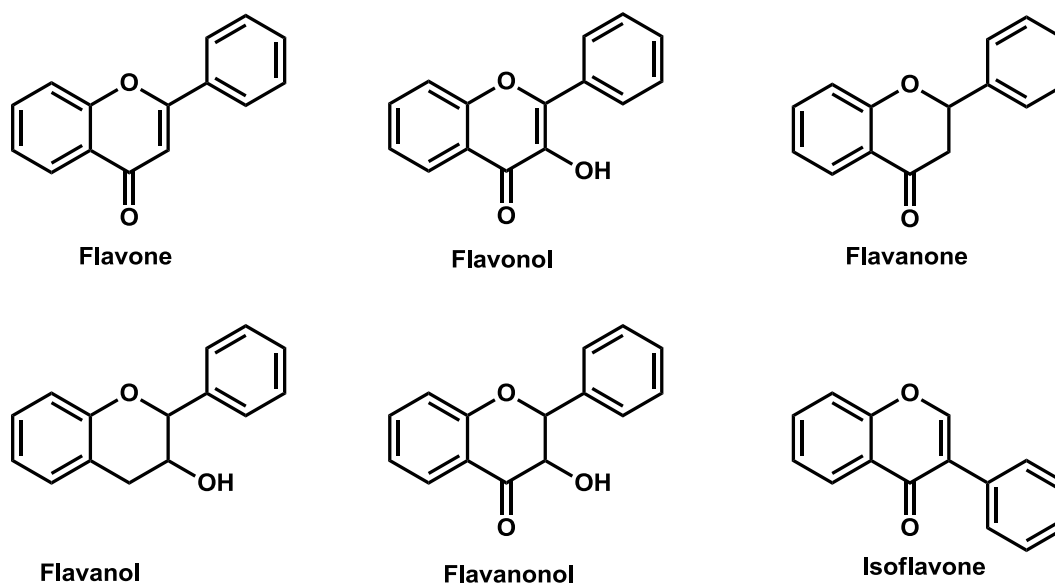


**Figure 1.11.** Chemical structures of the flavonoid family

In plants, flavonoids play many roles such as plant pigments, UV filters (absorb in the 280-315 nm region), chemical messengers, physiological regulators, and cell cycle inhibitors. Important sources of flavonoids are green tea, grapes, apple, cocoa, soybean, parsley, blueberry *etc.* Two plants, which are rich sources of flavones and anthocyanidins, are shown in figure 1.12.



**Figure 1.12.** (a) Parsley leaves-source of flavones (b) Blueberries-source of dietary anthocyanidins

Flavonoids have been reported to have anti-bacterial, anti-cancer, anti-inflammatory and anti-Alzheimer's properties.

#### 1.2.2.2. Terpenoids (Terpenes)

Terpenoids, also known as isoprenoids are a diverse class of organic compounds produced by a wide variety of plants, microorganisms and animals. They play a vital role

in the chemical ecology of plants derived from C<sub>5</sub> isoprene units [Mc Garvey 1995]. Terpenoids were originally known as terpenes and the suffix “ene” in terpenes indicates the presence of olefinic double bonds. In other words, the term “terpene” indicate hydrocarbons resulting from the combination of several isoprene units and the term “terpenoids” can be considered as modified terpenes, wherein methyl groups have been moved or removed, or oxygen atoms added. It is to be noted that sometimes the term "terpene" is used more broadly even to include the terpenoids. Plant terpenoids are extensively used for their aromatic qualities. They play a role in traditional herbal remedies and are under investigation for their anti-bacterial, anti-neoplastic and other pharmaceutical functions. Two biosynthetic pathways are available for terpenoid compounds *viz* mevalonic acid pathway and mevalonic acid-independent pathway.

Based on the number of isoprene units, terpenoids can be mainly classified into seven groups as depicted in Table 1.1.

**Table 1.1.** Classification of terpenoids

n	No. of carbon atoms	Molecular formula	Class of compound
2	10	C <sub>10</sub> H <sub>16</sub>	Monoterpenoid
3	15	C <sub>15</sub> H <sub>24</sub>	Sesquiterpenoid
4	20	C <sub>20</sub> H <sub>32</sub>	Diterpenoid
5	25	C <sub>25</sub> H <sub>40</sub>	Sesterterpenoid
6	30	C <sub>30</sub> H <sub>48</sub>	Triterpenoid
8	40	C <sub>40</sub> H <sub>64</sub>	Tetraterpenoid (Carotenoid)
> 8	> 40	(C <sub>5</sub> H <sub>8</sub> ) <sub>n</sub>	Polyterpenoid

Sources of natural products such as plants, marine world, microbial world and animal world produce a wide spectrum of terpenoid compounds. Examples for various classes of terpenoids are shown in figure 1.13.

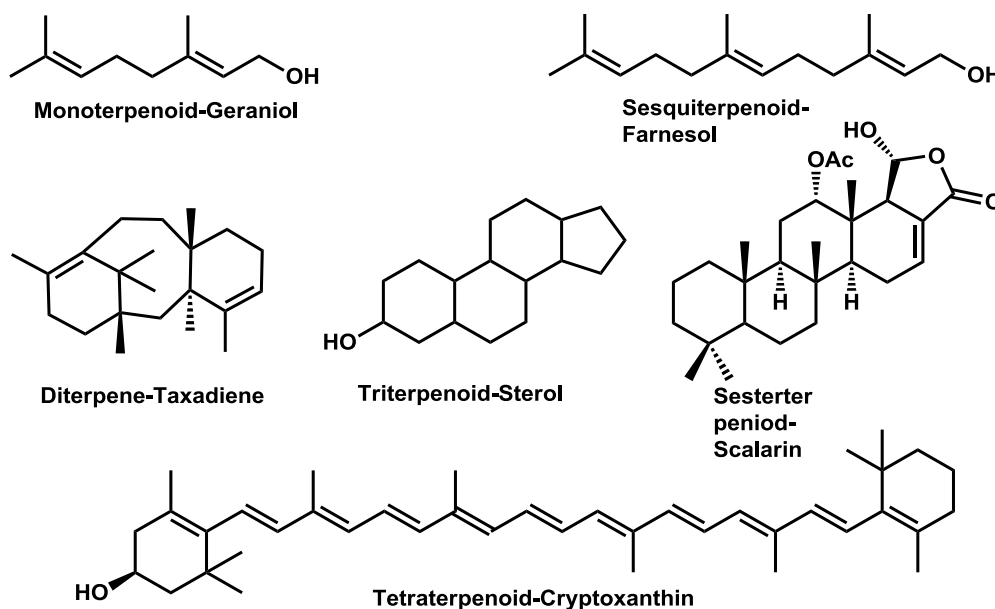


**Figure 1.13.** Structures of different terpenoids

### 1.2.2.3. Glycosides

A glycoside is a molecule in which sugar is bound to a non-sugar molecule *via* glycosidic bond. The sugar unit of the glycoside is known as glycone and the non-sugar part is known as aglycone (or genin). So the definition of glycosides can be again stated as organic natural compounds present in plants and animals, which upon hydrolysis give one or more glycone/s and aglycone. Depending up on the nature of glycosidic linkage, glycosides can be classified as *O*-glycosides, *N*-glycosides (glycosylamine), *S*-glycosides (thioglycoside) and *C*-glycosides. Two pharmaceutically important glycosides are shown in figure 1.14 [Brito-Arias and Marco 2007].

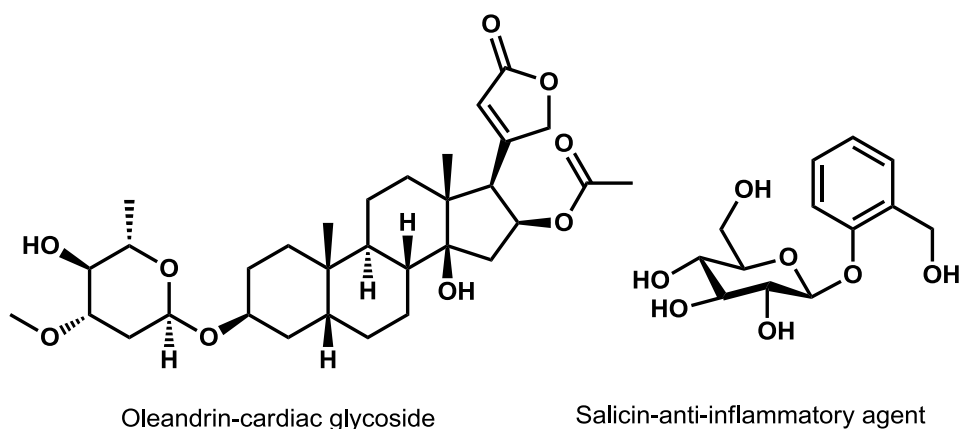


**Figure 1.14.** Glycosides

### 1.3. Nature as source of new drug compounds

Natural products have played a key role in drug discovery. Most of the medicines are either natural products or derivatives thereof. In fact, it is estimated that about 40% of all medicines are either natural products or their semi- synthetic derivatives. Scientific evaluation of traditional medicines, which were derived predominantly from plants, laid a very strong platform for the development of most of the early medicines such as aspirin, digitoxin, morphine, quinine, and pilocarpine. A graphical representation of chemical entities from 1981 to 2002 is depicted in figure 1.15.

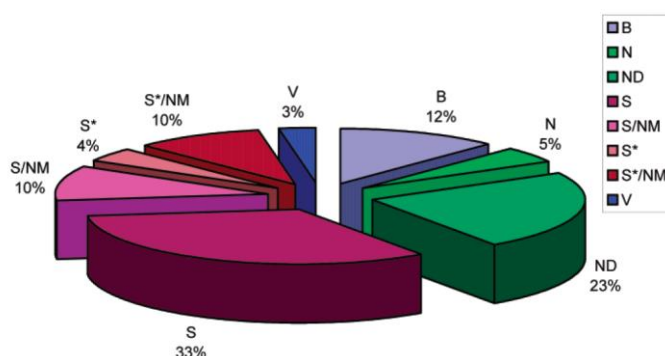


**Figure 1.15.** All new chemical entities from 1981- 2002 ( B = “biological” peptide or protein, N = natural product, ND = natural product derived, S = totally synthetic, S\* = made by total synthesis, but the pharmacophore is/was from a natural product, V = vaccine, sub class NM = natural product mimic)

**Source:** *J. Nat. Prod.* **2003**, *66*, 1022-1037

Interestingly, of the 877 novel medicines that were developed in the period 1981-2002, 6% were natural products, 27% were derivatives of natural products and 16% were synthetic molecules developed on the model of a natural product [Newman *et al.* 2003]. The data demonstrates the fact that nature is an important source for developing novel leads for medicines.

At least 80% of the world population is estimated to be still using traditional medicines in primary health care, including 40,000 to 70,000 medicinal plants representing about 20% of all higher-plant species. Although extensive research on medicinal plants is published every year, only a few plants have been comprehensively studied for pharmacological activity. Considering these facts, medicinal plants obviously represent a great source of novel leads for drug development.

Even though modern methods of drug discovery like combinatorial chemistry came into forefront, natural products are still providing their fair share of new clinical candidates and drugs. Their contribution to new drugs in the area of cancer, hypertension, infective disease, immune-suppression and neurological disease are commendable.

#### 1.4. Important natural product derived drugs

The importance of natural products in drug discovery can be easily understood from the number of natural product derived drugs available in the market. A list of natural product derived drugs is given in Table 1.2. From the list, it is apparent that natural sources are continuing their contribution to modern medicine. Structures of some selected drugs are shown in figure 1.16.

**Table 1.2. List of natural product derived modern drugs**

<b>Year of Introduction</b>	<b>Drug</b>	<b>Natural product; Commercialized as</b>	<b>Indication</b>	<b>Company</b>
1826	Morphine	Natural compound (p)	Analgesic	E. Merck
1899	Acetyl salicylic acid	Salicin (p) Synthetic	Analgesic, Anti-phlogistic <i>etc.</i>	Bayer

	(Aspirin)	analogue		
1941	Penicillin	Natural compound (m)	Anti-bacterial	Merck
1964	First cephalosporin antibiotic (cephalothin)	Semi-synthetic derivative based on 7-ACA (m)	Anti-bacterial	Eli Lilly
1983	Cyclosporin A	Natural compound (m)	Immunosuppressant	Sandoz
1987	Artemisinin	Natural compound (p)	Anti-malarial	Baiyunshan
1987	Lovastatin	Natural compound (m)	Anti-hyperlipidemic	Merck
1988	Simvastatin	Lovastatin (m). Semi-synthetic derivative	Anti-hyperlipidemic	Merck
1889	Pravastatin	Mevastatin (m). Semi-synthetic derivative	Anti-hyperlipidemic	Sankyo/BMS
1994	Fluvastatin	Lovastatin, mevastatin (m), synthetic analogue	Anti-hyperlipidemic	Sandoz
1990	Acarbose	Natural product (m)	Anti-diabetic (type II)	Bayer
1993	Paclitaxel (Taxol)	Natural compound (p) as a semi synthetic derivative of baccatin III (p)	Anti-cancer	BMS

1993	FK 506 (tacrolimus)	Natural compound (m)	Immunosuppressant	Fujisawa
1995	Docetaxel (Taxotere)	10-deacetyl baccatin III (p); semi- synthetic derivative	Anti-cancer	Rhone-PR
1996	Topotecan, Irinotecan	Camptothecin (p); semi- synthetic derivative	Anti-cancer	SKB- Pharmacia & Upjohn
1996	Miglitol	1- deoxynojirimycin (m, p); synthetic analogue	Anti-diabetic (type II)	Bayer
1999	Orlistat	Lipstatin (m); synthetic analogue	Obesity	Roche

m = microbial metabolite

p = plant metabolite

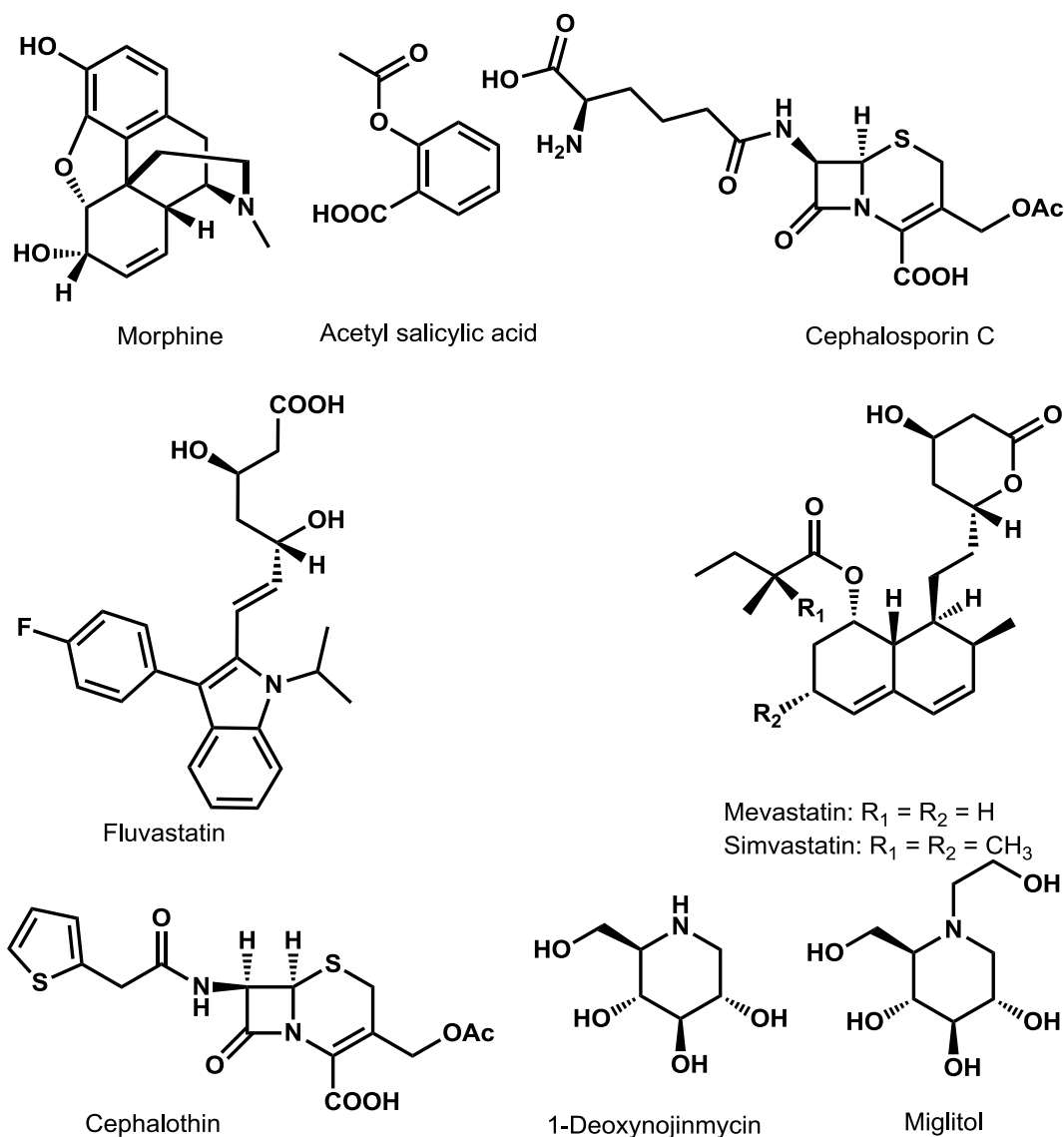


**Figure 1.16.** Structures of some drugs

### 1.5. Approaches in natural product drug discovery

To tap the endless natural sources for novel drugs, two definite approaches are available: the reductionist approach (based on the paradigm single target, single compound) used in present-day drug development and a holistic approach (based on measuring the effect of a traditional medicine in an *in vivo* system) (Figure 1.17) [Bogers *et al.* 2006].



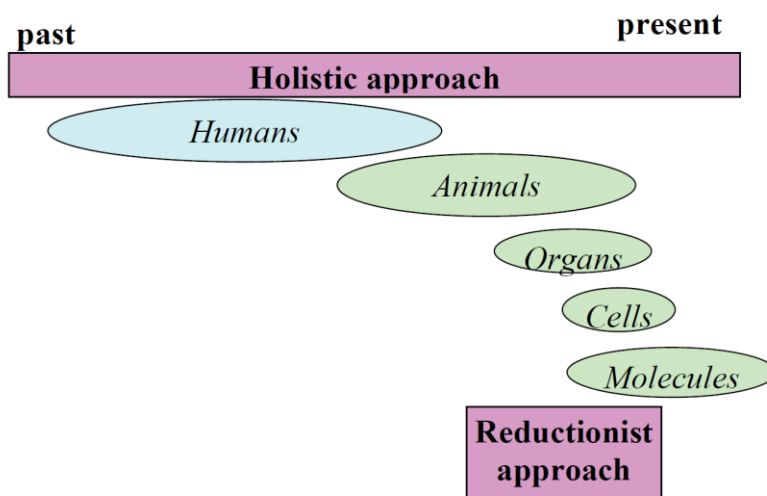


**Figure 1.17.** History of drug development since ancient times

**Source:** Bogers *et al.* 2006

### 1.5.1. The holistic approach

The holistic approach sticks to traditional medicines. The traditional healer makes a diagnosis based on a thorough examination of the patient and then prescribes a personalized medicine, usually consisting of a mixture of different ingredients. Because of the holistic approach of the traditional medicine, a holistic approach to study drug activity of these medicines seems more appropriate than a reductionist approach. Several reasons for a holistic evaluation can be discerned, including the possibility of synergy among plant extract constituents and the occurrence of prodrugs (the formation of the active compound(s) after intake of the medicine). Both of these factors are realistic assumptions [Chan 2005].

Studying traditional medicines in a holistic approach can be done by clinical trials, systems biology, or a combination of the two. In well-documented traditional medical systems such as in Asia, the safety of the medicines can be assumed based on the well-documented thousands of years of use. Clinical studies can thus easily be done. The first years in drug development spent to identify a target and find a safe lead compound (Investigational New Drug) as well as the phase-1 clinical trials can be skipped, allowing traditional medicines to enter directly into phase-2 clinical trials.

### 1.5.2. The reductionist approach

In this modern approach, the drug discovery consists of mainly of two phases: the first stage is the identification of a novel chemical entity, which will be approved as an Investigational New Drug (IND) for clinical trials (Figure 1.18 and Figure 1.19). The second stage concerns with the clinical trials, which includes three phases. If the drug passes all these three phases, the final stage will be the official registration.

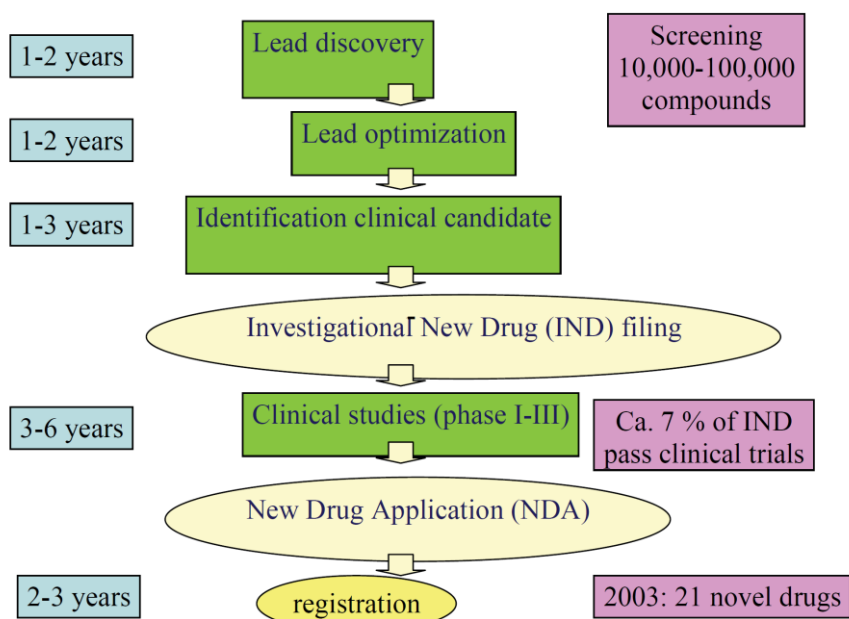


**Figure 1.18.** Scheme of present-day drug development

**Source:** Bogers *et al.* 2006

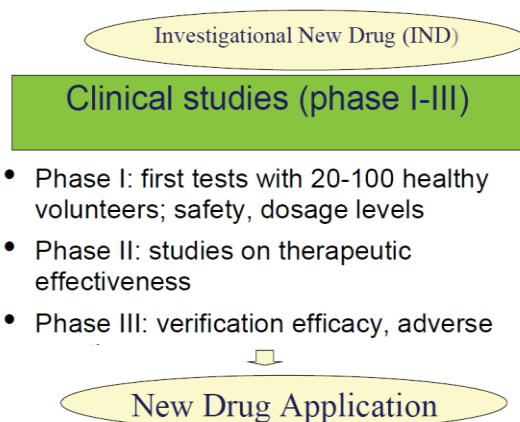


**Figure 1.19.** Clinical phases of drug development, which might be applied for traditional medicines. **Source:** Bogers *et al.* 2006

---

---

## 1.6. Importance of synthetic methodologies in modern drug discovery

Natural products as such find use as drugs in modern era of chemotherapy. However, its use is limited because of many reasons. One of the most important reasons is the solubility of the natural products. The bioactives, which have potent activity under *in vitro* condition sometime, show poor or no activity under *in vivo* conditions due to the poor water solubility or lipophilicity. Other reasons include the limited availability from the natural source, poor/moderate activity, lack of chiral centres, adverse side effects, need of high dosage, very high cost of production *etc* [Gryniewicz *et al.* 2008]. Hence, it is very important to develop novel and enantioselective reactions to synthesize new and potent analogues of the natural products. Some important natural products, their drawbacks and the synthesis of new derivatives are discussed in the following sections.

### 1.6.1. Camptothecin and its derivatives

Camptothecin **12** is a quinoline alkaloid isolated from the bark and stem of Camptotheca (Happy tree), native to china. In traditional Chinese medicine, the tree is used for the treatment of cancer. A systematic bioassay guided isolation and characterization resulted in the isolation of Camptothecin by M. E. Wall and M. C. Wani in 1966 [Wall *et al.* 1966; Govindachari *et al.* 1972; Efferth *et al.* 2007]. In clinical trials, it showed a noticeable anti-cancer activity. However, the low solubility and adverse drug reactions of camptothecin prompted the synthetic organic chemists to invest their time on making derivatives with an aim to improve its drug activity and the solubility. As a result, two novel anti-cancer drugs took birth *viz.* topotecan **13** and irinotecan **14** (Figure 1.20) [Zunino *et al.* 2002].

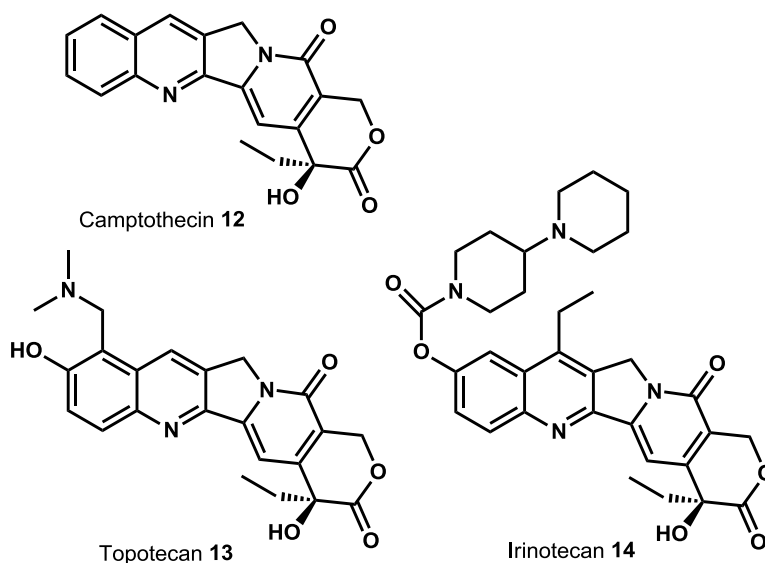


**Figure 1.20.** Camptothecin **12** and its derivatives **13** and **14**

### 1.6.2. Podophyllotoxin and its derivatives

Podophyllotoxin **15** is a non-alkaloid toxic lignan isolated from the roots and rhizomes of *Podophyllum* species [Borsche and Niemann 1932; Hartwell and Schrecker 1951]. It displays a wide range of activities such as cathartic, purgative, antiviral, vesicant and antihelminthic. However, its application immediately followed by burning or itching. In addition, small sores, itching and peeling resulted. To minimize these adverse side effects and to improve pharmacological activity, podophyllotoxin has been synthetically manipulated. Etoposide **16**, an important anti-cancer drug and teniposide **17** are the two main drug molecules synthesized from podophyllotoxin. (Figure 1.21) [You 2005].

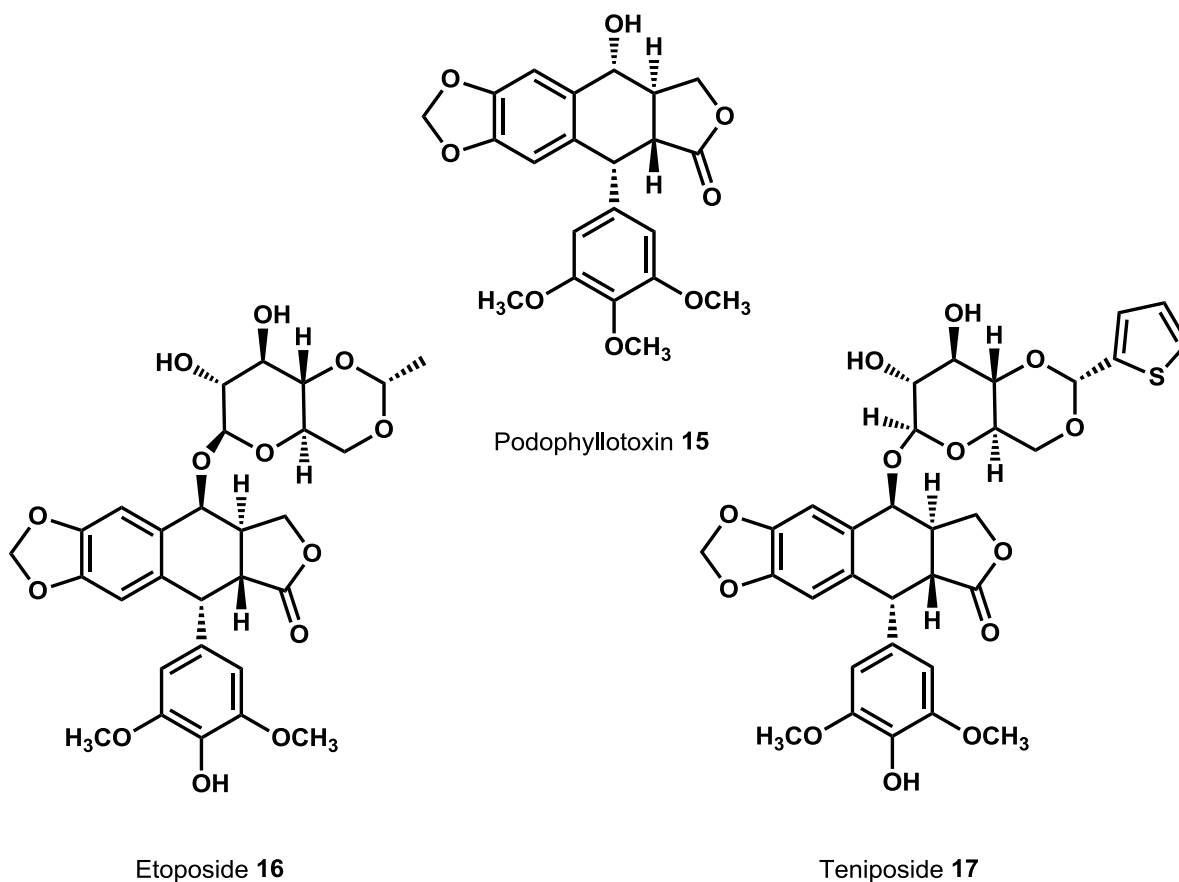


**Figure 1.21.** Podophyllotoxin **15** and its derivatives (**16** and **17**)

### 1.6.3. Penicillin and its derivatives

The poor oral activities and a narrow range of spectrum activity of natural penicillins (eg. Penicillin G **18** and Penicillin V **19**), forced the chemists to develop their derivatives. Most of the semi-synthetic derivatives were prepared from 6-APA (6-aminopenicillanic acid) **20** having the same nucleus as that of the penicillin (Figure 1.22). Derivatives prepared showed many improvements like bioavailability, broad spectrum of activities, stability, tolerance *etc* over natural ones. Examples are amoxicillin **21** and ampicillin **22** [AHFS Drug Information 2006].

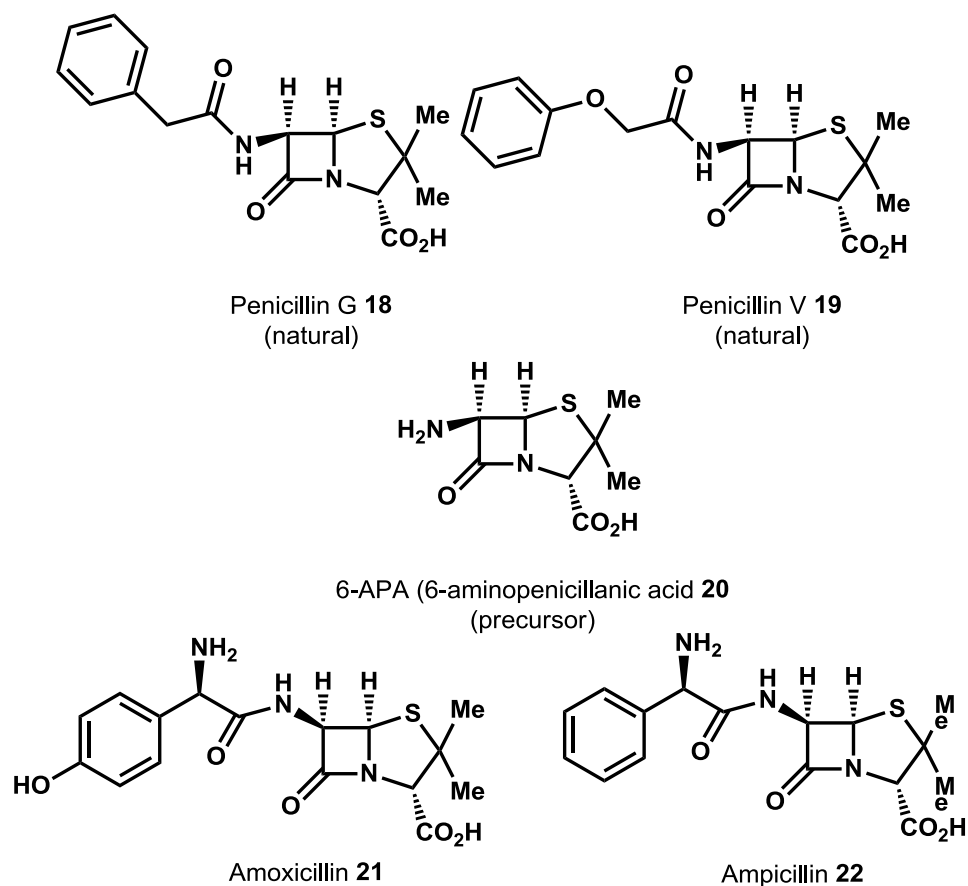


**Figure 1.22.** Structures of compounds **18-22**

#### 1.6.4. Semisynthesis of paclitaxel from 10-deacetylbaccatin III

Paclitaxel **1** is a diterpenoid anti-cancer drug isolated from Pacific yew (*Taxus brevifolia*). Since its occurrence in this yew tree is very low, one cannot isolate paclitaxel from the natural source in bulk amount for the drug production. In addition, its total synthesis is too tedious, complex and expensive. Here comes the importance of other natural sources and the synthetic methodologies. Synthetic organic chemists invested their time on semi-synthesis of paclitaxel from a comparatively cheap precursor 10-deacetylbaccatin III **23** (isolated from the European yew) which provided a possible route for its commercial production (Figure 1.23) [Faye 1994; Frank 2003].

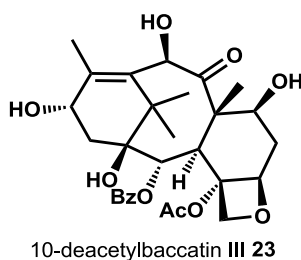


**Figure 1.23.** 10-deacetylbaccatin III 23

## 1.7. Conclusion and present work

From the above discussions, it is clear that natural products and its analogues play a pivotal role in modern drug designing and discovery. Even though new approaches like combinatorial chemistry are available, natural sources still play a major role in the development of drugs. Drugs, especially in the cancer treatment are coming out from the natural sources. From the literature reports, it is evident that novel and efficient synthetic methodologies help to make a variety of drugs from a single natural product. Penicillin and its derivatives are classical examples for such group of medicines. The semi-synthesis of paclitaxel from 10-deacetylbaccatin III also portrays the significance of synthetic manipulation in a natural product to make them more useful for the humankind.

Inspired by this observation and previous literature reports on the medicinal plant *Zingiber zerumbet* (L.) Smith, we decided to isolate the bioactives from its rhizomes with an aim to synthesize novel derivatives for biological evaluation. One of the most attractive facts about the *Z. zerumbet* is the abundance of highly potent sesquiterpene zerumbone in it. Sabu *et al.* recently reported that the rhizomes of *Z. zerumbet* found in South India contain 80% of zerumbone. Moreover this attractive phytochemical shows a diverse reactivity pattern and versatile bioactivities like anti-inflammatory, anti-cancer, anti-HIV *etc.* Nevertheless, the real trouble in testing the biological activity phytochemicals under *in vivo* condition is its poor solubility. Hence, we undertook this challenge and invested our time in isolation, characterization and synthetic transformations of phytochemicals from the rhizomes of *Z. zerumbet* with a special focus on zerumbone.

---

An overview of importance of the natural products and their analogues in modern drug discovery is presented in the first chapter of the thesis. Chapter 2 discusses the efforts toward the isolation, characterization and biological evaluation of phytochemicals from dried rhizomes of *Z. zerumbet*. Seven phytochemicals, including four sesquiterpenes and three flavonoids were isolated from the acetone extract. In addition, we synthesized a flavonoid glycoside from one of the isolated compounds. We then turned our attention to evaluate the unknown biological activities of phytochemicals against various targets in the treatment of diabetes mellitus type II.

Zerumbone, having a good latent reactivity, has been subjected to various metal catalyzed synthetic manipulations with an aim to improve its activities and solubility. For this, we have developed palladium and rhodium catalyzed regio- and diastereoselective 1,4-conjugate addition of zerumbone using boronic acids. The reaction worked well with phenyl boronic acids having electron withdrawing and electron donating groups. This work constitutes the first part of chapter three of the thesis. Second part includes a regioselective palladium catalyzed decarboxylative coupling reactions of zerumbone using commercially available arene carboxylic acids. All the derivatives synthesized by this methodology were extremely good in inhibiting the action of  $\alpha$ -glucosidase enzyme compared to the parent molecule.

In the final chapter, we discuss our efforts toward the synthesis and biological evaluation of carbohydrate-appended carbocycles. The major disadvantage of carbocycles in drug discovery and development is its low hydrophilicity. In order to improve the solubility and hence the activities, we utilized naturally abundant chiral sugar molecules. This carbohydrate appendage not only increases the water solubility, but also improves the biological activities. Recently we have reported a novel palladium/Lewis acid catalyzed synthesis of alkylidene cyclopentenones from fulvene derived strained olefins. We synthesized two such molecules and coupled them with various monosaccharides *via* a triazole linker.



---

### Isolation, Characterization and Biological Evaluation of Phytochemicals from *Zingiber zerumbet* (L.) Smith

---

#### 2.1. *Zingiber zerumbet* (L.) Smith: An Overview

Among the genus of plants in Zingiberaceae, *Zingiber* is the genus having about 141 species. This genus is found mainly in Asia and Pacific islands. It gets the name *Zingiber* from Sanskrit, meaning 'Bull's Horn' [Burkill 1966; Yob *et al.* 2011]. An important plant in this genus, which has gained the interest of scientists due to its medicinal value, is *Zingiber zerumbet* (L.) Smith. *Zingiber zerumbet* (in Malayalam, 'Malayinji' or 'Kolinji') is a vigorous ginger with leafy stems growing to about 1.2 m tall. It is a perennial herb with tuberous root that is normally found in the damp, shaded region of low land and hill slopes. In the midst of summer, a separate stalk starts growing out of the ground with green cone shaped bracts, which resembles that of pinecones. Within a couple of weeks, the green cone turns red and then small creamy yellow flowers appear on the cone. So it is known as 'pinecone ginger' in some region. However, it is most widely known as the "shampoo ginger" because of the creamy liquid substance produced in the cones (Figure 2.1) [Holttum 1950; Nalawade *et al.* 2003; Sabu 2003].

As the name suggests, shampoo ginger is used as shampoo and as the ingredient in many shampoos. The leaves have good flavor and is used in cooked food. Its flowers are eaten as a vegetable. The rhizome itself is a ginger and can be used in the same way as any other ginger is used. The cone shaped flowers are used in cut flower arrangements.

The plant *Z. zerumbet* has enormous medicinal uses. It is used as medicine for sprains and indigestion. Traditionally, the rhizome is used for injury, stomachache and toothache. It is used for the treatment of many other diseases like kidney stone, dysentery, seizures in children, diarrhoea, jaundice, sore skin, cold *etc.* [Huang *et al.* 2005; Singh *et al.* 2012].



**Figure 2.1.** *Zingiber zerumbet* Smith

## 2.2. Various names of *Zingiber zerumbet*

*Zingiber zerumbet* is known by various names in different countries [Yob *et al.* 2011]. Few of them are listed in Table 2.2.

**Table 2.2.** Different names of *Zingiber zerumbet*

Name	Country
Lempoyang	Malaysia and Indonesia
Ghatian and Yaiimu	India
Jangli adha	Bangladesh
Awapuhi	Hawaii
Zurunbah	Arab
Hong qiu jiang	China
Haeo dam or Hiao dam	Northern Thailand

### 2.3. Scientific classification

Scientific classification of *Zingiber zerumbet* is given in Table 2.1 [Prakash *et al.* 2011]. *Zingiber zerumbet* belongs to the family Zingiberaceae and this family is commonly known as ginger family.

**Table 2.1. Scientific classification of *Zingiber zerumbet***

Kingdom	Plantae – <i>Plants</i>
Subkingdom	<i>Tracheobionta – Vascular plants</i>
Superdivision	<i>Spermatophyta – Seed plants</i>
Division	<i>Magnoliophyta – Flowering plants</i>
Class	<i>Liliopsida – Monocotyledons</i>
Sub class	Zingiberidae
Order	Zingiberales
Family	Zingiberaceae – <i>Ginger family</i>
Genus	Zingiber Mill – <i>Ginger</i>
Species	<i>Zingiber zerumbet</i> Smith – <i>Bitter ginger</i>

### 2.4. Distribution

*Zingiber zerumbet* is native to Southeast Asia, but has been widely cultivated in tropical and subtropical areas around the world. The main countries in which the plant is distributed are India, Bangladesh, Malaysia, Nepal and Sri Lanka. It is common in moist forests and mangrove margins from sea level to over 500 m [Prakash *et al.* 2012].

## 2.5. Phytochemical investigation of *Zingiber zerumbet*

### 2.5.1. Phytochemistry of leaf and rhizome essential oil

Jaripa Begum and co-workers have reported the results of phytochemical investigation on leaf and rhizome oils of *Zingiber zerumbet*. The leaf and rhizome oils, obtained by hydrodistillation, were analyzed by gas chromatography mass spectrometry (GC-MS). Twenty nine components were identified from the leaf oil. The major components were zerumbone (36.98%),  $\alpha$ -caryophyllene (16.35%) and camphene (9.24%). Thirty components were identified from the rhizome oil with the main components being zerumbone (46.83%),  $\alpha$ -caryophyllene (19.00%) and 1,5,5,8-tetramethyl-12-oxabicyclo[9.1.0]dodeca-3,7-diene (4.28%). The compositions of both oils varied qualitatively and quantitatively [Bhuiyan *et al.* 2009].

Zerumbone and  $\alpha$ -caryophyllene are the main common components in leaves and rhizomes oils. Zerumbone,  $\alpha$ -caryophyllene, caryophyllene, camphor, caryophyllene oxide, limonene,  $\alpha$ -pinene, eucalyptol, camphene, 3-carene, linalool, borneol, 4-terpineol cycloheptane and 4-methylene-1-methyl-2-(2-methyl-1-propen-1-yl)-1-vinyl were observed as the fourteen versatile common compounds present in both the oils with variations in percent content (Table 2.3).

**Table 2.3. Essential oil components of leaf and rhizome**

Sl. No.	Name of constituents from leaf oil	%	Name of constituents from rhizome oil	%
1	Tricyclene	0.56	$\alpha$ -Pinene	1.17
2	$\alpha$ -Pinene	2.23	Camphene	3.56
3	Camphene	9.24	3-Carene	0.82
4	3-Carene	1.02	$\beta$ -Cymene	0.21
5	Eucalyptol	1.69	Limonene	0.88
6	Limonene	1.14	Eucalyptol	1.27
7	Linalool	0.85	Linalool	0.57
8	Camphor	2.75	Camphor	2.80
9	Borneol	0.52	Borneol	0.29
10	Bornel	0.81	4-Terpineol	0.23

11	4-Terpineol	0.54	$\beta$ -Terpinyl acetate	0.30
12	$\alpha$ -Terpineol	0.45	Caryophyllene	3.98
13	Caryophyllene	3.25	$\alpha$ -Caryophyllene	19.00
14	$\alpha$ -Caryophyllene	16.35	2,4-Diisopropenyl-1-methylcyclohexane	0.45
15	Cycloheptane,4-methylene-1-methyl-2-(2-methyl-1-propen-1-yl)-1-vinyl	0.68	Anisole, p-styryl-	0.41
16	1,6,10-Dodecatrien-3-ol, 3,7,11-trimethyl, -[S-(z)]	0.53	trans-Nerolidol	0.45
17	Caryophyllene oxide	2.54	Germacrene D-4-ol	0.20
18	1,2-Dihydropyridine,1-(1-oxobutyl),	5.82	Caryophyllene oxide	3.70
19	3-Cyclohexen-1-carboxaldehyde, 3,4-Dimethyl	3.91	1,5,5,8-Tetramethyl-12-oxabicyclo[9.1.0]dodeca-3,7-diene	4.28
20	Azulene 1,2,3,4,5,6,7,8-octahydro-1,4-dimethyl-7-(1-methylethylidene), -(IS-cis)-	0.48	2-Naphthalenemethanol, 1,2,3,4,4a,5,6,7-octahydro-.alpha.,.alpha.,4a,8-tetramethyl-, (2R-cis)-	0.37
21	2,6-Dimethylbicyclo [3,2,1]octane	0.69	Bicyclo[3.1.0]hexane-6-methanol, 2-hydroxy-1,4,4-trimethyl-	0.88
22	7-Octylidenebicyclo[4.1.0]heptan-	0.69	Kauran-18-al, 17-(acetyloxy)-, (4.beta.)-	2.16
23	1,5-Cycloundecadien,8,8-dimethyl-9-methylene	1.13	1H-Cycloprop[e]azulen-4-ol, decahydro-1,1,4,7-tetramethyl-, [1ar-(1a.alpha.,4.beta.,4a.beta.,7.alpha.,7a.beta.,7b.alpha.)]-	1.89
24	3-Isopropyltricyclo [4.3.1.1] (2,5) undec -3-en-10-ol	0.78	4-Isopropenyl-4,7-dimethyl-1-oxaspiro[2.5]octane	0.21
25	$\beta$ -Eudesmol	0.71	2-Methylenecholestan-3-ol	1.02
26	Agerospirol	0.97	Carveol	0.92

27	3a,9-Dimethyldodecahydrocyclohepta[d] inden-3-one	0.72	Norethynodrel	0.24
28	trans-Longipinene	1.65	zerumbone	46.83
29	Zerumbone	36.98	Bicyclo[5.3.0]decane, 2-methylene-5-(1-methylvinyl)-8-methyl-	0.43
30	--	--	Cycloheptane, 4-methylene-1-methyl-2-(2-methyl-1-propen-1-yl)-1-vinyl-	0.46

### 2.5.2. Phytochemicals from the rhizomes of *Zingiber zerumbet*

In 1960, Dev *et al.* isolated zerumbone, a cyclic sesquiterpene for the first time from the rhizomes of *Zingiber zerumbet*. The compound was structurally elucidated in 1965 and later characterized by NMR and X-ray analysis [Dev 1960; Dev 1965]. In 1962, Bhattacharya and co-workers successfully isolated and characterized two terpenoids namely humulene monoxide and humulene dioxide from the rhizome [Ramaswami and Bhattacharya 1962].

Later in 1991, Nakatani *et al.* reported the occurrence of flavonoid glycosides from the chloroform soluble part of rhizomes of *Z. zerumbet*. Structures of the isolated compounds were determined to be kaempferol-3,4'-*O*-dimethylether, kaempferol-3-*O*-methylether, kaempferol-3-*O*-(3,4-*O*-diacetyl- $\alpha$ -L-rhamnopyranoside) and kaempferol-3-*O*-(2,4-*O*-diacetyl- $\alpha$ -L-rhamnopyranoside). Zerumbone-6,7-epoxide and curcumin were also reported from the same extract [Nakatani *et al.* 1991].

Masuda *et al.* identified three new acetylated kaempferol glycosides from the acetone extract of dried rhizome and their structures determined to be the 3-*O*-(2-*O*-acetyl- $\alpha$ -L-rhamnopyranoside), 3-*O*-(3-*O*-acetyl- $\alpha$ -L-rhamnopyranoside) and 3-*O*-(4-*O*-acetyl- $\alpha$ -L-rhamnopyranoside) [Masuda *et al.* 1991]. 5-Hydroxyzerumbone, 6-methoxy-2*E*,9*E*-humaladiene-8-one, zederone, 4-hydroxy benzaldehyde and vanillin were also isolated from the rhizome extract of *Z. zerumbet* [Kader *et al.* 2009]. The Compounds isolated from the rhizomes of *Z. zerumbet* are shown in figure 2.2.

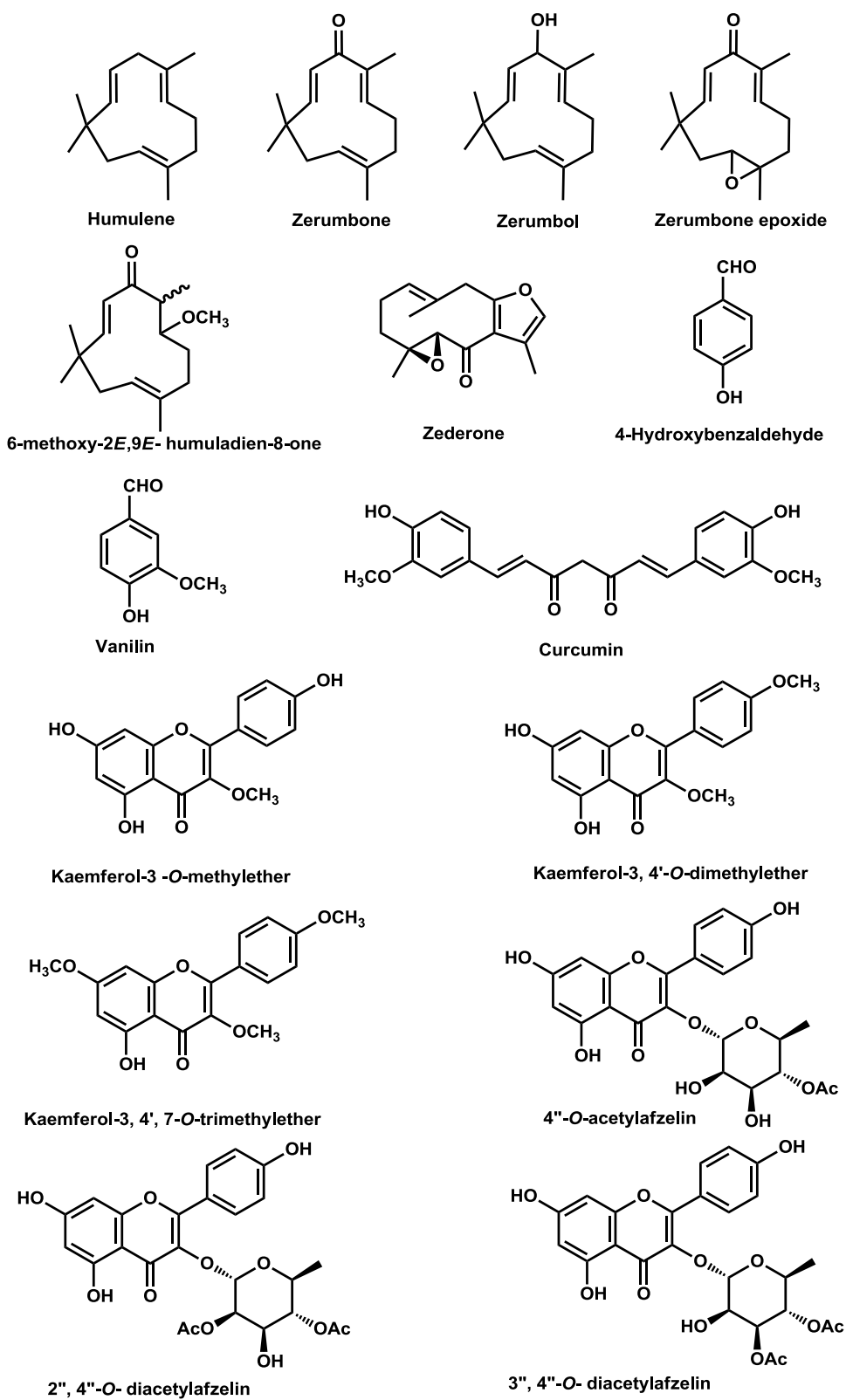


**Figure 2.2.** Selected compounds from *Z. zerumbet*

## 2.6. Multipotential bioactivities of *Zingiber zerumbet*

### 2.6.1. Biological properties of extracts of *Z. zerumbet*

Various compounds have been isolated from *Z. zerumbet* and they serve as very potent and reliable drug candidates for various diseases. They have been investigated for their prospects of effectiveness against a number of diseases using various *in vitro* as well as *in vivo* methods. Many researchers have reported the different potential bioactivities of various extracts of *Z. zerumbet* [Singh *et al.* 2012]. They are listed in table 2.4.

**Table 2.4. Biological properties various extracts of rhizomes of *Z. zerumbet***

Extract	Bioactivity
Pentane	Dementia
Hexane	Inhibit the proliferation of human colonic adenocarcinoma cell lines in a dose dependent manner, while the growth of normal human dormal and colon fibroblast was less affected
Methanol	Anti-inflammatory property Antiflatulant property Chemopreventive, free radical scavenging activities and activating properties Potential drug for the treatment of several cancers as well as Leukemia Anti-tumour activity Anti-tumour promoting effect Prevent colon and skin cancer Redox regulated mechanism may account for zerumbone's ability to suppress cancer cell proliferation Antinociceptic activity Against normal mouse fibroblast Suppress free radicals (superoxide anion) generation from NADPH oxidase xanthine



	oxidase
	Curative effect of zerumbone in a dose dependent manner on the osteoarthritic knee joints, and reported that oral administration
	Chemopreventive activity
	Hepatoprotective activity
	Immune-modulatory activity
	Anti-edema activity when assessed using the carrageenan induced paw edema test and the cotton-pellet induced granuloma test
	Antipancreatic activity
	The various beneficial effects of b-eudesmol isolated
	Treating epileptic seizures
	Angiogenic diseases
Ethanol	The effective activity of <i>Zingiber zerumbet</i> against <i>Staphylococcus aureus</i>
	HIV inhibitory and other cytotoxic activities
Aqueous	Elicitate moderate to marked antipyretic activities which was dose dependent
	Anti-tumour/anti-apoptotic activity
	Development of anti-AD (Alzheimer's disease) treatment

Thus from the above table, it is clear that *Z. zerumbet* is a medicinal plant with diverse activities against various life threatening diseases. These scientific reports support the use of *Z. zerumbet* in traditional medicines at various countries.

### 2.6.2. Biological properties of compounds from *Z. zerumbet*

From the literature survey it is evident that most of the properties of *Z. zerumbet* are due to the presence of an eleven membered sesquiterpene zerumbone. It has been investigated for its prospects of effectiveness against number of activities in *in vitro* as well as *in vivo* conditions. The  $\alpha$ ,  $\beta$ -unsaturated carbonyl group of zerumbone is the

---

moiety responsible for its biological activities [Kitayama *et al.* 1999; Kitayama *et al.* 2001].

The anti-tumour initiating and promoting activities of zerumbone in mouse skin were evaluated using a conventional 2-stage carcinogenesis model. The results indicate that zerumbone is a promising agent for the prevention of both tumour initiating and promoting processes, through induction of anti-oxidative and phase II drug metabolizing enzymes as well as attenuation of proinflammatory signaling pathways [Murakami *et al.* 2004].

Zerumbone suppressed NF- $\kappa$ B activation induced by tumour necrosis factor (TNF), okadaic acid, cigarette smoke condensate, phorbol myristate acetate, and H<sub>2</sub>O<sub>2</sub> and that the suppression was not cell type specific. Interestingly,  $\alpha$ -humulene, a structural analogue of zerumbone lacking the carbonyl group, was completely inactive. Overall, results indicate that zerumbone inhibits the activation of NF- $\kappa$ B and NF- $\kappa$ B-regulated gene expression induced by carcinogens and that this inhibition may provide a molecular basis for the prevention and treatment of cancer by zerumbone [Takada *et al.* 2005].

Kim *et al.* reported that the dietary administration of zerumbone effectively suppresses mouse colon and lung carcinogenesis through multiple modulatory mechanisms of growth, apoptosis, inflammation and expression of NF- $\kappa$ B and HO-1 that are involved in carcinogenesis in the colon and lung [Kim *et al.* 2007]. Zerumbone is investigated for its activity and mechanism in human liver cancer cell lines by Sakinah *et al.* in 2007. They found that zerumbone induces the apoptotic process in HepG2 cells through the up and down regulation of Bax/Bcl-2 protein independently of functional p53 activity [Sakainah *et al.* 2007].

Xian *et al.* demonstrated that zerumbone significantly suppressed the proliferation of promyelocytic leukemia NB4 cells among several leukemia cell lines, but not human umbilical vein endothelial cells (HUVECs), by inducing G2/M cell cycle arrest followed by apoptosis with 10  $\mu$ M of IC<sub>50</sub> [Xian *et al.* 2007].

The anti-inflammatory activity of zerumbone was investigated using carrageenan-induced paw edema and cotton pellet-induced granuloma tissue formation test in mice. It was demonstrated that intraperitoneal administration of zerumbone at a dose of 5, 10, 50 and 100 mg/kg produced significant dose-dependent inhibition of paw edema induced by

carrageenan. They also demonstrated that zerumbone at similar doses significantly suppressed granulomatous tissue formation in cotton pellet-induced granuloma test [Sulaiman *et al.* 2010].

Zerumbone produces pronounced antinociception against chemical models of nociception in mice. The results suggest that the L-arginine-nitric oxide-cGMP-PKC-K<sup>+</sup> ATP channel pathways, the TRPV1 and kinin B2 receptors play an important role in the zerumbone-induced antinociception [Perimal *et al.* 2010].

Keong *et al.* in 2010 reported the immunomodulatory effects of zerumbone towards the lymphocytes proliferation (mice thymocytes, micesplenocytes and human peripheral blood mononuclear cells, PBMC), cell cycle progression and cytokine (intraleukin 2 and 12) induction [Keong *et al.* 2010]. The hepatoprotective activity of zerumbone may be through the enhancement of drug-metabolising enzyme activity [Nakamura *et al.* 2004]. It is postulated that in the hepatocytes, the antioxidant effect of zerumbone is through the neutralisation of lipid peroxidation.

## 2.7. Objective of the present work

Interests for biologically active compounds derived from plants are increasing day by day because of its valuable uses in medicinal field. *Zingiber zerumbet* or shampoo ginger, a member of Zingiberaceae family is well known for its medicinal as well as cosmetic applications. In traditional medicine, rhizomes of *Z. zerumbet* are employed against cough, stomachache, asthma and used as a vermifuge. It has been reported that the methanol extract of rhizomes show various pharmacological properties such as anti-inflammatory, anti-tumour, anti-flatulant, anti-cancer, anti-nociceptic, anti-atherosclerotic, anti-pancreatic, anti-AD (Alzheimer's disease), anti-HIV activities *etc.* Moreover, this plant is reported to have high content of biologically active compound, zerumbone, an eleven membered sesquiterpene. Intrigued by these facts about the plant *Z. zerumbet*, we decided to invest our time on isolation, characterization and biological evaluation of phytochemicals from its rhizomes for further synthetic manipulations and evaluations.

## 2.8. Results and discussion

Fresh rhizomes of *Z. zerumbet* were collected from Thiruvananthapuram, India and was deposited at Herbarium of JNTBGRI with voucher specimen no. TBGRI 60680. The rhizomes were then dried, ground into powder (1 kg) and extracted using acetone at room temperature. Removal of solvent under reduced pressure gave 150 g of crude extract. This crude extract was washed with hexane to separate the low polar components. The hexane fraction (90 g) on column chromatography gave compounds **1-4** and acetone fraction gave compounds **5-7**. Compound **7** on alkaline hydrolysis gave natural product **8**.

### 2.8.1. Identification of compounds 1-7

#### 2.8.1.1. Identification of compound 1

Hexane fraction was subjected to column chromatography on silica gel (100-200 mesh) using hexane as eluent, which afforded compound **1** as a colourless viscous liquid (340 mg). This compound was UV active and gave a blue charring in Enholm yellow solution. The structure of compound **1** was established by various spectroscopic analysis and confirmed as  **$\alpha$ -humulene** (Figure 2.3).

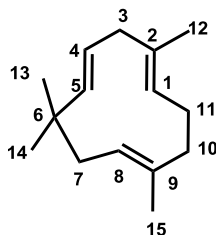


**Figure 2.3.**  $\alpha$ -humulene **1**

IR spectrum of the compound showed a signal at  $1662\text{ cm}^{-1}$  corresponding to the C=C bond stretching. In the  $^1\text{H}$  NMR spectrum, the signal due to the C4 proton was discernible as a multiplet at  $\delta$  5.59-5.54 (Figure 2.4). The doublet at  $\delta$  5.13 was due the olefinic proton at C5. The proton at C1 showed a triplet at  $\delta$  4.93. Another triplet at  $\delta$  4.85 was responsible for olefinic proton at C8. Protons on four methyl groups were visible at  $\delta$  1.63, 1.42 and 1.06 as singlets. In  $^{13}\text{C}$  NMR spectrum, the olefinic carbons C5, C2, C9, C4, C1 and C8 resonated at  $\delta$  140.9, 139.0, 132.9, 127.7, 125.9 and 124.9 respectively (Figure 2.5). All the spectral data were also in good agreement with the literature report [Neuenschwander *et al.* 2012]. The mass spectrum showed a molecular ion peak at  $m/z$  204.1876  $[\text{M}]^+$  (Figure 2.6).

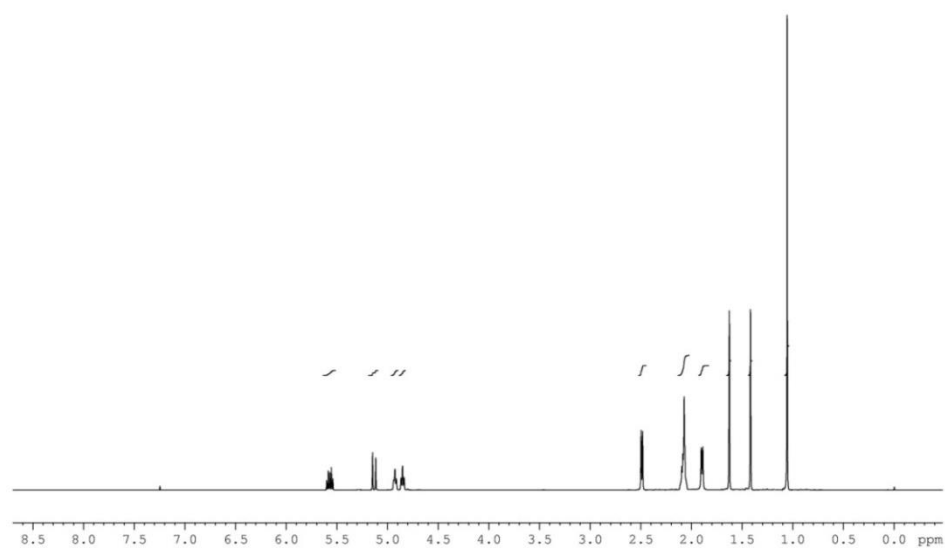


**Figure 2.4.**  $^1\text{H}$  NMR of compound 1 ( $\alpha$ -humulene)

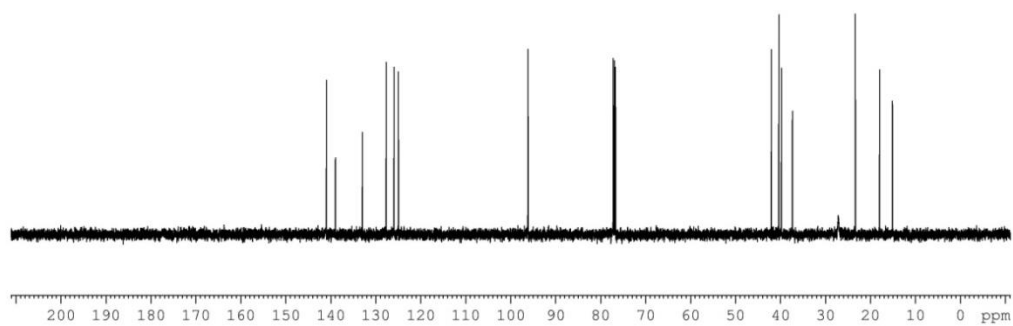


**Figure 2.5.**  $^{13}\text{C}$  NMR of compound 1 ( $\alpha$ -humulene)

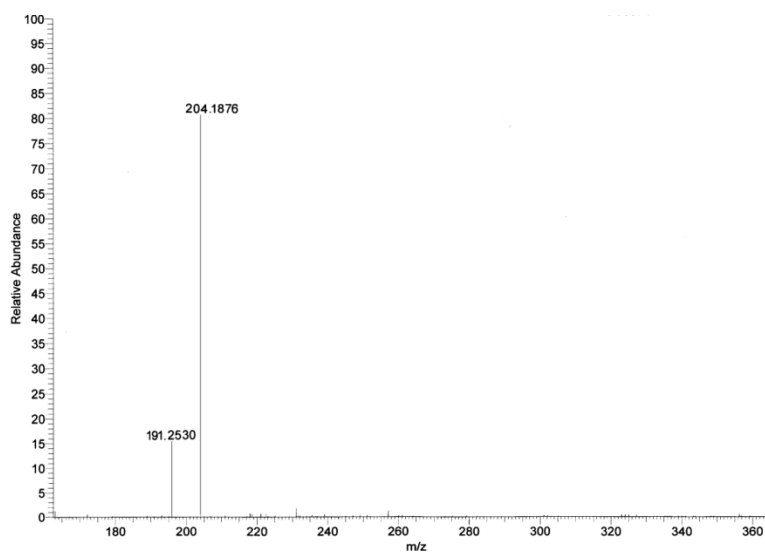


**Figure 2.6.** Mass spectrum of compound 1 ( $\alpha$ -humulene)

### 2.8.1.2. Identification of compound 2

The hexane extract on column chromatography using 3% EtOAc:hexane as eluent afforded compound **2** as a white solid (26 g), which was then recrystallised in pure form using distilled hexane (25.1 g, 50% yield). Using various spectroscopic analysis, compound **2** was identified as **zerumbone** (Figure 2.7).

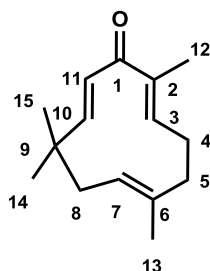


**Figure 2.7.** Zerumbone **2**

The IR spectrum showed a strong absorption at  $1656\text{ cm}^{-1}$ , indicating the presence of a dienone moiety. The  $^1\text{H}$  NMR spectrum showed the presence of three olefinic protons between  $\delta$  6.02-5.81 as a multiplet and another as a broad doublet centered at  $\delta$  5.24 (Figure 2.8). Four singlets at  $\delta$  1.76, 1.51, 1.18 and 1.05, each accounting for three protons could be readily identified as four methyl groups. The  $^{13}\text{C}$  spectrum showed fifteen signals (Figure 2.9). The key feature of the spectrum was the signal at  $\delta$  204.2 indicating the carbonyl group. All other signals in the  $^1\text{H}$  and  $^{13}\text{C}$  NMR spectra were in agreement with the literature reports [Nakatani *et al.* 1991]. The mass spectrum showed a molecular ion peak at  $m/z$  241.1565  $[\text{M}+\text{Na}]^+$  (Figure 2.10).

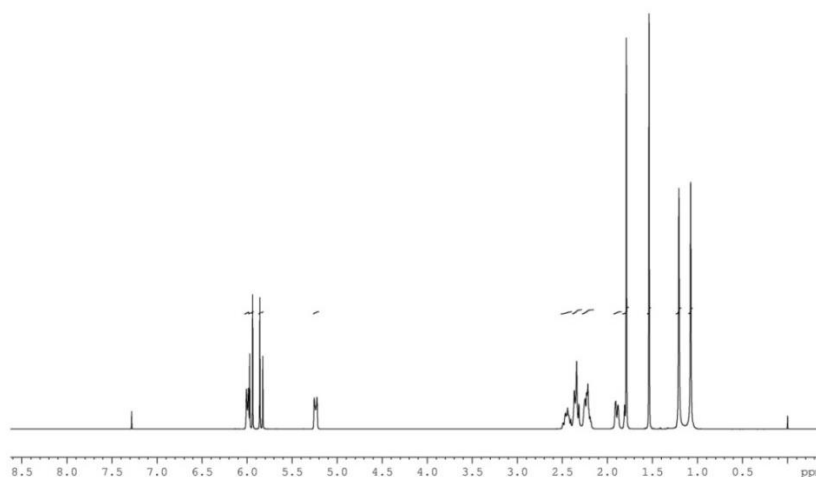


**Figure 2.8.**  $^1\text{H}$  NMR of compound **2** (zerumbone)

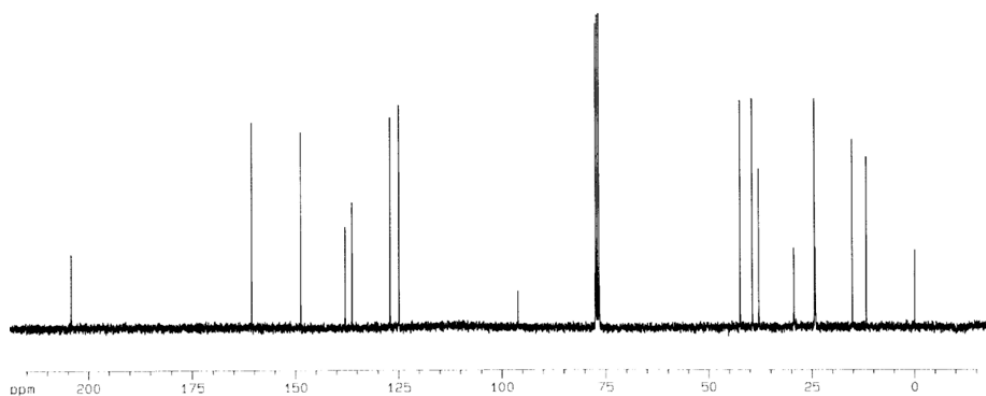


**Figure 2.9.**  $^{13}\text{C}$  NMR of compound **2** (zerumbone)

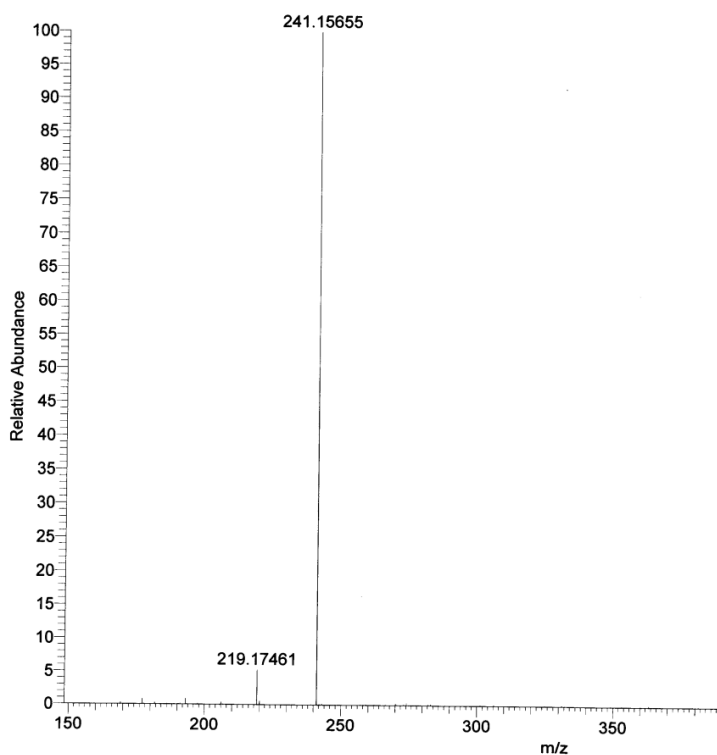


**Figure 2.10.** Mass spectrum of compound **2** (zerumbone)

### 2.8.1.3. Identification of compound **3**

The hexane extract on elution using 5% EtOAc:hexane solvent mixture gave compound **3** as a colourless viscous liquid (220 mg). The compound was thoroughly studied by IR, NMR and mass spectroscopic analysis and finally confirmed as zerumbol (Figure 2.11).

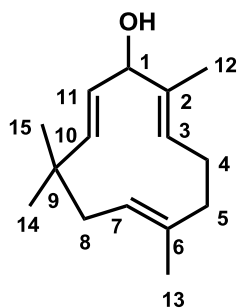


**Figure 2.11.** Zerumbol 3

IR spectrum of the compound showed a broad signal at  $3292\text{ cm}^{-1}$ , characteristic of hydroxyl functionality. The  $^1\text{H}$  NMR spectrum displayed a doublet of doublet centered at  $\delta$  5.56 responsible for the olefinic proton at C11 (Figure 2.12). The proton on carbon (C1) having a hydroxyl group resonated at  $\delta$  4.63 as a doublet.  $^{13}\text{C}$  NMR spectrum displayed a peak at  $\delta$  78.7 corresponding to carbon (C1) containing hydroxyl group (Figure 2.13). All other values were in good agreement with the previous reports. The mass spectrum showed a molecular ion peak at  $m/z$  219.1753  $[\text{M}-\text{H}]^+$  (Figure 2.14).

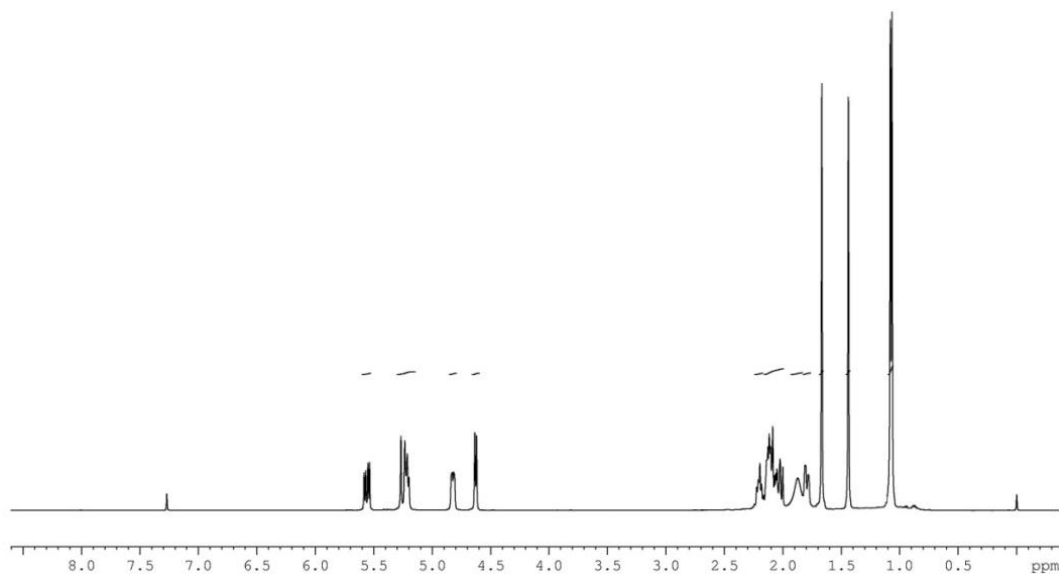


**Figure 2.12.**  $^1\text{H}$  NMR of compound 3 (zerumbol)



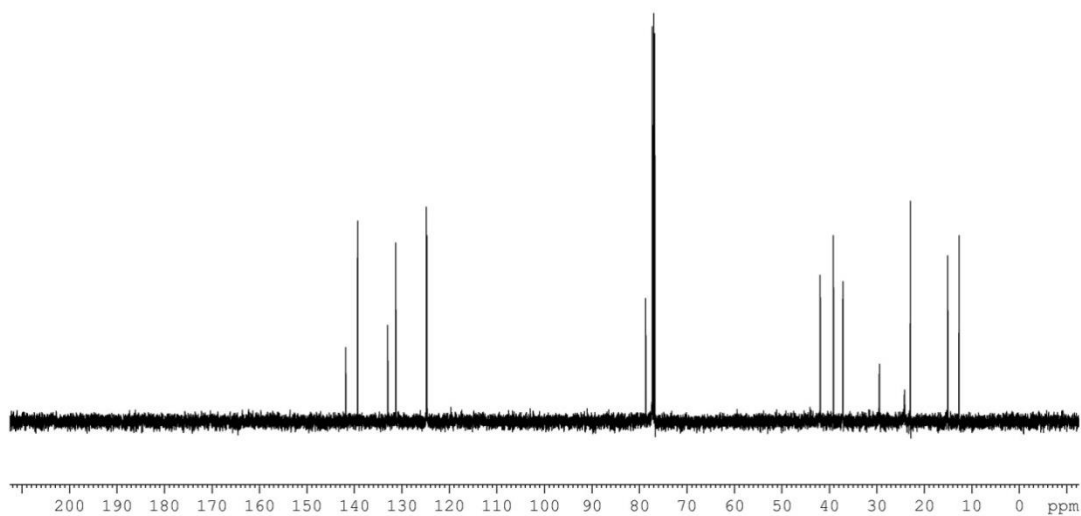


Figure 2.13.  $^{13}\text{C}$  NMR of compound 3 (zerumbol)

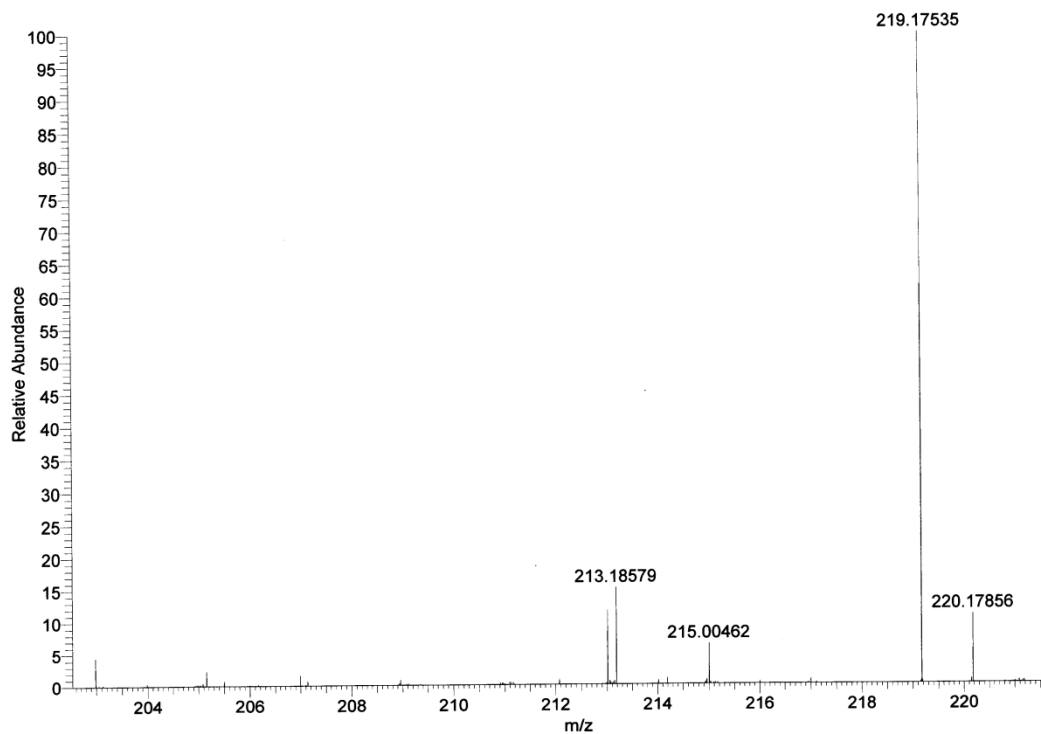
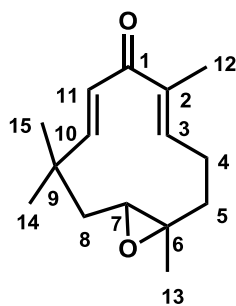


Figure 2.14. Mass spectrum of compound 3 (zerumbol)

#### 2.8.1.4. Identification of compound 4

The hexane extract on column chromatography using 7% EtOAc: hexane as eluent afforded the compound 4 as a white solid (400 mg), which was then recrystallised in pure form using distilled hexane (350 mg). Using various spectroscopic analysis the compound 4 was identified as **zerumbone epoxide** (Figure 2.15).



**Figure 2.15.** Zerumbone epoxide **4**

IR spectrum showed a peak at  $1646\text{ cm}^{-1}$  corresponding to the carbonyl group. The  $^1\text{H}$  NMR spectrum displayed a multiplet in the region  $\delta$  6.15-6.08 responsible for three olefinic protons at C3, C10 and C11 (Figure 2.16). The proton on C7 resonated at  $\delta$  2.75 as a doublet. In  $^{13}\text{C}$  NMR spectrum, the carbonyl carbon (C1) resonated at  $\delta$  202.9 (Figure 2.17). Two carbons (C7 and C6) of epoxide ring displayed the peaks at  $\delta$  62.8 and 61.4. All other signals in the  $^1\text{H}$  and  $^{13}\text{C}$  NMR spectra were in agreement with the literature report [Nakatani *et al.* 1991]. The mass spectrum showed a peak at  $m/z$  257.1513  $[\text{M}+\text{Na}]^+$  (Figure 2.18).

Finally, the structure and stereochemistry of compound **3** was unambiguously confirmed by single crystal X-ray analysis (Figure 2.19).

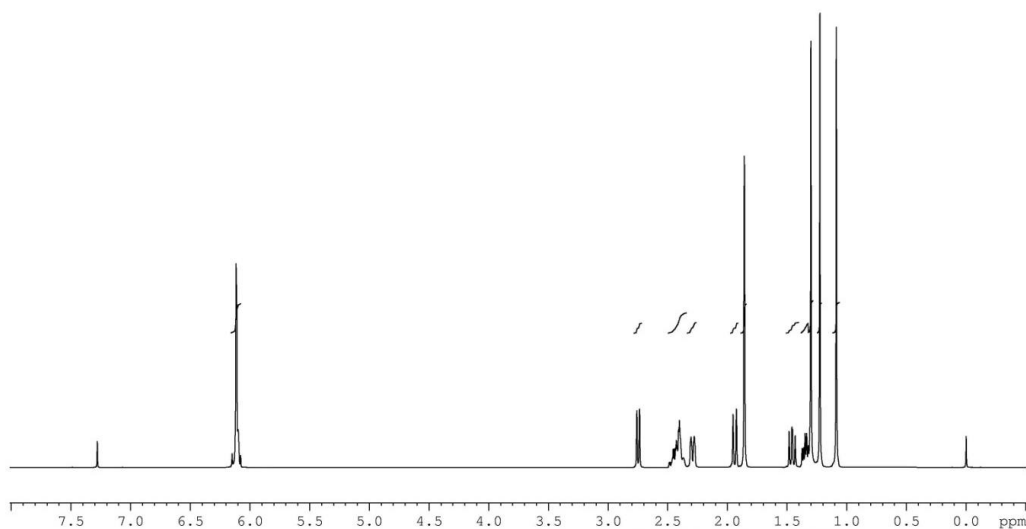


**Figure 2.16.**  $^1\text{H}$  NMR of compound **4** (zerumbone epoxide)

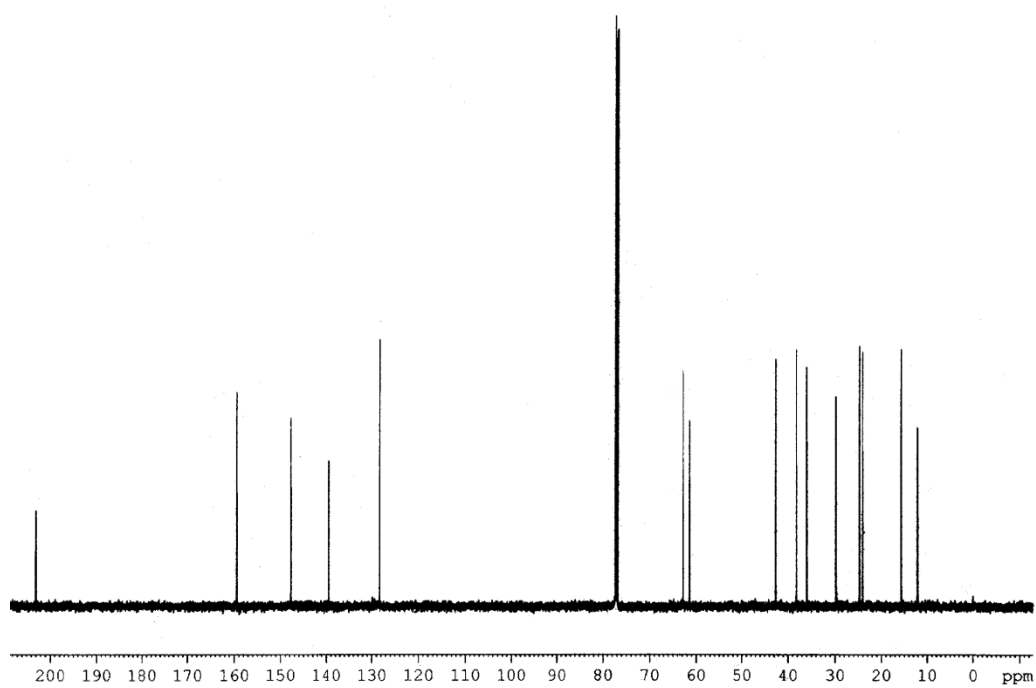


Figure 2.17.  $^{13}\text{C}$  NMR of compound 4 (zerumbone epoxide)

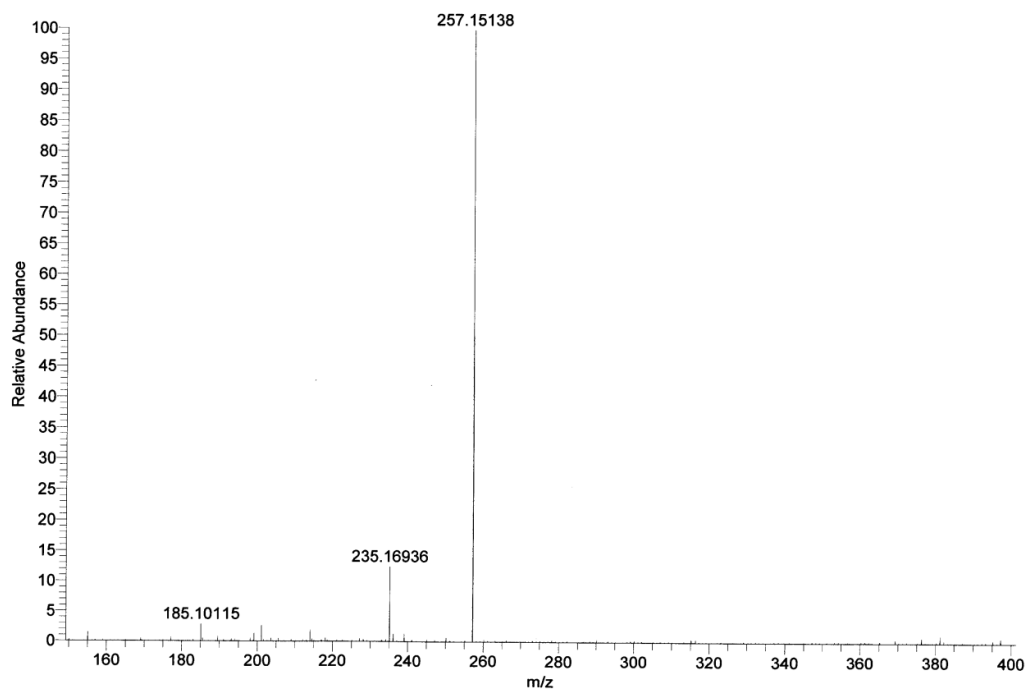
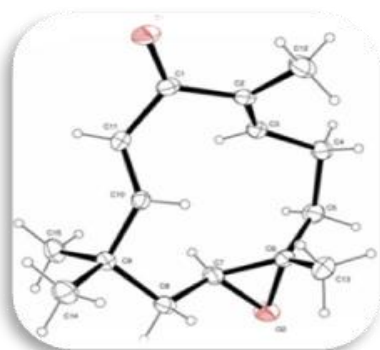


Figure 2.18. Mass spectrum of compound 4 (zerumbone epoxide)



**Figure 2.19.** Single crystal X-ray structure of zerumbone epoxide

### 2.8.1.5. Identification of compound 5

Acetone extract on elution using 30% EtOAc:hexane mixture afforded compound **5** as a yellow solid. Using various spectroscopic techniques and literature reports compound **5** was identified as a flavonol named **kaempferol** (Figure 20).

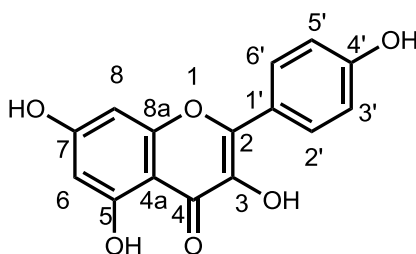


**Figure 2.20.** Kaempferol 5

IR spectrum of the compound presented a broad and a sharp peak at 3326 and 1668  $\text{cm}^{-1}$  corresponding to the hydroxyl and carbonyl groups respectively. The  $^1\text{H}$  NMR spectrum showed two peaks at  $\delta$  12.19 and 9.29 responsible for the protons of hydroxyl groups (Figure 2.21). Two similar aromatic protons at C2' and C6' resonated at  $\delta$  8.16 as a doublet with a coupling constant of 9.0 Hz. Another doublet seen at  $\delta$  7.02 was responsible for the protons at C3' and C5'. The aromatic proton at C8 position presented a doublet at  $\delta$  6.54. The doublet visible at  $\delta$  6.28 was assigned as the proton of C6.

$^{13}\text{C}$  NMR spectrum of kaempferol displayed a peak at  $\delta$  176.6 corresponding to the carbonyl carbon of the enone moiety (Figure 2.22). The  $\alpha$  and  $\beta$  carbon of the same enone moiety resonated at  $\delta$  147.1 (C2) and 136.7 (C3). All other signals in the  $^1\text{H}$  and  $^{13}\text{C}$  NMR spectra were in agreement with the literature report. The mass spectrum showed a peak at  $m/z$  309.0371  $[\text{M}+\text{Na}]^+$  (Figure 2.23).

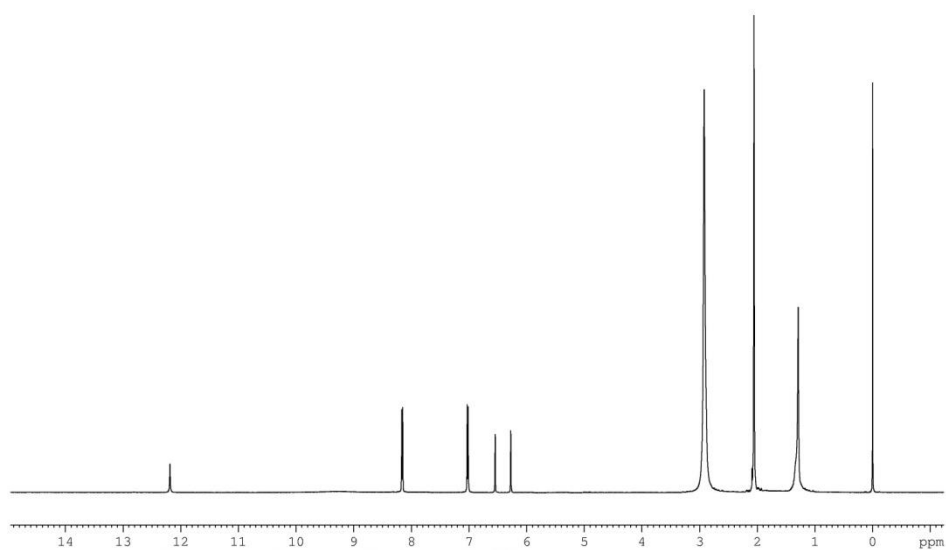


**Figure 2.21.**  $^1\text{H}$  NMR of compound **5** (kaempferol)

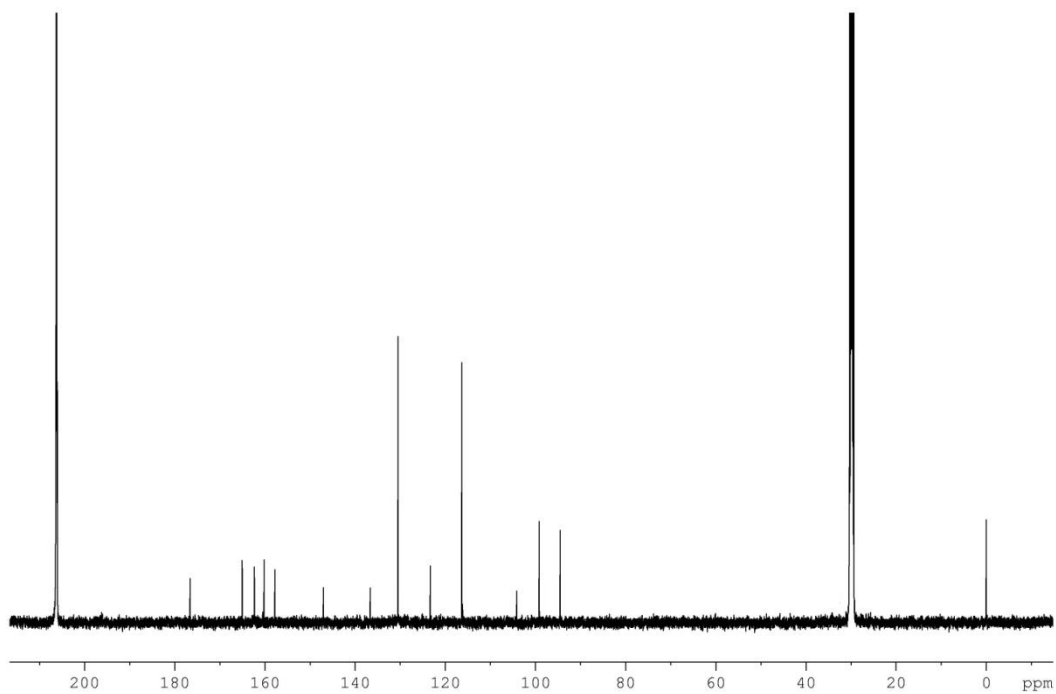


**Figure 2.22.**  $^{13}\text{C}$  NMR of compound **5** (kaempferol)

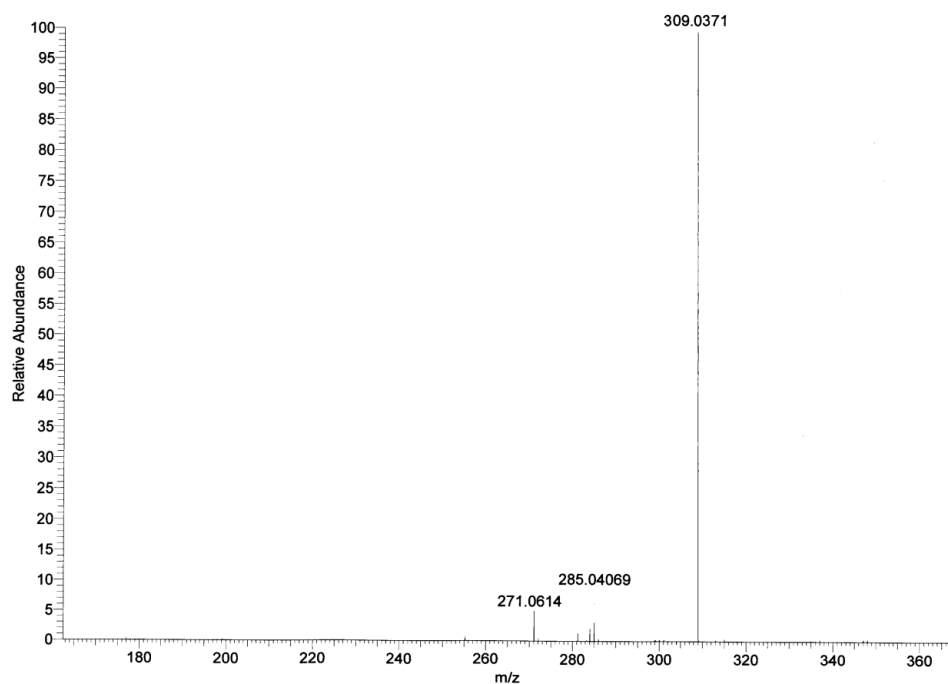


**Figure 2.23.** Mass spectrum of compound **5** (kaempferol)

#### 2.8.1.6. Identification of compound **6**

Compound **6** was identified as **kaempferol-3-O-methylether** or isokaempferide using various spectroscopic techniques and literature reports (Figure 2.24). It is a yellow solid with melting point 250 °C.

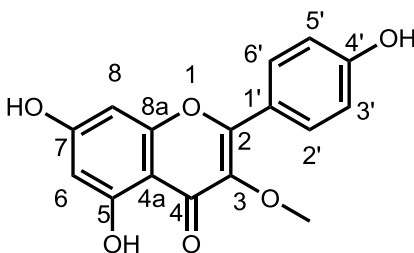


**Figure 2.24.** Kaempferol-3-O-methylether **6**

IR spectrum of the compound showed a broad peak at 3325  $\text{cm}^{-1}$  which is responsible for the hydroxyl group. The signal at 1654  $\text{cm}^{-1}$  was due to the presence of carbonyl group of the  $\alpha,\beta$ -unsaturated ketone system. The protons of the hydroxyl groups resonated at  $\delta$  12.81 and 9.40 as sharp and broad singlet respectively (Figure 2.25). The four aromatic protons on C2'/C6' and C3'/C5' were observed as doublets at  $\delta$  8.04 and 7.02 respectively. The two protons of aromatic ring A displayed two distinct doublets at  $\delta$

6.50 (H at C8) and 6.26 (H at C6). The characteristic methoxy protons appeared as a singlet at  $\delta$  3.87.

In  $^{13}\text{C}$  NMR the carbonyl carbon of the enone moiety was visible at  $\delta$  178.7 (Figure 2.26). All other signals of  $^1\text{H}$  and  $^{13}\text{C}$  NMR spectra were in agreement with the literature report [Nakatani *et al.* 1991]. The mass spectrum showed a peak at  $m/z$  323.0537  $[\text{M}+\text{Na}]^+$  (Figure 2.27).

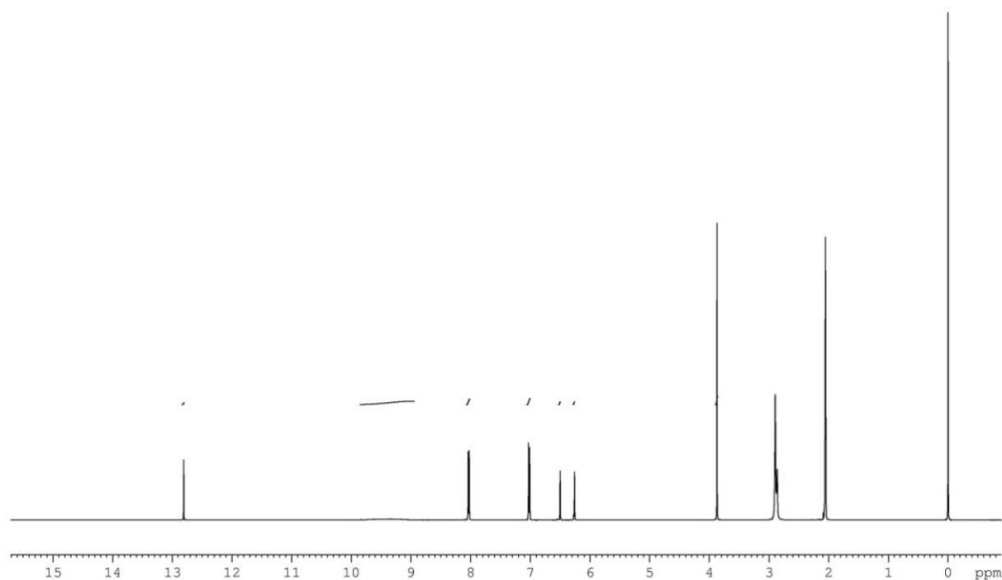


**Figure 2.25.**  $^1\text{H}$  NMR of compound **6** (kaempferol-3-*O*-methylether)

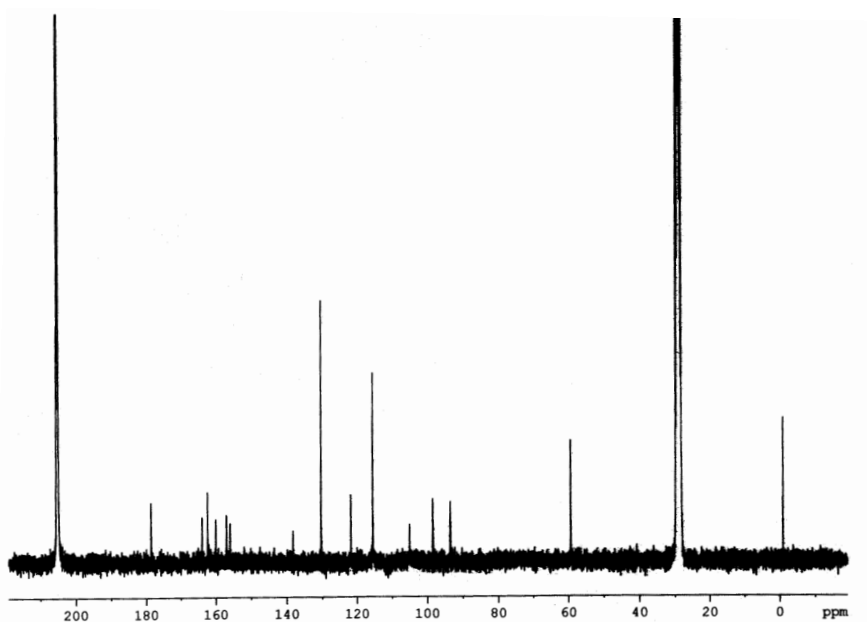


**Figure 2.26.**  $^{13}\text{C}$  NMR of compound **6** (kaempferol-3-*O*-methylether)

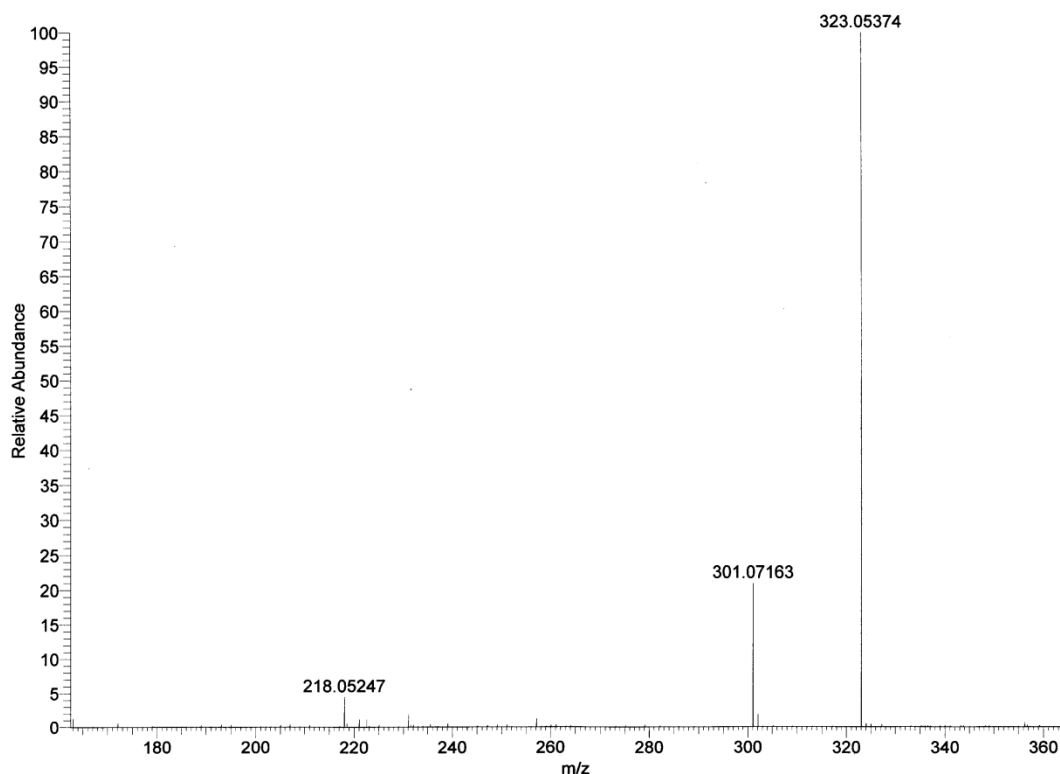


**Figure 2.27.** Mass spectrum of compound **6** (kaempferol-3-*O*-methylether)

### 2.8.1.7. Identification of compound **7**

Elution using 80% EtOAc:hexane mixture afforded compound **7** as a pale yellow solid. Using various spectroscopic techniques and literature reports, compound **7** was identified as a flavonol glycoside named kaempferol-3-*O*-(3,4-diacetyl- $\alpha$ -L-rhamnopyranoside) or 3'',4''-*O*-diacetyl afzelin (Figure 2.28).

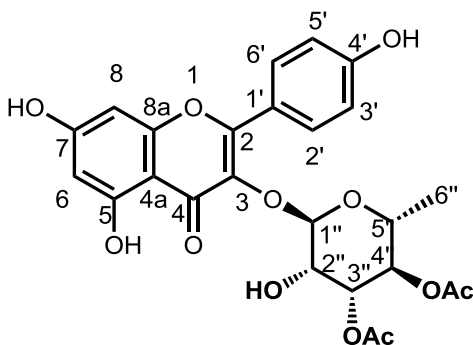


**Figure 2.28.** 3'',4''-*O*-Diacetyl afzelin **7**

The protons of three phenolic hydroxyl groups were visible at  $\delta$  12.58, 11.02 and 10.34 as singlets. The aromatic protons on the ring B presented two doublets centered at  $\delta$  7.80 (C2' and C6') and 6.99 (C3' and C5') (Figure 2.29). The protons on the carbons C8



and C6 appeared as singlets at  $\delta$  6.48 and 6.28. The anomeric proton of the rhamnopyranoside ring was observed as a doublet at  $\delta$  5.76. The proton at C3'' presented a doublet of doublet at  $\delta$  5.03 while the proton at C4'' gave a triplet centered at  $\delta$  4.96. The broad singlet at  $\delta$  4.28 was due to the proton at C2''. The proton on the carbon C5'' presented a multiplet at  $\delta$  3.49-3.42. The protons of two acetyl moieties showed singlets at  $\delta$  2.08 and 2.03. The methyl protons of rhamnopyranoside ring were observed as a doublet at  $\delta$  0.80.

$^{13}\text{C}$  NMR analysis also supported the proposed structure. The characteristic carbonyl carbon of enone moiety appeared in the spectrum at  $\delta$  177.4, where as the carbonyl carbons of acetyl moieties were observed at  $\delta$  169.9 and 169.6 (Figure 2.30). The anomeric carbon presented a peak at  $\delta$  100.9. The peaks at  $\delta$  20.8 and 20.7 were assigned to two methyl carbons of acetyl groups. The methyl group of rhamnopyranoside ring appeared at  $\delta$  16.9. The structure assigned was further confirmed by HOMO and HETERO COSY 2D NMR studies. The HOMO COSY spectrum of the compound showed good correlations between the adjacent protons. All other signals of  $^1\text{H}$  NMR and  $^{13}\text{C}$  NMR spectra were in agreement with the literature report [Nakatani *et al.* 1991]. The mass spectrum showed a peak at  $m/z$  515.1190  $[\text{M}-\text{H}]^+$  (Figure 2.31).

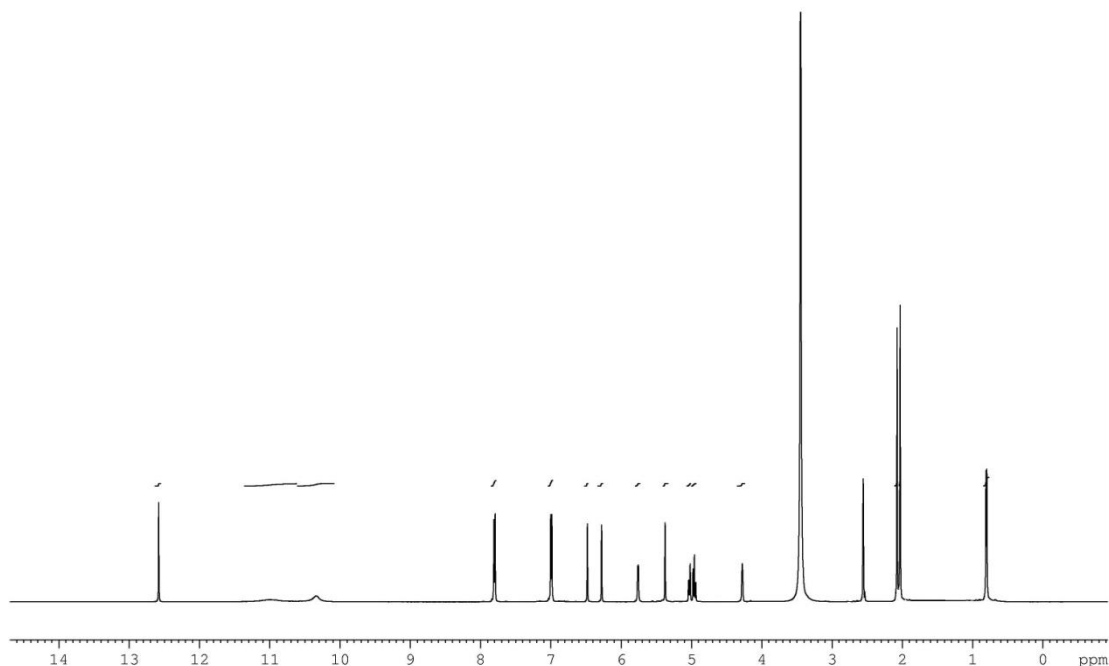


**Figure 2.29.**  $^1\text{H}$  NMR of compound 7 (3'',4''-O-diacetylfazelin)

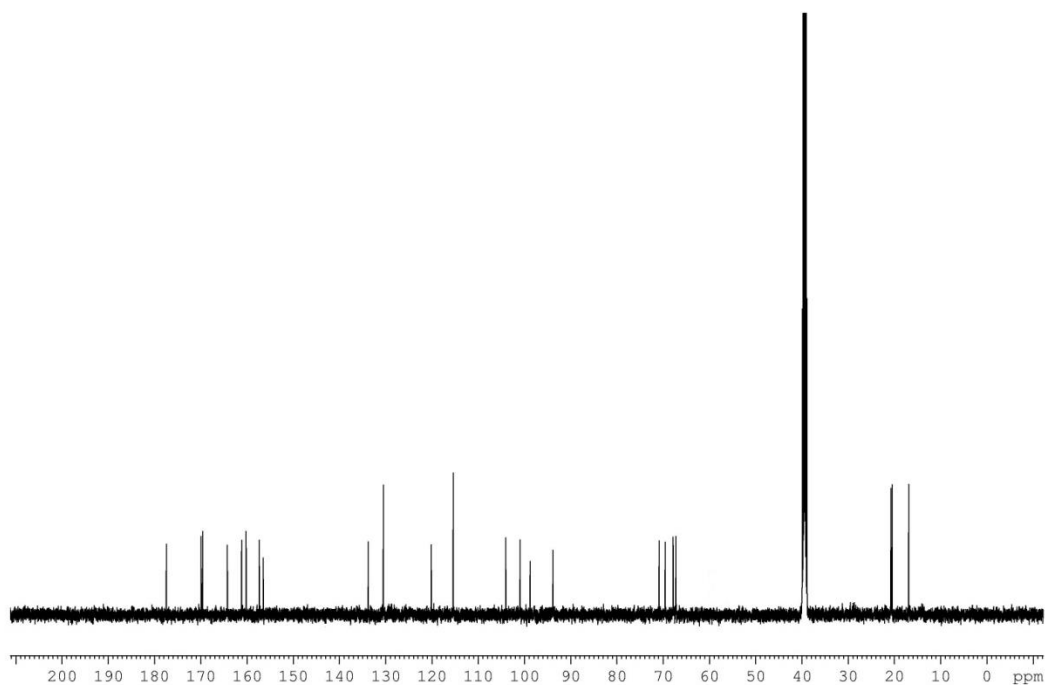


**Figure 2.30.**  $^{13}\text{C}$  NMR of compound **7** (3'',4''-*O*-diacetylfzelin)

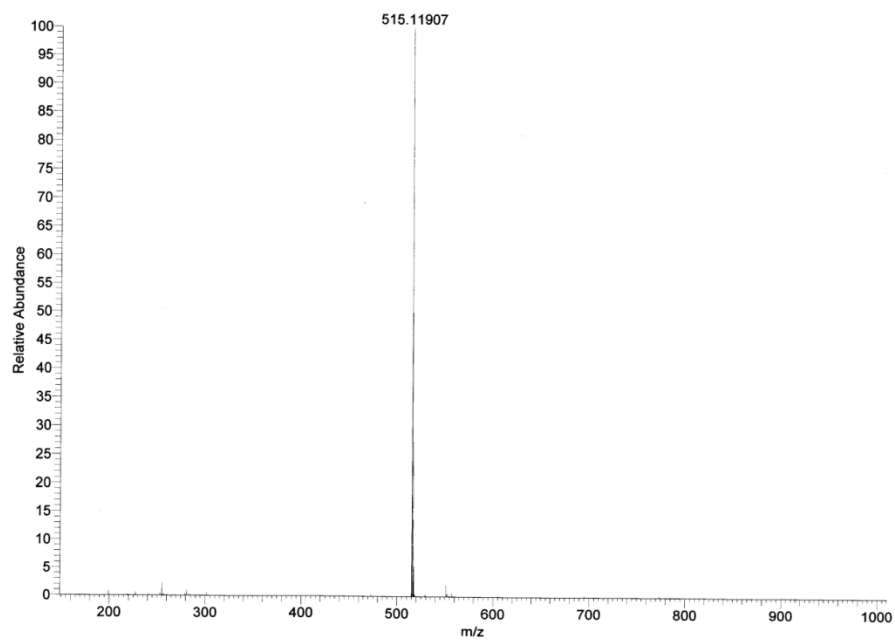


**Figure 2.31.** Mass spectrum of compound **7** (3'',4''-*O*-diacetylfzelin)

### 2.8.2. Synthesis and characterization of compound 8 (Afzelin)

Sodium hydroxide (40 mg, 0.716 mmol) was dissolved in methanol (5 mL) at 0-5 °C. Compound 7 (100 mg, 0.179 mmol) was added and stirred at room temperature for 1 hour. After the completion of the reaction (as indicated by TLC analysis), the reaction mixture was poured into 1N HCl solution (10 mL). It was then extracted with ethyl acetate (3 x 50 mL) and the solvent was evaporated off. The residue on column chromatography using methanol: chloroform mixture afforded the product as a pale yellow amorphous solid in 90% yield (Figure 2.32).

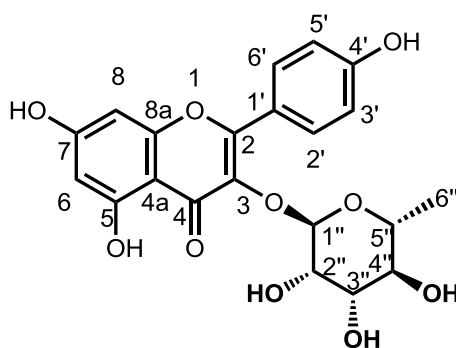


**Figure 2.32.** Afzelin 8

IR spectrum of the compound showed a broad peak at  $3365\text{ cm}^{-1}$  corresponding to the hydroxyl groups. Carbonyl group of enone moiety appeared at  $1655\text{ cm}^{-1}$ .

Three protons of phenolic hydroxyl groups appear at  $\delta$  12.7, 9.94 and 9.29 as singlets (Figure 2.33). The protons on the carbons C3'/C5' and C2'/C6' presented two separate doublets centered at  $\delta$  7.86 and 7.02. A doublet was visible for the proton on the carbon C8 at  $\delta$  6.47 and a singlet for proton on the carbon C6 at  $\delta$  6.27. The anomeric proton appeared as a singlet at  $\delta$  5.54. A broad singlet at  $\delta$  4.24 was counted as a proton on the C2'' carbon. The multiplet at  $\delta$  3.72-3.68, integrating for one proton represented the proton on C3'' carbon. The two protons at the carbons C4'' & C5'' together presented a multiplet at  $\delta$  3.38-3.29. A doublet at  $\delta$  0.90 was credited to the methyl protons on C6'' carbon.

In  $^{13}\text{C}$  NMR, the peak at  $\delta$  179.3 was assigned to the carbonyl carbon of the enone moiety (Figure 2.34). All other signals of  $^{13}\text{C}$  NMR spectra were in agreement with the proposed structure [Nakatani *et al.* 1991]. The mass spectrum showed a peak at  $m/z$  455.0970  $[\text{M}+\text{Na}]^+$  (Figure 2.35).

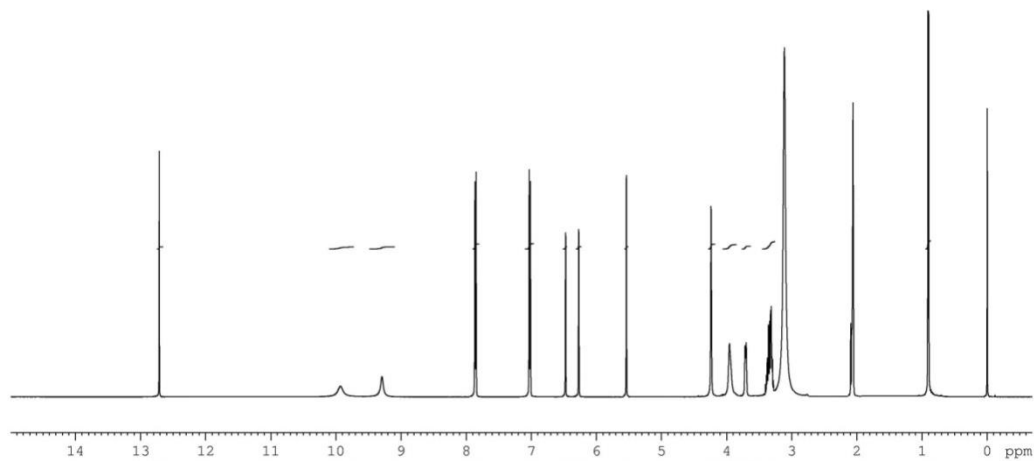


**Figure 2.33.**  $^1\text{H}$  NMR of compound **8** (afzelin)

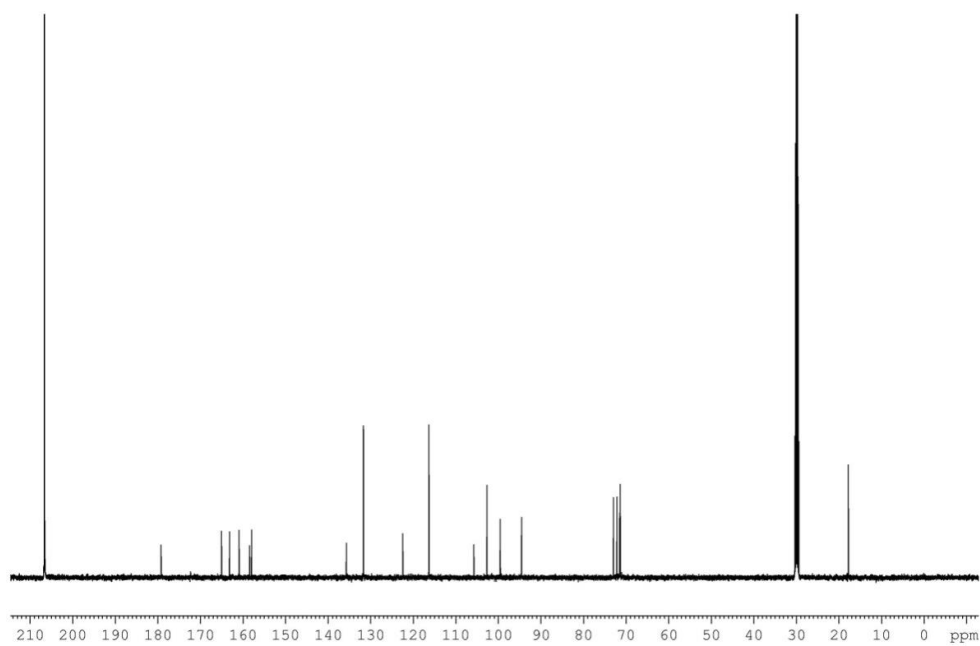


**Figure 2.34.**  $^{13}\text{C}$  NMR of compound **8** (afzelin)

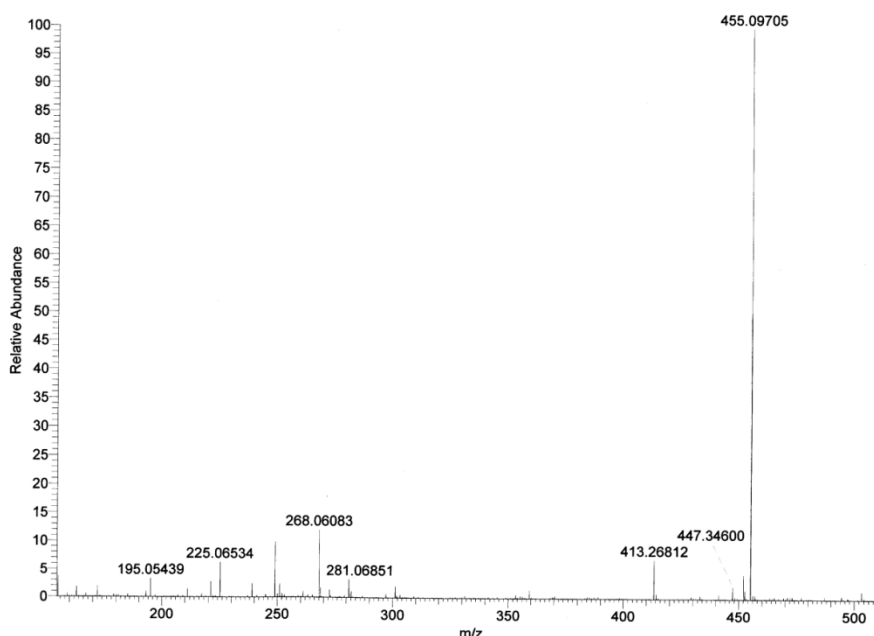


**Figure 2.35.** Mass spectrum of compound **8** (afzelin)

## 2.9. Biological evaluation of compounds

### 2.9.1. $\alpha$ -Glucosidase enzyme inhibition properties

Diabetes mellitus or simply diabetes, is a group of metabolic diseases in which a person has high blood sugar. This high blood sugar is either because of the pancreas does not produce enough insulin or because cells do not respond to the insulin that is produced. This condition produces the classical symptoms of polyuria, polydipsia and polyphagia. There are two main and common types of diabetes mellitus. They are type 1 diabetes and type 2 diabetes. Type 1 diabetes results from the body's failure to produce insulin and the person affected by the same requires insulin injection. In type 2 diabetes, cells fail to use insulin properly [Vinay *et al.* 2005].

Nowadays, type 2 diabetes has developed worldwide into an epidemic [Danaei *et al.* 2011]. Hyperglycemia, due to faulty insulin secretion and function, is the major determinant of diabetes and its secondary complications. Intestinal  $\alpha$ -glucosidase aids in breakdown of disaccharides to monosaccharide. Its inhibition is an attractive drug target as first line of treatment for type 2 diabetes to control the postprandial hyperglycemia. In addition, there are reports regarding additional therapeutic properties of  $\alpha$ -glucosidase inhibitors like protection against pancreatic beta cell apoptosis, inhibition of attachment

of macrophage to vascular endothelium and amelioration of development of atherosclerosis [Osonoi *et al.* 2010].

All the eight compounds were screened against  $\alpha$ -glucosidase enzyme by a procedure reported by Apostolidis *et al.* [Apostolidis *et al.* 2002 and Priya *et al.* 2011] with slight modifications. A wide range of concentrations starting from 5  $\mu$ M to 500  $\mu$ M were checked for each compound. The results are depicted in Table 1. It is clear from the results that kaempferol (**5**) and kaempferol-3-*O*-methylether (or isokaempferide, **6**) showed potent inhibitory activity with an  $IC_{50}$  value of 9.00  $\mu$ M and 7.88  $\mu$ M respectively. Interestingly both the compounds exhibited significantly better activity compared to the existing drug (acarbose), the standard used in the study. Acarbose showed an  $IC_{50}$  value of 47.2  $\mu$ M. The glycosylated derivatives (compound **7** and **8**) showed inferior activity compared to the non-glycosylated partners (**5** and **6**) with a higher  $IC_{50}$  value of 64.18 and 81.16  $\mu$ M respectively. This observation was in good agreement with the recent literature reports, in which the authors clearly says that flavonoids show better inhibition against  $\alpha$ -glucosidase enzyme compared to their respective glycosylated ones [Jianbo *et al.* 2013]. In the case of four sesquiterpenes, all of them showed poor activity compared to the flavonoids and standard acarbose. Thus, we conclude that flavonoid constituents of *Zingiber zerumbet* contribute more to the the  $\alpha$ -glucosidase enzyme inhibition compared to its sesquiterpene components (Table 2.5).

**Table 2.5.  $IC_{50}$  values of compounds 1-8 against  $\alpha$ -glucosidase enzyme**

Sl. No.	Compounds	$IC_{50}$ value ( $\mu$ M)
1	$\alpha$ -Humulene	197.2 $\pm$ 0.06
2	Zerumbone	95.7 $\pm$ 1.04
3	Zerumbol	116.10 $\pm$ 1.50
4	Zerumbone epoxide	170.25 $\pm$ 0.09
5	Kaempferol	9.00 $\pm$ 0.08
6	Kaempferol-3- <i>O</i> -methylether	7.88 $\pm$ 0.06
7	Kaempferol-3- <i>O</i> -(3,4- <i>O</i> -diacetyl- $\alpha$ -L-rhamnopyranoside)	64.18 $\pm$ 1.01
8	Afzelin	81.16 $\pm$ 1.65
9	Acarbose	47.2 $\pm$ 0.95

### 2.9.2. Anti-glycation properties

Protein glycation is a consequence of hyperglycemia in which the excess glucose present in the blood reacts non-enzymatically with proteins resulting in advanced glycation end products (AGEs). This forms stable cross-links with other peptides, enzymes, structural proteins *etc.* and alters their biological function. The formation and accumulation of AGE's have been implicated in the progression of diseases such as Alzheimer's disease, cardiovascular disease and stroke. Nowadays the development of antiglycation agents has gained high demand in pharma industry [Goldin *et al.* 2006].

All compounds were tested for its ability to inhibit the formation of advanced glycated end products (AGEs) using a reported procedure [Riya *et al.* 2013]. In this study, a total of 6 groups were present for each compound. Results were expressed in terms of relative fluorescence units (RFU). Among the eight compounds tested, significant decrease ( $P < 0.05$ ) in fluorescence was observed in compounds **1**, **5**, **6** & **7** at 100  $\mu\text{M}$  concentration. However, compound **6** was found to be most active under both day 1 and day 7 experiments. Quercetin (100  $\mu\text{M}$ ) showed significant ( $P < 0.05$ ) reduction in fluorescence with respect to control (Figure 2.36 & Figure 2.37).

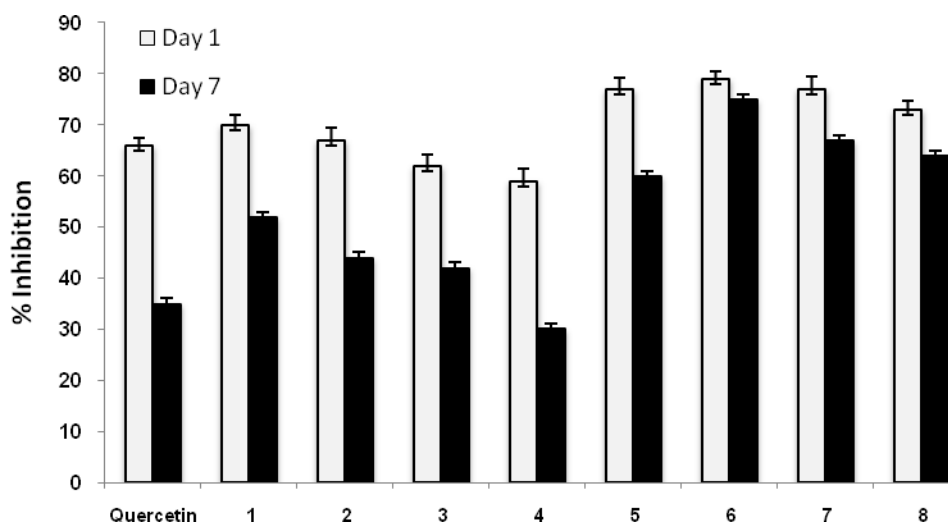


**Figure 2.36.** Glycation inhibition of compounds **1-8** at 100  $\mu\text{M}$  concentration

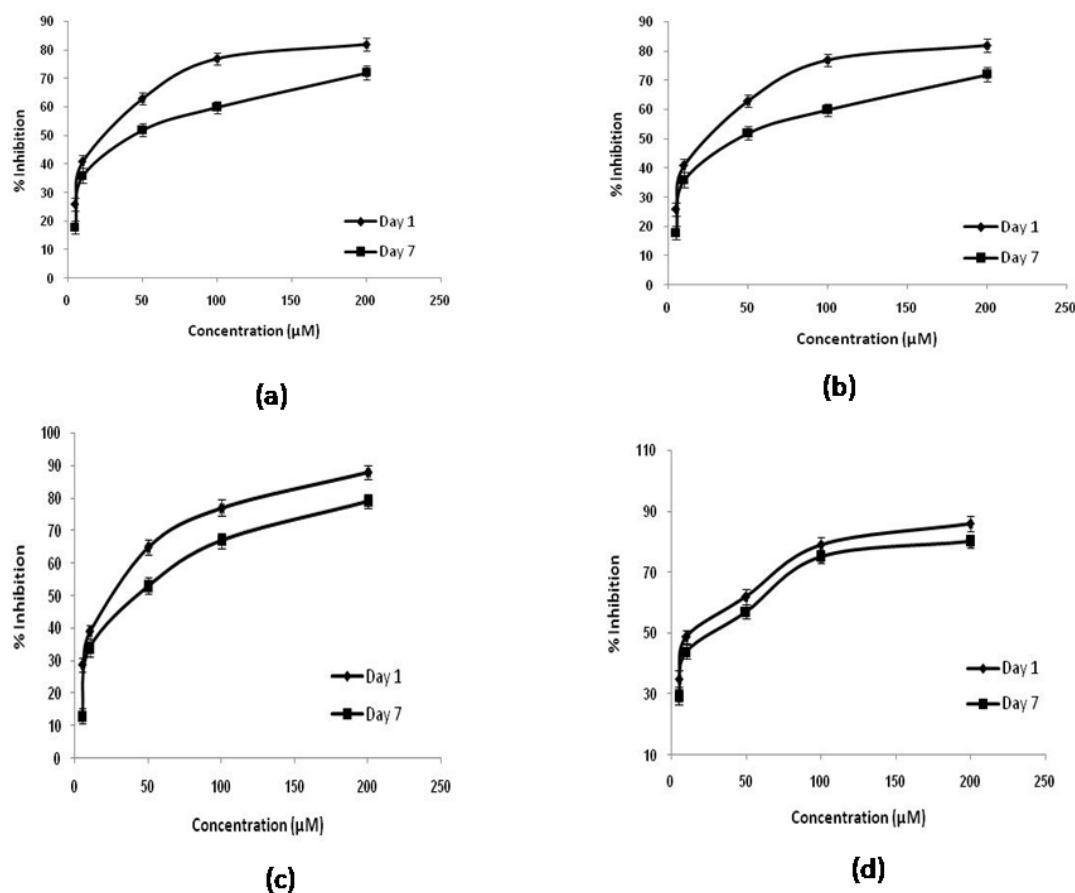


**Figure 2.37.** Percentage of inhibition of protein glycation reaction by (a) compound 1 (b) compound 5 (c) compound 6 (d) compound 7

### 2.9.3. Aldose reductase enzyme inhibition studies

Aldose reductase enzyme is primarily known for catalyzing the reduction of glucose to sorbitol using NADPH as cofactor. In diabetic patients, since the glucose level is high, the sorbitol formation and accumulation will be also high. These conditions in turn produce high osmotic pressure in eye leading to retinopathy in diabetic patients. So it is very important in therapeutic point of view to inhibit the action of aldose reductase in diabetic patients. Herein we report a series of phytochemicals, isolated from *Zingiber zerumbet* with aldose reductase inhibition properties under *in vitro* conditions using a reported procedure [Hayman and Kinoshita 1965]. All the phytochemicals except zerumbone epoxide showed promising inhibitory potential (Table 2.6). The compound with highest activity was afzelin, which displayed an  $IC_{50}$  value of 5.54 μM. In this assay, flavonoid class of compounds exhibited greater activity compared to the sesquiterpene



compounds. The standard used was zopolrestat, which showed an  $IC_{50}$  value  $1.34 \mu\text{M}$  (Figure 2.38).

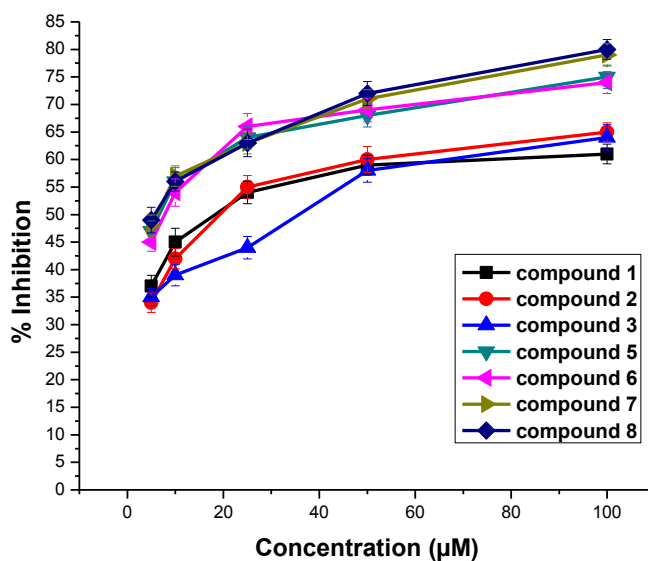


**Figure 2.38.** Aldose reductase inhibition of compounds 1-3 and 5-8

**Table 2.6.**  $IC_{50}$  values of compounds 1-8 against aldose reductase enzyme

Sl. No.	Compounds	$IC_{50}$ value ( $\mu\text{M}$ )
1	a-Humulene	$18.85 \pm 1.06$
2	Zerumbone	$19.27 \pm 1.11$
3	Zerumbol	$36.25 \pm 2.50$
4	Zerumbone epoxide	--
5	Kaempferol	$6.74 \pm 1.08$
6	Kaempferol-3-O-methylether	$7.93 \pm 1.56$
7	Kaempferol-3-O-(3,4-O-diacetyl - $\alpha$ -L-rhamnopyranoside)	$6.34 \pm 1.01$
8	Afzelin	$5.54 \pm 1.08$
9	Zopolrestat (std)	$1.34 \pm 1.35$

Thus, a detailed investigation on the inhibition assays of  $\alpha$ -glucosidase enzyme, aldose reductase enzyme and protein glycation reaction has been carried out under *in vivo*

conditions. The results revealed that all the sesquiterpenes show low to moderate inhibition against the carbohydrate digestive enzyme,  $\alpha$ -glucosidase. Among the four flavonoid molecules, the non-glycosylated flavonoids showed potent activity compared to the glycosylated ones. In aldose reductase inhibition assay, the four flavonoid molecules showed superior inhibition properties than the four sesquiterpene. Finally, in glycation inhibition reaction, the three out of four flavonoid showed potent activity along with one sesquiterpene *viz*  $\alpha$ -humulene. Thus, from the overall results it is clear that kaempferol and kaempferol-3-*O*-methylether are potent inhibitors of  $\alpha$ -glucosidase, aldose reductase and protein glycation reaction.

## 2.10. Conclusion

In conclusion, we have isolated seven phytochemicals from *Zingiber zerumbet* and synthesized a natural product from one of the isolated compounds. All the eight compounds were screened against  $\alpha$ -glucosidase enzyme, aldose reductase enzyme and protein glycation reaction. Kaempferol and kaempferol-3-*O*-methylether were found to be potent  $\alpha$ -glucosidase, aldose reductase as well as protein glycation inhibitors. Compared to the four-sesquiterpene components of *Zingiber zerumbet*, the flavonoid constituents exhibited a greater activity against both  $\alpha$ -glucosidase and aldose reductase enzymes. But in preventing the protein glycation reaction, compounds  $\alpha$ -humulene, kaempferol, kaempferol-3-*O*-methylether and 3",4"-*O*-diacetylfazelin displayed promising inhibitory activities.

## 2.11. Experimental details

General methods: All the chemicals were of the best grade commercially available and were used without further purification. All the solvents were purified according to standard procedures; dry solvents were prepared according to the literature methods and stored over molecular sieves. Analytical thin layer chromatography was performed on glass plates coated with silica gel containing calcium sulfate binder. Gravity column chromatography was performed using 100-200 mesh silica gel, mixtures of hexane-ethyl acetate were used for elution. Melting point was determined on a Buchi melting point apparatus and is uncorrected. NMR spectra were recorded at 300 or 500 ( $^1\text{H}$ ) and 75 or 125 ( $^{13}\text{C}$ ) MHz respectively on a Bruker Advance DPX-300 and 500 MHz NMR spectrometer. Chemical shifts are reported in  $\delta$  (ppm) relative to TMS ( $^1\text{H}$ ) or  $\text{CDCl}_3$

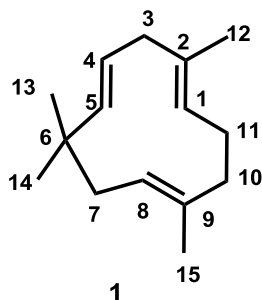
( $^{13}\text{C}$ ) as internal standards. Multiplicities ( $^1\text{H}$  NMR) were given as: s (singlet); br.s (broad singlet); d (doublet); br.d (broad doublet); ddd (doublet of double doublet); t (triplet); m (multiplet). Mass spectra were recorded under ESI/HRMS at 61800 resolution using Thermo Scientific Exactive mass spectrometer. IR spectra were recorded on Bruker Alpha FT-IR spectrometer. For enzyme inhibition assays, absorbance was measured in microplate reader (Biotek Synergy 4, US).

## 2.12. Spectral details of compounds 1-8

### $\alpha$ -Humulene [(1*E*,4*E*,8*E*)-2,6,6,9-tetramethylcycloundeca-1,4,8-triene] 1

**IR** (neat)  $\nu_{\text{max}}$ : 1662, 1443, 1354, 1178, 969, 824, 675  $\text{cm}^{-1}$ .

**$^1\text{H}$  NMR** (500 MHz,  $\text{CDCl}_3$ ):  $\delta$  5.59-5.54 (m, 1H, H at C4), 5.13 (d,  $J = 16$  Hz, 1H, H at C5), 4.93 (t,  $J = 6.5$  Hz, 1H, H at C1), 4.85 (t,  $J = 7.5$  Hz, 1H, H at C8), 2.49 (d,  $J = 7.5$  Hz, 2H, H at C3), 2.09-2.07 (m, 4H, H at C10 & C11), 1.89 (d,  $J = 7.5$  Hz, 2H, H at C7), 1.63 (s, 3H, H at C12), 1.42 (s, 3H, H at C13), 1.06 (s, 6H, H at C14 & C15).

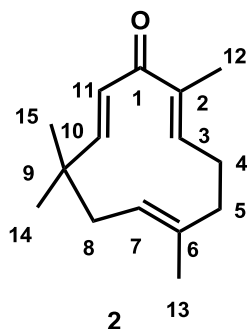


**$^{13}\text{C}$  NMR** (125 MHz,  $\text{CDCl}_3$ ):  $\delta$  140.9 (C5), 139.0 (C2), 132.9 (C9), 127.7 (C4), 125.9 (C1), 124.9 (C8), 42.0 (C7), 40.4 (C3), 39.8 (C10), 37.4 (C6), 27.2 (C14 or C15), 23.4 (C14 or C15), 17.9 (C12), 15.1 (C15).

Mass spectroscopic analysis: **HRMS** (ESI):  $m/z$  calcd for  $\text{C}_{15}\text{H}_{24}$ : 204.1878, found: 204.1876.

### Zerumbone [(2*E*,6*E*,10*E*)-2,6,9,9-tetramethylcycloundeca-2,6,10-trienone] 2

**IR** (KBr)  $\nu_{\text{max}}$ : 3026, 2964, 2924, 2856, 1656 (dienone), 1455, 1431, 1386, 1363, 1299, 1264, 1211, 1183, 1166, 1104, 1062, 1023, 966, 949, 906, 848, 827, 697, 627, 576, 533  $\text{cm}^{-1}$ .



UV  $\lambda_{\text{max}}$  (MeOH) nm: 250

$^1\text{H NMR}$  (500 MHz,  $\text{CDCl}_3$ ):  $\delta$  6.01-5.81 (m, 3H, H at C3, C9 and C10), 5.24 (br.d, 1H, H at C7), 2.37-2.2 (m, 5H, H at C8, C4 & C5), 1.90-1.86 (m, 1H, H at C8), 1.76 (s, 3H, H at C12), 1.51 (s, 3H, H at C13), 1.18 (s, 3H, H at C14 or C15), 1.05 (s, 3H, H at C14 or C15).

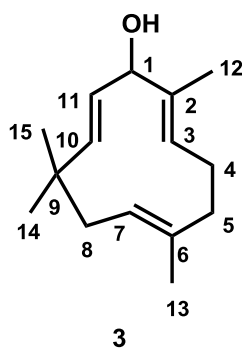
$^{13}\text{C NMR}$  (125 MHz,  $\text{CDCl}_3$ ):  $\delta$  204.2 (C1), 160.7 (C10), 148.7 (C3), 137.9 (C2), 136.2 (C6), 127.1 (C11), 124.9 (C7), 42.4 (C8), 39.4 (C5), 37.8 (C9), 29.4 (C14 or C15), 24.4 (C4), 24.1 (C14 or C15), 15.2 (C12), 11.7 (C13).

Mass spectroscopic analysis: **HRMS** (ESI):  $m/z$  calcd for  $\text{C}_{15}\text{H}_{22}\text{ONa}$ : 241.1568, found: 241.1565.

### Zerumbol [(2*E*,6*E*,10*E*)-2,6,9,9-tetramethylcycloundeca 2,6,10-trienol] **3**

**IR** (neat)  $\nu_{\text{max}}$ : 3292, 2956, 1444, 1264, 1070, 1025, 974, 731  $\text{cm}^{-1}$ .

$^1\text{H NMR}$  (500 MHz,  $\text{CDCl}_3$ ):  $\delta$  5.56 (dd,  $J_1 = 16.5$  Hz,  $J_2 = 7.5$  Hz, 1H, H at C11), 5.29-5.20 (m, 2H, H at C10 & C3), 4.82 (dd,  $J_1 = 9.5$  Hz,  $J_2 = 3.5$  Hz, 1H, H at C7), 4.63 (d,  $J = 7.5$  Hz, 1H, H at C1), 2.23-2.16 (m, 1H, H at C4), 2.14-2.00 (m, 4H H at C4, C5 & C8), 1.87 (brs, 1H, OH), 1.81-1.79 (m, 1H, C8), 1.67 (s, 3H, H at C12), 1.44 (s, 3H, H at C13), 1.08 (s, 3H, H at C14 or C15), 1.07 (s, 3H, H at C14 or C15).



$^{13}\text{C NMR}$  (125 MHz,  $\text{CDCl}_3$ ):  $\delta$  141.9 (C2), 139.3 (C10), 133.0 (C6), 131.3 (C11), 124.9 (C7), 124.8 (C3), 78.7 (C1), 41.9 (C8), 39.1 (C5), 37.2 (C9), 29.59 (C14 or C15), 24.2 (C14 or

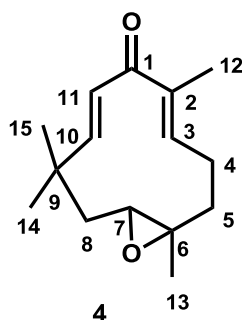
C15), 22.9 (C4), 15.1 (C13), 12.7 (C12).

Mass spectroscopic analysis: **HRMS** (ESI):  $m/z$  calcd for  $C_{15}H_{24}O$ : 219.1749  $[M-H]^+$ , found: 219.1753.

**Zerumbone epoxide [(4*E*,7*E*)-1,5,9,9-tetramethyl-12-oxabicyclo[9.1.0]dodeca-4,7-dien-6-one] 4**

**IR** (KBr)  $\nu_{\max}$ : 2962, 1646, 1457, 1385, 1247, 1118, 1057, 970, 882, 765, 678  $cm^{-1}$ .

**UV**  $\lambda_{\max}$  (MeOH) nm: 2637



**$^1H$  NMR** (500 MHz,  $CDCl_3$ ):  $\delta$  6.15-6.08 (m, 3H, H at C3, C10 & C11), 2.75 (d,  $J = 11$  Hz, 1H, C7), 2.45-2.40 (m, 2H, H at C4), 2.29 (d,  $J = 13$  Hz, 1H, H at C5), 1.93 (d,  $J = 14$  Hz, 1H, H at C8), 1.86 (s, 3H, H at C12), 1.48-1.43 (m, 1H, H at C8), 1.37-1.32 (m, 1H, H at C5), 1.30 (s, 3H, C14 or C15), 1.23 (s, 3H, H at C13), 1.09 (s, 3H, H at C14 or C15).

**$^{13}C$  NMR** (125 MHz,  $CDCl_3$ ):  $\delta$  202.9 (C1), 159.5 (C10), 147.8 (C3), 139.4 (C2), 128.3 (C11), 62.8 (C7), 61.4 (C6), 42.6 (C8), 38.2 (C5), 35.9 (C9), 29.8 (C14 or C15), 24.7 (C4), 24.0 (C14 or C15), 15.6 (C13), 12.1 (C12).

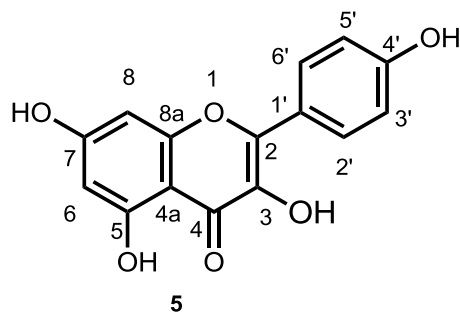
Mass spectroscopic analysis: **HRMS** (ESI):  $m/z$  calcd for  $C_{15}H_{22}O_2Na$ : 257.1517, found: 257.1513.

Crystal data of compound **4**: The unit cell parameters are:  $a = 22.168(5)$  Å,  $b = 9.755(5)$  Å,  $c = 15.629(5)$  Å and  $\alpha = 90.000(5)$  deg.  $\beta = 124.982(5)$  deg.,  $\gamma = 90.000(5)$  deg. The space group of the crystal system is  $C2/c$ .

**3,5,7-Trihydroxy-2-(4-hydroxyphenyl)-4H-chromen-4-one (Kaempferol) 5**

**IR** (KBr)  $\nu_{\max}$ : 3326, 1668, 1620, 1513  $\text{cm}^{-1}$ .

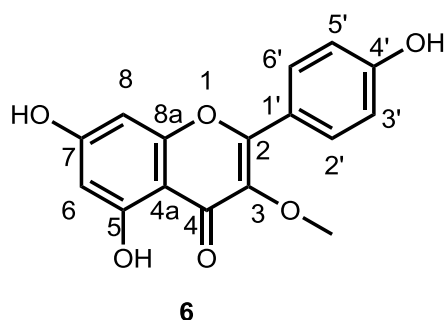
**UV**  $\lambda_{\max}$  (MeOH) nm: 265, 365



**$^1\text{H}$  NMR** (500 MHz, acetone- $d_6$ ):  $\delta$  12.19 (s, 1H, OH at C5), 9.29 (br.s, 1H, OH), 8.16 (d,  $J = 9.0$  Hz, 2H, H at C2' and C6'), 7.02 (d,  $J = 9$  Hz, 2H, H at C3' and C5'), 6.54 (d,  $J = 2.0$  Hz, 1H, H at C8), 6.28 (d,  $J = 2.0$  Hz, 1H, H at C6).

**$^{13}\text{C}$  NMR** (125 MHz, acetone- $d_6$ ):  $\delta$  176.6 (C4), 165.1 (C7), 162.4 (C5), 160.2 (C4'), 157.8 (C8a), 147.1 (C2), 136.7 (C3), 130.5 (C2', 6') 123.3 (C1'), 116.4 (C3' and C5'), 104.2 (C4a), 99.2 (C6), 94.5 (C8).

Mass spectroscopic analysis: **HRMS** (ESI):  $m/z$  calcd for  $\text{C}_{15}\text{H}_{10}\text{O}_6\text{Na}$ : 309.0375, found: 309.0371.

**5,7-Dihydroxy-2-(4-hydroxyphenyl)-3-methoxy-4H-chromen-4-one****(Isokaempferide) 6**

**IR** (KBr)  $\nu_{\max}$ : 3325, 1654, 1625, 1513  $\text{cm}^{-1}$ .

**UV**  $\lambda_{\max}$  (MeOH) nm: 266, 350

**$^1\text{H}$  NMR** (500 MHz, acetone- $d_6$ ):  $\delta$  12.81 (s, 1H, OH), 9.40 (br.s, 1H, OH), 8.04 (d,  $J = 9.0$  Hz, 2H, H at C2' and C6'), 7.02 (d,  $J = 9.0$  Hz, 2H, H at C3' and C5'), 6.50 (d,  $J = 2.0$  Hz, 1H, H at C8), 6.26 (d,  $J = 1.5$  Hz, 1H, H at C6), 3.87 (s, 3H, OMe).

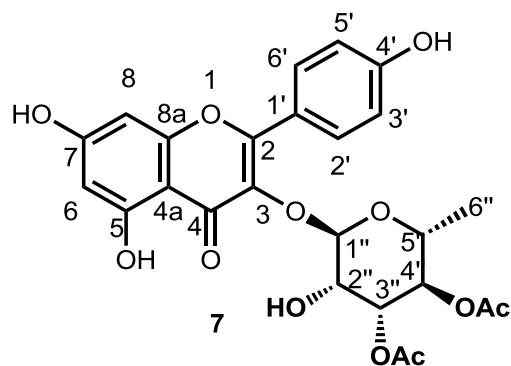
**$^{13}\text{C}$  NMR** (125 MHz, acetone- $d_6$ ):  $\delta$  178.7 (C4), 163.9 (C7), 162.1 (C5), 160.0

(C4'), 156.9 (C2 or C8a), 155.9 (C2 or C8a), 138.3 (C3), 130.3 (C2' or C6'), 129.6 (C2' or C6'), 121.8 (C1'), 115.5 (C3' & C5'), 105.1 (C4a), 98.5 (C6), 93.6 (C8), 59.3 (OMe).

Mass spectroscopic analysis: **HRMS** (ESI):  $m/z$  calcd for  $C_{16}H_{12}O_6Na$ : 323.0532, found: 323.0537.

**Kaempferol-3-O-(3,4- O-diacetyl- $\alpha$ -L-rhamnopyranoside) (3'',4''-O-diacetylafzelin)**

7



**IR** (KBr)  $\nu_{\max}$ : 3360, 2945, 1657, 1615, 845  $\text{cm}^{-1}$ .

**UV**  $\lambda_{\max}$  (MeOH) nm: 265, 365

**$^1\text{H}$  NMR** (500 MHz, DMSO- $d_6$ ):

12.58 (s, 1H, OH), 11.02 (br.s, 1H, OH), 10.34 (br.s, 1H, OH), 7.80 (d,  $J = 8.5$  Hz, 2H, H at C2' and C6'), 6.99 (d,  $J = 8.5$  Hz, 2H, H at C3' and C5'), 6.48 (s, 1H, H at C8), 6.28 (s, 1H, H at C6), 5.76 (d,  $J = 4.5$  Hz, 1H, H at C1''), 5.38 (s, 1H), 5.03 (dd,  $J_1 = 10.0$  Hz,  $J_2 = 2.5$  Hz, 1H, H at C3''), 4.96 (t,  $J = 9.5$  Hz, 1H, H at C4''), 4.28 (br.s, 1H, H at C2''), 3.49-3.42 (m, 1H, H at C5''), 2.08 (s, 3H, Ac), 2.03 (s, 3H, Ac), 0.80 (d,  $J = 6.5$  Hz, 3H, H at C6'').

**$^{13}\text{C}$  NMR** (125 MHz, DMSO- $d_6$ ):  $\delta$  177.4 (C4), 169.9 (Ac), 169.6 (Ac), 164.3 (C7), 161.2 (C5), 160.2 (C4'), 157.4 (C2), 156.5 (C8a), 133.8 (C3), 130.5 (C2' and C6'), 120.2 (C1'), 115.4 (C3' and C5'), 104.1 (C4a), 100.9 (C1''), 98.8

(C6), 93.8 (C8), 70.9 (C3''), 69.6 (C4''),  
67.9 (C2'' or C5''), 67.2 (C2'' or C5''),  
20.8 (Ac), 20.7 (Ac), 16.9 (C6'').

Mass spectroscopic analysis: **HRMS** (ESI):  $m/z$  calcd for  $C_{25}H_{23}O_{12}$ : 515.1190 [M-H]<sup>+</sup>, found: 515.1190.

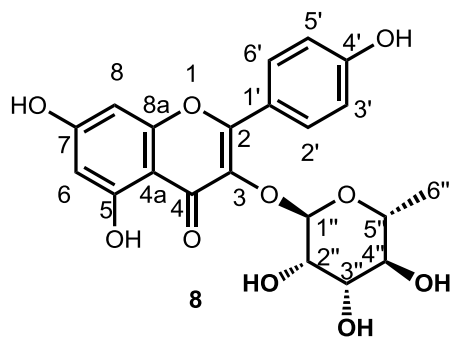
### Kaempferol-3-O-rhamnopyranoside (Afzelin) **8**

Sodium hydroxide (40 mg, 0.716 mmol) was dissolved in methanol (5 mL) at 0-5°C. Compound **7** (100 mg, 0.179 mmol) was added and stirred at room temperature for 1 hour. After the completion of the reaction (as indicated by TLC analysis), the reaction mixture was poured into 1N HCL solution (10 mL). It was then extracted with ethyl acetate (3 x 50 mL) and the solvent was evaporated off. The residue on column chromatography using methanol: chloroform mixture afforded the compound **8** in 90% yield. Pale yellow amorphous powder.

**IR** (KBr)  $\nu_{\max}$ : 3365, 2935, 1655,  
1610, 845  $\text{cm}^{-1}$ .

**<sup>1</sup>H NMR** (500 MHz, acetone-d<sub>6</sub>):  $\delta$   
12.7 (s, 1H, OH), 9.94 (br.s, 1H, OH), 9.29  
(br.s, 1H, OH), 7.86 (d,  $J = 8.5$  Hz, 2H, H  
at C2' & C6'), 7.02 (d, 2H,  $J = 8.5$  Hz, H  
at C3' & C5'), 6.47 (d,  $J = 1.0$  Hz, 1H, H at  
C8), 6.27 (s, 1H, H at C6), 5.54 (s, 1H, H  
at C1''), 4.24 (br.s, 1H, H at C2''), 3.96  
(br.s, 1H), 3.72-3.68 (m, 1H, H at C3''),  
3.38-3.29 (m, 2H, H at C4'' and C5''), 0.90  
(d,  $J = 6.0$  Hz, 3H, H at C6'').

**<sup>13</sup>C NMR** (125 MHz, acetone-d<sub>6</sub>):  $\delta$   
179.3 (C4), 165.1 (C7), 163.2 (C5), 160.9  
(C4'), 158.5 (C8a), 157.9 (C2), 135.7 (C3),  
131.7 (C2' and C6'), 122.5 (C1'), 116.3  
(C3' and C5'), 105.8 (C4a), 102.7 (C1''),





99.6 (C6), 94.6 (C8), 72.9 (C4"), 72.1 (C3"), 71.5 (C2"), 71.4 (C5"), 17.8 (C6").

Mass spectroscopic analysis: **HRMS** (ESI): m/z calcd for C<sub>21</sub>H<sub>20</sub>O<sub>10</sub>Na: 455.0954, found: 455.0970.

## 2.13. Procedures for various biological assays

### 2.13.1. Procedure for $\alpha$ -glucosidase inhibition assay

$\alpha$ -Glucosidase inhibition was assayed using different concentrations of sample stock solution (5  $\mu$ M -500  $\mu$ M), 20  $\mu$ L of 0.1 M phosphate buffer (pH 6.9) containing  $\alpha$ -glucosidase solution (1.0 U/mL), and was incubated in 96 well plates at 25 °C for 10 min. After pre-incubation, 50  $\mu$ L of 5 mM p-nitrophenyl- $\alpha$ -D-glucopyranoside solution in 0.1 M phosphate buffer (pH 6.9) was added to each well at timed intervals. The reaction mixtures were incubated at 25 °C for 5 min. Before and after incubation, absorbance readings were recorded at 405 nm by a Synergy 4 Biotek multiplate reader (Biotek Instruments Inc., Highland Park, PO Box 998, Winooski, Vermont-0504-0998, USA) and compared with a control that had an adequate amount of buffer solution in place of the compounds. Acarbose was used as the standard. The  $\alpha$ -glucosidase inhibitory activity was expressed as the inhibition percentage and was calculated as follows:

$$\% \text{ inhibition} = (A_{\text{control}} - A_{\text{sample}}) / A_{\text{control}} \times 100$$

Where  $A_{\text{control}}$  is the absorbance of control without sample and  $A_{\text{sample}}$  is the absorbance of the sample. The concentration of the extract having 50% inhibition ( $IC_{50}$ ) was calculated from the concentration inhibition response curve.

### 2.13.2. Procedure for aldose reductase inhibition assay

The enzyme source was the eye lenses from streptozotocin-induced diabetic Sprague-Dawley rats. Animals were sacrificed by cervical dislocation, immediately the lenses were enucleated through posterior approach. A 10% lens homogenate (w/v) was prepared in 0.1 M phosphate buffered saline (pH 7.4). After centrifugation at 5000 $\times$ g for 15 min at 4 °C, the supernatant was collected and used for the determination of enzyme activity [Jaiswal *et al.* 2012]. Lens aldose reductase activity was measured according to the method of Hayman and Kinoshita with slight modifications. In brief, reaction mixture contains 0.7 mL of sodium phosphate buffer (67 mM, pH 6.2), 0.1 mL of NADPH (25 $\times$ 10<sup>-5</sup> M) and 0.1 mL of lens homogenate, in a final volume of 1 mL. The enzyme

---

reaction was started by the addition of the 0.1 ml substrate (DL-Glyceraldehyde, 1 mM) and absorbance was recorded at 340 nm for 3 min at 30 sec time interval. Enzyme activity was expressed as  $\Delta OD/\text{min}/\text{mg}$  protein. Each compound was added to the reaction mixture at various concentrations to determine the percentage inhibition. The  $IC_{50}$  was calculated for each compound by plotting percent inhibition versus concentration.

### **2.13.3. Procedure for anti-glycation activity assay**

Bovine serum albumin (BSA) derived advanced glycation endproducts were quantified based on a previous report [Riya *et al.* 2013]. AGE fluorescence ( $\lambda_{\text{ex}}$  370 nm;  $\lambda_{\text{em}}$  440 nm) was measured using Biotek microplate reader after 24 h and 7 days (day1 and day7). BSA ( $25 \text{ mg mL}^{-1}$ ) in presence of glucose (500 mM) in phosphate buffered saline (PBS) was used as control. The data was compared with the reference compound quercetin ( $100 \mu\text{M}$ ).

# Chapter 3

## Synthesis and Biological Evaluation of Novel Derivatives of Zerumbone

---

### Part A

#### Transition Metal Catalyzed Regio- and Diastereoselective 1,4-Conjugate Addition of Zerumbone Using Boronic Acids: A Simple Route toward Novel Zerumbone Derivatives

---

#### 3.1. Introduction

Zerumbone **1** is a monocyclic sesquiterpene containing a cross-conjugated dienone system, with potent biological activity, and is abundantly available from the essential oil of wild ginger, *Zingiber zerumbet* (L.) Smith (Figure 3.1) [Dev 1960; Danodaran and Dev 1965; Dev *et al.* 1968; Hall *et al.* 1981; Fransworth and Bunyaphatsara 1992; Sawada *et al.* 2002]. This natural product demonstrates a wide spectrum of biological activity including anti-tumor, anti-inflammatory, anti-cancer and anti-HIV [Murakami *et al.* 2004; Kirana *et al.* 2003; Ozaki *et al.* 1991; Sulaiman *et al.* 2010; Szabolcs *et al.* 2007; Murakami and Ohigashi 2007; Murakami *et al.* 2004; Aggarwal *et al.* 2008; Taha *et al.* 2010; Abdelwahab 2011; Sung *et al.* 2012; Abdelwahab *et al.* 2012; Dai 1997]. Studies have revealed that the rhizome oil of the *Zingiber zerumbet* plant that grows in southern India contains about 80% zerumbone and this compound can be easily obtained by simple distillation and recrystallization techniques [Baby *et al.* 2009].

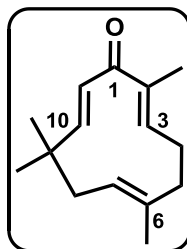
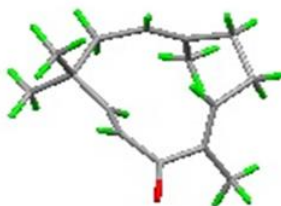


Figure 3.1. Zerumbone **1**

Zerumbone was first isolated by Dev in 1960, structurally elucidated in 1965 and later characterized by NMR and X-ray spectroscopy (Figure 3.2) [Dev 1960; Damodaran and Dev 1965].



**Figure 3.2.** X-ray structure of zerumbone

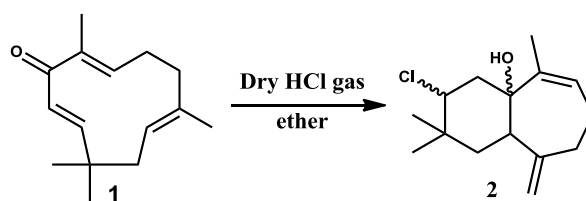
It has a great latent reactivity and contains three double bonds; an isolated double bond and two double bonds as part of a cross-conjugated dienone moiety. Out of these, the double bond at C6 position is found to be least hindered being furthest from the gem-dimethyl groups at C9. It is evident from the X-ray crystal structure that the dienone system lies in a slightly distorted plane perpendicular to that of the isolated double bond [Hall *et al.* 1981]. The great abundance and interesting biological properties make it an important and attractive phytochemical. These facts about zerumbone and its derivatives prompted us to invest our time on developing new synthetic methodologies for its derivatization with an aim to enhance its biological properties. Before going into the details, a brief account of the reactions of zerumbone is given in the following sections.

### 3.2. Reactions of zerumbone: An overview

Zerumbone **1** has been subjected to a number of chemical investigations as it has got an attractive and diverse reactivity pattern. It undergoes various reactions like cyclization, reduction, ring-expansion, ring-opening, epoxidation, conjugate addition *etc.* The reactions are discussed in detail in the following segments.

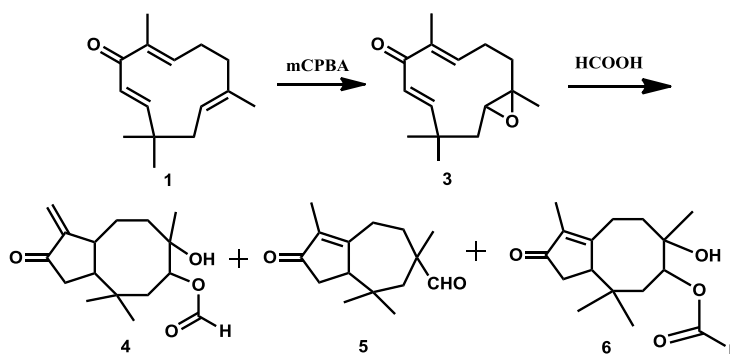
#### 3.2.1. Cyclization reaction

The acid catalyzed cyclization of zerumbone has been studied by Chhabra *et al.* The reaction product of **1** with dry hydrochloric acid gas in ether yielded a compound, which was reported to be a potent pesticide against the stored grain pest *Triboliumcastenium*. This compound had a unique [5.4.0]-undecane skeleton and the structure **2** has been assigned to it. The reaction is shown in scheme 3.1 [Chhabra *et al.*1985].



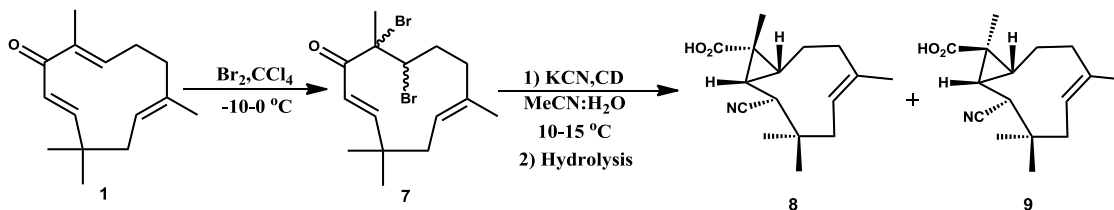
Scheme 3.1

Zerumbone **1** can be converted to zerumbone-6,7-epoxide **3** readily on treatment with perbenzoic acid [Matthes *et al.* 1982]. The transannular cyclization of zerumbone epoxide has been studied by various groups. Zerumbone-6,7-epoxide on treatment with formic acid yielded three compounds possessing the rare bicyclo[6.3.0]decane skeletons as shown in scheme 3.2.



Scheme 3.2

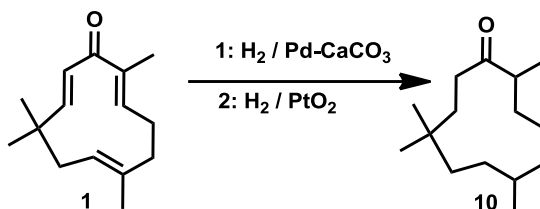
Selective synthesis of 6,7-dibromide **7** and its rearrangement studies in presence of aqueous potassium cyanide from zerumbone **1** has also been investigated [Kitayama and Okamoto 1999]. This has resulted in providing the Favorskii rearrangement products **8** and **9** having the bicyclic carboxylic acid structures as depicted in scheme 3.3.



Scheme 3.3

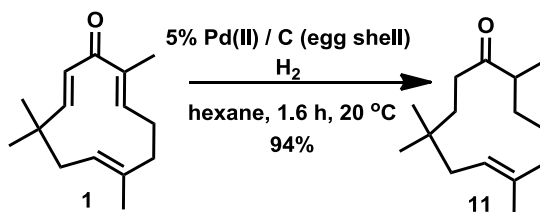
### 3.2.2. Reduction reaction

In 1960, Dev and co-workers demonstrated the reduction of zerumbone to hexahydrozerumbone **10** in a two step reaction pathway using hydrogen gas, Lindlar's catalyst and platinum(IV)oxide (Scheme 3.4) [Dev *et al.* 1960].



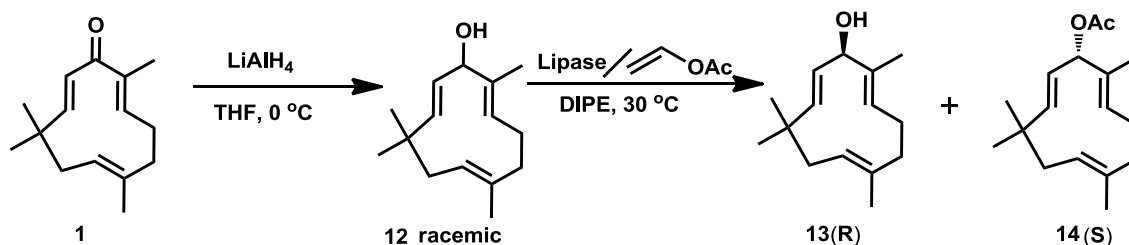
Scheme 3.4

Later in 2010, Kitayama *et al.* presented a regioselective reduction of zerumbone into tetrahydrozerumbone **11** instead of hexahydrozerumbone **10**. The isolated double bond remained as such and the two double bonds of dienone moiety got reduced. The reaction afforded the product in 94% yield (Scheme 3.5) [Kitayama *et al.* 2010].



Scheme 3.5

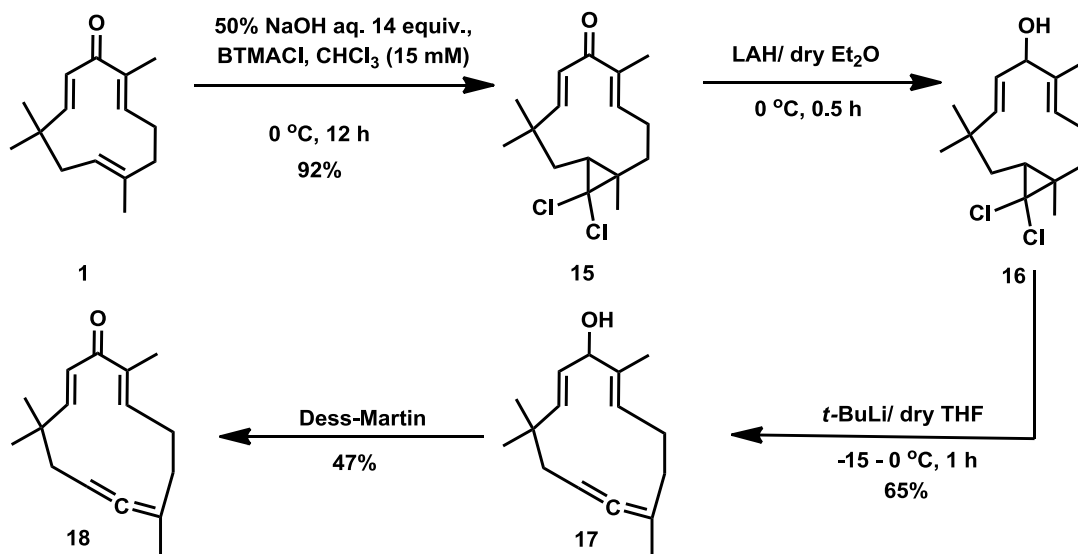
Kitayama *et al.* reported the synthesis of optically active zerumbol **13** and its acetate **14** from zerumbone **1** by reduction followed by lipase-catalyzed stereoselective trans-esterification. In the best conditions found, a lipase from *Pseudomonas fluorescens* (Amano AK) and vinyl acetate in THF at 30 °C afforded (*R*)-**13** and (*S*)-**14** with an *E*-value of 56. The absolute configuration of (*R*)-**13** was determined by Sharpless epoxidation with *l*-diethyltartrate (*l*-DET) to a bis-epoxide of known configuration (Scheme 3.6) [Kitayama *et al.* 2002].



Scheme 3.6

### 3.2.3. Ring expansion reaction

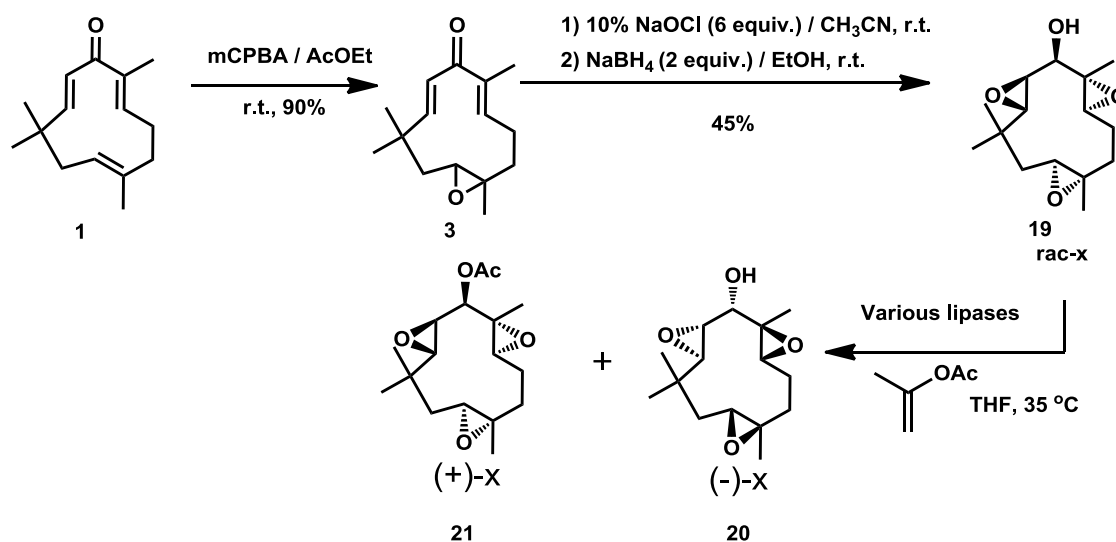
Kitayama *et al.* also succeeded in the synthesis of a zerumbone derivative with 12-membered ring, an allene type zerumbone **18**. For the first time, a Doering–LaFlamme allene synthesis method was adopted and the structure of the product was confirmed by monocrystal X-ray diffraction analysis. The overall yield of the reaction was 27.7% (Scheme 3.7) [Kitayama *et al.* 2006].



Scheme 3.7

### 3.2.4. Epoxidation reaction

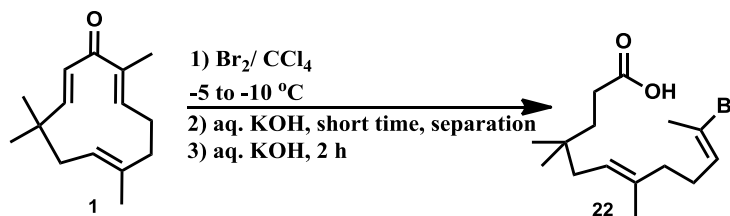
Optically active triepoxyzerumbol(-)-**20** and its acetate (+)-**21** were synthesized by lipase-catalyzed enantioselective transesterification of racemic **19** by the same group. Under optimized conditions, a lipase from *Alcaligenes* sp. (Meito QL) catalyzed the reaction of racemic **19** with isopropenyl acetate in THF at 35 °C to afford (1S)-**20** and (1R)-**21** with an *E*-value of 79. The absolute configuration of (1R)-**21** was determined by single crystal X-ray diffraction of its ester with a chlorine atom using the anomalous dispersion effect (Scheme 3.8) [Kitayama *et al.* 2007].



Scheme 3.8

### 3.2.5. Ring opening reaction

The pioneering report on the ring opening reaction of zerumbone was reported by Kitayama *et al.* [Kitayama *et al.* 2010]. The product obtained by this reaction has shown remarkable histidine-kinase inhibition properties (Scheme 3.9).

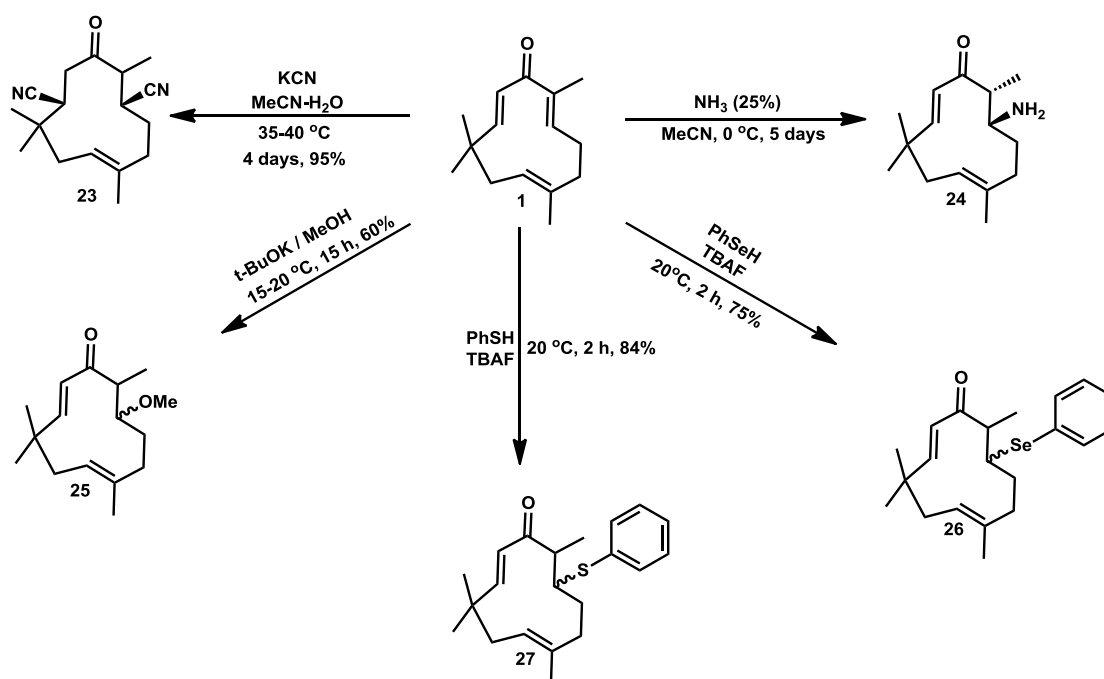


Scheme 3.9

### 3.2.6. 1,4-Conjugate addition reaction

Due to the presence of conjugated double bonds, zerumbone undergoes 1,4-conjugate addition reaction by various nucleophiles. Kitayama *et al.* have synthesized many such derivatives using KCN, NH<sub>3</sub>, MeOH and PhSH. The reactions and conditions are shown in scheme 3.10 [Kitayama *et al.* 1999; Ohe *et al.* 2002].



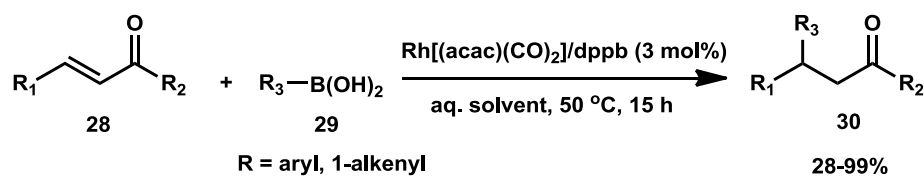


Scheme 3.10

### 3.3. Rhodium catalyzed 1,4-conjugate addition reactions using boronic acids

Boronic acids are versatile class of compounds first reported by Frankland in 1860 [Frankland and Duppa 1860]. They can be synthesized from a variety of precursors and are usually stable and easily stored. A wide range of boronic acids are commercially available and in particular they are environmentally safer than other organometallic reagents. Their unique properties as mild organic Lewis acids and their mitigated reactivity profile coupled with their stability and ease of handling, makes boronic acids a particularly attractive class of synthetic intermediates. Moreover, because of their low toxicity and their ultimate degradation into the environmentally friendly boric acid, boronic acids can be regarded as “green” compounds.

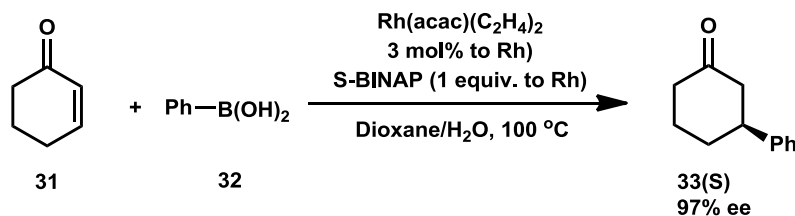
Rhodium catalyzed 1,4-conjugate addition reactions using boronic acids were first reported by Miyaura and co-workers in 1997 [Sakai *et al.* 1997]. They described a rhodium(I)-catalyzed conjugate addition of aryl- or 1-alkenylboronic acids to enones at 50 °C in an aqueous solvent. A combination of [Rh(acac)(CO)<sub>2</sub>] and dppb was recognized to be highly effective for the addition to acyclic and cyclic enones (Scheme 3.11).



Scheme 3.11

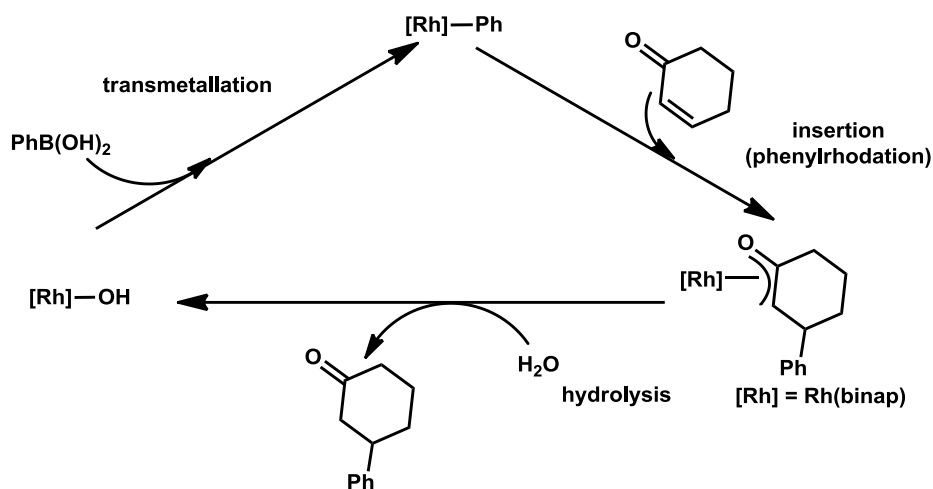
Work on the mechanistic details was in progress at that time, but they proposed a catalytic cycle that involves the transmetalation between the rhodium(I) enolate and arylboronic acid to give the arylrhodium(I) species and the insertion of the enone into the Ar-Rh bond.

Immediately after the first report, Hayashi *et al.* developed a new catalytic system for the asymmetric 1,4-conjugate addition reactions on enones. All the reactions proceeded with high enantioselectivity for both cyclic and linear  $\alpha,\beta$ -unsaturated ketones with a variety of aryl- and alkenylboronic acids (Scheme 3.12) [Hayashi *et al.* 2002].

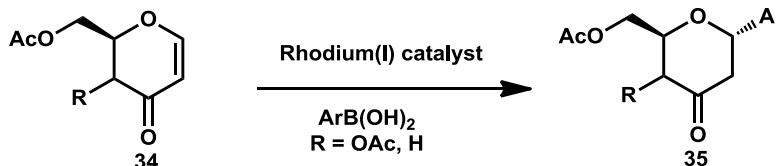


Scheme 3.12

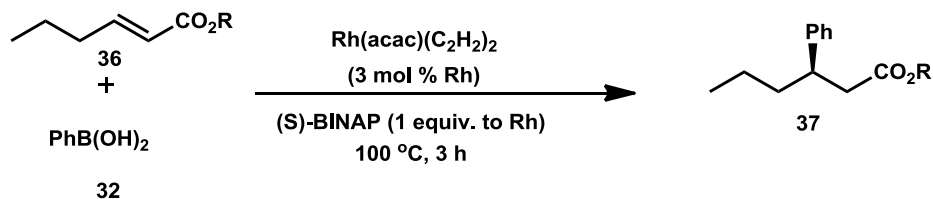
The same group proposed a detailed mechanism for the asymmetric 1,4-conjugate addition of boronic acids to  $\alpha,\beta$ -unsaturated ketone catalyzed by a rhodium-BINAP complex and this was established by the use of  $\text{RhPh}(\text{PPh}_3)(\text{BINAP})$  as the key intermediate. Using NMR spectroscopic techniques, they suggested that the reaction proceeds *via* three intermediates phenylrhodium, oxa- $\pi$ -allylrhodium and hydroxorhodium complexes. The transformations between the three intermediates, that is, insertion, hydrolysis and transmetalation, were also observed in the NMR experiments (Scheme 3.13).



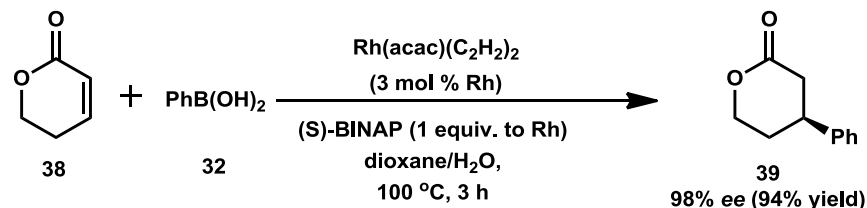
Later in 2001, Ramnauth *et al.* reported an efficient synthesis of C-glycosides by employing a cationic rhodium(I)-catalyzed 1,4-conjugate addition of arylboronic acids to enones derived from glycals [Ramnauth *et al.* 2001]. The reaction is stereoselective for the  $\alpha$ -anomer and is highly dependent on the nature of the rhodium catalyst (Scheme 3.14).



Not only the  $\alpha,\beta$ -unsaturated ketone but  $\alpha,\beta$ -unsaturated esters also undergo asymmetric 1,4-conjugate addition reaction. Takaya and co-workers reported phenylation of (*E*)-hexenoate esters with high enantioselectivity (Scheme 3.15) [Takaya *et al.* 1999].

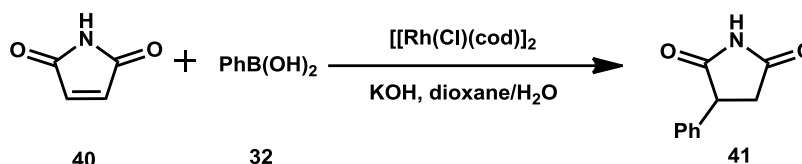


The reaction of cyclic  $\alpha,\beta$ -unsaturated esters also proceeded with high enantioselectivity. The arylation reaction of six membered cyclic ester using various phenylboronic acids gave the products in 97-98% *ee* in high yields (Scheme 3.16).



Scheme 3.16

Iyer *et al.* demonstrated the 1,4-conjugate addition to unprotected maleimide **40**. Various boronic acids were treated with a rhodium(I) catalyst enabling their 1,4-conjugate addition. The reaction was general with both electron-rich and electron poor boronic acids. These reactions were also performed in the microwave condition resulting in reduced reaction times and improved efficiencies (Scheme 3.17) [Iyer *et al.* 2007].



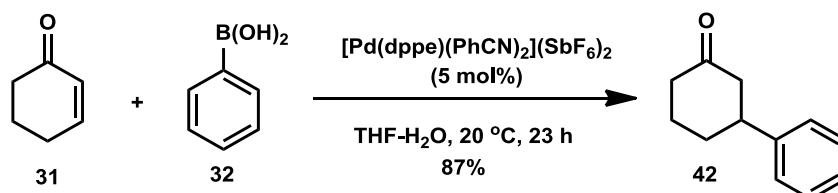
Scheme 3.17

Thus from the literature reports, it is clear that the rhodium catalyzed 1,4-conjugate addition reaction of boronic acids to various  $\alpha,\beta$ -unsaturated ketones and esters is as an important synthetic tool for its arylation or alkenylation. Asymmetric version of these reactions provides products in high isolated yield with high *ee* ratio.

### 3.4. Palladium catalyzed 1,4-conjugate addition reactions

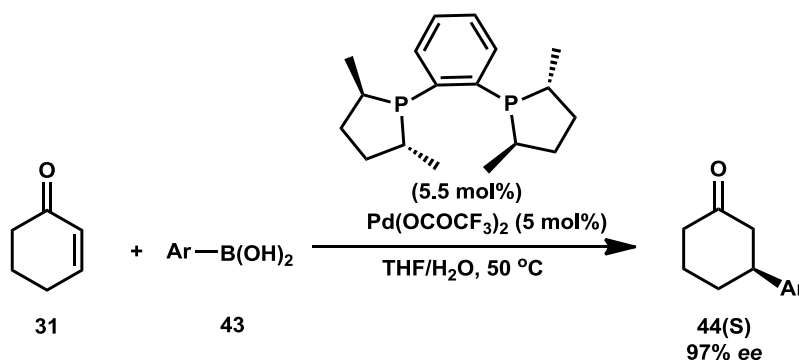
Palladium catalyzed 1,4-conjugate addition reaction using boronic acids is also reported in the literature. But there are only a few reports on this class of reactions. This is because in contrast to the formation of O-bound enolates in the insertion of enones into a C-Rh bond, a palladium catalyst yields C-bound enolates, resulting in  $\beta$ -hydride elimination. Thus, the reaction of enones with  $\text{RPdX}$ , generated *in situ* by transmetalation of  $\text{PdX}_2$  with an organometallic reagent or by the oxidative addition of  $\text{RX}$  to a palladium(0) complex, affords Heck coupling products with precipitation of palladium black.

But in 2003, Nishikata *et al.* reported the first example of 1,4- conjugate addition of boronic acids to enones by using a cationic palladium (II) catalyst. All the reactions afforded the conjugate addition product in good to excellent yield. Both the cyclic as well as non-cyclic  $\alpha,\beta$ -unsaturated ketones worked well under the optimized condition (Scheme 3.18) [Nishikata *et al.* 2003].



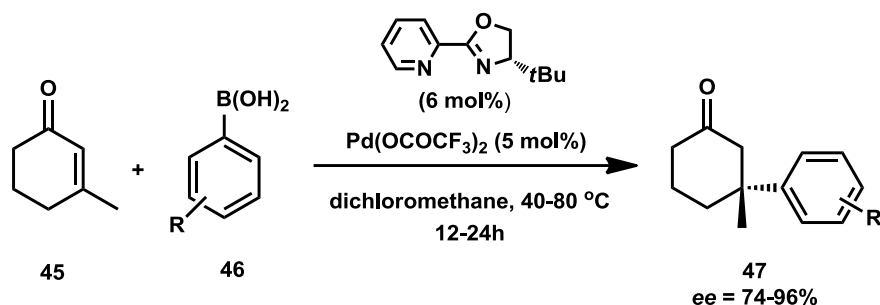
**Scheme 3.18**

Followed by this report, Gini *et al.* demonstrated the first asymmetric palladium-catalyzed conjugate addition of arylboronic acids to  $\alpha,\beta$ -unsaturated aldehydes, ketones, and esters using chiral bidentate phosphine ligands. For cyclic substrates, excellent chemo-, regio- and enantioselectivities are achieved when a  $\text{Pd}(\text{O}_2\text{CCF}_3)_2/\text{DuPHOS}$  catalyst is applied (Scheme 3.19) [Gini 2005].



**Scheme 3.19**

Later in 2011, a palladium-catalyzed asymmetric conjugate addition of arylboronic acids to five-, six-, and seven-membered  $\beta$ -substituted cyclic enones was reported by Stoltz *et al.* using a catalyst prepared from  $\text{Pd}(\text{OCOCF}_3)_2$  and a chiral pyridinooxazoline ligand, yielding enantioenriched products bearing benzylic stereocenters (Scheme 3.20) [Stoltz *et al.* 2012].



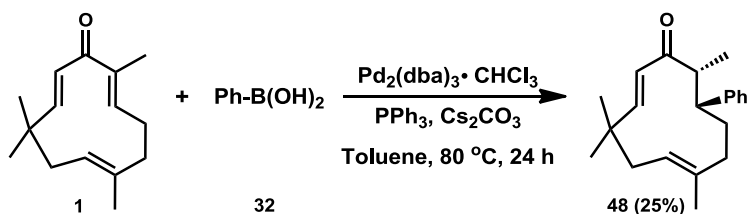
Scheme 3.20

### 3.5. Objective of the present work

The literature survey indicated that there are no reports on transition metal catalyzed synthetic transformations of zerumbone. It has been documented that zerumbone undergoes conjugate addition, ring-expansion, ring opening, reduction, epoxidation and asymmetric induction reactions. Most of the conjugate addition reactions of zerumbone reported so far suffer from drawbacks such as long reaction times (4–5 days), lack of generality, non-stereoselectivity and non-regioselectivity. This prompted us to investigate the conjugate addition reactions under transition-metal catalysis on this challenging sesquiterpene. Rhodium-catalyzed conjugate addition of organometallic compounds to  $\alpha,\beta$ -unsaturated ketones plays a pivotal role in organic synthesis. Most of the rhodium-catalyzed reactions reported so far are mild, general and, most importantly, highly stereoselective. Palladium-catalyzed 1,4-conjugate addition reactions of boronic acids to cyclic/acyclic enones are also known, albeit they are not as common as those mediated by rhodium. In this work, we disclose our efforts toward developing a new and general route to synthesize novel zerumbone derivatives *via* palladium and rhodium-catalyzed 1,4-conjugate addition reactions using organoboronic acids.

### 3.6. Results and discussion

In an initial reaction, zerumbone **1** (1 equiv.) was treated with phenylboronic acid **32** (2 equiv.) in the presence of tris(dibenzylideneacetone)dipalladium-chloroform [Pd<sub>2</sub>(dba)<sub>3</sub>·CHCl<sub>3</sub>] (5 mol%), cesium carbonate (Cs<sub>2</sub>CO<sub>3</sub>) (2 equiv.) and triphenylphosphine (PPh<sub>3</sub>) (10 mol%) in toluene at 80 °C for 24 hours. The reaction afforded the corresponding 1,4-conjugate addition product **48** in 25% yield (Scheme 3.21).



Scheme 3.21

The structure assigned to the product **48** was supported by spectral analysis. The IR spectrum of the compound showed characteristic carbonyl absorption at 1693 cm<sup>-1</sup>. In the <sup>1</sup>H NMR spectrum, the aromatic protons resonated at δ 7.38-7.33 and 7.28-7.25 as two separate multiplets. The protons on the olefinic carbons of enone moiety (C10 and C11) were discernible as a multiplet at δ 6.36-6.28. The doublet of doublet at δ 5.11 was assigned to the proton of isolated double bond at C7 carbon. The proton on the carbon (C4) containing phenyl ring was visible at δ 3.42 as a broad doublet. The peak due to proton at C2 carbon appeared as doublet of double doublet at δ 2.72. The protons at C8 carbon presented two separate peaks at δ 2.31 and 1.97-1.90 as a triplet and a multiplet respectively. The methylene protons at C5 carbon showed two multiplets at δ 2.03-1.99 and 1.05-0.99. The peaks due to one multiplet at δ 1.97-1.90 and one triplet at δ 1.55 correspond to two protons on the C4 carbon atom (Figure 3.3)

In <sup>13</sup>C NMR spectrum, the carbonyl carbon was seen at δ 202.8. The β-carbon of unsaturated ketone moiety was visible at δ 151.3. The carbon (C7) of isolated olefinic bond resonated at δ 126.4. The remaining two olefinic carbons and aromatic carbons appeared at δ 143.8, 137.8, 128.5, 128.4, 128.2 and 122.2. When the C2 carbon resonated at δ 46.2, the carbon with phenyl ring appeared at δ 53.9. Carbon of methyl group attached to the isolated double bond presented a signal at δ 16.7. The peak at δ 7.4 corresponds to the carbon of methyl group connected to C2 carbon atom (Figure 3.4). All other signals in the <sup>1</sup>H and <sup>13</sup>C NMR spectra were in good agreement with the proposed structure. The mass spectral analysis showed a peak at *m/z* 319.2030 (M+Na)<sup>+</sup>, which also supported the proposed structure (Figure 3.5).

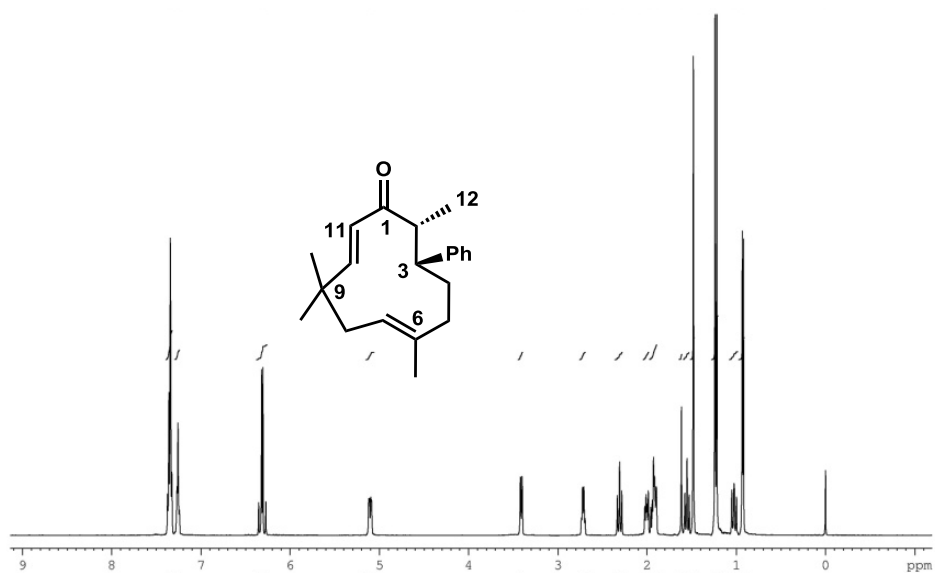


**Figure 3.3.**  $^1\text{H}$  NMR spectrum of compound 48

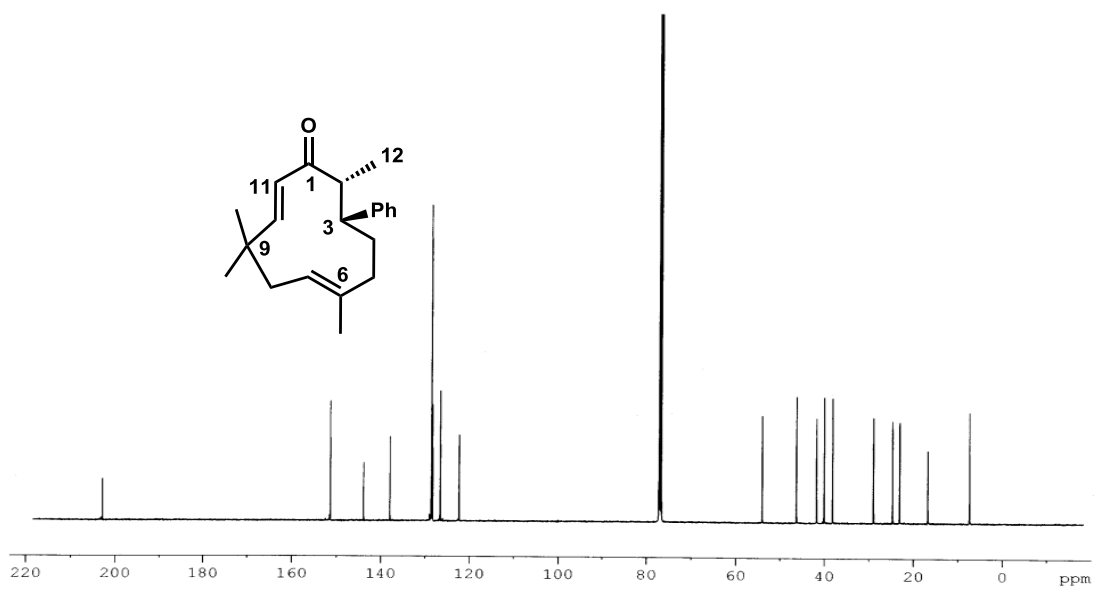


**Figure 3.4.**  $^{13}\text{C}$  NMR of compound 48



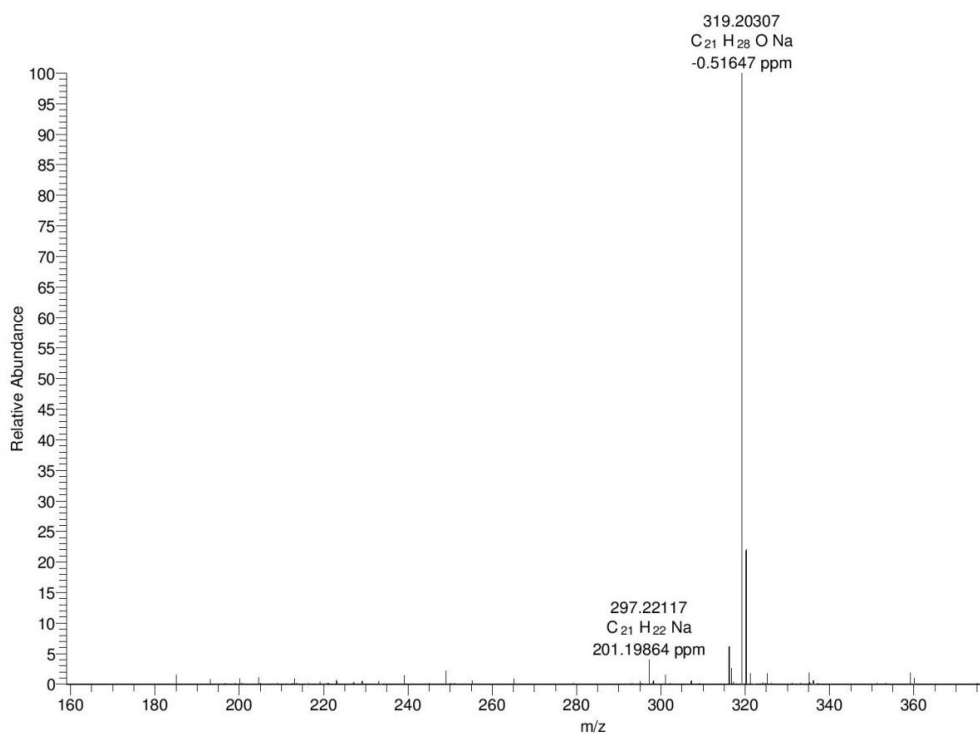


**Figure 3.5.** Mass spectra of compound **48**

The structure and stereochemistry of the product **48** was confirmed unambiguously by single crystal X-ray analysis (Figure 3.6). Compound **48** was crystallized from EtOAc–hexane to give crystals, which were suitable for single crystal X-ray analysis. The crystal data has been deposited at Cambridge Crystallographic Data Centre (CCDC) with deposition number CCDC: 910243.

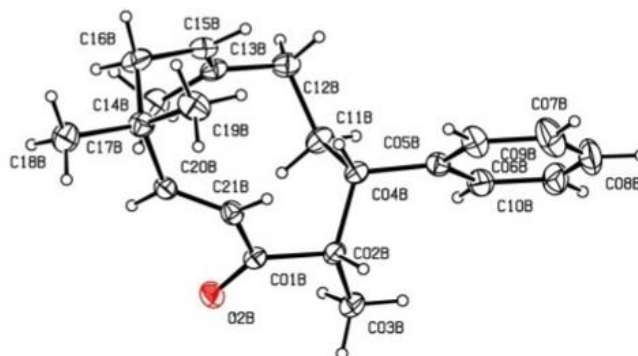


**Figure 3.6** Single crystal X-ray structure (ORTEP representation) of product **48**

In order to find a suitable catalytic system, detailed screening studies were carried out using different catalysts, ligands and bases. Our efforts toward optimizing the various reaction parameters are listed in Table 3.1. An investigation of the base revealed that

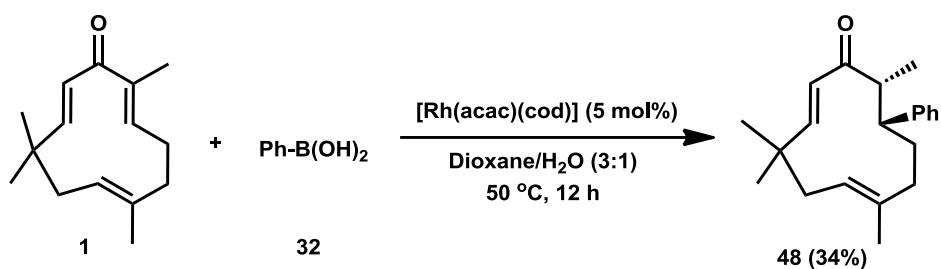
cesium carbonate was more effective than potassium carbonate ( $\text{K}_2\text{CO}_3$ ) and triethylamine ( $\text{Et}_3\text{N}$ ) (Table 3.1, entries 1, 4 and 5). We next turned our attention to ligand effects. From the ligands screened, triphenylphosphine was found to be the best (Table 3.1, entries 1, 8 and 9). Unfortunately, the palladium-catalyzed 1,4-conjugate addition reactions did not give the desired product in more than 30% yield.

**Table 3.1. Optimizatiion studies for palladium catalyzed 1,4-conjugate addition**

Entry <sup>a</sup>	Catalyst	Ligand	Base	Temp (°C)	Yield (%) <sup>b</sup>
1	$\text{Pd}_2(\text{dba})_3\cdot\text{CHCl}_3$	$\text{PPh}_3$	$\text{Cs}_2\text{CO}_3$	80	25
2	$\text{Pd}_2(\text{dba})_3\cdot\text{CHCl}_3$	$\text{PPh}_3$	$\text{Cs}_2\text{CO}_3$	100	30
3 <sup>c</sup>	$\text{Pd}_2(\text{dba})_3\cdot\text{CHCl}_3$	$\text{PPh}_3$	$\text{Cs}_2\text{CO}_3$	100	28
4	$\text{Pd}_2(\text{dba})_3\cdot\text{CHCl}_3$	$\text{PPh}_3$	$\text{K}_2\text{CO}_3$	100	–
5	$\text{Pd}_2(\text{dba})_3\cdot\text{CHCl}_3$	$\text{PPh}_3$	$\text{Et}_3\text{N}$	100	–
6 <sup>d</sup>	$\text{Pd}_2(\text{dba})_3\cdot\text{CHCl}_3$	$\text{PPh}_3$	$\text{Cs}_2\text{CO}_3$	120	30
7 <sup>e</sup>	$\text{Pd}_2(\text{dba})_3\cdot\text{CHCl}_3$	$\text{PPh}_3$	$\text{Cs}_2\text{CO}_3$	120	–
8	$\text{Pd}_2(\text{dba})_3\cdot\text{CHCl}_3$	dppe	$\text{Cs}_2\text{CO}_3$	100	–
9	$\text{Pd}_2(\text{dba})_3\cdot\text{CHCl}_3$	dppf	$\text{Cs}_2\text{CO}_3$	100	–
10	$\text{Pd}(\text{OAc})_2$	$\text{PPh}_3$	$\text{Cs}_2\text{CO}_3$	100	–
11	$\text{PdCl}_2$	$\text{PPh}_3$	$\text{Cs}_2\text{CO}_3$	100	–
12 <sup>f</sup>	$\text{Pd}(\text{OAc})_2$	$\text{PPh}_3$	$\text{Cs}_2\text{CO}_3$	100	–

<sup>a</sup> Reaction condition: Zerumbone (1 equiv.), boronic acid (2 equiv.), catalyst (5 mol%), ligand (10 mol%), base (1 equiv.), toluene (2 mL). <sup>b</sup> Isolated yield. <sup>c</sup> In presence of 0.01 mL water. <sup>d</sup> Reaction carried out in a sealed tube. <sup>e</sup> DMF as the solvent. <sup>f</sup> In presence of 0.01 mL of water and chloroform (2 mL)

We next turned our attention to the 1,4-conjugate addition of zerumbone using boronic acids under rhodium catalysis. In a test reaction, zerumbone (**1**) was treated with phenylboronic acid (**32**) in the presence of the rhodium(I) catalyst,  $[\text{Rh}(\text{acac})(\text{cod})]$ , which afforded the 1,4-addition product **48** in 34% yield (Scheme 3.22).



Scheme 3.22

The rhodium-catalyzed 1,4-conjugate addition reaction required a detailed optimization study to find the best conditions (Table 3.2). The reaction temperature proved to have a very important outcome (Table 3.2, entries 1–4); a yield of 61% was obtained when the reaction was performed at 100 °C (Table 3.2, entry 4). Various catalysts including [Rh(acac)(cod)], [Rh(Cl)(cod)]<sub>2</sub>, [Rh(OH)(cod)]<sub>2</sub> and [Rh(Cl)(coe)<sub>2</sub>]<sub>2</sub> were screened from which [Rh(acac)(cod)] gave the highest yield (Table 3.2, entries 5–9). Other parameters such as the ligand and solvent were also investigated. Addition of a ligand led to a reduction in the yield (Table 3.2, entries 9 and 10). Of the solvents tested, a mixture of 1,4-dioxane–water (3:1) gave a superior result compared to N,N-dimethylformamide and toluene. The optimized conditions were as follows: a 1:2 mixture of zerumbone–boronic acid, [Rh(acac)(cod)] (10 mol%) and 1,4-dioxane/H<sub>2</sub>O (3:1, 2 mL) as the solvent.

**Table 3.2. Optimization studies for rhodium catalyzed 1,4-conjugate addition**

Entry <sup>a</sup>	Catalyst	Mol %	Temp (°C)	Solvent	Time (h)	Yield 3 (%) <sup>b</sup>
1	[Rh(acac)(cod)]	5	50	dioxane/H <sub>2</sub> O	12	34
2	[Rh(acac)(cod)]	5	RT	dioxane/H <sub>2</sub> O	24	—
3	[Rh(acac)(cod)]	5	80	dioxane/H <sub>2</sub> O	24	48
4	[Rh(acac)(cod)]	5	100	dioxane/H <sub>2</sub> O	24	61
5	[Rh(acac)(cod)]	10	100	dioxane/H <sub>2</sub> O	12	70
6	[Rh(Cl)(cod)] <sub>2</sub>	10	100	dioxane/H <sub>2</sub> O	24	64
7	[Rh(Cl)(cod)] <sub>2</sub>	10	100	dioxane/H <sub>2</sub> O	24	Trace
8	[Rh(OH)(cod)] <sub>2</sub>	10	100	dioxane/H <sub>2</sub> O	24	5
9	[Rh(Cl)(coe) <sub>2</sub> ] <sub>2</sub>	10	100	dioxane/H <sub>2</sub> O	24	—
10 <sup>c</sup>	[Rh(acac)(cod)]	10	100	dioxane/H <sub>2</sub> O	12	61
11 <sup>d</sup>	[Rh(acac)(cod)]	10	100	dioxane/H <sub>2</sub> O	12	40
12 <sup>e</sup>	[Rh(acac)(cod)]	10	100	dioxane	12	10
13	[Rh(acac)(cod)]	10	100	DMF/H <sub>2</sub> O	12	7
14	[Rh(acac)(cod)]	10	100	Toluene	12	—

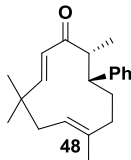
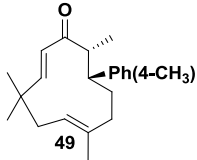
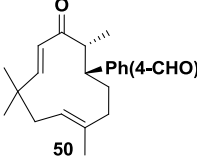
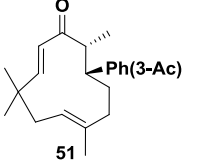
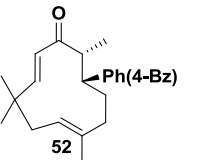
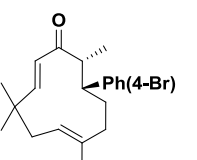
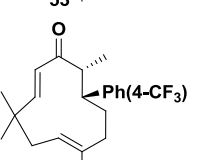
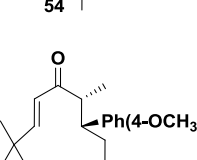
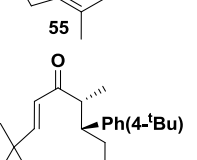
<sup>a</sup>Conditions: 1 (1 equiv.), 2 (2 equiv.), rhodium catalyst (x mol%), solvent (2 mL). <sup>b</sup>

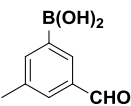
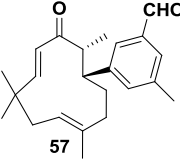
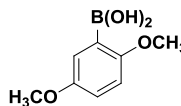
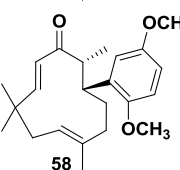
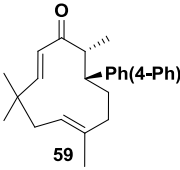
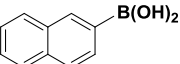
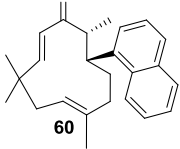
Isolated yield. <sup>c</sup> In presence of BINAP (10 mol%). <sup>d</sup> In presence of PPh<sub>3</sub> (10 mol%).

<sup>e</sup>Without water.

Subsequently, the scope of the reaction was explored under the optimized conditions using different substituted phenylboronic acids. In all cases, the desired 1,4-addition product was formed in moderate to good yield. The results are shown in Table 3.3. It is noteworthy that functionalized boronic acids such as **32a–32k** could be used in this 1,4-conjugate addition process, which should make it valuable for further development toward biologically important zerumbone derivatives.

Table 3.3. Generality of rhodium-catalyzed 1,4-conjugate addition

Entry <sup>a</sup>	Boronic acid	Time (h)	Product	Yield (%) <sup>b</sup>
1	PhB(OH) <sub>2</sub> 32	12		70
2	Ph(4-CH <sub>3</sub> )B(OH) <sub>2</sub> 32a	24		71
3	Ph(4-CHO)B(OH) <sub>2</sub> 32b	24		63
4	Ph(3-Ac)B(OH) <sub>2</sub> 32c	12		71
5	Ph(4-Bz)B(OH) <sub>2</sub> 32d	12		68
6	Ph(4-Br)B(OH) <sub>2</sub> 32e	12		40
7	Ph(4-CF <sub>3</sub> )B(OH) <sub>2</sub> 32f	24		60
8	Ph(4-OCH <sub>3</sub> )B(OH) <sub>2</sub> 32g	24		60
9	Ph(4- <sup>t</sup> Bu)B(OH) <sub>2</sub> 32h	24		66

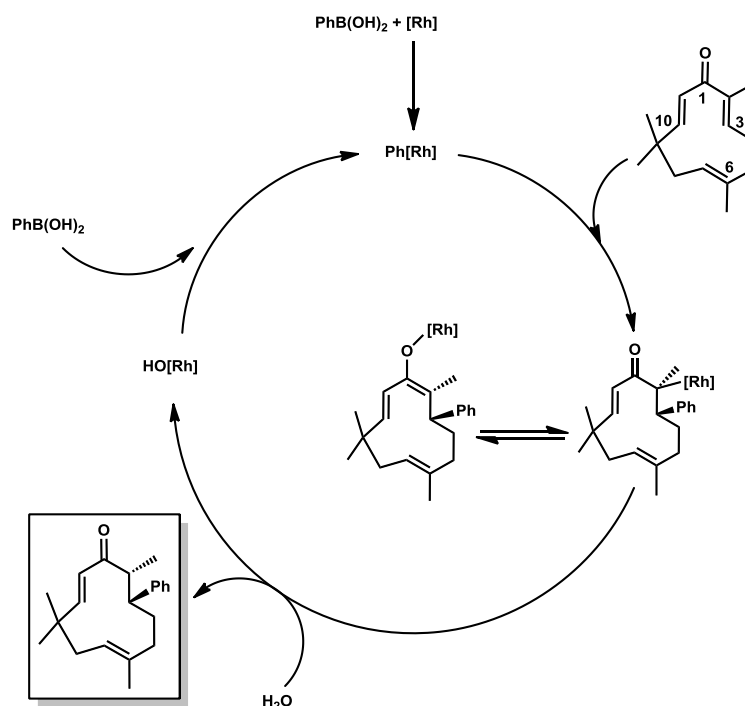
10	 <p>32i</p>	24	 <p>57</p>	30
11	 <p>32j</p>	24	 <p>58</p>	50
12	<p>Ph(4-Ph)B(OH)<sub>2</sub></p> <p>32l</p>	24	 <p>59</p>	75
13	 <p>32k</p>	24	 <p>60</p>	85

<sup>a</sup>Reaction conditions: Zerumbone (1equiv.), boronic acid (2 equiv.), [Rh(acac)(cod)] (10 mol%), solvent: Dioxane: water (3:1), (2 mL). <sup>b</sup> Isolated yield.

Unfortunately, the reaction did not work with heteroarylboronic acids such as pyridinyl and thienyl boronic acids.

### 3.7. Mechanistic pathway

The first step of the proposed mechanism involves transmetallation followed by the addition of the organometallic species to the double bond of the enone in a regio- and stereoselective manner. Subsequent hydrolysis of the Rh–O bond furnishes the conjugate addition product **48** (Scheme 3.23). The selective formation of a single diastereo-isomer is mainly due to the steric hindrance resulting from the methyl group at C-2 and the distorted structure of the conjugated double bonds in the parent molecule, zerumbone.



Scheme 3.23

### 3.8. Biological evaluation of 1,4-adducts

#### 3.8.1. Anti-bacterial properties

1,4-adducts were tested against gram negative and gram positive bacteria. As the parent molecule, the derivatives did not show any anti-bacterial properties under tested conditions.

#### 3.8.2. $\alpha$ -Glucosidase enzyme inhibition properties

Since, zerumbone showed a good  $\text{IC}_{50}$  value of  $95.7 \mu\text{M}$  against  $\alpha$ -glucosidase enzyme, we decided to check the activities of the synthesised adducts. Selected compounds were screened against  $\alpha$ -glucosidase enzyme, one of the leading targets in the treatment of diabetes mellitus type II. Unfortunately, none of them showed any significant inhibition in the range of  $5\text{-}100 \mu\text{M}$

### 3.9. Conclusion

In conclusion, we have developed a straightforward, catalytic and general method for the synthesis of novel zerumbone derivatives, *via* rhodium (I)-catalyzed 1,4-conjugate addition reactions using various boronic acids. The addition across the enone moiety of zerumbone took place in a regio- and diastereoselective manner. A comparative study of the reactivity of organopalladium and organorhodium reagents toward this 1,4-conjugate

addition reaction showed that, in most cases, the organopalladium reagents were inferior in terms of reactivity compared to organorhodium reagents. The synthesized molecules are expected to have high synthetic utility for the preparation of a number of biologically relevant molecules. We have evaluated the anti-microbial and  $\alpha$ -glucosidase inhibitory potential of the newly synthesized molecules under *in vitro* conditions. Unfortunately, the derivatives did not show any promising inhibitory activity as compared to zerumbone. However, analysis of the newly synthesized molecules against other targets is under way in our laboratory.

### 3.10. Experimental section

General information about the experiments is given in Section 2.11 of Chapter 2.

#### General Procedure for the synthesis of 1,4-adducts

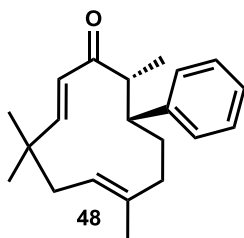
Zerumbone **1** (1 equiv.), arylboronic acid (2 equiv.) and rhodium catalyst (10 mol %) were taken in a Schlenk tube and degassed. The mixture was dissolved in 3:1 mixture of dioxane and water (2 mL) and stirred at 100 °C for 12-24 h under argon atmosphere. After the completion of the reaction (as indicated by TLC analysis), the solvent was evaporated in vacuo. The residue on silica gel (100-200 mesh) column chromatography using ethyl acetate in hexane afforded the product.

#### (2*E*,6*E*)-4,4,7,11-Tetramethyl-10-phenylcycloundeca-2,6-dienone **48**

Following the general experimental procedure, the zerumbone **1** (30 mg, 0.14 mmol), phenylboronic acid **32** (33.5 mg, 0.28 mmol), catalyst [Rh(acac)(cod)] (8.52 mg, 0.03 mmol) in 1,4-dioxane-H<sub>2</sub>O (3:1, 2 mL) at 100 °C for 12 h under argon atmosphere gave the product **48** as a white crystalline solid (28.5 mg, 70%). R<sub>f</sub>: 0.46 (1:9 EtOAc-hexane); Mp: 70 °C.

**IR** (KBr)  $\nu_{\text{max}}$ : 3024, 2959, 2938, 2871, 1693, 1628, 1452, 1383, 1301, 1042, 999, 840, 743, 701 cm<sup>-1</sup>.

**<sup>1</sup>H NMR** (500 MHz, CDCl<sub>3</sub>):  $\delta$  7.38-7.33 (m, 4H), 7.28-7.25 (m, 1H), 6.36-6.28 (m, 2H), 5.11 (dd,  $J_1 = 11.5$  Hz,  $J_2 = 4.0$  Hz, 1H), 3.42 (br.d, 1H), 2.72





(ddd,  $J_1 = 13.0$  Hz,  $J_2 = 6.5$  Hz,  $J_3 = 2.5$  Hz, 1H), 2.31 (t,  $J = 12.5$  Hz, 1H), 2.03-1.99 (m, 1H), 1.97-1.90 (m, 2H), 1.55 (t,  $J = 12.0$  Hz, 1H), 1.49 (s, 3H), 1.24 (s, 3H), 1.22 (s, 3H), 1.05-0.99 (m, 1H), 0.93 (d,  $J = 5.0$  Hz, 3H).

$^{13}\text{C}$  NMR (125 MHz,  $\text{CDCl}_3$ ):  $\delta$  202.8, 151.3, 143.8, 137.8, 128.5, 128.4, 128.2, 126.4, 122.2, 53.9, 46.2, 41.7, 40.0, 38.1, 28.9, 24.7, 23.1, 16.7, 7.4.

Mass Spectrometric Analysis: **HRMS** (ESI):  $m/z$  calcd for  $\text{C}_{21}\text{H}_{28}\text{ONa}$ : 319.2038, found: 319.2030.

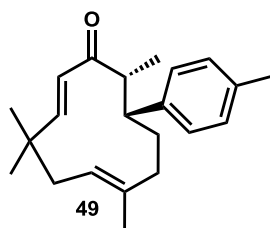
Crystal data of compound **48**: The unit cell parameters of the crystal are: a 11.3478(5), b 12.8754(6), c 12.5373(6) and beta 95.178(2) with space group P21.

**(2E,6E)-4,4,7,11-Tetramethyl-10-(p-tolyl)cycloundeca-2,6-dienone 49**

Following the general experimental procedure, the zerumbone **1** (30 mg, 0.14 mmol), 4-methyl phenylboronic acid **32a** (37.39 mg, 0.28 mmol), catalyst  $[\text{Rh}(\text{acac})(\text{cod})]$  (8.52 mg, 0.03 mmol) in 1,4-dioxane- $\text{H}_2\text{O}$  (3:1, 2 mL) at 100 °C for 24 h under argon atmosphere gave the product **49** as a pale yellow viscous liquid (30.5 mg, 71%). R<sub>f</sub>: 0.56 (1:9 EtOAc-hexane).

**IR** (neat)  $\nu_{\text{max}}$ : 2921, 2853, 1738, 1690, 1624, 1599, 1454, 1379, 1264, 1118, 1040, 810, 699, 647  $\text{cm}^{-1}$ .

$^1\text{H}$  NMR (500 MHz,  $\text{CDCl}_3$ ):  $\delta$  7.26-7.13 (m, 4H), 6.35-6.20 (m, 2H), 5.09 (br.d, 1H), 3.36 (br.d, 1H), 2.67 (ddd,  $J_1 = 13.0$  Hz,  $J_2 = 6.5$  Hz,  $J_3 = 2.5$  Hz, 1H), 2.35 (s, 3H), 2.31 (t,  $J = 13.2$  Hz, 1H), 2.02-1.84 (m, 3H), 1.57-1.50 (m, 1H), 1.48 (s, 3H), 1.24 (s, 3H), 1.22 (s, 3H), 1.05-



0.96 (m, 1H), 0.91 (d,  $J = 6.6$  Hz, 3H).

$^{13}\text{C}$  NMR (125 MHz,  $\text{CDCl}_3$ ):  $\delta$  203.3, 151.5, 140.7, 137.9, 136.1, 129.2, 129.1, 128.8, 128.7, 128.4, 122.2, 54.1, 45.9, 41.7, 40.1, 38.1, 29.1, 24.7, 23.1, 21.0, 16.9, 7.6.

Mass Spectrometric Analysis: **HRMS** (ESI):  $m/z$  calcd for  $\text{C}_{22}\text{H}_{30}\text{ONa}$ : 333.2194, found: 333.2183.

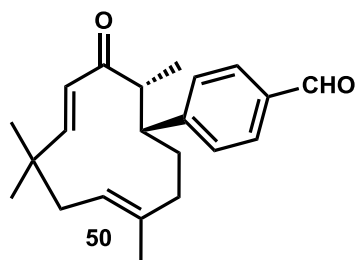
**4-((4E,8E)-2,6,6,9-Tetramethyl-3-oxocycloundeca-4,8-dien-1-yl)benzaldehyde 50**

Following the general experimental procedure, the zerumbone **1** (30 mg, 0.14 mmol), 4-formylphenylboronic acid **32b** (37.39 mg, 0.28 mmol), catalyst  $[\text{Rh}(\text{acac})(\text{cod})]$  (8.52 mg, 0.03 mmol) in 1,4-dioxane- $\text{H}_2\text{O}$  (3:1, 2 mL) at 100 °C for 24 h under argon atmosphere gave the product **50** as a colourless viscous liquid (28 mg, 63%).  $R_f$ : 0.29 (1:9 EtOAc-hexane).

**IR** (neat)  $\nu_{\text{max}}$ : 2920, 2852, 1736, 1682, 1654, 1600, 1511, 1457, 1420, 1254, 1120, 1041, 846, 698, 645  $\text{cm}^{-1}$ .

$^1\text{H}$  NMR (500 MHz,  $\text{CDCl}_3$ ):  $\delta$  10.01 (s, 1H), 7.87 (d,  $J = 8.0$  Hz, 2H), 7.51 (d,  $J = 8.0$  Hz, 2H), 6.31 (s, 2H), 5.08 (dd,  $J_1 = 11.5$  Hz,  $J_2 = 4.0$  Hz, 1H), 3.48 (br.d, 1H), 2.67 (ddd,  $J_1 = 9.0$  Hz,  $J_2 = 6.5$  Hz,  $J_3 = 2.0$  Hz, 1H), 2.31 (t,  $J = 12.5$  Hz, 1H), 2.06-1.89 (m, 3H), 1.54-1.48 (m, 1H), 1.47 (s, 3H), 1.25 (s, 3H), 1.24 (s, 3H), 1.12-1.00 (m, 1H), 0.93 (d,  $J = 6.5$  Hz, 3H).

$^{13}\text{C}$  NMR (125 MHz,  $\text{CDCl}_3$ ):  $\delta$  202.5, 191.8, 152.1, 151.1, 137.6, 135.1, 130.1, 130.0, 129.4, 129.2, 127.9, 122.6,



53.6, 46.7, 41.2, 40.2, 38.1, 29.1, 24.5,  
23.2, 16.9, 7.6.

Mass Spectrometric Analysis: **HRMS** (ESI):  $m/z$  calcd for  $C_{22}H_{28}O_2Na$ : 347.1987, found: 347.1980.

**(2E,6E)-10-(3-acetylphenyl)-4,4,7,11-tetramethylcycloundeca-2,6-dienone 51**

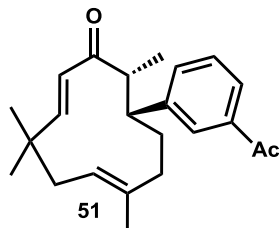
Following the general experimental procedure, the zerumbone **1** (30 mg, 0.14 mmol), 3-acetylphenylboronic acid **32c** (45.09 mg, 0.28 mmol), catalyst [Rh(acac)(cod)] (8.52 mg, 0.03 mmol) in 1,4-dioxane- $H_2O$  (3:1, 2 mL) at 100 °C for 12 h under argon atmosphere gave the product **51** as a pale yellow viscous liquid (33 mg, 68%).  $R_f$ : 0.27 (1:9 EtOAc-hexane).

**IR** (neat)  $\nu_{max}$ : 2957, 2929, 2855, 1689, 1628, 1453, 1362, 1269, 1173, 1043, 999, 844, 794, 699, 588  $cm^{-1}$ .

**$^1H$  NMR** (500 MHz,  $CDCl_3$ ):  $\delta$  7.94 (s, 1H), 7.84 (d,  $J = 7.5$  Hz, 1H), 7.55 (d,  $J = 8$  Hz, 1H), 7.47 (t,  $J = 7.5$  Hz, 1H), 6.37-6.29 (m, 2H), 5.11 (dd,  $J_1 = 11.5$  Hz,  $J_2 = 4$  Hz, 1H), 3.47 (br.d, 1H), 2.72 (ddd,  $J_1 = 13$  Hz,  $J_2 = 6.5$  Hz,  $J_3 = 2.5$  Hz, 1H), 2.64 (s, 3H), 2.36-2.28 (m, 1H), 2.05-1.90 (m, 3H), 1.52 (t,  $J = 12$  Hz, 1H), 1.49 (s, 3H), 1.25 (s, 3H), 1.23 (s, 3H), 1.05 (m, 1H), 0.91 (d,  $J = 6.5$  Hz, 3H).

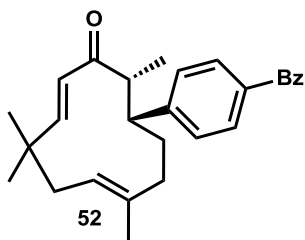
**$^{13}C$  NMR** (125 MHz,  $CDCl_3$ ):  $\delta$  202.3, 197.8, 151.7, 144.5, 137.7, 137.6, 133.0, 128.6, 127.9, 127.8, 126.8, 122.4, 53.7, 46.2, 41.6, 40.0, 38.1, 29.3, 26.4, 24.7, 23.2, 16.7, 7.4.

Mass Spectrometric Analysis: **HRMS** (ESI):  $m/z$  calcd for  $C_{23}H_{30}O_2Na$ : 361.2143, found: 361.2131.



**(2E,6E)-10-(4-benzoylphenyl)-4,4,7,11-tetramethylcycloundeca-2,6-dienone 52**

Following the general experimental procedure, the zerumbone **1** (30 mg, 0.14 mmol), 4-benzoylphenylboronic acid **32d** (62.16 mg, 0.28 mmol), catalyst [Rh(acac)(cod)] (8.52 mg, 0.03 mmol) in 1,4-dioxane-H<sub>2</sub>O (3:1, 2 mL) at 100 °C for 12 h under argon atmosphere gave the product **52** as a colourless viscous liquid (36 mg, 68%). R<sub>f</sub>: 0.32 (1:9 EtOAc-hexane).



**IR** (neat)  $\nu_{\max}$ : 3028, 2957, 2934, 2869, 1692, 1658, 1627, 1603, 1449, 1382, 1313, 1279, 1177, 1042, 1000, 923, 855, 738, 703, 625 cm<sup>-1</sup>.

**<sup>1</sup>H NMR** (500 MHz, CDCl<sub>3</sub>):  $\delta$  7.83-7.81 (m, 4H), 7.60 (t,  $J = 7.5$  Hz, 1H), 7.53-7.44 (m, 4H), 6.33 (s, 2H), 5.12 (dd,  $J_1 = 11.5$  Hz,  $J_2 = 4.5$  Hz, 1H), 3.51 (br.d, 1H), 2.75 (ddd,  $J_1 = 13.0$  Hz,  $J_2 = 6.5$  Hz,  $J_3 = 2.0$  Hz, 1H), 2.35-2.30 (m, 1H), 2.07-2.03 (m, 1H), 2.00-1.91 (m, 2H), 1.58 (t,  $J = 12.0$  Hz, 1H), 1.49 (s, 3H), 1.25 (s, 3H), 1.23 (s, 3H), 1.05-1.01 (m, 1H), 0.95 (d,  $J = 7.0$  Hz, 3H).

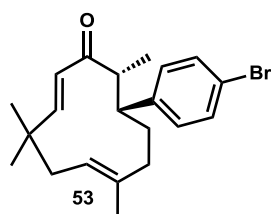
**<sup>13</sup>C NMR** (125 MHz, CDCl<sub>3</sub>):  $\delta$  202.2, 195.9, 151.8, 148.8, 137.9, 137.6, 136.2, 132.2, 130.3, 129.8, 128.3, 128.2, 127.9, 122.4, 53.6, 46.4, 41.7, 40.1, 38.1, 28.9, 24.6, 23.1, 16.8, 7.4.

Mass Spectrometric Analysis: **HRMS** (ESI):  $m/z$  calcd for C<sub>28</sub>H<sub>32</sub>O<sub>2</sub>Na: 423.2300, found: 423.2293.

**(2E,6E)-10-(4-bromophenyl)-4,4,7,11-tetramethylcycloundeca-2,6-dienone 53**

Following the general experimental procedure, the zerumbone **1** (30 mg, 0.14 mmol), 4-bromophenylboronic acid **32e** (55.22 mg, 0.28 mmol), catalyst [Rh(acac)(cod)] (8.52 mg, 0.03 mmol) in 1,4-dioxane-H<sub>2</sub>O (3:1, 2 mL) at 100 °C for 12 h under argon

atmosphere gave the product **53** as a pale yellow viscous liquid (20 mg, 40%).  $R_f$ : 0.45 (1:9 EtOAc-hexane).



**IR** (neat)  $\nu_{\max}$ : 2958, 2934, 2870, 1693, 1628, 1488, 1453, 1407, 1382, 1302, 1264, 1077, 1008, 817, 720, 556  $\text{cm}^{-1}$ .

**<sup>1</sup>H NMR** (500 MHz, CDCl<sub>3</sub>):  $\delta$  7.46 (d,  $J$  = 8.5 Hz, 2H), 7.21 (d,  $J$  = 8.5 Hz, 2H), 6.29 (s, 2H), 5.08 (dd,  $J_1$  = 11.5 Hz,  $J_2$  = 4.0 Hz, 1H), 3.36 (dd,  $J_1$  = 8.0 Hz,  $J_2$  = 1.0 Hz, 1H), 2.66 (ddd,  $J_1$  = 13.0 Hz,  $J_2$  = 6.5 Hz,  $J_3$  = 2.0 Hz, 1H), 2.30 (t,  $J$  = 12.5 Hz, 1H), 2.03-1.99 (m, 1H), 1.92-1.82 (m, 2H), 1.50 (t,  $J$  = 12.5 Hz, 1H), 1.47 (s, 3H), 1.23 (s, 3H), 1.21 (s, 3H), 1.05-0.99 (m, 1H), 0.90 (d,  $J$  = 7.0 Hz, 3H).

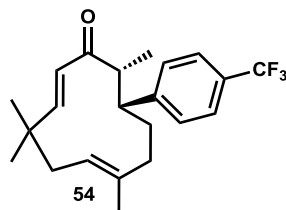
**<sup>13</sup>C NMR** (125 MHz, CDCl<sub>3</sub>):  $\delta$  202.5, 151.7, 142.8, 137.6, 131.6, 130.1, 127.9, 122.3, 120.3, 53.7, 45.8, 41.7, 40.0, 38.0, 28.9, 24.7, 23.1, 16.7, 7.3.

Mass Spectrometric Analysis: **HRMS** (ESI):  $m/z$  calcd for C<sub>21</sub>H<sub>27</sub>BrONa: 397.1143, found: 397.1137.

#### **(2*E*,6*E*)-4,4,7,11-Tetramethyl-10-(4-(trifluoromethyl)phenyl)cycloundeca-2,6-dienone **54****

Following the general experimental procedure, the zerumbone **1** (30 mg, 0.14 mmol), 4-(trifluoromethyl)phenylboronic acid **32f** (52.53 mg, 0.28 mmol), catalyst [Rh(acac)(cod)] (8.52 mg, 0.03 mmol) in 1,4-dioxane-H<sub>2</sub>O (3:1, 2 mL) at 100 °C for 12 h under argon atmosphere gave the product **54** as a white crystalline solid (30 mg, 60%).  $R_f$ : 0.49 (1:9 EtOAc-hexane). Mp: 104-106 °C.

**IR** (KBr)  $\nu_{\max}$ : 3041, 2920, 2853,



1738, 1693, 1624, 1453, 1418, 1382, 1325, 1264, 1163, 1122, 1069, 1042, 999, 845, 715, 668, 646 cm<sup>-1</sup>.

<sup>1</sup>H NMR (500 MHz, CDCl<sub>3</sub>): δ 7.62 (d, *J* = 8.0 Hz, 2H), 7.45 (d, *J* = 8.0 Hz, 2H), 6.32 (s, 2H), 5.10 (dd, *J*<sub>1</sub> = 11.5 Hz, *J*<sub>2</sub> = 4.0 Hz, 1H), 3.47 (br.d, 1H), 2.70 (ddd, *J*<sub>1</sub> = 9.0 Hz, *J*<sub>2</sub> = 6.6 Hz, *J*<sub>3</sub> = 2.5 Hz, 1H), 2.31 (t, *J* = 13.0 Hz, 1H), 2.05-2.01 (m, 1H), 1.96-1.89 (m, 2H), 1.53-1.48 (m, 1H), 1.49 (s, 3H), 1.24 (s, 3H), 1.23 (s, 3H), 1.09-1.04 (m, 1H), 0.92 (d, *J* = 7.0 Hz, 3H).

<sup>13</sup>C NMR (125 MHz, CDCl<sub>3</sub>): δ 202.6, 152.0, 147.8, 137.6, 129.1, 128.8, 127.9, 125.5, 125.4, 125.2, 122.4, 53.6, 46.3, 41.6, 40.2, 38.0, 28.9, 24.5, 23.1, 16.8, 7.5.

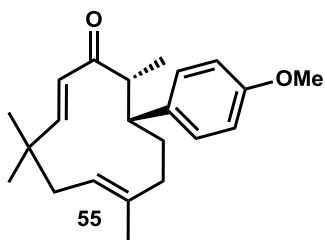
Mass Spectrometric Analysis: **HRMS** (ESI): *m/z* calcd for C<sub>22</sub>H<sub>27</sub>F<sub>3</sub>ONa: 387.1912, found: 387.1904.

**(2*E*,6*E*)-10-(4-methoxyphenyl)-4,4,7,11-tetramethylcycloundeca-2,6-dienone 55**

Following the general experimental procedure, the zerumbone **1** (30 mg, 0.14 mmol), 4-methoxyphenylboronic acid **32g** (41.79 mg, 0.28 mmol), catalyst [Rh(acac)(cod)] (8.52 mg, 0.03 mmol) in 1,4-dioxane-H<sub>2</sub>O (3:1, 2 mL) at 100 °C for 24 h under argon atmosphere gave the product **55** as a colourless viscous liquid (26 mg, 60%). R<sub>f</sub>: 0.44 (1:9 EtOAc-hexane).

**IR** (neat) ν<sub>max</sub>: 2919, 2851, 1735, 1687, 1607, 1511, 1457, 1419, 1378, 1248, 1117, 1038, 832, 700, 646 cm<sup>-1</sup>.

<sup>1</sup>H NMR (500 MHz, CDCl<sub>3</sub>): δ 7.25



(d,  $J = 8.5$  Hz, 2H), 6.90 (d,  $J = 8.5$  Hz, 2H), 6.34-6.26 (m, 2H), 5.10 (dd,  $J_1 = 12.0$  Hz,  $J_2 = 4.0$  Hz, 1H), 3.82 (s, 3H), 3.34 (br.d, 1H), 2.68 (ddd,  $J_1 = 9$  Hz,  $J_2 = 7.0$  Hz,  $J_3 = 2.5$  Hz, 1H), 2.30 (t,  $J = 12.5$  Hz, 1H), 2.01-1.97 (m, 1H), 1.92-1.83 (m, 2H), 1.54 (t,  $J = 12$  Hz, 1H), 1.47 (s, 3H), 1.23 (s, 3H), 1.21 (s, 3H), 1.03-0.97 (m, 1H), 0.91 (d,  $J = 7.0$  Hz, 3H).

$^{13}\text{C}$  NMR (125 MHz,  $\text{CDCl}_3$ ):  $\delta$  203.5, 158.2, 151.5, 137.9, 135.7, 129.4, 128.3, 122.1, 113.8, 55.3, 54.2, 45.5, 41.6, 40.1, 38.1, 29.0, 24.9, 23.1, 16.9, 7.5.

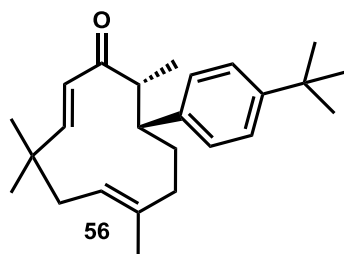
Mass Spectrometric Analysis: HRMS (ESI):  $m/z$  calcd for  $\text{C}_{22}\text{H}_{30}\text{O}_2\text{Na}$ : 349.2143, found: 349.2137.

**(2E,6E)-10-(4-(tert-butyl)phenyl)-4,4,7,11-tetramethylcycloundeca-2,6-dienone 56**

Following the general experimental procedure, the zerumbone **1** (30 mg, 0.14 mmol), 4-tert-butylphenylboronic acid **32h** (48.96 mg, 0.28 mmol), catalyst  $[\text{Rh}(\text{acac})(\text{cod})]$  (8.52 mg, 0.03 mmol) in 1,4-dioxane- $\text{H}_2\text{O}$  (3:1, 2 mL) at 100 °C for 24 h under argon atmosphere gave the product **56** as a pale yellow viscous liquid (32 mg, 66%).  $R_f$ : 0.44 (1:9 EtOAc-hexane).

IR (neat)  $\nu_{\text{max}}$ : 2925, 2851, 1735, 1690, 1626, 1599, 1451, 1377, 1263, 1118, 1040, 810, 699, 647  $\text{cm}^{-1}$ .

$^1\text{H}$  NMR (500 MHz,  $\text{CDCl}_3$ ):  $\delta$  7.36 (d,  $J = 8.5$  Hz, 2H), 7.25 (d,  $J = 8$  Hz, 2H), 6.35-6.26 (m, 2H), 5.09 (dd,  $J_1 = 11.5$  Hz,  $J_2 = 4$  Hz, 1H), 3.37 (br.d, 1H), 2.72 (ddd,  $J_1 = 13$  Hz,  $J_2 = 6.5$  Hz,  $J_3 = 2$  Hz, 1H), 2.30 (t,  $J = 12.5$  Hz, 1H), 2.02-1.98 (m,



1H), 1.92-1.88 (m, 2H), 1.62-1.55 (m, 1H), 1.48 (s, 3H), 1.33 (s, 9H), 1.23 (s, 3H), 1.21 (s, 3H), 1.03-0.98 (m, 1H), 0.93 (d,  $J = 7$  Hz, 3H).

$^{13}\text{C}$  NMR (125 MHz,  $\text{CDCl}_3$ ):  $\delta$  203.6, 151.4, 149.3, 140.6, 137.9, 128.3, 128.1, 125.3, 122.1, 53.9, 45.6, 41.7, 40.1, 38.2, 34.4, 31.4, 29.0, 24.7, 23.1, 16.8, 7.6.

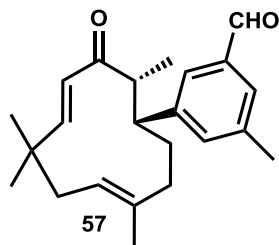
Mass Spectrometric Analysis: **HRMS** (ESI):  $m/z$  calcd for  $\text{C}_{25}\text{H}_{36}\text{ONa}$ : 375.2664, found: 375.2651.

### 3-Methyl-5-((4E,8E)-2,6,6,9-tetramethyl-3-oxocycloundeca-4,8-dienyl)benzaldehyde 57

Following the general experimental procedure, the zerumbone **1** (30 mg, 0.14 mmol), 3-formyl-5-methylphenylboronic acid **32i** (45.11 mg, 0.28 mmol), catalyst  $[\text{Rh}(\text{acac})(\text{cod})]$  (8.52 mg, 0.03 mmol) in 1,4-dioxane- $\text{H}_2\text{O}$  (3:1, 2 mL) at  $100^\circ\text{C}$  for 24 h under argon atmosphere gave the product **57** as a pale yellow viscous liquid (13 mg, 30%).  $R_f$ : 0.28 (1:9 EtOAc-hexane).

**IR** (neat)  $\nu_{\text{max}}$ : 2956, 2926, 2855, 2724, 1696, 1627, 1601, 1454, 1348, 1264, 1144, 1044, 999, 862, 701, 668,  $564\text{ cm}^{-1}$ .

$^1\text{H}$  NMR (500 MHz,  $\text{CDCl}_3$ ):  $\delta$  10.02 (s, 1H), 7.65 (s, 1H), 7.58 (s, 1H), 7.39 (s, 1H), 6.36-6.30 (m, 2H), 5.11 (dd,  $J_1 = 11.5$  Hz,  $J_2 = 4.0$  Hz, 1H), 3.45 (br.d, 1H), 2.71 (ddd,  $J_1 = 13.3$  Hz,  $J_2 = 7.0$  Hz,  $J_3 = 2.5$  Hz, 1H), 2.48 (s, 3H), 2.31 (t,  $J = 12.5$  Hz, 1H), 2.06-2.02 (m, 1H), 1.99-1.91 (m, 2H), 1.63 (s, 3H), 1.54-1.51 (m, 1H), 1.26 (s, 3H), 1.23 (s, 3H), 1.05-1.02 (m, 1H), 0.91 (d,  $J = 6.5$  Hz, 3H).



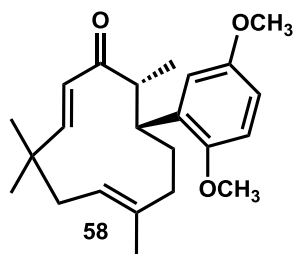


$^{13}\text{C}$  NMR (125 MHz,  $\text{CDCl}_3$ ):  $\delta$  202.2, 192.2, 151.8, 144.9, 139.1, 137.6, 135.3, 133.7, 129.0, 127.9, 126.3, 122.4, 53.7, 46.1, 41.6, 40.0, 38.1, 28.9, 24.6, 23.2, 21.2, 16.8, 7.4.

Mass Spectrometric Analysis: **HRMS** (ESI):  $m/z$  calcd for  $\text{C}_{23}\text{H}_{30}\text{O}_2\text{Na}$ : 361.2143, found: 361.2131.

**(2E,6E)-10-(2,5-Dimethoxyphenyl)-4,4,7,11-tetramethylcycloundeca-2,6-dienone 58**

Following the general experimental procedure, the zerumbone **1** (30 mg, 0.14 mmol), 2,5-dimethoxyphenylboronic acid **32j** (50.04 mg, 0.28 mmol), catalyst [Rh(acac)(cod)] (8.52 mg, 0.03 mmol) in 1,4-dioxane- $\text{H}_2\text{O}$  (3:1, 2 mL) at 100 °C for 24 h under argon atmosphere gave the product **58** as a white crystalline solid (24.40 mg, 68%).  $R_f$ : 0.34 (1:9 EtOAc-hexane). Mp: 138-140 °C.



**IR** (KBr)  $\nu_{\text{max}}$ : 2956, 2928, 2871, 1693, 1629, 1612, 1586, 1503, 1458, 1367, 1291, 1208, 1154, 1039, 837, 798, 632  $\text{cm}^{-1}$ .

$^1\text{H}$  NMR (500 MHz,  $\text{CDCl}_3$ ):  $\delta$  7.15 (d,  $J = 8.5$  Hz, 1H), 6.53-6.45 (m, 3H), 6.22 (d,  $J = 16.0$  Hz, 1H), 5.08 (dd,  $J_1 = 11.5$  Hz,  $J_2 = 4.0$  Hz, 1H), 3.93 (s, 3H), 3.86 (br.d, 1H), 3.81 (s, 3H), 2.60 (ddd,  $J_1 = 13.5$  Hz,  $J_2 = 7.0$  Hz,  $J_3 = 2.0$  Hz, 1H), 2.30 (t,  $J = 12.5$  Hz, 1H), 1.94-1.82 (m, 3H), 1.47 (s, 3H), 1.41 (t,  $J = 12.0$  Hz, 1H), 1.26 (s, 3H), 1.21 (s, 3H), 0.91-0.89 (m, 1H), 0.83 (d,  $J = 7.0$  Hz, 3H).

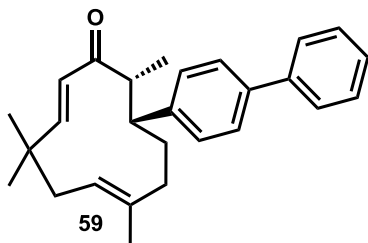
$^{13}\text{C}$  NMR (125 MHz,  $\text{CDCl}_3$ ):  $\delta$  203.4, 159.4, 158.5, 150.1, 137.5, 128.7, 128.0, 124.3, 122.2, 103.7, 98.9, 55.4,

55.2, 51.6, 41.9, 40.0, 38.0, 37.0, 29.1, 23.8, 22.8, 16.7, 7.2.

Mass Spectrometric Analysis: **HRMS** (ESI):  $m/z$  calcd for  $C_{23}H_{32}O_3Na$ : 379.2249, found: 379.2242.

**(2E,6E)-10-(Biphenyl-4-yl)-4,4,7,11-tetramethylcycloundeca-2,6-dienone 59**

Following the general experimental procedure, the zerumbone **1** (30 mg, 0.14 mmol), 4-biphenylboronic acid **32k** (54.45 mg, 0.28 mmol), catalyst [Rh(acac)(cod)] (8.52 mg, 0.03 mmol) in 1,4-dioxane- $H_2O$  (3:1, 2 mL) at 100 °C for 12 h under argon atmosphere gave the product **59** as a colourless viscous liquid (38 mg, 75%).  $R_f$ : 0.44 (1:9 EtOAc-hexane).



**IR** (neat)  $\nu_{max}$ : 3028, 2958, 2934, 2869, 1693, 1628, 1486, 1452, 1382, 1366, 1301, 1042, 1001, 843, 755, 697, 562  $cm^{-1}$ .

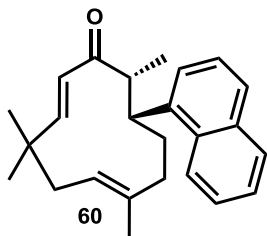
**$^1H$  NMR** (500 MHz,  $CDCl_3$ ):  $\delta$  7.61-7.56 (m, 4H), 7.45-7.39 (m, 4H), 7.35-7.32 (m, 1H), 6.37-6.28 (m, 2H), 5.12 (dd,  $J_1 = 11.0$  Hz,  $J_2 = 3.5$  Hz, 1H), 3.46 (br.d, 1H), 2.76 (ddd,  $J_1 = 13.5$  Hz,  $J_2 = 6.5$  Hz,  $J_3 = 2.5$  Hz, 1H), 2.32 (t,  $J = 12.5$  Hz, 1H), 2.06-2.01 (m, 1H), 1.99-1.90 (m, 2H), 1.59 (t,  $J = 11.5$  Hz, 1H), 1.45 (s, 3H), 1.25 (s, 3H), 1.23 (s, 3H), 1.05-1.01 (m, 1H), 0.96 (d,  $J = 7.0$  Hz, 3H).

**$^{13}C$  NMR** (125 MHz,  $CDCl_3$ ):  $\delta$  202.7, 151.6, 142.9, 142.8, 140.8, 139.5, 137.8, 128.9, 128.8, 128.2, 127.2, 127.1, 126.9, 122.3, 53.9, 45.9, 41.7, 40.1, 38.2, 28.9, 24.8, 23.1, 16.8, 7.6.

Mass Spectrometric Analysis: **HRMS** (ESI):  $m/z$  calcd for  $C_{27}H_{32}ONa$ : 395.2351, found: 395.2344.

**(2E,6E)-4,4,7,11-Tetramethyl-10-(naphthalen-1-yl)cycloundeca-2,6-dienone 60**

Following the general experimental procedure, the zerumbone **1** (30 mg, 0.14 mmol), 1-naphthylphenylboronic acid **32i** (47.29 mg, 0.28 mmol), catalyst [Rh(acac)(cod)] (8.52 mg, 0.03 mmol) in 1,4-dioxane- $H_2O$  (3:1, 2 mL) at 100 °C for 24 h under argon atmosphere gave the product **60** as a pale yellow viscous liquid (40 mg, 85%).  $R_f$ : 0.45 (1:9 EtOAc-hexane).



**IR** (neat)  $\nu_{max}$ : 3047, 2960, 2935, 2870, 1693, 1629, 1511, 1472, 1381, 1299, 1264, 1042, 997, 846, 795, 779, 729, 677, 565  $cm^{-1}$ .

**$^1H$  NMR** (500 MHz,  $CDCl_3$ ):  $\delta$  8.34 (d,  $J = 8.5$  Hz, 1H), 7.94 (d,  $J = 8.0$  Hz, 1H), 7.85 (d,  $J = 8.0$  Hz, 1H), 7.66-7.63 (m, 1H), 7.56- 7.48 (m, 3H), 6.63 (d,  $J = 16.0$  Hz, 1H), 6.41 (d,  $J = 16.0$  Hz, 1H), 5.19 (dd,  $J_1 = 11.5$  Hz,  $J_2 = 4.0$  Hz, 1H), 4.45 (br.d, 1H), 2.75 (ddd,  $J_1 = 13.5$  Hz,  $J_2 = 7.0$  Hz,  $J_3 = 2.5$  Hz, 1H), 2.38 (t,  $J = 12.5$  Hz, 1H), 2.24-2.18 (m, 1H), 2.01-1.94 (m, 2H), 1.55 (s, 3H), 1.43 (t,  $J = 7.5$  Hz, 1H), 1.41 (s, 3H), 1.27 (s, 3H), 1.15-1.05 (m, 1H), 0.91 (d,  $J = 6.5$  Hz, 3H).

**$^{13}C$  NMR** (125 MHz,  $CDCl_3$ ):  $\delta$  203.1, 151.9, 138.8, 138.2, 134.5, 132.6, 129.6, 127.9, 127.2, 126.2, 125.3, 125.2, 122.4, 121.9, 51.8, 41.7, 40.4, 40.1, 38.1, 29.0, 25.3, 23.3, 16.9, 7.9.

Mass Spectrometric Analysis: **HRMS** (ESI):  $m/z$  calcd for  $C_{25}H_{30}ONa$ : 369.2194, found: 369.2188.

# Synthesis and Biological Evaluation of Novel Derivatives of Zerumbone

---

## Part B

### Synthesis of Novel Zerumbone Derivatives *via* Regio- and Stereoselective Palladium Catalyzed Decarboxylative Coupling Reactions: A New Class of $\alpha$ -Glucosidase Inhibitors

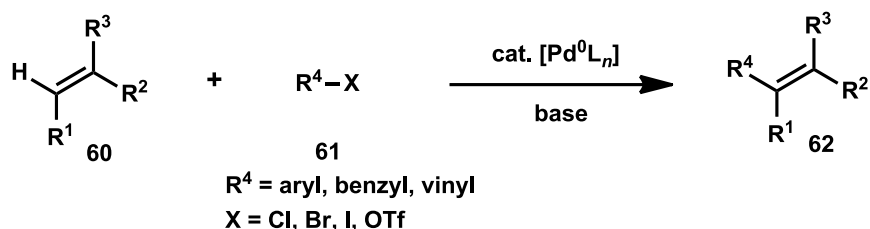
---

#### 3.11. Introduction

Palladium-catalyzed coupling reactions have become a great tool in organic synthesis. The palladium catalyzed carbon-carbon and carbon-heteroatom bond forming reactions find numerous applications in the preparation of pharmaceuticals, agrochemicals and advanced materials both on laboratory and industrial scale. The importance of palladium catalysis was underlined by the 2010 Nobel Prize to R. Heck, A. Suzuki, and E. Negishi for their revolutionary work in this field. Among all the palladium-catalyzed coupling reactions, the first carbon-carbon bond forming Heck reaction plays a vital role in synthesizing simple to complex molecules [Hartwig *et al.* 2002; Miyaura 2002; Hassan *et al.* 2002]

#### 3.12. Heck reaction

The Heck reaction or Mizoroki-Heck reaction is a palladium catalyzed carbon-carbon bond forming reaction of alkenyl or aryl ( $sp^2$ ) halides or triflates with an alkene in presence of a base to form substituted alkenes (Scheme 3.24) [Mizoroki *et al.* 1971; Heck *et al.* 1985].

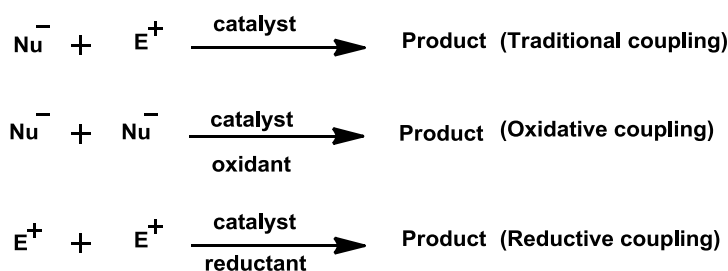


Scheme 3.24

The major advantage of Heck coupling reaction is its substrate scope. Simple olefins to substituted olefins smoothly undergo coupling reaction in a stereoselective manner. Moreover, most of these reactions are quite general, simple and efficient and can be utilized in the synthesis of various natural products and many pharmaceutically important molecules. For example, Heck reaction is industrially applied in the production of naproxen, a nonsteroidal anti-inflammatory drug. Apart from this classic reaction, different types of Heck reactions are known like Heck oxyarylation reaction, amino-Heck reaction, oxidative-Heck reactions *etc.* Among this category, one of the most important class is oxidative Heck coupling reaction.

### 3.12.1. Oxidative Heck coupling reaction

Metal catalyzed coupling reactions between nucleophiles and electrophiles have received great attention and have become the classical or traditional methodology for the construction of carbon-carbon bonds. However, coupling between two nucleophiles or two electrophiles has not gained much attention. Since nucleophiles are electron-rich species, they cannot form chemical bonds directly unless an appropriate oxidant is introduced to remove the extra electrons. Similarly, to couple two electrophiles, an extra reductant is required. Such reactions in which extra oxidant/reductant is required are known as oxidative coupling/reductive coupling reactions respectively. In contrast to the oxidative coupling reaction, the classical or traditional coupling reactions do not use any external oxidant. But to combine two nucleophiles together, an extra oxidant is absolutely needed to take away two redundant electrons [Shi *et al.* 2011]. The schematic representation of the traditional, oxidative and reductive coupling reactions is shown in scheme 3.25.



Scheme 3.25

Taking the “Pd(0)–Pd(II) catalytic cycle” as an example, the steps involved in the oxidative coupling reaction can be explained as; transmetalation of two nucleophiles (RM and R<sub>1</sub>M<sub>1</sub>) with the catalyst to form R–Pd(II)–R<sub>1</sub>. This was followed by reductive elimination to form coupling product and the release of low-valent catalyst Pd (0) species. In order to complete the catalytic cycle, an oxidant X–Y is required to reoxidize the Pd(0) species to regenerate Pd(II). The product of the oxidative coupling reaction carries groups from both the nucleophiles. The quantitative use of oxidant only acts as an electron acceptor without going into the cross-coupling product. The homo-coupling of the two nucleophiles and the direct reaction of the nucleophiles with the oxidant are the two main side reactions.

### 3.12.2. Decarboxylative coupling reaction-An oxidative Heck reaction

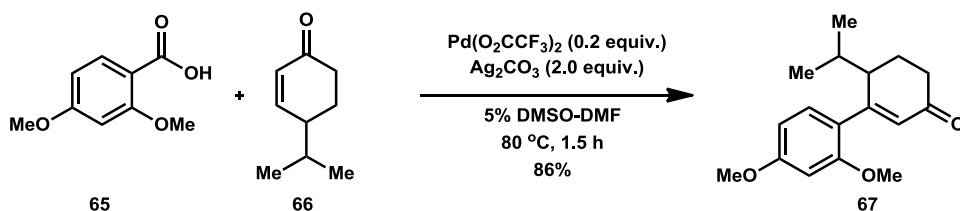
In 2002, Myers *et al.* reported the first palladium catalyzed decarboxylative coupling reaction of arene carboxylates with olefinic substrates [Mayers *et al.* 2002]. This new carbon-carbon bond forming reaction uses commercially available and cheap carboxylic acids as an alternative to organometallic reagents. The new synthetic methodology proceeds mainly through two steps as depicted in scheme 3.26.



Scheme 3.26

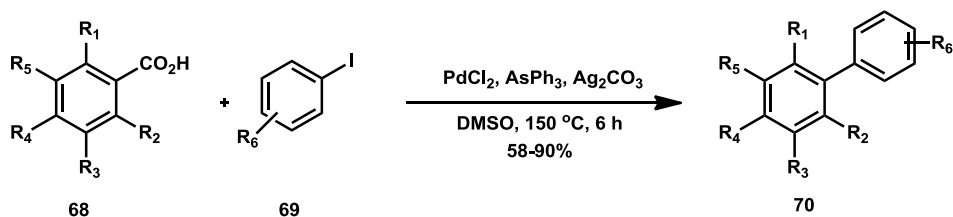
The two steps involved are (i) An initial Ar–S<sub>E</sub> reaction, involving *ipso* attack of an electrophilic Pd(II) intermediate on an arene carboxylate to form an arylpalladium(II) species with loss of carbon dioxide. (ii) This intermediate is then proposed to react with an olefinic substrate by steps common to the Heck coupling process.

Immediately after the first report, the same group demonstrated the vinylic arylation of 2-cycloalken-1-one substrates using a number of different arene carboxylic acids [Tanaka and Myers 2004]. The external oxidant used was two equivalents of silver carbonate. All the reactions afforded product in good to excellent yield just in 0.5-15 h. Moreover, the reaction was free from phosphine ligands (Scheme 3.27).



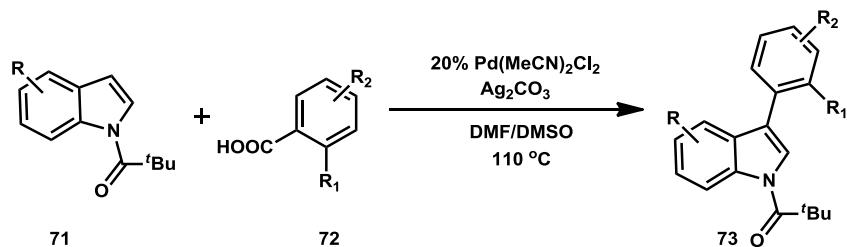
Scheme 3.27

Becht *et al.* reported a simple and efficient biaryl synthesis *via* palladium catalyzed decarboxylative coupling reaction of aryl iodides and arene carboxylic acids [Becht *et al.* 2007]. The PdCl<sub>2</sub>/AsPh<sub>3</sub> catalytic system in the presence of Ag<sub>2</sub>CO<sub>3</sub> in DMSO was found to be particularly efficient to perform this transformation. This reaction can be extended to the synthesis of various biaryls, including sterically hindered biaryls, with yields ranging from 58% to 90% (Scheme 3.28).



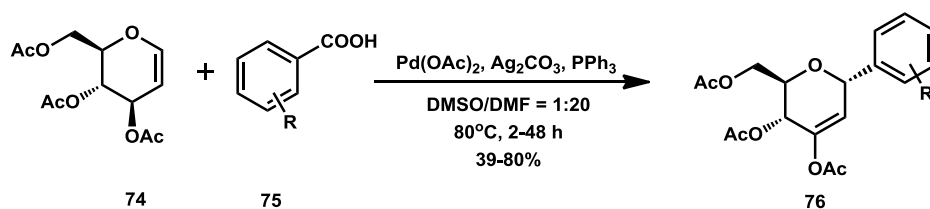
Scheme 3.28

The decarboxylative coupling methodology provided a new and efficient C-3 arylation of indoles using benzoic acids [Cornella *et al.* 2009]. Indoles with both electron donating and electron withdrawing groups afforded the arylated product in good to excellent yield (Scheme 3.29).



Scheme 3.29

A regio- and stereoselective synthesis of C-glycosides have been reported by Xiang *et al.* in 2011 [Xiang *et al.* 2011]. The palladium catalyzed decarboxylative Heck reaction of arene carboxylic acids and glycal provided a series of biologically important 2-deoxy-C-aryl glycosides. This is the first metal-catalyzed method for decarboxylative C-glycosylative coupling (Scheme 3.30).



Scheme 3.30

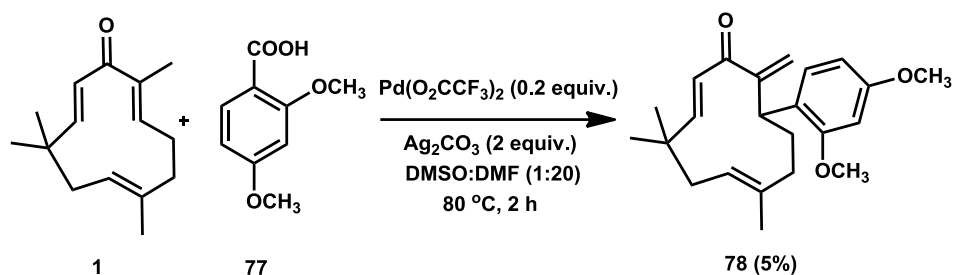
### 3.13. Objective of the present study

Since the endocyclic double bond of cross-conjugated dienone system of zerumbone is more stable and less reactive, we decided to synthesize zerumbone derivatives with new active centers for further derivatization. In order to achieve this goal, we turned our attention to transition metal catalyzed decarboxylative coupling reactions. Myers *et al.* reported the first palladium catalyzed decarboxylative olefination of arene carboxylates. Inspired by this idea, different groups have sought to replicate this process to perform decarboxylative carbon-carbon bond formation reaction. To the best of our knowledge, there is no report on palladium catalyzed decarboxylative coupling with zerumbone and its derivatives. In this chapter, we describe the first regio- and stereoselective palladium catalyzed decarboxylative coupling of arene carboxylic acids to zerumbone. This methodology provides novel zerumbone derivatives having a new dienone system with an exocyclic double bond and these new zerumbone derivatives are potent  $\alpha$ -glucosidase inhibitors.

### 3.14. Results and discussion

We commenced our investigation with the coupling reaction of zerumbone **1** with 2,4-dimethoxybenzoic acid **77** in presence of Pd(O<sub>2</sub>CCF<sub>3</sub>)<sub>2</sub> as a catalyst and silver carbonate as an oxidant in DMSO:DMF (1:20, 3 mL) solvent system at room temperature. Surprisingly, the reaction afforded coupled product **78** with an exocyclic double bond in 5% yield, instead of the expected endocyclic dienone product (Scheme 3.31).





Scheme 3.31

The structure assigned to the product **78** was supported by various spectral analysis. IR spectrum of the compound showed characteristic carbonyl absorption at  $1677\text{ cm}^{-1}$ . In the  $^1\text{H}$  NMR spectrum of compound **78**, the three aromatic protons presented three separate peaks at  $\delta$  7.25, 6.52 and 6.49 as singlet, doublet of doublet and doublet respectively. The olefinic protons on the endocyclic enone moiety were visible at  $\delta$  6.59 and 6.17 as doublets. But the two protons on the exocyclic double bond showed two distinct peaks at  $\delta$  5.58 and 4.79 as a doublet and a singlet respectively. A doublet of doublet noticed at  $\delta$  5.21 integrated for one proton was due to the proton of isolated double bond. The proton on the carbon containing phenyl ring gave a signal at  $\delta$  4.29 as doublet. The protons of two methoxy groups resonated at  $\delta$  3.84 and 3.82 as singlets. A triplet and a doublet of doublet observed at  $\delta$  2.27 and 1.95 were responsible for the protons at C8 position. The protons on the carbon C4 presented two different multiplets at  $\delta$  2.19-2.14 and 1.43-1.38. The protons at C5 carbon displayed a doublet of doublet and a triplet at  $\delta$  2.04 and 1.67 respectively. The singlet at  $\delta$  1.49 was due to the protons of methyl group at the isolated double bond. In addition, the geminal methyl groups were seen at  $\delta$  1.24 and 1.23 (Figure 3.7).

$^{13}\text{C}$  NMR showed the characteristic carbonyl peak at  $\delta$  198.4. The methylenic carbon of exocyclic double bond resonated at  $\delta$  117.8. Two carbons of methoxy groups were appeared at  $\delta$  55.4 and 55.3 (Figure 3.8). All other signals in the  $^1\text{H}$  NMR and  $^{13}\text{C}$  NMR were in good agreement with the proposed structure. Mass spectrum well supported the structure with  $[\text{M}+\text{Na}]^+$  ion peak at  $m/z$  377.2085 (Figure 3.9).

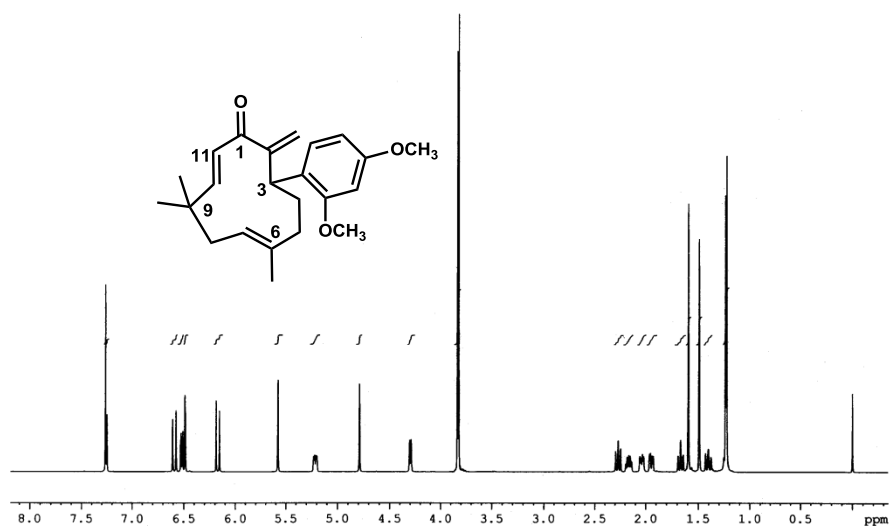


Figure 3.7.  $^1\text{H}$  NMR spectrum of compound 78

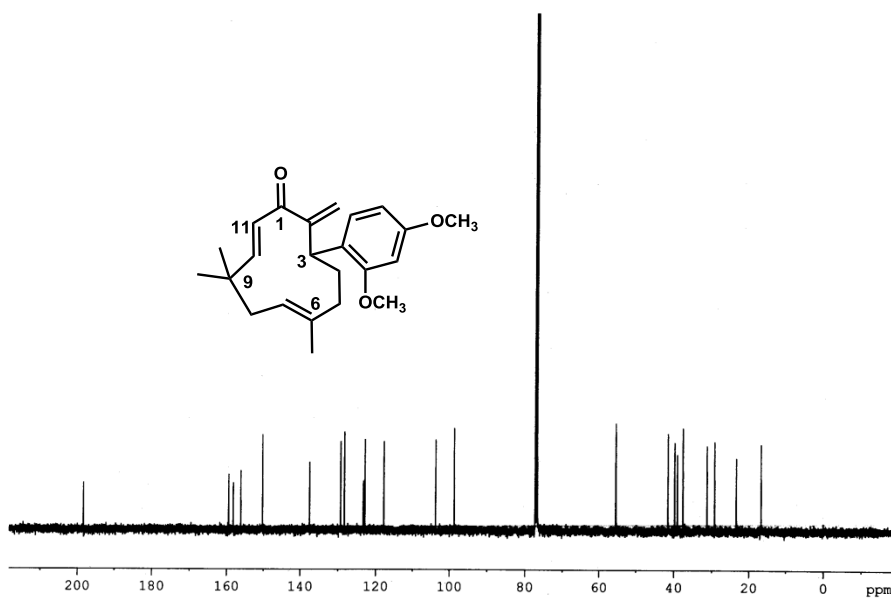
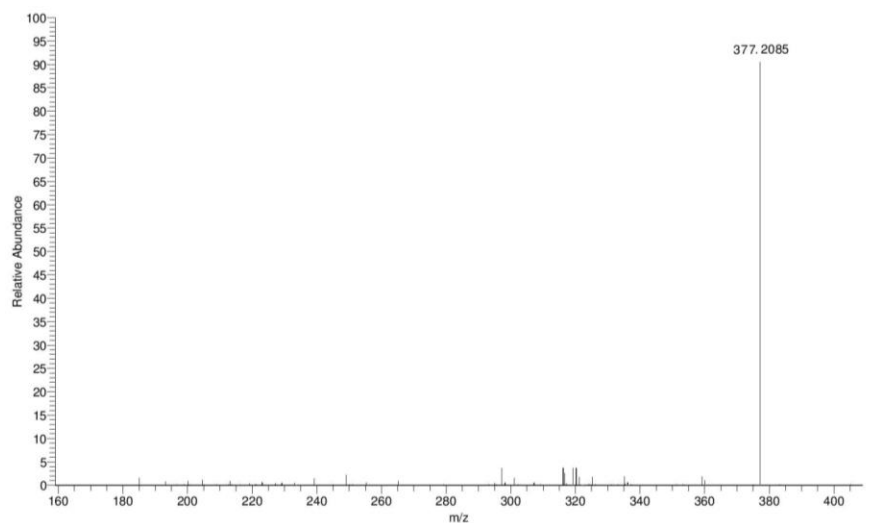
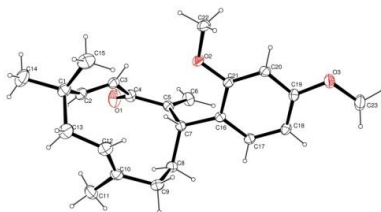


Figure 3.8.  $^{13}\text{C}$  NMR spectrum of compound 78



**Figure 3.9.** Mass spectra of compound **78**

Finally, the structure and stereochemistry of the product **78** was unambiguously confirmed by single crystal X-ray analysis (Figure 3.10). The crystal data has been deposited at Cambridge Crystallographic Data Centre (CCDC) with deposition number CCDC: 933883.



**Figure 3.10.** Single crystal X-ray structure (ORTEP representation) of product **78**

Form the crystal structure, it is clear that the ring conformation of zerumbone has changed tremendously during the reaction. The change in conformation between the parent molecule, zerumbone and the product **78** is shown in figure 3.11.

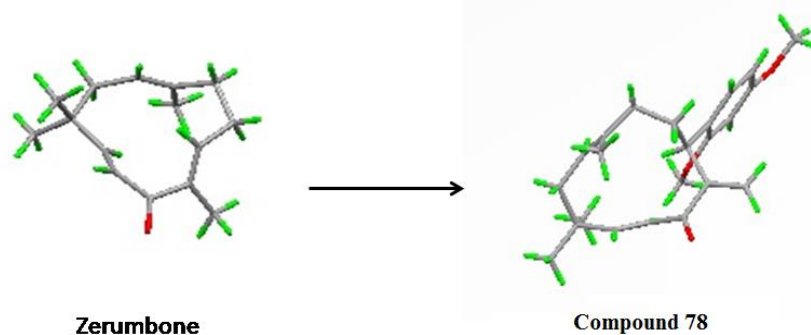
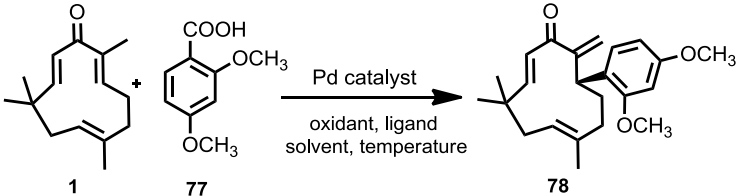


**Figure 3.11.** Conformational change from zerumbone **1** to compound **78**

Encouraged by this result, different reaction temperatures, a variety of palladium catalysts, ligands, oxidants and solvent systems were screened to optimize the reaction conditions. Among various catalysts employed,  $\text{Pd}(\text{O}_2\text{CCF}_3)_2$  gave the best results (Table 3.4, Entry 4). Oxidants showed a remarkable effect in the coupling process. Oxidants other than silver carbonate were found to be ineffective in improving the reaction yield (Table 3.4, Entry 4-7). Interestingly, subsequent examination of the solvent effect revealed their significant influence on this reaction. Using  $\text{Pd}(\text{O}_2\text{CCF}_3)_2$  as catalyst,  $\text{Ag}_2\text{CO}_3$  as oxidant and  $\text{PPh}_3$  as ligand, the effect of different solvents were studied, among which DMSO/DMF (1:20) was found to be the best solvent system for this transformation. Other solvents, such as toluene, dioxane, acetonitrile *etc.* have also been employed in this reaction but none of them gave a better yield than DMSO/DMF (1:20) (Table 3.4, Entry 13-15). Thus, consolidating the results of our optimization, we concluded that the reaction between zerumbone **1** (1.0 equiv.) and arene carboxylic acid **77** (2.0 equiv.) using  $\text{Pd}(\text{O}_2\text{CCF}_3)_2$  (0.2 equiv.),  $\text{Ag}_2\text{CO}_3$  (3.0 equiv.), and  $\text{PPh}_3$  (0.4 equiv.) in DMSO/DMF (1:20) solvent mixture at 100 °C for 4 h represents the most suitable set of conditions for the formation of coupled product **78** (Table 3.4, Entry 12).

**Table 3.4. Optimization studies of palladium catalyzed decarboxylative coupling reaction of aryl carboxylic acids with zerumbone 1**

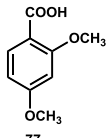
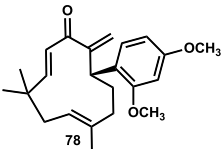
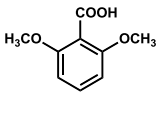
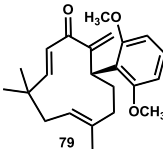
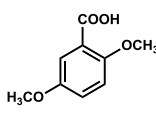
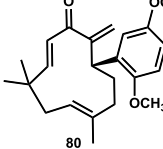
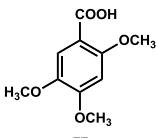
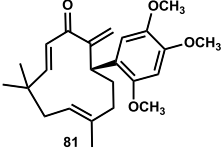
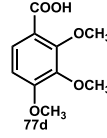
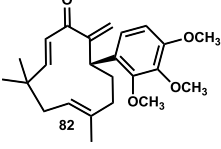
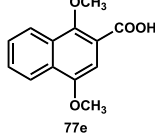
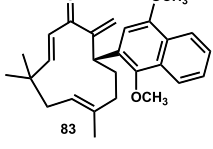
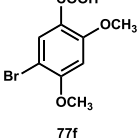
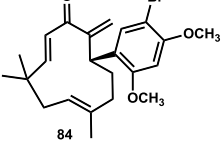
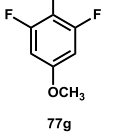
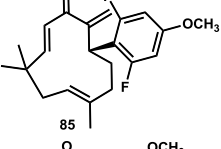
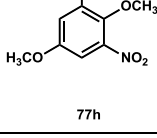
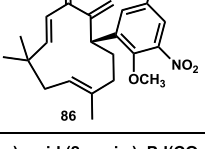


Entry <sup>a</sup>	Catalyst	Oxidant	Temperature(°C)	Time	Yield <sup>b</sup> (%)
1	Pd(O <sub>2</sub> CCF <sub>3</sub> ) <sub>2</sub>	Ag <sub>2</sub> CO <sub>3</sub>	RT	2	5
2	Pd(O <sub>2</sub> CCF <sub>3</sub> ) <sub>2</sub>	Ag <sub>2</sub> CO <sub>3</sub>	50	12	10
3	Pd(O <sub>2</sub> CCF <sub>3</sub> ) <sub>2</sub>	Ag <sub>2</sub> CO <sub>3</sub>	80	2	25
4	Pd(O <sub>2</sub> CCF <sub>3</sub> ) <sub>2</sub>	Ag <sub>2</sub> CO <sub>3</sub>	80	4	31
5	Pd(O <sub>2</sub> CCF <sub>3</sub> ) <sub>2</sub>	Ag <sub>2</sub> O	80	2	-
6	Pd(O <sub>2</sub> CCF <sub>3</sub> ) <sub>2</sub>	Cu(OAc) <sub>2</sub>	80	2	8
7	Pd(O <sub>2</sub> CCF <sub>3</sub> ) <sub>2</sub>	Cu(OAc) <sub>2</sub> .H <sub>2</sub> O	80	2	5
8	Pd(OAc) <sub>2</sub>	Ag <sub>2</sub> CO <sub>3</sub>	80	2	16
9	PdCl <sub>2</sub>	Ag <sub>2</sub> CO <sub>3</sub>	80	2	14
10	Pd(PPh <sub>3</sub> ) <sub>2</sub> Cl <sub>2</sub>	Ag <sub>2</sub> CO <sub>3</sub>	80	2	12
11 <sup>c</sup>	Pd(OAc) <sub>2</sub>	Ag <sub>2</sub> CO <sub>3</sub>	80	2	20
12 <sup>c</sup>	Pd(O <sub>2</sub> CCF <sub>3</sub> ) <sub>2</sub>	Ag <sub>2</sub> CO <sub>3</sub>	100	4	49
13 <sup>d</sup>	Pd(O <sub>2</sub> CCF <sub>3</sub> ) <sub>2</sub>	Ag <sub>2</sub> CO <sub>3</sub>	100	4	trace
14 <sup>e</sup>	Pd(O <sub>2</sub> CCF <sub>3</sub> ) <sub>2</sub>	Ag <sub>2</sub> CO <sub>3</sub>	100	4	trace
15 <sup>f</sup>	Pd(O <sub>2</sub> CCF <sub>3</sub> ) <sub>2</sub>	Ag <sub>2</sub> CO <sub>3</sub>	80	4	trace

<sup>a</sup>Reaction conditions: Zerumbone (1 equiv.), carboxylic acid (2 equiv.), catalyst (0.2 equiv.) and oxidant (3 equiv.) in DMSO:DMF (1:20) solvent mixture (3 mL).<sup>b</sup> Isolated yield; <sup>c</sup>In presence of PPh<sub>3</sub> (0.4 equiv.); <sup>d</sup>In toluene; <sup>e</sup>In dioxane; <sup>f</sup>In acetonitrile.

With the optimal reaction conditions identified, we then turned our attention to the evaluation of arene carboxylic acid generality in the reaction. Gratifyingly, the reaction was found to be general. Noteworthy, excellent regio- and stereoselectivities were observed in all reactions. The results are depicted in Table 3.5.

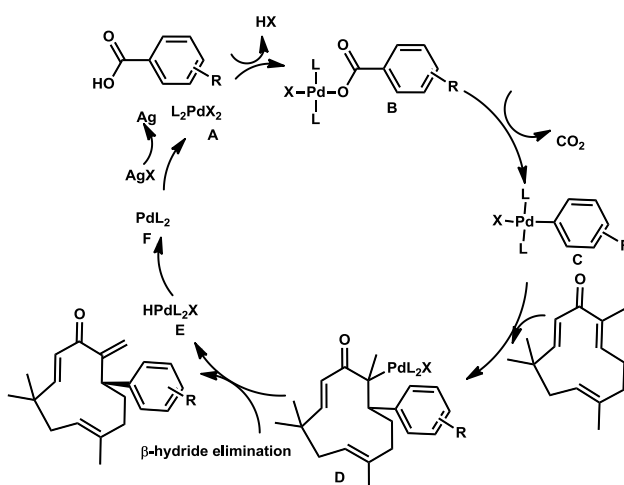
Table 3.5. Palladium catalyzed decarboxylative coupling of various carboxylic acids

Entry <sup>a</sup>	Acid	Product	Yield <sup>b</sup>
1	 77	 78	49
2	 77a	 79	90
3	 77b	 80	14
4	 77c	 81	11
5	 77d	 82	26
6	 77e	 83	23
7	 77f	 84	17
8	 77g	 85	NR
9	 77h	 86	NR

<sup>a</sup> Reaction conditions: Zerumbone (1equiv.), acid (2 equiv.), Pd(CO<sub>2</sub>CF<sub>3</sub>)<sub>2</sub> (0.2 equiv.) Ag<sub>2</sub>CO<sub>3</sub> (3 equiv.) and PPh<sub>3</sub> (0.4 equiv.) in (1:20) DMSO:DMF solvent mixture (3 mL).<sup>b</sup> Isolated yield.

### 3.15. Mechanism

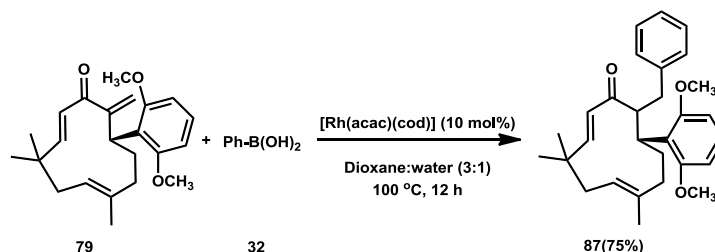
Based on our work and the previous reports on the palladium-catalyzed decarboxylative reaction, we proposed the mechanism to be as shown in Scheme 3.32 [Tanaka *et al.* 2005; Xiang *et al.* 2011]. The first step of the catalytic cycle involves the formation of palladium complex **B** from Pd II complex **A** via a salt exchange mechanism and subsequent decarboxylation generates an intermediate **C**. Carbopalladation of the zerumbone would then give the intermediate **D**. Finally,  $\beta$ -hydride elimination from the methyl group results in the formation of coupled product.



Scheme 3.32

### 3.16. Synthetic utility of decarboxylative coupled product

In order to explore the synthetic utility of the synthesized zerumbone derivatives, we carried out rhodium catalyzed 1,4-conjugate addition of **79** with phenyl boronic acid **32**; the reaction afforded the product **87** in a regio- and stereoselective manner (Scheme 3.33).



Scheme 3.33

The structure of the product was ascertained by spectroscopic data. In the  $^1\text{H}$  NMR spectrum, six protons resonated at  $\delta$  7.24-7.21, 7.13-7.09 and 7.04-7.02 as multiplets. The

remaining two protons together presented a doublet at  $\delta$  6.63. The olefinic protons of enone moiety produced two doublets at  $\delta$  6.44 and 6.30. A doublet of doublet at  $\delta$  5.09 was responsible for the proton at the isolated double bond. The proton on the carbon bearing the benzyl ring appeared as a broad doublet at  $\delta$  4.05. A singlet at  $\delta$  3.87 integrated for six protons was identified as the protons of two  $-\text{OCH}_3$  groups (Figure 3.12). In the  $^{13}\text{C}$  NMR spectrum, the characteristic carbonyl carbon appeared at  $\delta$  202.2. A signal at  $\delta$  61.4 was assigned to the carbon with benzyl group. The carbons of methoxy groups were discernible at  $\delta$  55.6 and 55.5 (Figure 3.13). All other signals in the  $^1\text{H}$  NMR and  $^{13}\text{C}$  NMR were in good agreement with the proposed structure. Mass spectroscopic analysis also confirmed the compound by showing a  $[\text{M}+\text{Na}]^+$  ion peak at 455.2598.

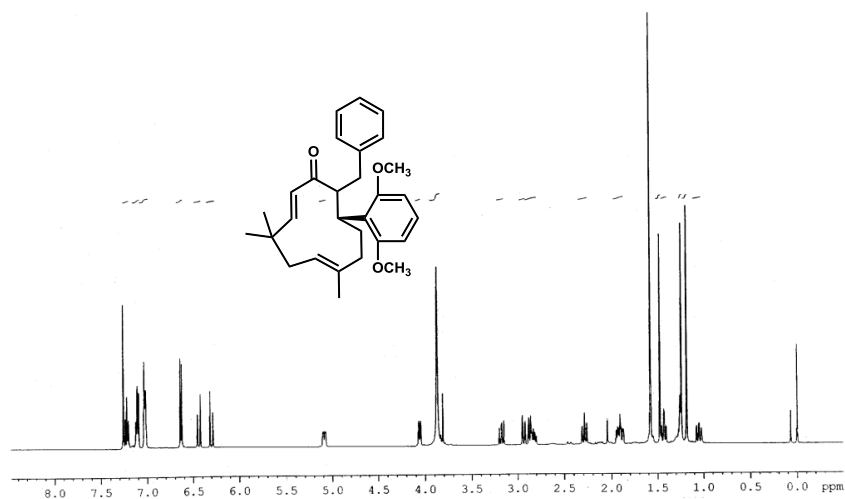


**Figure 3.12.**  $^1\text{H}$  NMR spectrum of compound **87**



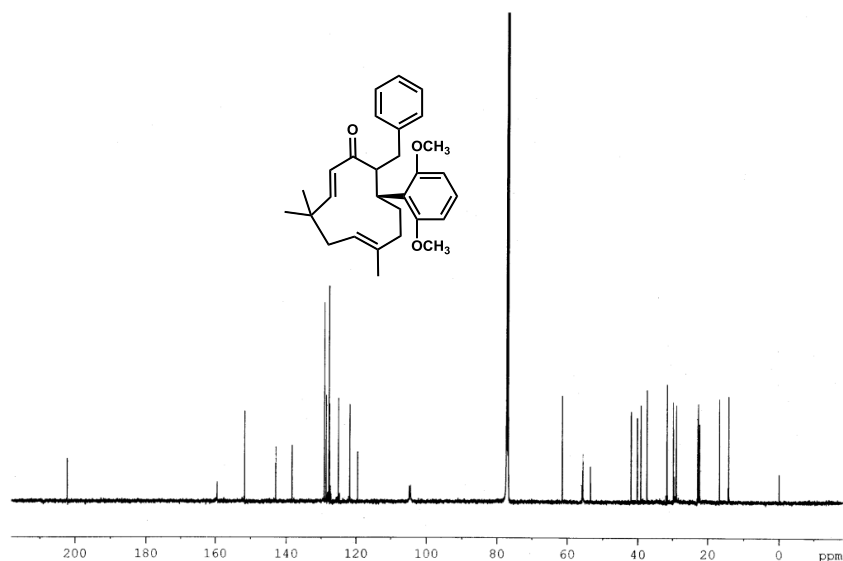


Figure 3.13.  $^{13}\text{C}$  NMR spectrum of compound 87

### 3.17. Biological evaluation of compounds 78-84

#### 3.17.1. $\alpha$ -Glucosidase inhibition assay of compounds 78-84

To showcase the biological activity of synthesized compounds, we targeted the  $\alpha$ -glucosidase inhibitory activity. *In vitro*  $\alpha$ -glucosidase inhibition assays of compound 78-84 were carried out using the procedure reported by Apostolidis *et al.* [Apostolidis *et al.* 2002]. Commercially available acarbose was used as standard. The results are shown in figure 3.14.

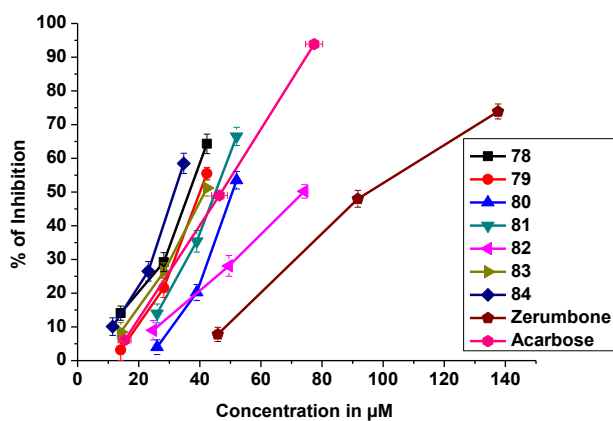


Figure 3.14.  $\alpha$ -Glucosidase enzyme inhibition properties of compounds 78-84, zerumbone and acarbose (standard) with varying concentration

From the results, it is clear that all the novel zerumbone derivatives except **82** are potent  $\alpha$ -glucosidase inhibitors compared to the standard acarbose. Out of the seven derivatives, compound **83** displayed the most potent activity with the lowest  $IC_{50}$  value of  $31.6 \pm 2.81 \mu\text{M}$ .  $IC_{50}$  values of the entire compounds are presented in Table 3.6. The newly formed dienone system and the significant conformational change may be the reason for the superior activity of derivatives over zerumbone [Hall *et al.* 1981].

**Table 3.6.  $IC_{50}$  values of compounds 78-84 against  $\alpha$ -glucosidase enzyme**

Sl.No.	Compounds	$IC_{50}$ value $\pm$ SD ( $\mu\text{M}$ )
1	<b>78</b>	$36.7 \pm 2.61$
2	<b>79</b>	$40.3 \pm 1.53$
3	<b>80</b>	$50.6 \pm 2.10$
4	<b>81</b>	$45.3 \pm 2.90$
5	<b>82</b>	$74.2 \pm 2.63$
6	<b>83</b>	$41.8 \pm 2.66$
7	<b>84</b>	$31.6 \pm 2.81$
8	Zerumbone	$95.7 \pm 2.26$
9	Acarbose (std)	$47.2 \pm 2.50$

### 3.18. Conclusion

In conclusion, we have developed for the first time a regio- and stereoselective palladium catalyzed decarboxylative coupling of arene carboxylic acids to the zerumbone. This straightforward synthetic route is successful in repositioning the rigid endocyclic double bond of parent molecule, zerumbone and provided a class of molecules having an exocyclic double bond with a new dienone system. Preliminary *in vitro*  $\alpha$ -glucosidase inhibition assays revealed that all the compounds except **82** show potent inhibitory activity compared to the zerumbone and the standard acarbose. The possibility for further functionalization of the novel derivatives was effectively demonstrated from the 1,4 conjugate addition reaction using phenyl boronic acid. Further investigations on the scope of the reaction and *in vivo* studies of the novel molecules for potential biological activity are in progress.

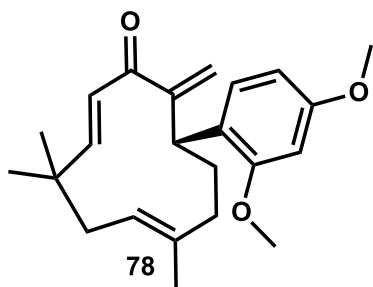
### 3.19. Experimental methods

#### General experimental procedure for the palladium catalyzed decarboxylative coupling of arene carboxylic acids with zerumbone (**1**)

Zerumbone (1equiv.), arenecarboxylic acid (2 equiv.), oxidant (3 equiv.) and Pd catalyst (0.2 equiv.) and ligand (0.4 equiv.) were taken in a Schlenk tube and degassed. The mixture was dissolved in DMSO-DMF (1:20, 3 mL) and stirred at 100 °C for 4 hours. After the completion of the reaction (as indicated by TLC), the reaction mixture was extracted with ethyl acetate (3 x 25 mL). The organic layer was then dried over anhydrous sodium sulphate and the solvent was evaporated in vacuo. The residue on silica gel (100-200 mesh) column chromatography using 4-7% ethyl acetate in hexane afforded the coupled product in low to moderate yield.

#### (2*E*,6*E*)-10-(2,4-dimethoxyphenyl)-4,4,7-trimethyl-11-methylenecycloundeca-2,6-dienone **78**

Following the general procedure, the zerumbone **1** (30 mg, 0.14 mmol), 2, 4-dimethoxybenzoic acid **77** (50.09 mg, 0.28 mmol), silver carbonate (113.74 mg, 0.41 mmol), palladium trifluoroacetate (6.16 mg, 0.03 mmol) and PPh<sub>3</sub> (14.42 mg, 0.55 mmol) in DMSO-DMF (1:20, 3 mL) at 100 °C for 4 hours under argon atmosphere gave the coupled product **78** as a white crystalline solid (23.88 mg, 49%). R<sub>f</sub>: 0.40 (3:17 EtOAc-hexane). Mp: 110-112 °C.



**IR** (KBr)  $\nu_{\max}$ : 3072, 2955, 2858, 1677, 1613, 1504, 1461, 1294, 1208, 1040, 839, 676 cm<sup>-1</sup>.

**<sup>1</sup>H NMR** (500 MHz, CDCl<sub>3</sub>):  $\delta$  7.25 (s, 1H), 6.59 (d,  $J = 16.5$  Hz, 1H), 6.52 (dd,  $J_1 = 8.0$  Hz,  $J_2 = 2.5$  Hz, 1H), 6.49 (d,  $J = 2.0$  Hz, 1H), 6.17 (d,  $J = 16.5$  Hz, 1H), 5.58 (d,  $J = 1.0$  Hz, 1H), 5.21 (dd,  $J_1 = 11.0$  Hz,  $J_2 = 4.5$  Hz, 1H), 4.79 (s, 1H), 4.29 (d,  $J = 7.5$  Hz, 1H), 3.84 (s, 3H), 3.82 (s, 3H) 2.27 (t,  $J = 13.0$  Hz, 1H),

2.19-2.14 (m, 1H), 2.04 (dd,  $J_1 = 12.5$  Hz,  $J_2 = 5.5$  Hz, 1H), 1.95 (dd,  $J_1 = 13$  Hz,  $J_2 = 4.5$  Hz, 1H), 1.67 (t,  $J = 12.0$  Hz, 1H), 1.49 (s, 3H), 1.43-1.38 (m, 1H), 1.24 (s, 3H), 1.23 (s, 3H) .

$^{13}\text{C}$  NMR (125 MHz,  $\text{CDCl}_3$ ):  $\delta$  198.4, 159.4, 158.2, 156.1, 150.2, 137.5, 129.3, 128.3, 123.3, 122.9, 117.8, 103.7, 98.7, 55.4, 55.3, 41.5, 39.8, 39.1, 37.6, 31.2, 29.2, 23.4, 16.7.

Mass spectroscopic analysis: **HRMS** (ESI):  $m/z$  calcd for  $\text{C}_{23}\text{H}_{30}\text{NaO}_3$ : 377.2093, found: 377.2085.

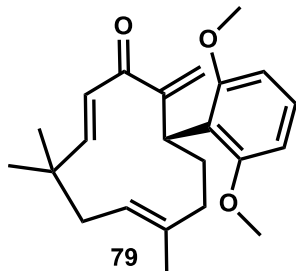
Crystal data of compound **78**: The unit cell parameters of the crystal are; a 10.3553(3), b 10.8243(3), c 11.4355(3), alpha 114.4940(10), beta 103.8700(10), gamma 105.1610(10) with space group P-1.

**(2E,6E)-10-(2,6-dimethoxyphenyl)-4,4,7-trimethyl-11-methylenecycloundeca-2,6-dienone 79**

Following the general procedure, the zerumbone **1** (30 mg, 0.14 mmol), 2, 6-dimethoxybenzoic acid **77a** (50.09 mg, 0.28 mmol), silver carbonate (113.74 mg, 0.41 mmol), palladium trifluoroacetate (6.16 mg, 0.03 mmol) and  $\text{PPh}_3$  (14.42 mg, 0.55 mmol) in DMSO-DMF (1:20, 3 mL) at 100 °C for 4 hours under argon atmosphere gave the coupled product **79** as a white crystalline solid (43.87 mg, 90%).  $R_f$ : 0.40 (3:17 EtOAc-hexane). Mp: 143-145 °C.

**IR** (KBr)  $\nu_{\text{max}}$ : 3073, 2932, 2842, 1674, 1625, 1590, 1467, 1282, 1205, 1036, 852, 679  $\text{cm}^{-1}$ .

$^1\text{H}$  NMR (500 MHz,  $\text{CDCl}_3$ ):  $\delta$  7.08 (t,  $J = 8.5$  Hz, 1H), 6.49 (d,  $J = 8.5$  Hz, 2H), 6.31 (d,  $J = 16.5$  Hz, 1H), 6.14 (d,  $J = 16.5$  Hz, 1H), 5.39 (s, 1H), 5.21



(dd,  $J_1 = 11.5$  Hz,  $J_2 = 4.5$  Hz, 1H), 5.02 (s, 1H), 4.45 (d,  $J = 6.0$  Hz, 1H), 3.76 (s, 6H), 2.39-2.34 (m, 1H), 2.20 (t,  $J = 12.5$  Hz, 1H), 1.93 (dd,  $J_1 = 12.5$  Hz,  $J_2 = 6.0$  Hz, 1H), 1.87 (dd,  $J_1 = 13.0$  Hz,  $J_2 = 4.0$  Hz, 1H), 1.62 (t,  $J = 12.5$  Hz, 1H), 1.49-1.48 (m, 1H), 1.42 (s, 3H), 1.18 (s, 3H), 1.16 (s, 3H).

$^{13}\text{C}$  NMR (125 MHz,  $\text{CDCl}_3$ ):  $\delta$  199.3, 158.5, 153.9, 151.1, 138.0, 128.6, 127.7, 122.6, 119.4, 117.3, 104.3, 55.5, 41.7, 40.3, 39.3, 35.9, 30.3, 29.3, 23.7, 16.4.

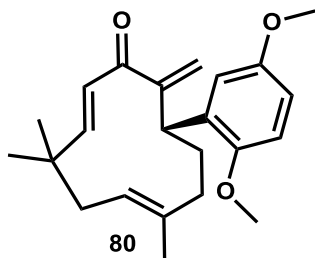
Mass spectroscopic analysis: HRMS (ESI):  $m/z$  calcd for  $\text{C}_{23}\text{H}_{30}\text{NaO}_3$ : 377.2093, found: 377.2083.

**(2E,6E)-10-(2,5-dimethoxyphenyl)-4,4,7-trimethyl-11-methylenecycloundeca-2,6-dienone 80**

Following the general procedure, the zerumbone **1** (30 mg, 0.14 mmol), 2,5-dimethoxybenzoic acid **77b** (50.09 mg, 0.28 mmol), silver carbonate (113.74 mg, 0.41 mmol), palladium trifluoroacetate (6.16 mg, 0.03 mmol) and  $\text{PPh}_3$  (14.42 mg, 0.55 mmol) in DMSO-DMF (1:20, 3 mL) at 100 °C for 4 hours under argon atmosphere gave the coupled product **80** as a viscous liquid (6.82 mg, 14%).  $R_f$ : 0.40 (3:17 EtOAc-hexane).

IR (neat)  $\nu_{\text{max}}$ : 2920, 2853, 1640, 1586, 1414, 1121, 755  $\text{cm}^{-1}$ .

$^1\text{H}$  NMR (500 MHz,  $\text{CDCl}_3$ ):  $\delta$  6.93 (d,  $J = 3.0$  Hz, 1H), 6.79 (d,  $J = 9.0$  Hz, 1H), 6.71 (dd,  $J_1 = 9.0$  Hz,  $J_2 = 3.0$  Hz, 1H), 6.59 (d,  $J = 16.5$  Hz, 1H), 6.14 (d,  $J = 16.5$  Hz, 1H), 5.60 (d,  $J = 1.0$  Hz, 1H), 5.21 (dd,  $J_1 = 11.0$  Hz,  $J_2 = 4.5$  Hz, 1H),



4.82 (s, 1H), 4.35 (d,  $J = 7.5$  Hz, 1H), 3.81 (s, 3H), 3.79 (s, 3H), 2.28-2.23 (m, 1H), 2.19-2.14 (m, 1H), 2.05 (dd,  $J_1 = 12.5$  Hz,  $J_2 = 6.0$  Hz, 1H), 1.94 (dd,  $J_1 = 13.5$  Hz,  $J_2 = 5.0$  Hz, 1H), 1.69-1.65 (m, 1H), 1.50 (s, 3H), 1.45-1.39 (m, 1H), 1.24 (s, 3H), 1.23 (s, 3H).

$^{13}\text{C}$  NMR (125 MHz,  $\text{CDCl}_3$ ):  $\delta$  198.4, 155.4, 153.6, 151.5, 149.8, 137.3, 132.4, 129.3, 122.9, 118.2, 115.3, 111.1, 110.6, 55.8, 55.5, 41.6, 39.8, 39.2, 38.1, 31.3, 29.3, 23.4, 16.6.

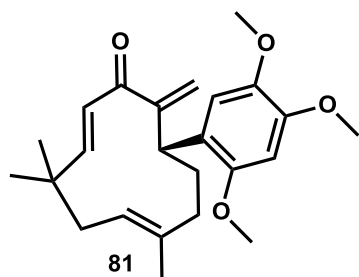
Mass spectrometric analysis: **HRMS** (ESI):  $m/z$  calcd for  $\text{C}_{23}\text{H}_{30}\text{NaO}_3$ : 377.2093, found: 377.2081.

**(2E,6E)-4,4,7-trimethyl-11-methylene-10-(2,4,5-trimethoxyphenyl)cycloundeca-2,6-dienone 81**

Following the general procedure, the zerumbone **1** (30 mg, 0.14 mmol), 2,4,5-trimethoxybenzoic acid **77c** (58.36 mg, 0.28 mmol), silver carbonate (113.74 mg, 0.41 mmol), palladium trifluoroacetate (6.16 mg, 0.03 mmol) and  $\text{PPh}_3$  (14.42 mg, 0.55 mmol) in DMSO-DMF (1:20, 3 mL) at 100 °C for 4 hours under argon atmosphere gave the coupled product **81** as a white crystalline solid (13.22 mg, 25%).  $R_f$ : 0.40 (3:17 EtOAc-hexane). Mp: 89-92 °C.

**IR** (KBr)  $\nu_{\text{max}}$ : 3071, 2932, 2852, 1675, 1615, 1511, 1460, 1208, 1037, 828, 680  $\text{cm}^{-1}$ .

$^1\text{H}$  NMR (500 MHz,  $\text{CDCl}_3$ ):  $\delta$  6.82 (s, 1H), 6.47 (s, 1H), 6.46 (d,  $J = 16.0$  Hz, 1H), 6.09 (d,  $J = 16.0$  Hz, 1H), 5.49 (s, 1H), 5.15 (dd,  $J_1 = 11$  Hz,  $J_2 = 4.5$  Hz, 1H), 4.75 (s, 1H), 4.27 (d,  $J = 7.0$  Hz, 1H),



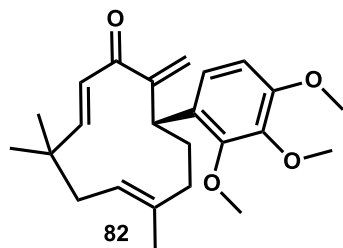
3.83 (s, 3H), 3.79 (s, 3H), 3.78 (s, 3H), 2.19 (t,  $J = 12.5$  Hz, 1H), 2.06- 1.96 (m, 2H), 1.88 (dd,  $J_1 = 13.0$  Hz,  $J_2 = 4.5$  Hz, 1H), 1.61 (t,  $J = 12.0$  Hz, 1H), 1.43 (s, 3H), 1.38 (t,  $J = 13.5$  Hz, 1H), 1.17 (s, 3H), 1.17 (s, 3H).

$^{13}\text{C}$  NMR (125 MHz,  $\text{CDCl}_3$ ):  $\delta$  196.8, 155.0, 150.5, 149.3, 147.2, 141.9, 136.3, 128.0, 121.9, 121.4, 116.6, 112.1, 96.7, 55.9, 55.2, 55.1, 40.5, 38.7, 38.0, 36.6, 30.6, 28.2, 22.5, 15.7.

Mass spectrometric analysis: **HRMS** (ESI):  $m/z$  calcd for  $\text{C}_{24}\text{H}_{32}\text{NaO}_4$ : 407.2198, found: 407.2190.

**(2E,6E)-4,4,7-trimethyl-11-methylene-10-(2,3,4-trimethoxyphenyl)cycloundeca-2,6-dienone **82****

Following the general procedure, the zerumbone **1** (30 mg, 0.14 mmol), 2,3,4-trimethoxybenzoic acid **77d** (58.36 mg, 0.28 mmol), silver carbonate (113.74 mg, 0.41 mmol), palladium trifluoroacetate (6.16 mg, 0.03 mmol) and  $\text{PPh}_3$  (14.42 mg, 0.55 mmol) in DMSO-DMF (1:20, 3 mL) at 100 °C for 4 hours under argon atmosphere gave the coupled product **82** as a colourless viscous liquid (13.75 mg, 26%).  $R_f$ : 0.40 (3:17 EtOAc-hexane).



**IR** (neat)  $\nu_{\text{max}}$ : 3585, 2927, 2855, 1676, 1606, 1493, 1460, 1267, 1199, 1095, 1019, 720, 665  $\text{cm}^{-1}$ .

$^1\text{H}$  NMR (500 MHz,  $\text{CDCl}_3$ ):  $\delta$  6.99 (d,  $J = 8.5$  Hz, 1H), 6.67 (d,  $J = 8.5$  Hz, 1H), 6.50 (d,  $J = 16.5$  Hz, 1H), 6.21 (d,  $J = 16.5$  Hz, 1H), 5.58 (s, 1H), 5.24 (dd,  $J_1 = 11.0$  Hz,  $J_2 = 4.5$  Hz, 1H), 4.76 (s, 1H), 4.25 (d,  $J = 7.5$  Hz, 1H), 3.91 (s, 3H), 3.88

(s, 3H), 3.87 (s, 3H), 2.26 (t,  $J = 13.0$  Hz, 1H), 2.13-2.03 (m, 2H), 1.95 (dd, ,  $J_1 = 13.0$  Hz,  $J_2 = 4.5$  Hz, 1H), 1.70 (t,  $J = 12.0$  Hz, 1H), 1.49 (s, 3H), 1.43 (t,  $J = 13.0$  Hz, 1H), 1.25 (s, 3H), 1.24 (s, 3H).

$^{13}\text{C}$  NMR (125 MHz,  $\text{CDCl}_3$ ):  $\delta$  197.7, 156.4, 152.3, 151.8, 150.7, 142.3, 137.5, 128.9, 128.2, 122.8, 122.4, 117.9, 106.9, 60.8, 60.6, 55.9, 41.4, 39.8, 39.2, 38.5, 31.6, 29.3, 23.7, 16.8.

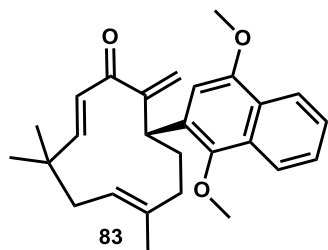
Mass spectroscopic analysis: **HRMS** (ESI):  $m/z$  calcd for  $\text{C}_{24}\text{H}_{32}\text{NaO}_4$ : 407.2198, found: 407.2188.

**(2E,6E)-10-(1,4-dimethoxynaphthalen-2-yl)-4,4,7-trimethyl-1methylenecycloundeca-2,6-dienone 83**

Following the general procedure, the zerumbone **1** (30 mg, 0.14 mmol), 1,4-dimethoxynaphthalenebenzoic acid **77e** (63.85 mg, 0.28 mmol), silver carbonate (113.74 mg, 0.41 mmol), palladium trifluoroacetate (6.16 mg, 0.03 mmol) and  $\text{PPh}_3$  (14.42 mg, 0.55 mmol) in DMSO-DMF (1:20, 3 mL) at 100 °C for 4 hours under argon atmosphere gave the coupled product **83** as a viscous liquid (12.79 mg, 23%).  $R_f$ : 0.38 (3:17 EtOAc-hexane).

**IR** (neat)  $\nu_{\text{max}}$ : 2922, 2853, 1641, 1593, 1405, 1122, 1042, 684  $\text{cm}^{-1}$ .

$^1\text{H}$  NMR (500 MHz,  $\text{CDCl}_3$ ):  $\delta$  8.22 (d,  $J = 8.5$  Hz, 1H), 8.01 (d,  $J = 8.5$  Hz, 1H), 7.55-7.52 (m, 1H), 7.48-7.44 (m, 1H), 6.73 (s, 1H), 6.47 (d,  $J = 16.5$  Hz, 1H), 6.33 (d,  $J = 16.5$  Hz, 1H), 5.57 (s, 1H), 5.37-5.36 (m, 1H), 4.99 (s, 1H), 4.58 (d,  $J = 7.0$  Hz, 1H), 3.99 (s, 3H), 3.92 (s, 3H), 2.32-2.27 (m, 1H), 2.18-2.16 (m, 1H),





2.07-1.99 (m, 2H), 1.82-1.77 (m, 1H),  
1.66-1.61 (m, 1H), 1.53 (s, 3H), 1.31 (s,  
3H), 1.27 (s, 3H).

$^{13}\text{C}$  NMR (125 MHz,  $\text{CDCl}_3$ ):  $\delta$   
178.2, 156.2, 152.0, 151.9, 137.6, 128.2,  
126.7, 125.2, 122.8, 122.5, 121.9, 117.7,  
104.2, 62.4, 55.6, 41.4, 39.7, 39.1, 37.4,  
32.8, 29.3, 24.0, 16.9.

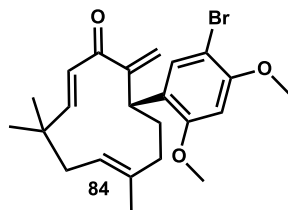
Mass spectrometric analysis: HRMS (ESI):  $m/z$  calcd for  $\text{C}_{27}\text{H}_{32}\text{NaO}_3$ : 427.2249,  
found: 427.2204.

**(2E,6E)-10-(5-bromo-2,4-dimethoxyphenyl)-4,4,7-trimethyl-1methylenecycloundeca-  
2,6-dienone 84**

Following the general procedure, the zerumbone **1** (30 mg, 0.14 mmol), 5-bromo-  
2,4-dimethoxybenzoic acid **77f** (59.45 mg, 0.28 mmol), silver carbonate (113.74 mg, 0.41  
mmol), palladium trifluoroacetate (6.16 mg, 0.03 mmol) and  $\text{PPh}_3$  (14.42 mg, 0.55 mmol)  
in DMSO-DMF (1:20, 3 mL) at 100 °C for 4 hours under argon atmosphere gave the  
coupled product **84** as a viscous liquid (10.11 mg, 17%).  $R_f$ : 0.30 (3:17 EtOAc-hexane).

IR (neat)  $\nu_{\text{max}}$ : 2956, 2852, 1674,  
1497, 1460, 1383, 1295, 1207, 1030, 738  
 $\text{cm}^{-1}$ .

$^1\text{H}$  NMR (500 MHz,  $\text{CDCl}_3$ ):  $\delta$  7.44  
(s, 1H), 6.50 (d,  $J = 16.0$  Hz, 1H), 6.48 (s,  
1H), 6.14 (d,  $J = 16.5$  Hz, 1H), 5.59 (d,  $J =$   
1.0 Hz, 1H), 5.18 (dd,  $J_1 = 11.0$  Hz,  $J_2 =$   
4.5 Hz, 1H), 4.80 (s, 1H), 4.25 (d,  $J = 7.5$   
Hz, 1H), 3.91 (s, 3H), 3.87 (s, 3H), 2.28-  
2.23 (m, 1H), 2.13-2.04 (m, 2H), 1.94 (dd,  
 $J_1 = 13.0$  Hz,  $J_2 = 4.5$  Hz, 1H), 1.66-1.61  
(m, 1H), 1.48 (s, 3H), 1.44-1.39 (m, 1H),  
1.23 (s, 6H).

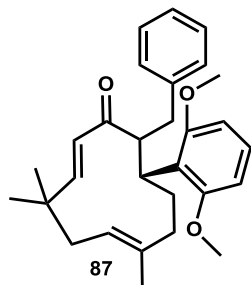


$^{13}\text{C}$  NMR (125 MHz,  $\text{CDCl}_3$ ):  $\delta$  197.2, 155.4, 155.2, 150.1, 137.3, 131.9, 129.1, 124.8, 122.9, 118.1, 102.0, 96.7, 56.3, 55.7, 41.6, 39.7, 39.1, 37.6, 31.3, 29.2, 23.5, 16.7.

Mass spectroscopic analysis: **HRMS** (ESI):  $m/z$  calcd for  $\text{C}_{23}\text{H}_{29}\text{NaO}_3$ : 455.1198, found: 455.1198

**(2E,6E)-11-benzyl-10-(2,6-dimethoxyphenyl)-4,4,7-trimethylcycloundeca-2,6-dienone 87**

Compound **79** (30 mg, 0.084 mmol), phenylboronic acid **32** (2, 0.169 mmol) and  $[\text{Rh}(\text{acac})(\text{cod})]$  (2.6 mg, 0.008 mmol) were added to a Schlenk tube and the contents degassed. The mixture was dissolved in 1,4-dioxane– $\text{H}_2\text{O}$  (3:1, 2 mL) and stirred at 100 °C for 24 h under an argon atmosphere. After completion of the reaction (as indicated by TLC analysis), the solvent was evaporated in vacuo. The residue was purified by silica gel column chromatography (EtOAc–hexane) to afford the product **87** as viscous liquid (28 mg, 75%).  $R_f = 0.53$  (3:17 EtOAc: Hex).



$^1\text{H}$  NMR (500 MHz,  $\text{CDCl}_3$ ):  $\delta$  7.24-7.21 (m, 1H), 7.13-7.09 (m, 2H), 7.04-7.02 (m, 3H), 6.63 (d,  $J = 8.5$  Hz, 2H), 6.44 (d,  $J = 16.0$  Hz, 1H), 6.30 (d,  $J = 16.0$  Hz, 1H), 5.09 (dd,  $J_1 = 12.0$  Hz,  $J_2 = 4.5$  Hz, 1H), 4.05 (br.d, 1H), 3.87 (s, 6H), 3.20-3.15 (m, 1H), 2.95-2.92 (m, 1H), 2.88-2.80 (m, 2H), 2.31-2.26 (m, 1H), 1.94-1.87 (m, 2H), 1.48 (s, 3H), 1.46-1.41 (m, 1H), 1.24 (s, 3H), 1.18 (s, 3H), 1.08-1.02 (m, 1H).

$^{13}\text{C}$  NMR (125 MHz,  $\text{CDCl}_3$ ):  $\delta$  202.2, 159.5, 151.7, 142.9, 138.3, 129.2, 128.6, 127.7, 125.1, 121.8, 119.5, 104.9, 104.5, 61.4, 55.6, 55.5, 53.4, 41.9, 40.1,

---

39.1, 37.4, 31.6, 29.8, 28.9, 16.7, 14.1.

Mass spectroscopic analysis: **HRMS** (ESI):  $m/z$  calcd for  $C_{29}H_{36}NaO_3$ : 455.2562, found: 455.2598.

---

# Synthesis and Biological Evaluation of Carbohydrate Appended Alkylidene Cyclopentenes

---

### 4.1. Introduction

Carbohydrates are one of the most abundant and widely distributed organic compounds on earth. Chemically, they are polyhydroxy aldehydes and ketones. For many years, carbohydrates were thought to be uninteresting compounds whose only biological purpose was to serve as structural materials and as energy sources. Although carbohydrates fulfill these two roles, recent works have shown that they perform other important biological functions as well. They are often found in intimate association with proteins and are involved in recognition of one protein by another and in adhesion processes. Many vital activities as diverse as healing, blood clotting, infection, prevention of infection, and fertilization all involve carbohydrates [Lemieux 1978; Springer 1990; Dumas *et al.* 2003].

Protein-carbohydrate interactions play an essential role in biological communication. Numerous normal and pathological processes including inflammatory response and metastatic spreading are mediated by such recognition events. Although the intrinsic binding ability of monovalent protein-carbohydrate interactions is low, presentation of carbohydrate epitopes in multivalent arrays usually results in highly specific and effective ligands. This specificity suggests a potential utility of synthetic multiantennated saccharide derivatives as carriers in drug or probe delivery to target sites and as inhibitors of undesired carbohydrate-receptor associations [Ouchi and Ohy 1994].

### 4.2. Glycosides in medicine: Role of glycosidic residue in biological activity

A glycoside is a molecule in which a sugar is bound to non-sugar molecule *via* a glycosidic bond. A saccharide with a leaving group at the anomeric center can be activated by a promoter to give a glycosyl cation. It is then attacked by an aglycone

moiety to form glycosides [Toshima and Tatsuta 1993]. Number of commercially available drugs are glycosides or glycoconjugates. Ribavirin **1**, salicin **2** and oleandrin **3** are few examples of drugs that come under this category (Figure 4.1).

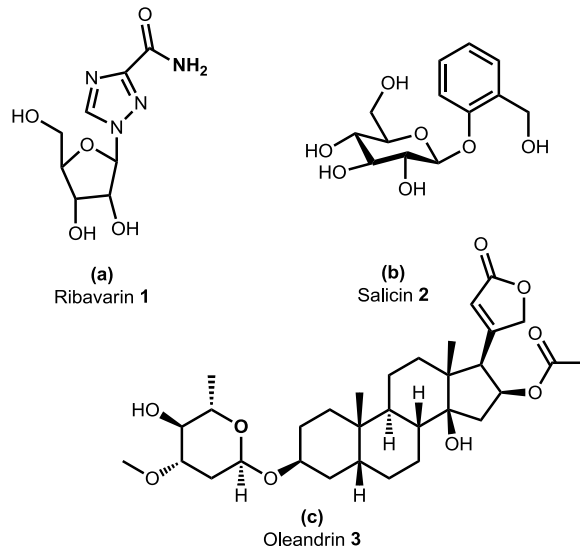


**Figure 4.1** (a) Ribavirin **1**-antiviral drug (b) Salicin **2** -anti-inflammatory agent (c) Oleandrin **3**-cardiac glycoside

The glycosidic residue on the drug molecule usually plays a vital role in their activity or helps to improve its pharmacokinetic parameters. In recent years, lots of developments were brought to molecular glycobiology which in turn helped to get deep understanding to aglycone vs glycoside activities and made possible to produce new and more active glycodrugs. Literature reports show that, it is nearly impossible to pinpoint the trends in the properties of glycosides with their respective aglycones. But, from selected examples, one can explain the general trends and effects of glycosides compared to their partner aglycons. One of the most common improvement in the glycosidic partner compared to its aglycone is the water solubility. This makes the molecule more hydrophilic and hence influences the pharmacokinetic properties like circulation, elimination and the concentrations in the body fluids. Modified hydrophilicity also influences the membrane transport. Some compounds enter the cells just because of their solubility in the membrane components. Interactions of some glycosidic moieties with receptors or lectins on the cell surfaces make possible active uptake of the glycosides. Another important aspect of the activity of glycosides is its susceptibility towards

glycosidic cleavage at various sites of application. Most of the glycosides undergo acid or enzyme catalyzed hydrolysis in stomach. But there are a few glycosides which are not easily hydrolyzed and this non-resorbed glycoconjugates can be cleaved later in the colon or metabolized by the intestinal microflora [Kren and Martinkova 2001; Kren 2008].

Medicinal importance of carbohydrate-metal complexes have been studied recently. These studies include the synthesis of carbohydrate appended *cis*-platin derivatives as anti-cancer agents. Mikato and Yano were successful in synthesizing platinum (II) complexes from carbohydrate-diamine conjugates and investigating the in-vivo antitumor activity of these complexes. They found that the carbohydrate moieties reduced the toxicity inherent with platinum (II) complexes. One of the carbohydrate-pendant *cis*-platin derivatives **4** is shown in figure 4.2 [Tsubomura *et al.* 1990; Mikata *et al.* 2001].

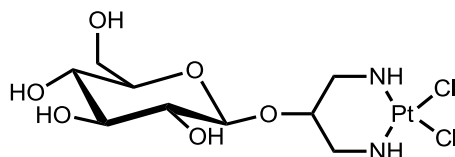


**Figure 4.2** Cis-platin derivative **4**

Thus developing more efficient and economic synthetic approaches for synthesizing glycosides remains to be an active area of research [Cao *et al.* 2011; Banville *et al.* 1990]. Before going into the details of our efforts toward the synthesis of novel glycohybrids and their biological evaluations, a brief account of click chemistry and palladium catalyzed ring-opening reaction of fulvene derived bicyclic hydrazines is presented.

### 4.3. Click chemistry in drug designing

Click chemistry, in particular, the copper(I)-catalyzed ligation of azides and acetylenes, promises to greatly simplify and accelerate the discovery of high-affinity carbohydrate mimetics. Click chemistry is a chemical philosophy introduced by K. B. Sharpless, in 2001 and describes chemistry tailored to generate substances quickly and reliably by joining small units together. This is inspired by the fact that nature also generates substances by joining small modular units [Kolb *et al.* 2001; Evans 2007; Moses and Moorhouse 2007].

Click chemistry is not a specific reaction; it is a concept that mimics nature. The reactions in click chemistry must (or would be desirable):

- Be modular.
- Be wide in scope.
- Give very high chemical yields.
- Generate only inoffensive by-products.
- Be stereospecific.
- Physiologically stable.
- Exhibit a large thermodynamic driving force  $> 84$  kJ/mol to favour a reaction with a single reaction product. A distinct exothermic reaction makes a reactant "spring loaded."
- High atom economy.

The process must (or would be desirable):

- Have simple reaction conditions.
- Use readily available starting materials and reagents.
- Use no solvent or use a solvent that is benign or easily removed (preferably water).
- Provide simple product isolation by non-chromatographic methods (crystallization or distillation).

Its applications are increasingly found in all aspects of drug discovery, ranging from lead finding through combinatorial chemistry and target-templated *in situ* chemistry, to proteomics and DNA research, using bioconjugation reactions. The copper-(I)-catalyzed 1,2,3-triazole formation from azides and terminal acetylenes is a particularly powerful linking reaction, due to its high degree of dependability, complete specificity, and the bio-compatibility of the reactants. It yields exclusively the 1,4-disubstituted 1,2,3-triazole.

The triazole products are more than just passive linkers; they readily associate with biological targets, through hydrogen bonding and dipole interactions. Yang and co-workers recently utilized the Huisgen 1,3-dipolar cycloaddition of azide and acetylenes to generate fifty triazole analogs of the clinically available antibiotic vancomycin. Sharpless and co-workers reported the synthesis of a femtomolar inhibitor of acetylcholinesterase

using click chemistry. HIV-1 protease inhibitor **5** synthesized by click chemistry is given in figure 4.3 [Yang *et al.* 2004; Meldal and Tornøe 2008].

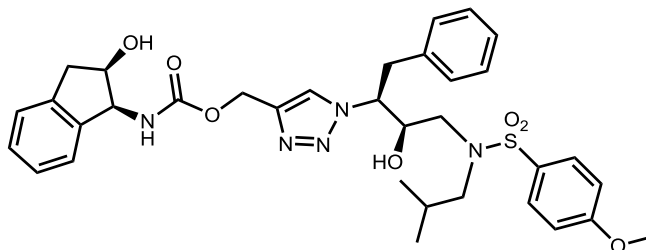


**Figure 4.3.** HIV-I protease inhibitor **5**

The triazole nucleus is one of the most important and well-known heterocycles which is a common and integral feature of a variety of natural products and medicinal agents. The triazole moiety is an excellent stable mimetic of the peptide bond that is not susceptible to proteolytic processing and may provide metabolically stable and efficient inhibitors of key mammalian, bacterial and viral proteases.

Triazole nucleus is present as a core structural component in an array of drug categories such as antimicrobial, antiinflammatory, analgesic, antiepileptic, antiviral, antineoplastic, antihypertensive, antimalarial, local anaesthetic, antianxiety, antidepressant, antihistaminic, antioxidant, antitubercular, antiParkinson's, antidiabetic, antiobesity and immunomodulatory agents *etc.* The broad and potent activity of triazole and their derivatives has established them as pharmacologically significant scaffolds. The basic heterocyclic rings present in various medicinal agents are 1,2,3-triazole and 1,2,4-triazole. A large volume of research has been carried out on triazole and their derivatives, which has proved the pharmacological importance of this heterocyclic nucleus (Figure 4.4) [Singhal *et al.* 2011; Kumar *et al.* 2008].

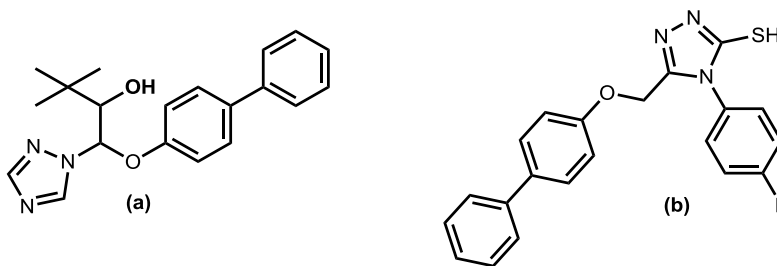


**Figure 4.4.** (a) Bitertanol **6**- broad spectrum fungicide (b) an analgesic **7**



In 2011, Song *et al.* reported the synthesis of triazole linked glycosylated  $\alpha$ -ketocarboxylic acid derivatives as new PTP1B inhibitors **8** (Figure 4.5) [Song *et al.* 2011].

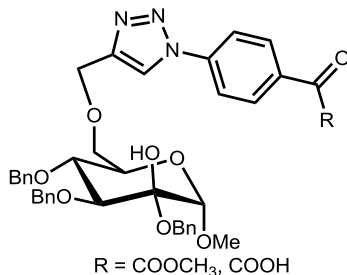
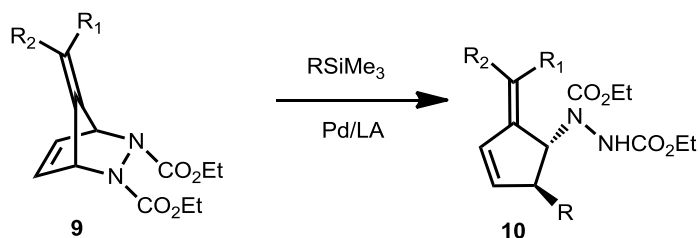


**Figure 4.5.** A new PTP1B inhibitor **8**

#### 4.4. Palladium catalyzed ring-opening reaction of fulvene derived bicyclic hydrazines

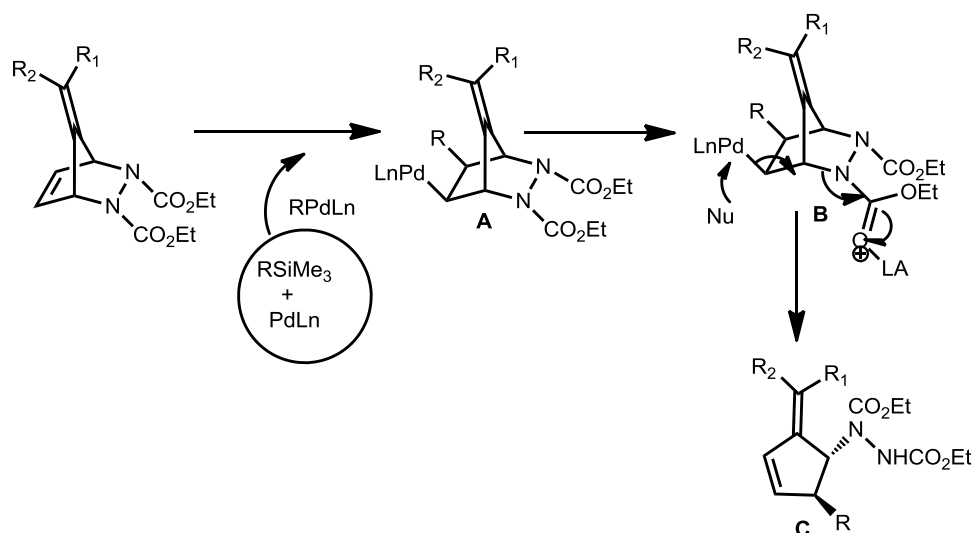
One of the ultimate goal and challenge in synthetic organic chemistry is to develop novel and efficient transformation for the creation of functionalized molecules with structural diversity. Cycloaddition of fulvenes provide versatile and powerful approaches to various natural products and biologically active molecules [Hare *et al.* 1982; Gleiter and Borzyk 1995]. In cycloadditions, pentafulvenes can participate as a  $2\pi$ ,  $4\pi$  or  $6\pi$  component depending on the number of electrons furnished by the competing partner [Hong 2005]. Our research group has unravelled a facile method for the functionalization of pentafulvenes *via* Pd/Lewis acid mediated ring opening of fulvene derived bicyclic hydrazines with a number of organometallic reagents (Scheme 4.1).



**Scheme 4.1**

The proposed mechanism for the reaction is given in scheme 4.2 [Anas *et al.* 2006; Anas *et al.* 2008]. First step involves the transmetalation of organostannane with palladium forming the active palladium species R-Pd-L<sub>n</sub>. Next step is the co-ordination followed by the addition of this species into the endocyclic C-C double bond to form the

intermediate **A**. In the final step, the Lewis acid assisted ring opening of intermediate **B** along with the elimination of  $L_n$ -Pd-Nu gives the product **C**. The Lewis acid assists the C-N bond cleavage by getting coordinated to the carboethoxy group. The addition of the species  $R$ -Pd- $L_n$  to the double bond is a *syn* addition, which results in the formation of the *trans*-disubstituted alkylidene cyclopentene as the product.



**Scheme 4.2**

The described methodology offers a conceptually new approach towards the synthesis of allyl, vinyl, heteroaryl and heteroatom substituted alkylidene cyclopentenes. Substituted cyclopentenes, due to their intermediacy in the synthesis of glycosidase inhibitors, prostaglandins and various other biologically active molecules are considered as versatile synthons and their synthesis have elicited great interest among the synthetic organic chemists.

The widespread occurrence and interesting biological activities of substituted cyclopentane derivatives in nature make them important targets for synthesis [Crimmins 1998; Berecibar 1999; Lillelund 2002]. Among various cyclopentane derivatives, alkylidene cyclopentanes hold special attention as intermediates in the construction of biologically interesting molecules including (+) and (-) - nigellamine  $A_2$ , guanacastepene *A* etc [Bian *et al.* 2006; Brady 2000]. Alkylidene cyclopentanes can easily be converted to piperidine alkaloids like streptazolins, odoriferous compounds like  $\beta$ -vetivone,  $\alpha$ -

vetispirene, hirsutene, liseaverticillols *etc.* Some of the structurally related compounds are shown in figure 4.6.

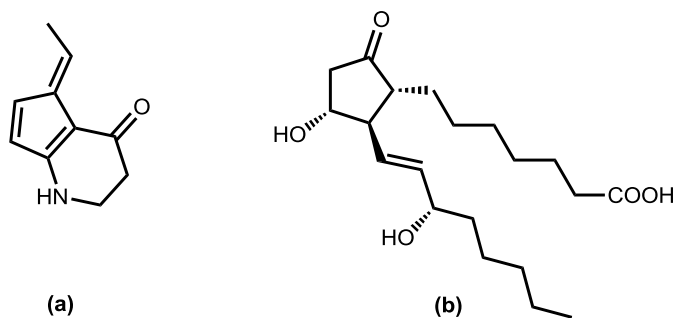


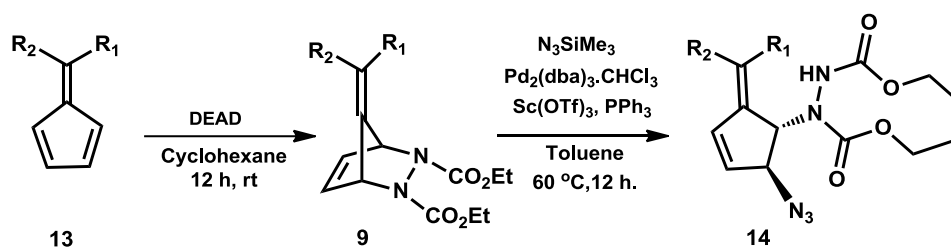
**Figure 4.6.** (a) Streptazon **11** (b) Prostaglandin E1 **12**

#### 4.5. Objective of the present work

Study of carbohydrates may offer novel opportunities for therapeutic treatment of diseases, which are difficult to treat. Therefore, design and synthesis of novel carbohydrate appended molecules capable of mimicking biological processes has gained much attention. The carbohydrate moieties can increase water solubility of drugs, decrease toxicity and/or contribute to the bioactivity of the natural products. The present work is focused on the design, synthesis and biological studies of novel glycohybrids. The key step in the synthesis of sugar-appended molecules is the glycosidation reaction of the sugar donor with an acceptor. Click chemistry, in particular, the copper-(I)-catalyzed ligation of azides and acetylenes, promises to greatly simplify and accelerate the discovery of high-affinity carbohydrate mimetics. Thus the present work is paying attention to the synthesis of a series of triazole linked glycohybrids using the Cu(I) catalyzed click coupling of carbohydrate derived acetylenes and azides derived from meso-bicyclic hydrazines *via* palladium catalyzed ring opening.

#### 4.6. Results and discussion

Our aim was to synthesize glycohybrids by connecting the azido alkylidenecyclopentenes with propargyl glycosides. The palladium catalyzed reaction of fulvene derived bicyclic hydrazines **9** with trimethylazidosilane afforded the *trans*-3-azido-4-hydrazino alkylidene cyclopentene **14** in good yield (Scheme 4.3.). The bicyclic hydrazines used for our strategy were prepared by Diels-Alder cycloaddition of pentafulvenes with diethyl azodicarboxylate (DEAD).



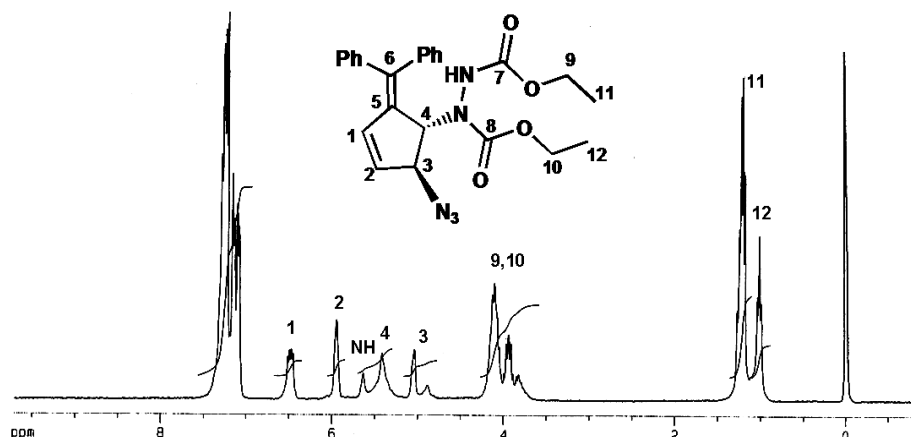
Scheme 4.3

Under this condition, the reaction between bicyclic hydrazine **15a** and trimethylsilylazide **16**, afforded 3-azido-4-hydrazino alkylidene cyclopentene **17a** in good yield. (Scheme 4.4).



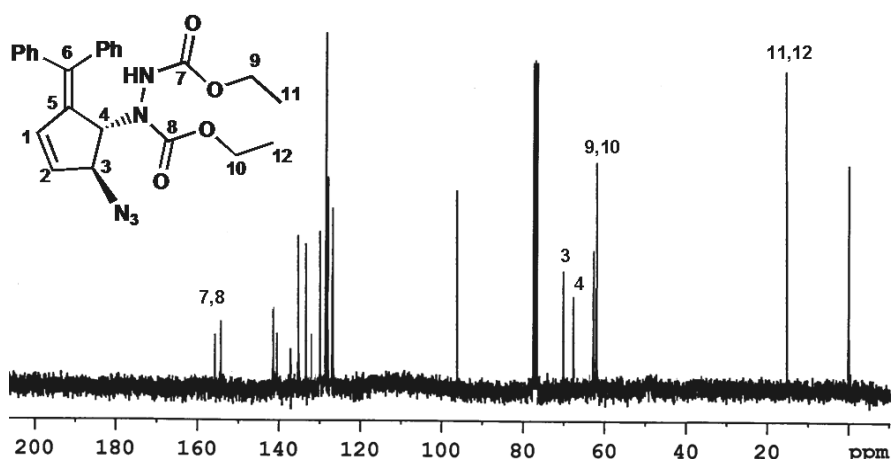
Scheme 4.4

The structure of the product **17a** was established based on spectroscopic analysis. IR spectrum showed absorptions at  $3312\text{ cm}^{-1}$  and  $1742\text{ cm}^{-1}$  indicating the presence of N-H and C=O functionalities. Azide group presented its absorption at  $2102\text{ cm}^{-1}$  as a sharp signal.  $^1H$  NMR spectrum (Figure 4.7) located the olefinic protons at C1 and C2 as a double doublet and a singlet at  $\delta$  6.52 and 5.99 respectively. The N-H proton was found to be merged with the multiplet signal due to proton at C3 in the region  $\delta$  5.67-5.45. The multiplets observed in the regions  $\delta$  4.19-4.09 and 4.03-3.92 were attributed to the protons at C9 and C10.



**Figure 4.7.**  $^1\text{H}$ NMR spectrum of compound **17a**

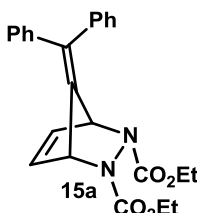
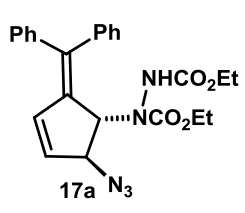
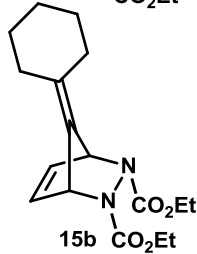
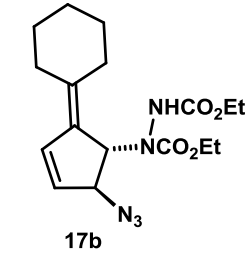
$^{13}\text{C}$  NMR spectrum of **17a** (Figure 4.8) marked carbonyl signals at  $\delta$  156.2 and 154.4. Carbon carrying the azide group C3 appeared at  $\delta$  70.3, while the C4 carbon was found to resonate at  $\delta$  67.8. The signals at  $\delta$  62.7 and 62.2 were assigned to the ethoxy carbons C9 and C10. The methyl carbons C11 and C12 were visible at  $\delta$  14.4 and 14.1. Mass spectra identified the molecular ion peak at  $m/z$  447.1904 and provided additional evidence for the structure.



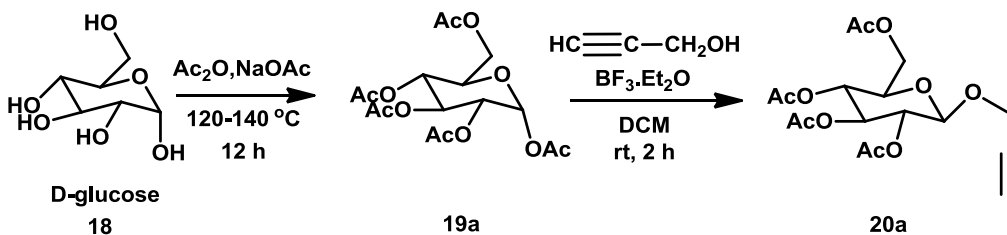
**Figure 4.8.**  $^{13}\text{C}$  NMR spectrum of compound **17a**

Similarly, another bicyclic olefin **15b** also reacted under the same reaction conditions to afford the desired product in 60% yield. The synthesized azido compounds are shown in table 4.1.

**Table 4.1. Palladium catalyzed synthesis of azido alkylidene cyclopentenes**

Entry	Bicyclic olefin	Product	Yield(%)
1	 15a	 17a	87
2	 15b	 17b	60

Propargyl glycosides were prepared by the reported procedure [Mereyala and Gurralla 1998]. Acetylated glucose, mannose and galactose were used as the glycosyl donors and propargyl alcohol as acceptor for the glycosidation reaction. The reaction pathway is shown in scheme 4.5.

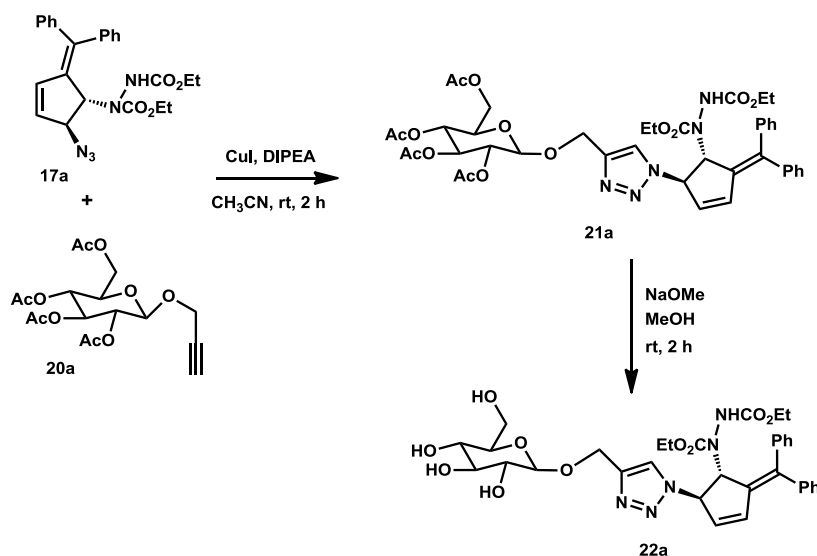
**Scheme 4.5**

All reactions afforded the propargylated glycosides in good yield. The results are shown in table 4.2.

Table 4.2. Propargyl glycosides

Entry	Donor	Product	Yield (%)
1			72
2			79
3			82

With the two coupling partners in hand, we conducted copper catalyzed 1,3-dipolar cycloaddition of azido alkylidencyclopentene with propargyl glycosides [Hotha and Kashyap 2006]. The reaction carried out at room temperature for 2 hours in acetonitrile followed by alkaline hydrolysis yielded the target glycohybrids in moderate to good yields (Scheme 4.6).



Scheme 4.6

The structure of the product was assigned based on various spectral analysis. IR spectrum of compound **21a** showed peaks at  $3445\text{ cm}^{-1}$  and  $1752\text{ cm}^{-1}$  which are due to -NH and carbonyl group of acetyl moiety respectively. In  $^1\text{H}$  NMR spectrum, proton of the triazole ring resonated at  $\delta$  7.95-7.87 as a multiplet. Ten aromatic protons presented a multiplet at  $\delta$  7.32- 7.16. The olefinic protons on the cyclopentene ring resonated at  $\delta$  6.88-6.70 and 6.35-6.25 as multiplets. The proton on the carbon attached to the triazole ring appeared as a broad singlet at  $\delta$  5.98. The -NH proton was merged with proton attached to carbon with hydrazine moiety and appeared as a multiplet at  $\delta$  5.75-5.55. The anomeric proton was merged with the methylene protons in the region  $\delta$  5.15-4.80. Four methylene protons of hydrazine moiety resonated at  $\delta$  4.26-4.09 as a multiplet. Twelve protons of acetyl moiety appeared at  $\delta$  2.10-2.00. The methyl protons of hydrazine part resonated at  $\delta$  1.20 and 1.00 as triplets with coupling constants 7 and 6.5 Hz respectively (Figure 4.9).

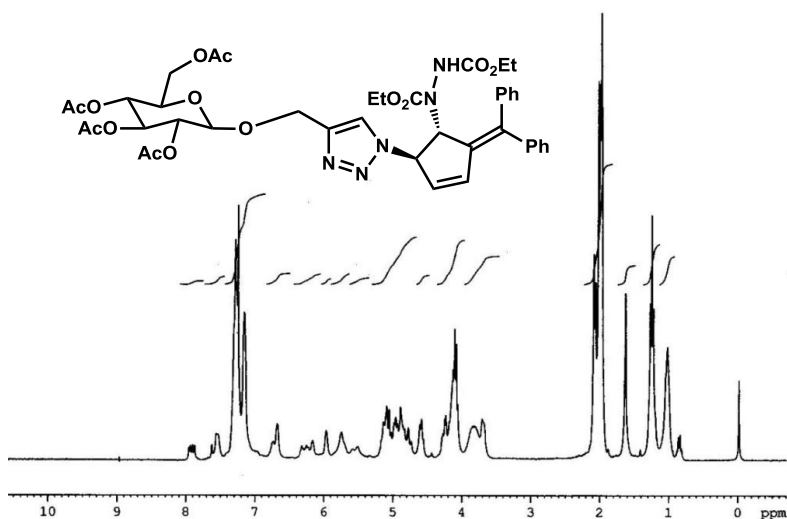


**Figure 4.9.**  $^1\text{H}$  NMR of Compound **21a**.

$^{13}\text{C}$  NMR spectrum presented peaks at  $\delta$  170.4, 170.3, 170.2, and 169.9, which attributed to the carbonyl carbons of acetyl moiety. The carbonyl groups of hydrazine part resonated at  $\delta$  157.3 and 154.3. The anomeric carbon presented a peak at  $\delta$  96.5. The signal due to methylene carbons of the carboethoxy groups appeared at  $\delta$  62.1 and 61.9. The methyl carbons of acetyl group resonated in the region  $\delta$  20.7-20.4 (Figure 4.10). All other signals were in good agreement with the proposed structure. Finally, the



structure of the compound was further confirmed by mass spectral analysis. The spectrum showed a molecular ion peak at  $m/z = 856.3011 [M+Na]^+$ .

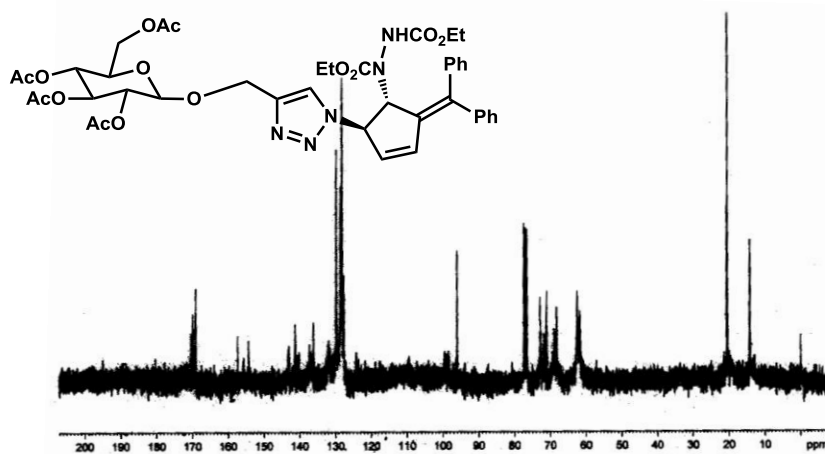


**Figure 4.10.**  $^{13}\text{C}$  NMR of compound **21a**

The product **22a** was also characterized by IR, NMR and mass spectral data. In IR spectrum, the peaks due to hydroxyl and -NH appeared as a broad band centered at  $3425\text{ cm}^{-1}$ . The carbonyl peak was observed at  $1716\text{ cm}^{-1}$ . In  $^1\text{H}$  NMR spectrum, proton on the triazole was observed at  $\delta$  8.10 as a singlet. Aromatic protons resonated in the region  $\delta$  7.30-7.20 as a multiplet. The olefinic protons on the cyclopentene ring were observed as doublet of doublet and doublet at  $\delta$  6.70 and 6.20 respectively. The proton on the carbon attached to the nitrogen atom of triazole ring appeared as multiplet at  $\delta$  6.15-6.05. The -NH proton was merged with the proton attached to the carbon with hydrazine moiety and appeared in the region  $\delta$  5.75-5.60. The methylene protons attached to triazole ring were observed at  $\delta$  5.05-4.98 as a multiplet (Figure 4.11). In the  $^{13}\text{C}$  NMR, the peak at  $\delta$  156.4 and 156.2 were attributed to the carbonyl carbons. The anomeric carbon was present at  $\delta$  103.5. The methyl carbons showed their peak at  $\delta$  14.8 (Figure 4.12). Finally, the structure of the compound was further confirmed by mass spectral analysis. The spectrum showed a molecular ion peak at  $m/z = 666.2770 [M+1]$ .

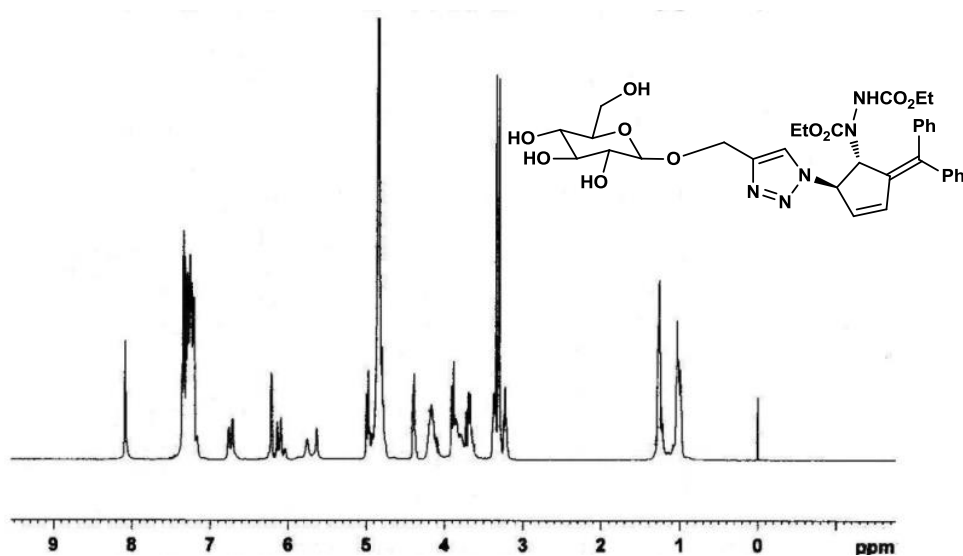


Figure 4.11. <sup>1</sup>H NMR of compound 22a

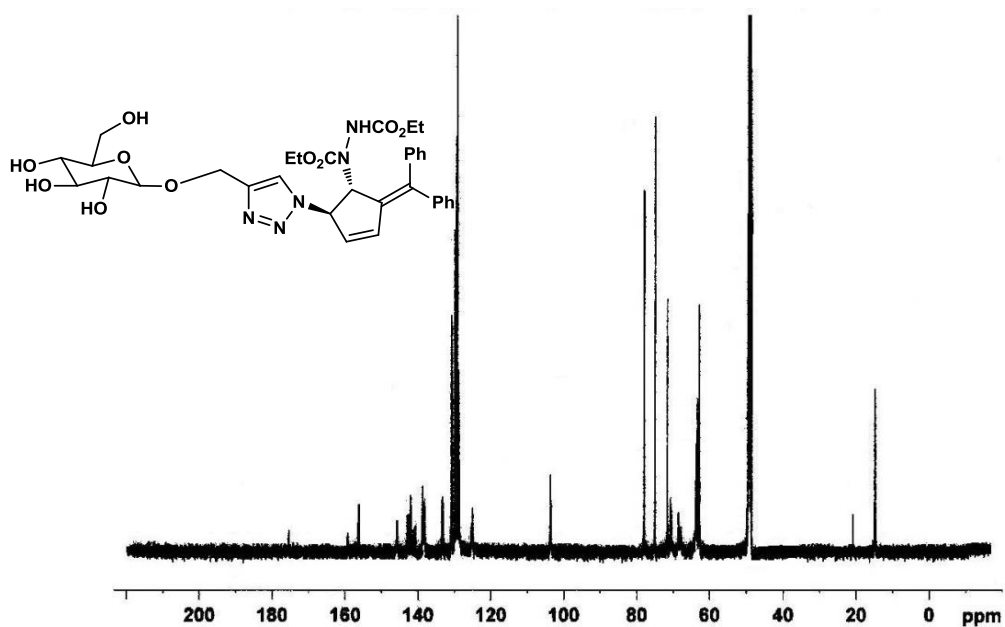


Figure 4.12. <sup>13</sup>C NMR of compound 22a

Using the same methodology we have synthesized a series of triazole linked glycohybrids. The results are summarised in Table 4.3.

Table 4.3: Novel Glycohybrids

Entry	Azide	Alkyne	Product	Yield (%)
1				R' = OAc, <b>21a</b> (70%) R' = H, <b>22a</b> (86%)
2				R' = OAc, <b>21b</b> (61%) R' = H, <b>22b</b> (85%)
3				R' = OAc, <b>21c</b> (77.5%) R' = H, <b>22c</b> (79%)
4				R' = OAc, <b>21d</b> (37%) R' = H, <b>22d</b> (86%)
5				R' = OAc, <b>21e</b> (40%) R' = H, <b>22e</b> (77%)
6				R' = OAc, <b>21f</b> (45%) R' = H, <b>22f</b> (96%)

Reaction conditions: azide (1 equiv.), alkyne (1.1 equiv.), CuI (2 equiv.), DIPEA (3 equiv.) in acetonitrile (10 mL) for 2 hours. For alkaline hydrolysis: Na metal (8 equiv.) and click product (1 equiv.) in methanol (10 mL) at rt for 2 hours.

## 4.7. Biological evaluation of glycohybrids

### 4.7.1. $\alpha$ -Amylase and $\alpha$ -glucosidase inhibition assay

Pancreatic  $\alpha$ -amylase breaks complex starch to oligosaccharides in the lumen of the small intestine, whereas the membrane-bound intestinal  $\alpha$ -glucosidases hydrolyze oligosaccharides, trisaccharides and disaccharides to glucose and carbohydrates and hence the level of sugar in blood [Gamblin et al. 2008; Park et al. 2009; Rawling et al. 2009]. With the glycohybrids in hand, we evaluated their inhibitory properties against  $\alpha$ -

glucosidase and  $\alpha$ -amylase enzymes using reported procedures [Apostolidis *et al.* 2009; Priya *et al.* 2011]. The results are shown in Figure 4.13. From the results, it is clear that the compound **22f** with a galactose appendage showed good  $\alpha$ -glucosidase inhibition activity, but others exhibited only moderate to poor inhibition properties. The standard used for this assay was acarbose, which showed an  $IC_{50}$  value of  $47.20 \pm 2.50 \mu M$  whereas compound **22f** gave a value of  $74.21 \pm 1.87 \mu M$ . All the  $IC_{50}$  values are given in table 4.4. But in the case of  $\alpha$ -amylase enzyme inhibition assay, the compounds showed poor or no inhibition activity.

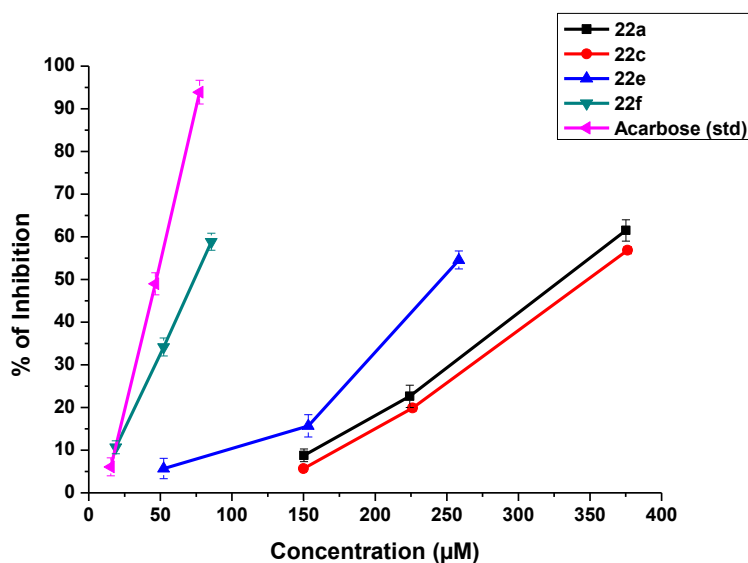


**Figure 4.13.**  $\alpha$ -Glucosidase inhibition of compounds **22a**, **22c**, **22e** and **22f** with varying concentrations

**Table 4.4.**  $IC_{50}$  values of compounds **22a**, **22c**, **22e** and **22f** against  $\alpha$ -glucosidase enzyme

Sl. No.	Compounds	$IC_{50} \pm SD$ ( $\mu M$ )
1	<b>22a</b>	$332.46 \pm 2.20$
2	<b>22c</b>	$351.19 \pm 2.30$
3	<b>22e</b>	$247.05 \pm 2.36$
4	<b>22f</b>	$74.21 \pm 1.87$
5	<b>Acarbose</b>	$47.20 \pm 2.50$

#### 4.7.2. Anti-glycation inhibition assay

We also checked the ability of our compounds to inhibit the protein glycation reaction using the procedure reported by Arom with slight modifications. Glycation is a non-enzymatic reaction in which the excess sugars present in the blood forms covalent bond with the blood protein leading to the formation of advanced glycated end-products (AGE's). The formation and accumulation of AGE's has been implicated in the progression of age-related diseases such as Alzheimer's disease, cardiovascular disease and stroke [Nagi *et al.* 2010; Ichihashi *et al.* 2011; Grillo and Colombatto 2008]. The results obtained are shown in figure 4.14. The results show that the compound **22f** with a galactose appendage is a potent anti-glycating agent with an  $IC_{50}$  value of just  $22.39 \pm 2.28 \mu\text{M}$  compared to the standard ascorbic acid ( $IC_{50} = 28.82 \pm 1.96 \mu\text{M}$ ) (Table 4. 5).

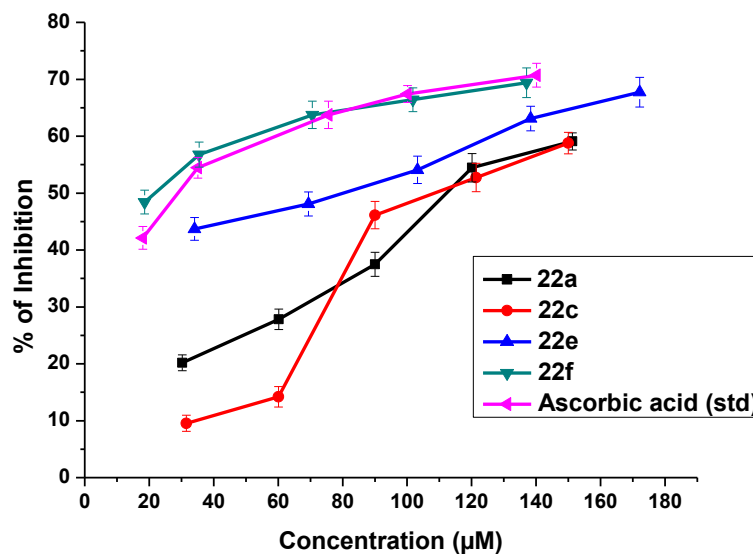


**Figure 4.14.** Glycation inhibition of compounds **22a**, **22c**, **22e** and **22f** with varying concentrations

**Table 4.5. IC<sub>50</sub> values of compounds 22a, 22c, 22e and 22f against glycation reaction**

Sl. No.	Compounds	IC <sub>50</sub> ± SD (μM)
1	22a	111.95 ± 1.86
2	22c	110 ± 2.00
3	22e	80.74 ± 2.25
4	22f	22.39 ± 2.28
5	Ascorbic acid	28.82 ± 1.96

#### 4.7.3. Cytotoxicity studies (MTT assay)

Moreover, the four compounds were found to be non-cytotoxic against H9c2 cardiac myoblast cell lines with MTT assay. The cytotoxicity assay results of compound **22f** are given in table 4.6. The assay proved that the compound **22f** is non-cytotoxic against H9c2 cardiac myoblast cell lines up to a concentration of 40 μM.

**Table 4.6. MTT assay results of compound 22f**

	Control	10 μM	20 μM	30 μM	40 μM
	0.501	0.489	0.486	0.464	0.442
	0.504	0.502	0.485	0.476	0.439
<b>Average</b>	0.503	0.496	0.486	0.470	0.441
<b>%toxicity</b>		2.687	3.284	7.662	12.040
	0.000	0.100	3.483	5.274	12.637
<b>Average</b>		1.393	3.383	6.468	12.338
<b>SD</b>		1.829	0.141	1.689	0.422

The morphological evaluation showed that cells had not undergone marked changes in structure from its spindle shape up to 40 μM concentration. At higher concentrations cells showed shrinkage, rounding up and membrane blebbing.

#### 4.8. Conclusion

In conclusion, we have synthesized a series of novel carbohydrate-alkylidenecyclopentene hybrids showing good biological activities. Out of the six compounds, four compounds were screened against α-glucosidase, α-amylase and protein

glycation reaction inhibition assays. From the results, it was found that the compound **22f** with a galactose appendage is a good  $\alpha$ -glucosidase inhibitor and a potent anti-glycating agent. Also, the MTT assay proved that the compound **22f** is non-cytotoxic against H9c2 cardiac myoblast cell lines upto a concentration of 40  $\mu$ M. Further *in vitro* as well as the *in vivo* studies of the active molecule are in progress with a hope to come up with a potent molecule against the diabetes mellitus type II.

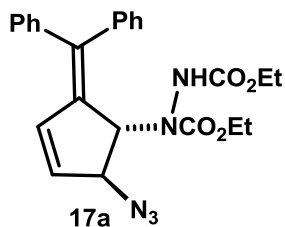
## 4.9. Experimental section

### Synthesis of azido alkylidene cyclopentenes

Bicyclic hydrazine (2 equiv.) and silane (1 equiv.) were taken in a schlenk tube. PPh<sub>3</sub> (20 mol %), Pd<sub>2</sub>(dba)<sub>3</sub>.CHCl<sub>3</sub> (5 mol %) were added to the reaction mixture followed by the addition of Sc(OTf)<sub>3</sub> (2 mol %) and evacuated. 4 mL dry toluene was added and degassed under Argon atmosphere. The reaction mixture was stirred at 60 °C for 12 hours. Completion of the reaction was monitored by TLC, solvent was removed and the reaction mixture was subjected to column chromatography using silica gel 100-200 mesh and EtOAc-hexane mixtures. (15% EtOAc)

### Diethyl-2-azido-5-(diphenylmethylene)cyclopent-3-en-1-yl)hydrazine-1,2 dicarboxylate **17a**

Following the general experimental procedure, bicyclic hydrazine **15a** (228 mg, 0.56 mmol), azidotrimethyl silane **16** (32.51 mg, 0.28 mmol), PPh<sub>3</sub> (14.8 mg, 20 mol %), Pd<sub>2</sub>(dba)<sub>3</sub>.CHCl<sub>3</sub> (14.6 mg, 5 mol %) and Sc(OTf)<sub>3</sub> (2.78 mg, 2 mol %), in 4 mL of dry toluene at 60 °C for 12 h gave the product **17a** as a white solid in 87% (110 mg) yield.



**IR** (KBr)  $\nu_{\max}$ : 3312, 2981, 2102, 1742, 1698, 1598, 1492, 1418, 1384, 1305, 1222, 1134, 1061, 954, 756, 703  $\text{cm}^{-1}$ .

**<sup>1</sup>H NMR** (300 MHz, CDCl<sub>3</sub>):  $\delta$  7.33-7.12 (m, 10H), 6.52 (dd,  $J_1 = 5.6$  Hz,  $J_2 = 12.4$  Hz, 1H), 5.99 (s, 1H), 5.67-5.45 (m, 2H), 5.08-4.93 (m, 1H), 4.19-4.09 (m, 2H), 4.03-3.92 (m, 2H), 1.32-1.23 (m, 4H), 1.06

(t,  $J = 6.9$  Hz, 2H).

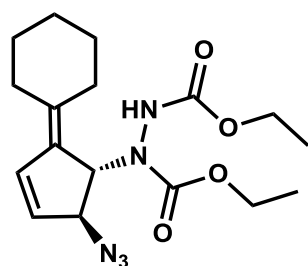
$^{13}\text{C}$  NMR (75 MHz,  $\text{CDCl}_3$ ):  $\delta$  156.2, 154.4, 141.5, 140.7, 138.2, 136.5, 135.8, 135.6, 133.7, 129.8, 129.7, 128.6, 128.4, 128.3, 128.1, 127.6, 70.3, 67.8, 62.7, 62.2, 14.4, 14.1.

Mass Spectrometric Analysis: HRMS (ESI):  $m/z$  calcd for  $\text{C}_{24}\text{H}_{25}\text{N}_5\text{O}_4$  ( $\text{M}^+$ ): 447.1907; found: 447.1904.

**Diethyl-2-azido-5-cyclohexylidenecyclopent-3-enyl)hydrazine-1,2-dicarboxylate 17b**

Following the general experimental procedure, bicyclic hydrazine **15b** (264 mg, 0.825 mmol), azidotrimethyl silane **2** (47.52 mg, 0.41 mmol),  $\text{PPh}_3$  (21.62 mg, 20 mol %),  $\text{Pd}_2(\text{dba})_3 \cdot \text{CHCl}_3$  (21.35 mg, 5 mol %) and  $\text{Sc}(\text{OTf})_3$  (4.06 mg, 2 mol %), in 4 mL of dry toluene at  $60^\circ\text{C}$  for 12 h gave the product **3b** as a yellow viscous liquid in 60% (88.5 mg) yield.

IR (neat)  $\nu_{\text{max}}$ : 3285, 2925, 2857, 2097, 1715, 1410, 1380, 1300, 1230, 1125, 1059, 966, 760  $\text{cm}^{-1}$ .



**17b**

$^1\text{H}$  NMR (300 MHz,  $\text{CDCl}_3$ ):  $\delta$  6.67 (d,  $J = 5.7$  Hz, 1H), 6.15 (s, 1H), 5.87 (s, 1H), 5.33-5.03 (m, 1H), 4.78 (s, 1H), 4.30-4.13 (m, 4H), 2.36-2.08 (m, 4H), 1.80-1.50 (m, 6H), 1.42-1.22 (m, 6H).

$^{13}\text{C}$  NMR (75 MHz,  $\text{CDCl}_3$ ):  $\delta$  156.6, 155.4, 141.6, 135.0, 131.0, 129.4, 70.7, 63.4, 62.4, 61.2, 31.5, 30.5, 29.9, 28.2, 25.7, 14.5, 14.4.



Mass Spectrometric Analysis: **LRMS** (FAB):  $m/z$  calcd for  $C_{17}H_{25}N_5O_4Na$  ( $M^+$ ): 386.1940; found: 386.1922.

#### General procedure for alkylation

The protected carbohydrate (1 equiv.) was dissolved in DCM, cooled to 0 °C and propargyl alcohol (1.2 equiv.) was added followed by  $BF_3 \cdot Et_2O$  (1.5 equiv.) and stirred at room temperature for 2 h under argon atmosphere. The completion of the reaction was monitored by TLC and quenched by stirring with anhydrous  $K_2CO_3$  for 30 minutes. It was then extracted with dichloromethane (3 x 50 mL), dried and concentrated. The reaction mixture was subjected to column chromatography using silica gel 60-120 mesh and EtOAc-hexane as eluent.

#### General procedure for click reaction

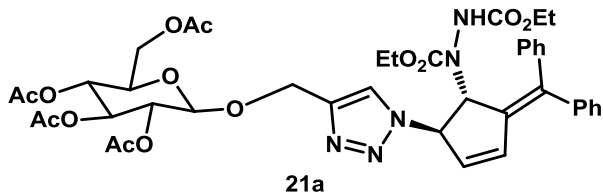
The alkylated carbohydrate (1.1 equiv.) and the azide (1 equiv.) are taken in a single neck RB and dissolved in dry acetonitrile. CuI (2 equiv.) was added followed by DIPEA (3 equiv.) and stirred at room temperature for 3 hours. Completion of the reaction was monitored by TLC and the reaction was quenched by adding  $NH_4Cl$  solution. It was then extracted with ethylacetate (3 x 50 mL), washed with brine and the solvent was removed. The reaction mixture was subjected to column chromatography using silica gel 60-120 mesh and EtOAc-hexane mixtures for elution.

#### Data for compound 21a

Following the general experimental procedure, the alkyne **20a** (209 mg, 0.54 mmol), azide **17a** (220 mg, 0.49 mmol), CuI (188 mg, 0.98 mmol) and DIPEA (191 mg, 1.48 mmol) in 20 mL dry acetonitrile gave the product as a very pale yellow frothing solid **21a** in 70% (288 mg) yield.  $R_f$ : 0.33 (70% EtOAc-hexane).  $Mp$  = 75 °C.

**IR** (KBr)  $\nu_{max}$ : 3445, 2925, 2855, 1752, 1635, 1446, 1413, 1379, 1309, 1227, 1160, 1041, 760, 703  $cm^{-1}$ .

**$^1H$  NMR** (500 MHz,  $CDCl_3$ ):  $\delta$  7.95-7.87 (m, 1H), 7.32-7.16 (m, 10H), 6.88-6.70 (m, 1H), 6.35-6.25 (m, 1H), 5.98



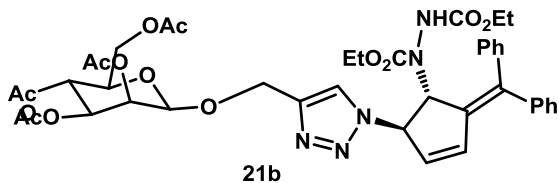
(br.s, 1H), 5.75-5.55 (m, 2H), 5.15-4.80 (m, 5H), 4.62-4.61 (m, 1H), 4.26-4.09 (m, 4H), 3.81-3.69 (m, 3H), 2.10- 2.00 (m, 12H), 1.20 (t,  $J = 7$  Hz, 3H), 1.00 (t,  $J = 6.5$  Hz, 3H).

$^{13}\text{C}$  NMR (125 MHz,  $\text{CDCl}_3$ ):  $\delta$  170.4, 170.3, 170.2, 169.9, 157.3, 154.3, 143.1, 141.3, 140.6, 140.2, 131.6, 130.7, 129.8, 129.2, 128.6, 128.3, 128.2, 127.7, 124.3, 96.5, 72.9, 71.7, 69.5, 68.3, 62.5, 62.1, 61.9, 61.2, 20.7, 20.6, 20.5, 20.4, 14.4, 14.3.

Mass Spectrometric Analysis: **LRMS** (FAB):  $m/z$  calcd for  $\text{C}_{41}\text{H}_{47}\text{N}_5\text{O}_{14}\text{Na}$ : 856.3017; found: 856.3011.

#### Data for compound 21b

Following the general experimental procedure, the alkyne **20b** (108 mg, 0.28 mmol), azide **17a** (114 mg, 0.254 mmol), CuI (96.9 mg, 0.509 mmol) and DIPEA (98.5 mg, 0.762 mmol) in 15 mL dry acetonitrile gave the product as a very pale yellow frothing solid **21b** in 61% (130 mg) yield.  $R_f$ : 0.33 (70% EtOAc-hexane).  $\text{Mp} = 78$  °C.



**IR** (KBr)  $\nu_{\text{max}}$ : 3429, 2926, 2855, 1751, 1632, 1445, 1409, 1374, 1309, 1225, 1133, 1047, 760, 703  $\text{cm}^{-1}$ .

$^1\text{H}$  NMR (300 MHz,  $\text{CDCl}_3$ ):  $\delta$  8.10-7.95 (m, 1H), 7.19-7.69 (m, 10H), 6.7 (d,  $J = 4.8$  Hz, 1H), 6.32 (d,  $J = 13.5$  Hz, 1H), 6.02 (s, 1H), 5.85-5.51 (m, 2H), 5.29-5.20 (m, 3H), 4.99-4.96 (m, 1H), 4.84-4.67 (m, 1H), 4.67-4.55 (m, 1H),

4.33-4.29 (m, 1H), 4.15-4.08 (m, 4H),  
3.92-3.84 (m, 2H), 2.16-1.97 (m, 12H),  
1.24-1.43 (m, 6H).

<sup>13</sup>C NMR (125 MHz, CDCl<sub>3</sub>): δ 170.5,  
170.4, 170.3, 169.9, 157.6, 154.3, 143.1,  
141.8, 140.6, 140.2, 131.6, 130.8, 129.8,  
129.2, 128.6, 128.3, 128.2, 127.7, 124.3,  
96.8, 72.9, 71.7, 69.5, 68.3, 62.5, 62.1,  
61.7, 61.2, 20.7, 20.6, 20.5, 14.6, 14.4

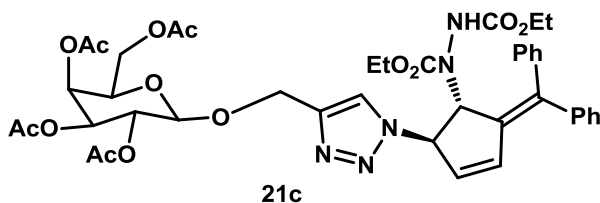
Mass Spectrometric Analysis: **LRMS** (FAB): *m/z* calcd for C<sub>41</sub>H<sub>47</sub>N<sub>5</sub>O<sub>14</sub>Na:  
856.31; found: 856.33.

#### Data for compound **21c**

Following the general experimental procedure, the alkyne **20c** (167 mg, 0.43 mmol), azide **17a** (176 mg, 0.39 mmol), CuI (148 mg, 0.78 mmol) and DIPEA (151 mg, 1.17 mmol) in 15 mL dry acetonitrile gave the product as a very pale yellow frothing solid **21c** in 75% (245 mg) yield. R<sub>f</sub>: 0.33 (70% EtOAc-hexane). Mp = 76 °C.

**IR** (KBr)  $\nu_{\max}$ : 3439, 2926, 2855,  
1750, 1634, 1444, 1409, 1373, 1309,  
1226, 1172, 1055, 760, 704 cm<sup>-1</sup>.

<sup>1</sup>H NMR (500 MHz, CDCl<sub>3</sub>): δ  
7.96-7.92 (m, 1H), 7.34-7.16 (m,  
10H), 6.69 (s, 1H), 6.35-6.25 (m, 1H),  
5.99 (s, 1H), 5.80-5.50 (m, 2H), 5.36  
(d, *J* = 2.5 Hz, 1H), 5.20-5.15 (m,  
1H), 4.98-4.20 (m, 2H), 4.80-4.75 (m,  
1H), 4.60-4.50 (m, 1H), 4.30-4.25 (m,  
1H), 4.17-4.09 (m, 4H), 3.94-3.75 (m,  
2H), 2.15-1.97 (m, 12H), 1.26 (t, *J* = 7



Hz, 6H).

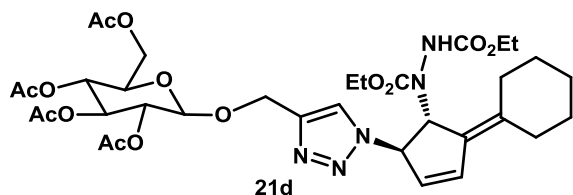
$^{13}\text{C}$  NMR (125 MHz,  $\text{CDCl}_3$ ):  $\delta$  170.5, 170.4, 170.1, 169.5, 157.4, 154.3, 143.4, 141.4, 141.2, 140.2, 137.4, 137.2, 129.8, 128.6, 128.2, 127.7, 96.1, 70.9, 69.3, 68.6, 67.2, 62.6, 62.4, 61.3, 20.8, 2.7, 2.6, 2.5, 14.4, 14.3.

Mass Spectrometric Analysis: **LRMS** (FAB):  $m/z$  calcd for  $\text{C}_{41}\text{H}_{47}\text{N}_5\text{O}_{14}\text{Na}$ : 856.31; found: 856.32.

#### Data for compound **21d**

Following the general experimental procedure, the alkyne **20a** (184 mg, 0.48 mmol), azide **17b** (157 mg, 0.43 mmol),  $\text{CuI}$  (165 mg, 0.87 mmol) and  $\text{DIPEA}$  (168 mg, 1.3 mmol) in 15 mL dry acetonitrile gave the product **21d** as a very pale brown frothing solid in 37% (119 mg) yield.  $R_f$ : 0.28 (70%  $\text{EtOAc}$ -hexane).  $\text{Mp} = 73^\circ\text{C}$ .

**IR** (KBr)  $\nu_{\text{max}}$ : 3300, 2934, 2856, 1755, 1512, 1445, 1410, 1378, 1226, 1171, 1121, 1043, 787, 761  $\text{cm}^{-1}$ .



$^1\text{H}$  NMR (300 MHz,  $\text{CDCl}_3$ ):  $\delta$  8.00-7.40 (m, 1H), 6.80 (s, 1H), 6.24 (s, 1H), 5.97-5.85 (m, 2H), 5.18-4.80 (m, 6H), 4.64 (d, 1H), 4.22-4.10 (m, 6H), 3.70 (s, 1H), 2.16-1.99 (m, 16H), 1.60 (s, 6H), 1.29 (t,  $J = 7.2$  Hz, 6H).

$^{13}\text{C}$  NMR (75 MHz,  $\text{CDCl}_3$ ): 170.3, 170.2, 170.1, 169.8, 157.4, 145.9, 142.3, 131.3, 130.3, 130.1, 122.9, 96.7, 74.8, 72.3, 70.7, 69.3, 65.9, 62.5, 61.7, 61.4,

56.0, 33.8, 29.0, 25.8, 20.76, 20.6, 20.5,  
20.4 14.6, 14.4.

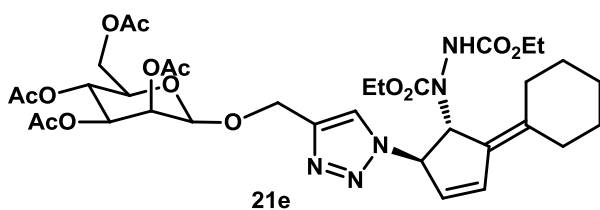
Mass Spectrometric Analysis: **LRMS** (FAB):  $m/z$ . calcd for  $C_{34}H_{47}N_5O_{14}Na$ :  
772.30; found: 772.29.

### Data for compound **21e**

Following the general experimental procedure, the alkyne **20b** (187 mg, 0.48 mmol), azide **17b** (160 mg, 0.44 mmol), CuI (168 mg, 0.88 mmol) and DIPEA (171 mg, 1.32 mmol) in 15 mL dry acetonitrile gave the product as a very pale yellow frothing solid **21e** in 40% (130 mg) yield.  $R_f$ : 0.28 (70% EtOAc-hexane).  $M_p = 75\text{ }^\circ\text{C}$ .

**IR** (KBr)  $\nu_{\max}$ : 3430, 2927, 2855,  
1752, 1632, 1514, 1445, 1410, 1376,  
1227, 1170, 1123, 1051  $\text{cm}^{-1}$ .

**$^1\text{H}$  NMR** (500 MHz,  $\text{CDCl}_3$ ):  $\delta$   
7.80-7.60 (m, 1H), 6.83 (s, 1H), 6.34  
(s, 1H), 6.05-5.95 (m, 2H), 5.31-5.22  
(m, 5H), 4.95 (s, 1H), 4.84 (d,  $J = 12$   
Hz, 1H), 4.68 (d,  $J = 12$  Hz, 2H),  
4.31-4.13 (m, 4H), 2.15-1.97 (m,  
16H), 1.63-1.58 (m, 6H), 1.30-1.25  
(m, 6H).



**$^{13}\text{C}$  NMR** (125 MHz,  $\text{CDCl}_3$ ):  
170.7, 170.3, 169.9, 169.7, 157.4,  
154.2, 145.9, 142.3, 131.3, 130.3,  
130.1, 122.9, 96.3, 74.8, 72.0, 70.7,  
69.3, 65.9, 62.5, 61.7, 61.4, 56.0,  
33.5, 29.0, 25.8, 20.8, 20.7, 2.6, 14.4,  
1.3

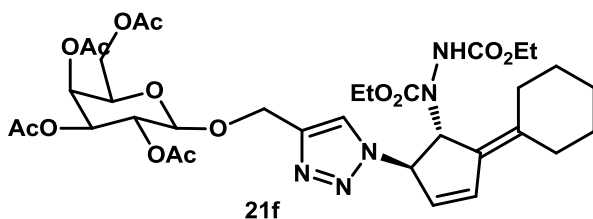
Mass Spectrometric Analysis: **LRMS** (FAB):  $m/z$  calcd for  $C_{34}H_{47}N_5O_{14}Na$ : 772.30; found: 772.30.

#### Data for compound **21f**

Following the general experimental procedure, the alkyne **20c** (214 mg, 0.55 mmol), azide **17b** (183 mg, 0.5 mmol), CuI (192 mg, 1.01 mmol) and DIPEA (195 mg, 1.5 mmol) in 20 mL dry acetonitrile gave the product as a very pale yellow frothing solid **21f** in 45% (170 mg) yield.  $R_f$ : 0.28 (70% EtOAc-hexane).  $M_p = 73$  °C.

**IR** (KBr)  $\nu_{max}$ : 3427, 2928, 2855, 1751, 1632, 1515, 1447, 1412, 1373, 1227, 1120, 1056, 760, 603  $cm^{-1}$ .

**$^1H$  NMR** (300 MHz,  $CDCl_3$ ):  $\delta$  7.80-7.50 (s, 1H), 6.74 (d, 1H), 6.25 (s, 1H), 6-05.5.85 (m, 2H), 5.30 (s, 1H), 5.13-5.08 (m, 2H), 4.99-4.73 (m, 3H), 4.56 (d,  $J = 8.1$  Hz, 1H), 4.31-4.08 (m, 6H), 3.94 (s, 1H), 2.17-1.97 (m, 16H), 1.60 (s, 6H), 1.26 (t,  $J = 7.2$  Hz, 6H).



**$^{13}C$  NMR** (75 MHz,  $CDCl_3$ ):  $\delta$  170.5, 170.4, 170.3, 157.1, 155.3, 143.9, 140, 135.6, 130, 128.4, 122.2, 97.0, 70.9, 69.9, 69.2, 67.1, 63.2, 62.4, 61.3, 31.8, 27.8, 26.2, 21.0, 20.7, 20.6, 14.4, 14.2.

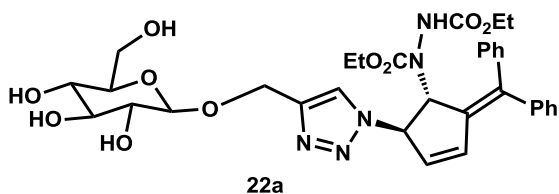
Mass Spectrometric Analysis: **LRMS** (FAB):  $m/z$  calcd for  $C_{34}H_{47}N_5O_{14}Na$ : 772.30; found: 772.29.

### General procedure for deprotection

Methanol (distilled) was taken in a single neck RB, cooled and Na pellets (8 eq.) were added and fully dissolved. The click product was added to it and stirred at room temperature for 2 h. Completion of the reaction was monitored by TLC, solvent was removed and the reaction mixture was subjected to column chromatography using silica gel 60-120 mesh and MeOH-CHCl<sub>3</sub> mixtures.

### Data for compound 22a

Following the general experimental procedure, Na (110 mg, 4.79 mmol) and compound **21a** (499 mg, 0.6 mmol) in dry MeOH gave the product as a pale yellow frothing solid **22a** in 86% (340 mg) yield. R<sub>f</sub>: 0.65 (30% MeOH-CHCl<sub>3</sub>). Mp = 78 °C.



**IR** (KBr)  $\nu_{\max}$ : 3425, 2980, 2925, 2500, 1716, 1600, 1492, 1467, 1444, 1413, 1381, 1337, 1307, 1229, 1156, 1079, 1046, 841, 757, 702 cm<sup>-1</sup>.

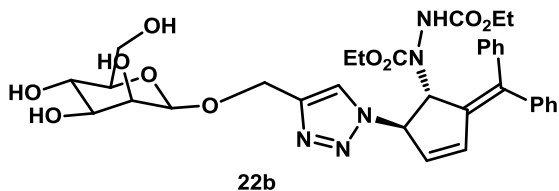
**<sup>1</sup>H NMR** (500 MHz, MeOD):  $\delta$  8.10 (s, 1H), 7.30-7.20 (m, 10H), 6.70 (dd, 1H), 6.20 (d,  $J = 5$  Hz, 1H), 6.15-6.05 (m, 1H), 5.75-5.60 (m, 2H), 5.05-4.98 (m, 2H), 4.40 (d,  $J = 7.5$  Hz, 1H), 4.18-4.14 (m, 2H), 3.91-3.85 (m, 3H), 3.73-3.67 (m, 3H), 3.40-3.20 (m, 2H), 1.28-1.25 (m, 3H), 1.04-1.01 (m, 3H)

**<sup>13</sup>C NMR** (125 MHz, MeOD):  $\delta$  156.4, 156.2, 145.8, 142.9, 141.3, 133.4, 133.2, 129.9, 129.3, 128.9, 103.5, 78.05, 75.09, 70.8, 70.6, 68.6, 63.9, 63.6, 63.4, 63.1, 62.9, 14.9.

Mass Spectrometric Analysis: **LRMS** (FAB):  $m/z$  calcd for  $C_{33}H_{39}N_5O_{10}$   $[M+1]^+$ : 666.2775; found: 666.2770.

#### Data for compound **22b**

Following the general experimental procedure, Sodium (11 mg, 0.48 mmol) and compound **21b** (50 mg, 0.06 mmol) in dry MeOH gave the product as a pale yellow frothing solid **22b** in 85% (34 mg) yield.  $R_f$ : 0.65 (30% MeOH- $CHCl_3$ ).  $M_p = 77$  °C.



**IR** (KBr)  $\nu_{max}$ : 3363, 2923, 2351, 2313, 1717, 1646, 1445, 1411, 1380, 1335, 1304, 1231, 1132, 1058, 842, 762, 703  $cm^{-1}$ .

**$^1H$  NMR** (300 MHz, MeOD):  $\delta$  8.08 (s, 1H), 7.35-7.22 (m, 10H), 6.80-6.73 (m, 1H), 6.22 (d,  $J = 5.7$  Hz, 1H), 6.20-6.09 (m, 1H), 5.75-5.65 (m, 2H), 4.65 (d,  $J = 13.2$  Hz, 1H), 4.17-4.06 (m, 2H), 3.88-3.59 (m, 8H), 1.45-1.29 (m, 6H)

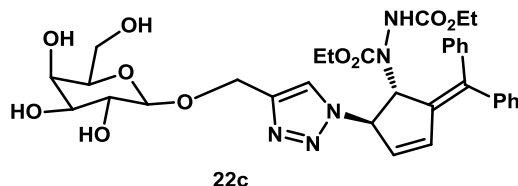
**$^{13}C$  NMR** (75 MHz, MeOD):  $\delta$  156.7, 146.2, 142.6, 131.3, 130.3, 128.6, 128.3, 127.9, 104.2, 83.4, 78.9, 76.6, 72.5, 70.4, 64.5, 63.9, 63.2, 63.1, 61.2, 14.8

Mass Spectrometric Analysis: **LRMS** (FAB):  $m/z$  calcd for  $C_{33}H_{39}N_5O_{10}$   $[M+1]^+$ : 666.27; found: 666.29.

#### Data for compound **22c**

Following the general experimental procedure, Na (31 mg, 1.44 mmol) and compound **21c** (150 mg, 0.18 mmol) in dry MeOH gave the product as a white solid **22c** in 79% (94 mg) yield.  $R_f$ : 0.65 (30% MeOH- $CHCl_3$ ).





**IR** (KBr)  $\nu_{\max}$ : 3426, 2924, 2854, 2471, 1699, 1641, 1492, 1442, 1424, 1383, 1342, 1312, 1277, 1232, 1151, 1047, 842, 758, 702  $\text{cm}^{-1}$ .

**$^1\text{H}$  NMR** (300 MHz, MeOD):  $\delta$  8.06 (d,  $J = 7.8$  Hz, 1H), 7.51-7.22 (m, 10H), 6.85-6.70 (m, 1H), 6.22-6.20 (m, 1H), 6.11 (d,  $J = 12.6$  Hz, 1H), 5.75-5.63 (m, 2H), 5.01- 4.98 (m, 1H), 4.67-3.55 (m, 12H), 1.29-1.01 (m, 6H).

**$^{13}\text{C}$  NMR** (75 MHz, MeOD):  $\delta$  156.4, 156.2, 145.8, 142.9, 131.3, 130.3, 128.6, 128.3, 127.9, 103.5, 83.4, 78.9, 76.6, 72.5, 70.4, 64.5, 63.9, 63.1, 63.0, 61.2, 14.8

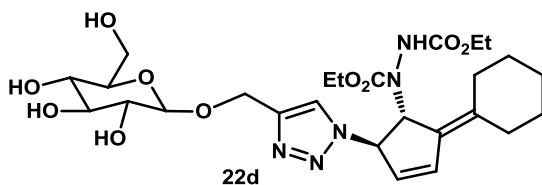
Mass Spectrometric Analysis: **LRMS** (FAB):  $m/z$  calcd for  $\text{C}_{33}\text{H}_{39}\text{N}_5\text{O}_{10}$   $[\text{M}+1]^+$ : 666.27; found: 666.27.

#### Data for compound **22d**

Following the general experimental procedure, Na (38 mg, 1.64 mmol) and compound **21d** (154 mg, 0.21 mmol) in dry MeOH gave the product as a pale brown frothing solid **22d** in 86% (103 mg) yield.  $R_f$ : 0.62 (30% MeOH- $\text{CHCl}_3$ ).

**IR** (KBr)  $\nu_{\max}$ : 3425, 2981, 2926, 1715, 1631, 1414, 1228, 1051  $\text{cm}^{-1}$ .

**$^1\text{H}$  NMR** (500 MHz, MeOD):  $\delta$  7.89 (s, 1H), 6.92 (d,  $J = 5.5$  Hz, 1H), 6.10-6.05 (m, 1H), 5.98 (s, 1H), 5.23 (br.s, 1H), 4.99-4.88 (m, 1H), 4.77-4.60 (m,



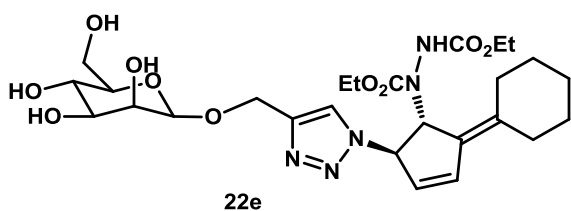
1H), 4.38 (d,  $J = 7.5$  Hz, 1 H), 4.19-4.08 (m, 5H), 3.90 (d, 1H), 3.68 (dd,  $J_1 = 5$  Hz,  $J_2 = 10$  Hz, 1H), 3.38-3.21 (m, 2H), 2.15-2.25 (m, 4H), 1.7-1.51 (m, 6H), 1.26-1.22 (m, 6H).

$^{13}\text{C}$  NMR (125 MHz, MeOD):  $\delta$  159.6, 146.1, 137.8, 131.6, 131.3, 129.1, 123.8, 104.4, 83.4, 78.9, 76.6, 72.5, 70.4, 64.5, 63.9, 63.1, 63, 61.2, 32.6, 28.8, 27.4, 14.9.

Mass Spectrometric Analysis: **LRMS** (FAB):  $m/z$  calcd for  $\text{C}_{26}\text{H}_{39}\text{N}_5\text{O}_{10}\text{Na}$ : 604.25; found: 604.23.

#### Data for compound 22e

Following the general experimental procedure, Na (32 mg, 1.39 mmol) and compound **21e** (130 mg, 0.17 mmol) in dry MeOH gave the product as a pale brown frothing solid **22e** in 77% (76 mg) yield.  $R_f$ : 0.65 (30% MeOH- $\text{CHCl}_3$ ).



**IR** (KBr)  $\nu_{\text{max}}$ : 3425, 2927, 2855, 1712, 1634, 1446, 1415, 1383, 1238, 1129, 1058, 586  $\text{cm}^{-1}$ .

$^1\text{H}$  NMR (500 MHz, MeOD):  $\delta$  7.89 (s, 1H), 6.92 (d,  $J = 5.5$  Hz, 1H), 6.05 (s, 1H), 5.98 (s, 1H), 5.24-5.20 (m, 1H), 4.86-4.78 (m, 1H), 4.65-4.58 (m, 1H), 4.17-4.09 (m, 5H), 3.83-3.59 (m, 5H), 2.25-2.15 (m, 4H), 1.74-1.51 (m, 6H), 1.25-1.22 (m, 6H).

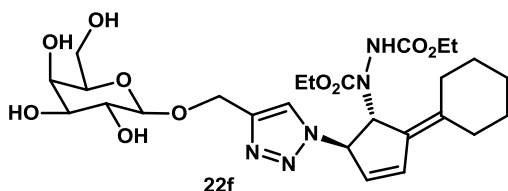
$^{13}\text{C}$  NMR (125 MHz, MeOD):  $\delta$  159.4, 145.9, 137.6, 131.6, 131.2, 129.1, 123.9,

104.3, 83.2, 78.9, 76.8, 72.7, 70.4, 64.5,  
63.9, 63.1, 63, 61.2, 32.5, 28.8, 27.4,  
14.8.

Mass Spectrometric Analysis: **LRMS** (FAB):  $m/z$  calcd for  $C_{26}H_{39}N_5O_{10}Na$ :  
604.25; found: 604.27.

#### Data for compound **22f**

Following the general experimental procedure, Na (37 mg, 1.6 mmol) and compound **21f** (150 mg, 0.2 mmol) in dry MeOH gave the product as a white solid **22f** in 96% (112 mg) yield.  $R_f$ : 0.65 (30% MeOH- $CHCl_3$ ).



**IR** (KBr)  $\nu_{max}$ : 3304, 2929, 2856,  
1709, 1520, 1444, 1410, 1381, 1290,  
1233, 1118, 1058, 835, 760  $cm^{-1}$ .

**<sup>1</sup>H NMR** (300 MHz, MeOD):  $\delta$  7.90  
(s, 1 H), 6.91 (br.d, 1H), 6.05-5.97 (m,  
2H), 5.23 (s, 1H), 4.99-4.95 (m, 1H),  
4.65-4.61 (m, 1H), 4.33 (d,  $J = 7.2$  Hz,  
1H), 4.18-4.13 (m, 5H), 4.00-3.30 (m,  
9H), 2.30-2.10 (m, 4H), 1.69-1.52 (m,  
6H), 1.24 (t,  $J = 7.2$  Hz, 6 H).

**<sup>13</sup>C NMR** (75 MHz, MeOD):  $\delta$  159.3,  
146.0, 137.6, 131.6, 131.3, 129.1, 123.9,  
104.3, 83.4, 78.9, 76.8, 72.5, 70.4, 64.5,  
63.9, 63.1, 63, 61.2, 32.6, 28.8, 27.4,  
14.9.

Mass Spectrometric Analysis: **LRMS** (FAB):  $m/z$  calcd for  $C_{26}H_{39}N_5O_{10}Na$ :  
604.25; found: 604.28.

---

**Procedure for the  $\alpha$ -Amylase inhibition assay of glycohybrids**

The  $\alpha$ -amylase inhibition assay was carried out by the method of Apostolidis *et al* [Apostolidis *et al.* 2009]. Briefly, 500 mL of 0.02 M sodium phosphate buffer (pH 6.9 with 0.006 M sodium chloride) containing  $\alpha$ -amylase solution (0.5 mg/mL) and different concentrations of the stock solution of compounds **1** and **2** (100–500  $\mu$ g/mL) were incubated at 25 °C for 10 min. After pre-incubation, 500 mL of 1% starch solution in 0.02 M sodium phosphate buffer (pH 6.9 with 0.006 M sodium chloride) was added to each tube at timed intervals. The reaction mixtures were then incubated at 25 °C for 10 min. The reaction was stopped with 1.0 mL dinitrosalicylic acid colour reagent. The test tubes were then incubated in a boiling water bath for 5 min and cooled to room temperature. The reaction mixture was then diluted after adding 10 mL distilled water and absorbance was measured at 540 nm using a Synergy 4 Biotek multiplate reader. Acarbose was used as the positive control. A graph was plotted with concentration along x-axis and percentage inhibition along y-axis to obtain the IC<sub>50</sub> value.

**Procedure for the  $\alpha$ -Glucosidase inhibition assay of glycohybrids**

Refer: Chapter 2, experimental section **2.13.1**

**Procedure for anti-glycation reaction assay**

Refer: Chapter 2, experimental section **2.13.3**

**Procedure for cytotoxicity assay****H9c2 cells and culture conditions**

H9c2 cells derived from rat embryonic cardiomyocytes were obtained from ATCC (American Type Culture Collection), USA. Cells were cultured in DMEM (Dulbecco's Modified Eagle's medium) supplemented with FBS (Foetal bovine serum), 100 U penicillin/mL, and 100  $\mu$ g streptomycin/mL and cultured in 5% CO<sub>2</sub> at 37 °C. Cells were passaged regularly and subcultured to 70% confluence before the experiments. Experimental group consist of (1) control cells; (2) cells treated with **22a**; (3) cells treated with **22c**; (4) cells treated with **22e**; (5) cells treated with **22f** for 24 h.

**Morphological analysis**

H9c2 cells at the exponential growth phase were trypsinized and resuspended in the medium. A total of  $5 \times 10^4$  cells per well were seeded in 24-well plate. After 48 h, cells

---

from all experimental groups were checked for morphological alterations under the phase-contrast microscope at 10x magnification.

**Cell viability assay (MTT assay)**

Cells were plated at  $5 \times 10^4$  cells in 24-well plate. After 48 h of incubation at 37 °C, cells were subjected to treatment with various compounds at a concentration of 10, 20, 30 and 40  $\mu\text{M}$ . 350  $\mu\text{L}$  of MTT (3-(4,5-dimethylthiazol-2-yl)-2,5-diphenyltetrazolium bromide) solution (5 mg MTT/mL DMEM) was added to each well and incubated for 3-4 h at 37 °C. The formazan crystals formed were dissolved in DMSO (Dimethyl sulfoxide). The plate was read after 45 min of incubation with shaking at room temperature in a microplate reader at 570 nm.

---

## Bibliography and References

---

- Abdelwahab, S. I.; Abdul, A. B.; Mohan, S.; Taha, M. M.; Syam, S.; Ibrahim, M. Y.; Mariod, A. A. "Zerumbone induces apoptosis in T-acute lymphoblastic leukemia cells" *Leuk Res.*, **2011**, *35*, 268-271.
- Abdelwahab, S. I.; Abdul, A. B.; Zain, Z. N.; Hadi, A. H. A. "Zerumbone inhibits interleukin-6 and induces apoptosis and cell cycle arrest in ovarian and cervical cancer cells" *Int Immunopharmacol.*, **2012**, *12*, 594-602.
- Aggarwal, B. B.; Ajaikumar, B. K.; Harikumar, K.B.; Sheeja, T. T.; Sung, B.; Anand, P. "Potential of Spice-Derived Phytochemicals for Cancer Prevention" *Planta Med.*, **2008**, *74*, 1560-1569 and references therein.
- AHFS Drug Information* American Society of Health-System Pharmacists, **2006**.
- Alexander, H.; Rolf, H., Chapter 5. ISBN, 3-7643-6081-X, Birkhauser Verlag, Basel-Boston-Berlin, **2003**.
- Anas, S.; Sajisha, V. S.; John, J.; Joseph, N.; George, S. C.; Radhakrishnan, K. V. "Facile synthesis of alkylidene cyclopentenes via palladium catalyzed ring opening of fulvene derived bicyclic hydrazines" *Tetrahedron*, **2008**, *64*, 9689-9697.
- Anas, S.; Sajisha, V. S.; Mohanlal, S.; Radhakrishnan, K. V. "Palladium/Lewis Acid Catalysed Desymmetrization of Fulvene Derived Bicyclic Hydrazines: A Facile Synthesis of Substituted Alkylidene Cyclopentenes" *Synlett*, **2006**, *15*, 2399-2402.
- Apostolidis, E.; Kwon, Y. I.; Shetty, K.; "Inhibitory potential of herb, fruit, and fungal-enriched cheese against key enzymes linked to type 2 diabetes and hypertension" *Innov Food Sci Emerg Technol*, **2002**, *8*, 46-54.
- Arom, J. "In Vitro Antiglycation Activity of Arbutin" *Naresuan University Journal*, **2005**, *13*, 35-41.

- Baby, S.; Dan, M.; Thaha, A. R. M.; Johnson, A. J.; Kurup, R.; Balakrishnapillai, P.; Lim, C. K. "High content of zerumbone in volatile oils of *Zingiber zerumbet* from southern India and Malaysia" *Flavour Fragr. J.*, **2009**, *24*, 301-308.
- Banville, D. L.; Keniry, M. A.; Kam, M.; Shafer, R. H. "NMR studies of the interaction of Chromomycin A<sub>3</sub> with small DNA duplexes: binding to GC containing sequences" *Biochemistry*, **1990**, *29*, 6521-6534.
- Becht, J. M.; Catala, C.; Drian, C. L.; Wagner, A. "Synthesis of Biaryls via Decarboxylative Pd-Catalyzed Cross-Coupling Reaction" *Org. Lett.*, **2007**, *9*, 1781-1783.
- Berecibar, A.; Grandjean, C.; Siriwardena, A. "Synthesis and Biological Activity of Natural Aminocyclopentitol Glycosidase Inhibitors: Mannostatins, Trehazolin, Allosamidins, and Their Analogues" *Chem. Rev.*, **1999**, *99*, 779-844.
- Bhuiyan, M. N. I.; Chowdhury, J. U.; Begum, J. "Chemical investigation of the leaf and rhizome essential oils of *Zingiber zerumbet* (L.) Smith from Bangladesh" *Bangladesh J Pharmacol*, **2009**, *4*, 9-12.
- Bian, J.; Wingerden, M. V.; Ready, J. M. "Enantioselective Total Synthesis of (+)- and (-)-Nigellamine A<sub>2</sub>" *J. Am. Chem. Soc.*, **2006**, *128*, 7428-7429.
- Blood pressure <http://www.medicinenet.com/captopril/article.htm>.
- Bogers, R. J.; Craker, L. E.; Lange, D. "Medicinal and Aromatic Plants", chapter 19, **2006**, 261-273. Netherlands.
- Bors, W.; Heller, W.; Michael, C.; Saran, M. "Flavonoids as antioxidants: Determination of radical scavenging efficiencies" *Methods Enzymol.*, **1990**, *186*, 343-355.
- Borsche, W.; Niemann J. "Über Podophyllin" *Justus Liebigs Ann. Chem.* **1932**, *494*, 126-142.
- Brady, S. F.; Singh, M. P.; Janso, J.; Clardy, J. "Guanacastepene, a Fungal-Derived Diterpene Antibiotic with a New Carbon Skeleton" *J. Am. Chem. Soc.*, **2000**, *122*, 2116-2117.

- Brito-Arias, M. “*Synthesis and Characterization of Glycosides*”. Springer, ISBN 978-0-387-26251-2, "IUPAC Gold Book - Glycosides **2007**.
- Burkill, I. “A Dictionary of the Economic Products of the Malay Peninsula” Ministry of Agriculture and Cooperative, Kuala, Lumpur, Malaysia, **1966**.
- Cao, H.; Hwang, J.; Chen, X. “Opportunity, Challenge and Scope of Natural Products in Medicinal Chemistry” **2011**, 411-431.
- Chan, K., “Chinese medicinal materials and their interface with Western medical concepts”. *Journal of Ethnopharmacology*, **2005**, 96, 1-18.
- Chhabra, B. R.; Kalsi, P. S.; Dhir, B. S.; Shirahama, H.; Dhillon, R. S. “Acid-Catalyzed Cyclization of Zerumbone” *Indian J. Chem* **1985**, 24, 499-501.
- Chin, Y. W.; Balunas, M. J.; Chai, H. B.; Kinghorn, A. D. “Drug discovery from natural sources”. *Aaps Journal*, **2006**, 8, E239–E253.
- Colerige Smith P. O, Thomas, P.; Scurr, J. H.; Dormandy, J. A. “Causes of various ulceration, a new hypothesis” *Br Med J*, **1980**, 296, 1726-1727.
- Cornella, J.; Lu, P.; Larrosa, I. “Intermolecular Decarboxylative Direct C-3 Arylation of Indoles with Benzoic Acids” *Org. Lett.*, **2009**, 11, 5506-5509
- Crimmins, M. T. “New developments in the enantioselective synthesis of cyclopentyl carbocyclic nucleosides” *Tetrahedron*, **1998**, 54, 9229-9272.
- Dai, J. R.; Cardellina, J. H.; McMahon, J. B.; Boyd, M. R. “Zerumbone, an HIV-Inhibitory and Cytotoxic Sesquiterpene of *Zingiber aromaticum* and *Z. zerumbet*” *Nat. Prod. Lett.*, **1997**, 10, 115-118.
- Danaei, G.; Finucane, M .M.; Lu, Y.; Singh, G. M.; Cowan, M. J.; Paciorek, C. J.; Lin, J. K.; Farzadfar, F.; Khang, Y. H.; Stevens, G. A.; Rao, M.; Ali, M. K.; Riley, L. M.; Robinson, C. A.; Ezzati, M. “National, regional, and global trends in fasting plasma glucose and diabetes prevalence since 1980: systematic analysis of health examination surveys and epidemiological studies with 370 country-years and 2.7 million participants” *Lancet* **2011**, 378, 31-40.
- Dev, S. “Studies in sesquiterpenes-xvi zerumbone, a monocyclic sesquiterpene ketone” *Tetrahedron*, **1960**, 8, 171-180.



- Dev, S.; Anderson, J. E.; Cormier, V.; Damodaran, N. P.; Roberts, J. D. "Nuclear magnetic resonance spectroscopy. The conformational mobility of humulene and zerumbone" *J. Am. Chem. Soc.*, **1968**, *90*, 1246-1248.
- Dumas, C.; Schibli, R.; Schubiger, P. A. "Versatile Routes to C-2- and C-6-Functionalized Glucose Derivatives of Iminodiacetic Acid" *J. Org. Chem.*, **2003**, *68*, 512-518.
- Efferth, .; Fu, Y. J.; Zu, Y. G.; Schwarz, G.; Konkimalla, V. S.; Wink, M. (2007). "Molecular target-guided tumor therapy with natural products derived from traditional Chinese medicine" *Current medicinal chemistry* **2007**, *14*, 2024-2032.
- Evans, R. A. "The Rise of Azide-Alkyne 1,3-Dipolar 'Click' Cycloaddition and its Application to Polymer Science and Surface Modification". *Australian Journal of Chemistry* **2007**, *60*, 384-395.
- Faye, F. "Race to synthesize Taxol ends in a tie" *Science* **1994**, *263*, 911.
- Frank, S. "A tale of taxol" *Florida State University Research in Review* **2003**, *12*.
- Frankland, E.; Duppa, B. F. "Preliminary Note on Borathyl" *Justus Liebigs Ann. Chem.*, *115*, **1860**, 319.
- Fransworth, N. R.; Bunyapraphatsara, N. "*Thai Medical plants*" **1992**, *261*, Bangkok, Thailand.
- Gamblin, D. P.; Scanlan, E. M.; Davis, B. G. "Glycoprotein Synthesis: An Update" *Chem. Rev.*, **2009**, *109*, 131-163.
- Gini, F.; Hessen, B.; Minnaard, A. J. "Palladium-Catalyzed Enantioselective Conjugate Addition of Arylboronic Acids" *Org. Lett.*, **2005**, *7*, 5309-5312.
- Gleiter, R.; Borzyk, O. "Synthesis of Rodlike Distillates" *Angew. Chem., Int. Ed. Engl.*, **1995**, *34*, 1001-1003.
- Goldin, A.; Beckman, J. A.; Schmidt, A. M.; Creager, M. A. "Advanced glycation end products: sparking the development of diabetic vascular injury" *Circulation* **2006**, *114*, 597-605.
- Govindachari, T. R.; Viswnathan, N. "The stem bark of *Mappia foetida*, a tree native to India, has proved to be another source significant for the isolation of camptothecin" *Phytochemistry* **1972**, *11*, 3529-3531.

- Graf, B. A.; Milbury, P. E.; Blumberg, J. B. Flavonols, Flavones, Flavanones, and Human Health: Epidemiological Evidence” *J. Med. Food*, **2005**, *8*, 281-290.
- Grillo, M. A.; Colombatto, S. “Advanced glycation end-products (AGEs): involvement in aging and in neurodegenerative diseases” *Amino Acids*, **2008**, *35*, 29-36.
- Gryniewicz, G.; Szeja, W.; Boryski, J. “Synthetic analogs of natural glycosides in drug discovery and development” *Acta Poloniae Pharmaceutica-Drug Research*, **2008**, *65*, 655-676.
- Haefner, B. “Drugs from the deep: marine natural products as drug candidates”. *Drug Discovery Today*, **2003**, *8*, 536–544.
- Hall, S. R.; Nimgirawath, S.; Raston, C. L.; Sittatrakul, A.; Thadaniti, S.; Thirasasana, N.; White, A. H. “Crystal structure of zerumbone” *Aus. J. Chem.*, **1981**, *34*, 2243-2247.
- Hanson, J. R. “Natural products: The secondary metabolites”, Royal Society of Chemistry, **2003**.
- Hare, M.; Raddatz, P.; Walenta, R.; Winterfeldt, E. “4-Oxo-2-cyclopentenyl Acetate—A Synthetic Intermediate” *Angew Chem., Int. Ed. Engl.*, **1982**, *21*, 480-492.
- Hartwell, J. L.; Schrecker, A. W. “Components of Podophyllin. V. The Constitution of Podophyllotoxin” *Journal of the American Chemical Society* **1951**, *73*, 2909–2916.
- Hartwig, J. F. In: Negishi, E. Ed. “Handbook of Organopalladium Chemistry for Organic Synthesis”, Wiley: New York, **2002**, *1*, 1051–1096.
- Hassan, J.; Sevignon, M.; Gozzi, C.; Schulz, E.; Lemaire, M. “Aryl–Aryl Bond Formation One Century after the Discovery of the Ullmann Reaction” *Chem. Rev.*, **2002**, *102*, 1359-1470.
- Hayashi, T.; Takahashi, M.; Takaya, Y.; Ogasawara, M. “Catalytic Cycle of Rhodium-Catalyzed Asymmetric 1,4-Addition of Organoboronic Acids. Arylrhodium, Oxa- $\delta$ -allylrhodium, and Hydroxorhodium Intermediates” *J. Am. Chem. Soc.*, **2002**, *124*, 5052-5058.
- Hayman, S.; Kinoshita, J. H. “Isolation and properties of lens aldose reductase” *J Biol Chem*, **1965**, *240*, 877-882.

- Heck, R. F. "Palladium Reagents in Organic Syntheses" Academic Press, London, **1985**.
- Holttum, R. E. "The *Zingiberaceae* of the Malay Peninsula" *Gardening Bulletin of Singapore*, **1950**, *13*, 1–249.
- Hong, B. C.; Chen, F. L.; Chen, S. H.; Liao, J. H.; Lee, G. H. "Intramolecular Diels–Alder Cycloadditions of Fulvenes. Application to the Kigelinol, Neoamphilectane, and Kempene Skeletons" *Org. Lett.*, **2005**, *7*, 557–560.
- Hotha, S.; Kashyap, S. "Click Chemistry" Inspired Synthesis of pseudo-Oligosaccharides and Amino acid Glycoconjugates" *J. Org. Chem.* **2006**, *71*, 364–367.
- Huang, G. .; Chien, T. Y.; Chen, L. G.; Wang, C. C. "Antitumour effects of zerumbone from *Zingiber zerumbet* in P-388D cells in vitro and in vivo" *Plant Med* **2005**, *71*, 219–224.
- Ichihashi, M.; Yagi, M.; Nomoto, K. "Glycation stress and photo-aging in skin" *Anti-Aging Medicine*, **2011**, *8*, 23–29.
- Iyer, P. S.; O'Malley, M. M.; Lucas, M. C. "Microwave-enhanced rhodium-catalyzed conjugate-addition of aryl boronic acids to unprotected maleimides" *Tetrahedron Lett.*, **2007**, *48*, 4413–4418.
- Jaiswal, N.; Srivastava, S. P.; Bhatia, V.; Mishra, A.; Sonkar, A. K.; Narender, T.; Srivastava, A. K.; Tamrakar, A. K. "Inhibition of alpha-glucosidase by *Acacia nilotica* prevents hyperglycemia along with improvement of diabetic complications via aldose reductase inhibition" *J Diabetes Metab*, **2012**, S6:004. doi:10.4172/2155-6156.S6-004.
- Jianbo, X.; Guoyin, K.; Koichiro, Y.; Xiaoqing, C. "Advance in Dietary Polyphenols as  $\alpha$ -Glucosidases Inhibitors: A Review on Structure-Activity Relationship Aspect" *Critical Reviews in Food Science and Nutrition* **2013**, *53*, 818–836.
- Kader, M. G.; Habib, M. R.; Nikkon, F.; Yeasmin, T.; Rashid, M. A.; Rahman, M. M.; Gibbons, S. "Zederone from the rhizomes of *Zingiber zerumbet* and its antistaphylococcal Activity" *Bol Latinoam Caribe Plant Med Aromat*, **2009**, *9*, 63 – 68.

- Keong, Y. S.; Noorjahan, B. A.; Mustafa, Sh.; Suraini, A. A.; Rahman, M. A.; Abdul, M. A. "Immunomodulatory effects of zerumbone isolated from roots of *Zingiber zerumbet*" *Pak J Pharm Sci* **2010**, *23*, 75–82.
- Kikushima, K.; Holder, J. C.; Gatti, M.; Stoltz, B. M. "Palladium-Catalyzed Asymmetric Conjugate Addition of Arylboronic Acids to Five-, Six-, and Seven-Membered  $\beta$ -Substituted Cyclic Enones: Enantioselective Construction of All-Carbon Quaternary Stereocenters" *J. Am. Chem. Soc.*, **2011**, *133*, 6902–6905.
- Kim, M.; Miyamoto, S.; Yasui, Y.; Oyama, T.; Murakami, A.; Tanaka, T. "Zerumbone, a tropical ginger sesquiterpene, inhibits colon and lung carcinogenesis in mice" *Int. J. Cancer* **2009** *124*, 264–271.
- Kirana, C.; McIntosh, G. H.; Record, I. R.; Jones, G. P. "Antitumor activity of extract of *Zingiber aromaticum* and its bioactive sesquiterpenoid zerumbone" *Nutr. Cancer*, **2003**, *45*, 218-225.
- Kitayama, T.; Masuda, T.; Sakai, K.; Chika Imada, C.; Yonekura, Y.; Kawai, Y. "Remarkable synthesis and structure of allene type zerumbone" *Tetrahedron*, **2006**, *62*, 10859–10864.
- Kitayama, T.; Iwabuchi, R.; Minagawa, S.; Sawada, S.; Okumura, R.; Hoshino, K.; Cappiellod, J.; Utsunia, R. "Synthesis of a novel inhibitor against MRSA and VRE: Preparation from zerumbone ring opening material showing histidine-kinase inhibition" *Bioorg. Med. Chem. Lett.*, **2007**, *17*, 1098–1101.
- Kitayama, T.; Nagao, R.; Masuda, T.; Richard K. Hill, R. K.; Masanori Morita, M.; Takatani, M.; Sawada, S.; Okamoto, T. "The chemistry of Zerumbone IV Asymmetric synthesis of Zerumbol" *Journal of Molecular Catalysis B: Enzymatic*, **2002**, *17* 75–79.
- Kitayama, T.; Ohta, S.; Nakayama, T.; Awata, M.; Kawai, Y. "Synthesis of optically active tetrahydrozerumbone" *Tetrahedron: Asymmetry*, **2010**, *21*, 11-15.
- Kitayama, T.; Okamoto, T.; Hill, R. K.; Kawai, Y.; Takahashi, S.; Yonemori, S.; Yamamoto, Y.; Ohe, K.; Uemura, S.; Sawada, S. "Chemistry of Zerumbone. 1. Simplified Isolation, Conjugate Addition Reactions, and a

- Unique Ring Contracting Transannular Reaction of Its Dibromide” *J. Org. Chem.*, **1999**, *64*, 2667-2672.
- Kitayama, T.; Yamamoto, K.; Utsumi, K.; Takatani, M.; Hill, R. K.; Kawai, Y.; Sawada, O. “Chemistry of zerumbone, regulation of ring bond cleavage and unique antibacterial activities of zerumbone derivatives” *Biosci Biotechnol Biochem* **2001** *65*, 2193–2199.
- Kitayama, T.; Yoshida, Y.; Furukawa, J.; Kawaic, Y.; Sawadad, S. Asymmetric synthesis of triepoxyzerumbol” *Tetrahedron: Asymmetry*, **2007**, *18*, 1676–1681.
- Koehn, F. E.; Carter, G. T. “The evolving role of natural products in drug discovery”. *Nat. Rev. Drug Discov.*, **2005**, *4*, 206–220.
- Kolb, H. C.; Finn, M. G.; Sharpless, K. B. “Click Chemistry: Diverse Chemical Function from a Few Good Reactions” *Angew. Chem. Int. Ed.* **2001**, *40*, 2004-2021.
- Kren, V. “Glycoside vs. aglycon: the role of glycosidic residue in biological activity” *Glycoscience*, Springer, **2008**.
- Kren, V.; Martinkova, L. “Glycosides in Medicine: The Role of Glycosidic Residue in Biological Activity” *Current Medicinal Chemistry* **2001**, *8*, 1303-1328.
- Kumar, H.; Javed, A. S.; Khan, A. S.; Amir, M. “1,3,4-Oxadiazole/thiadiazole and 1,2,4-triazole derivatives of biphenyl-4-yloxy acetic acid: Synthesis and preliminary evaluation of biological properties” *Eur J Med Chem*, **2008**, *43*, 2688-2698.
- Lemieux, R. U. “Review of oligosaccharide synthesis” *Chem. Soc. Rev.*, **1978**, *7*, 423.
- Lillelund, V. H.; Jensen, H. H.; Liang, X.; Bols, M. “Recent Developments of Transition-State Analogue Glycosidase Inhibitors of Non-Natural Product Origin” *Chem. Rev.*, **2002**, *102*, 515-554.
- Masuda, T.; Jitoe, A.; Kato, S.; Nakatani, N. “Acetylated Flavonoid Glycosides from *Zingiber zerumbet*” *Phytochemistry*, **1991**, *30*, 2391-2392.
- Matthes, H. W. D.; Luu, B.; Ourisson, G. “Transannular cyclizations of zerumbone epoxide” *Tetrahedron*, **1982**, *38*, 3129-3135.
- McGarvey, D. J.; Croteau, R. “Terpenoid metabolism” *Plant Cell* **1995**, *7*, 1015–1026.
- Meldal, M.; Tornøe, C. W. “Cu-Catalyzed Azide Alkyne Cycloaddition” *Chem. Rev.*, **2008**, *108*, 2952-3015.

- Mereyala, H. B.; Gurralla, S. R. "A highly diastereoselective, practical synthesis of allyl, propargyl 2,3,4,6-tetra-*O*-acetyl- $\beta$ -d-glucopyranosides and allyl, propargyl heptaacetyl- $\beta$ -d-lactosides" *Carbohydrate Res.*, **1998**, *307*, 351-354.
- Mikata, Y.; Shinohara, Y.; Yoneda, K.; Nakamura, Y.; Brudzinska, I.; Tanase, T.; Takagi, R.; Okamoto, T.; Kinoshita, I.; Doe, M.; Orvig, C.; Yano, S. "Unprecedented sugar-dependent in vivo antitumor activity of carbohydrate-pendant *cis*-diamminedichloroplatinum(II) complexes" *Bioorg. Med. Chem. Lett.*, **2001**, *11*, 3045-3047.
- Miyaura, N. "Cross-coupling reactions: a practical guide (topics in current chemistry)" Springer: Berlin, **2002**.
- Moses, J. E.; Moorhouse, A. D. "The growing applications of click chemistry" *Chem. Soc. Rev.*, **2007**, *36*, 1249-1262.
- Murakami, A.; Miyamoto, M.; Ohigashi, H. "Zerumbone, an anti-inflammatory phytochemical, induces expression of proinflammatory cytokine genes in human colon adenocarcinoma cell lines" *Biofactor*, **2004**, *21*, 95-101
- Murakami, A.; Ohigashi, H. "Targeting NOX, INOS and COX-2 in inflammatory cells: Chemoprevention using food phytochemicals" *Int. J. Cancer*, **2007**, *121*, 2357-2363.
- Murakami, A.; Tanaka, T.; Lee, J. Y.; Surh, Y. J.; Kim, H. W.; Kawabata, K.; Nakamura, Y.; Jiwajinda, S.; Ohigashi, H. "Zerumbone, a sesquiterpene in subtropical ginger, suppresses skin tumor initiation and promotion stages in ICR mice" *Int. J. Cancer.*, **2004**, *110*, 481-490.
- Myers, A. G.; Tanaka, D.; Mannion, M. R. "Development of a Decarboxylative Palladation Reaction and Its Use in a Heck-type Olefination of Arene Carboxylates" *J. Am. Chem. Soc.*, **2002**, *124*, 11250- 11251.
- Nagai, R.; Mori, T.; Yamamoto, Y. "Significance of advanced glycation end products in aging-related disease" *Anti-Aging Medicine*, **2010**, *7*, 112-119.

- Nakamura, Y.; Yoshida, C.; Murakami, A.; Ohigashi, H.; Osawa, T.; Uchida, K. "Zerumbone, a tropical ginger sesquiterpene, activates phase II drug metabolizing enzymes" *FEBS Lett* **2004**, *572*, 245–250.
- Nakatani, N.; Jitoe, A.; Masuda, T.; Yonemori, S. "Flavonoid Constituents of Zingiber zerumbet Smith" *Agric. Biol. Chem.*, **1991**, *55*, 455-460.
- Nalawade, S. M.; Sagare, A. P.; Lee, C. Y.; Kao, C. L.; and Tsay, H. S. "Studies on tissue culture of Chinese medicinal plant resources in Taiwan and their sustainable utilization" *Botanical Bulletin of Academia Sinica*, **2003**, *44*, 79–98.
- Newman, D. J.; Cragg, G. M.; Snader, K. M. "Natural Products as Sources of New Drugs over the Period 1981-2002" *J. Nat. Prod.*, **2003**, *66*, 1022-1037.
- Nishikata, T.; Yamamoto, Y.; Miyaura, N. "Conjugate Addition of Aryl Boronic Acids to Enones Catalyzed by Cationic Palladium(II)–Phosphane Complexes" *Angew. Chem. Int. Ed.*, **2003**, *42*, 2768 – 2770.
- Ohe, K.; Miki, K.; Yanagi, S.; Tanaka, T.; Sawada, S.; Uemura, S. "Selective conjugate addition to zerumbone and transannular cyclization of its derivatives" *J. Chem. Soc., Perkin Trans.. 1* **2000**, *21*, 3627-3634.
- Osonoi, T.; Saito, M.; Mochizuki, K.; Fukaya, N.; Muramatsu, T.; Inoue, S.; Fuchigami, M.; Goda, T. "The alpha-glucosidase inhibitor miglitol decreases glucose fluctuations and inflammatory cytokine gene expression in peripheral leukocytes of Japanese patients with type 2 diabetes mellitus" *Metabolism* **2010**, *59*, 1816-1822.
- Ouchi, T.; Ohy, Y. "In Neoglycoconjugates: Preparation and Applications", Academic Press, San Diego, **1994**, 465-499.
- Ozaki, Y.; Kawahara, N.; Harada, M. "Anti-inflammatory effect of Zingiber *cassumunar* Roxb and its active principles" *Chem. Pharm. Bull.*, **1991**, *39*, 2353-2356.
- Perimal, E. K.; Akhtar, M. N.; Mohamad, A. S.; Khalid, M. H.; Ming, O. H.; Khalid, S.; Tatt, L. M.; Kamaldin, M. N.; Zakaria, Z. A.; Israf, D. A.; Lajis, N.; Sulaiman, M. R. "Zerumbone-Induced Antinociception: Involvement of the L-Arginine-Nitric Oxide-cGMP -PKC-K+ATP Channel Pathways" *Basic & Clinical Pharmacology & Toxicology* **2010**, *108*, 155–162.

- Park, H.; Hwang, K. Y.; Kim, Y. H.; Oh, K. H.; Lee, J. Y.; Kim, K. "Discovery and biological evaluation of novel alpha-glucosidase inhibitors with in vivo antidiabetic effect" *Bioorg. Med. Chem.Lett.*, **2008**, *18*, 3711-3715.
- Prakash, R. O.; Rabinarayan, A.; Kumar, M. S. "Zingiber zerumbet (L.) Sm., a reservoir plant for therapeutic uses: A Review" *International Journal of Pharma World Research*, **2011**, *2*, 1-23.
- Priya Rani, M.; Padmakumari, K. P.; Sankarikutty, B.; Lijocheriyam, O.; Nisha, V. M.; Raghu, K. G. "Inhibitory potential of ginger extracts against enzymes linked to type 2 diabetes, inflammation and induced oxidative stress" *International Journal of Food Sciences and Nutrition*, **2011**, *62*, 106.
- Ramaswami, S. K.; Bhattacharya, S. C. "Isolation of Humulene Monoxide and Humulene Dioxide" *Tetrahedron*, **1962**, *18*, 575-579.
- Ramnauth, J.; Poulin, O.; Bratovanov, S. S.; Rakhit, S.; Maddaford, S. P. "Stereoselective C-Glycoside Formation by a Rhodium(I)-Catalyzed 1,4-Addition of Arylboronic Acids to Acetylated Enones Derived from Glycals" *Org. Lett.*, **2001**, *3*, 2571-2573.
- Rawling, A. J.; Lomas, H.; Adam, W. P.; Marvin, J. R. L.; Dominic, S. A.; Shane, J. S. R.; Sarah, F. J.; George, W. J. F.; Raymond, A. D.; John, H. J.; Terry, D. B. "Synthesis and Biological Characterisation of Novel N-Alkyl-Deoxynojirimycin  $\alpha$ -Glucosidase Inhibitors" *ChemBioChem*, **2009**, *10*, 1101-1105.
- Riya, M. P.; Antu, K. A.; Vinu, T.; Chandrakanth, K. C.; Anilkumar, K. S.; Raghu K. G. "An in vitro study reveals nutraceutical properties of *Ananas comosus* (L.) Merr. var. Mauritius residue beneficial to diabetes" *J. Sci. Food Agric.*, **2014**, *94*, 943-950.
- Sabu, M. "Revision of the genus *Zingiber* in South India" *Folia Malesiana*, **2003**, *4*, 25-52.
- Sakai, M.; Hayashi, H.; Miyaura, N. "Rhodium-Catalyzed Conjugate Addition of Aryl- or 1-Alkenylboronic Acids to Enones" *Organometallics* **1997**, *16*, 4229-4231.



- Sakinah, S. A. S.; Handayani, S. T.; Hawariah, L. P. A. "Zerumbone induced apoptosis in liver cancer cells via modulation of Bax/Bcl-2 ratio" *Cancer Cell International* **2007**, *7*, 4-6.
- Sawada, S.; Yokoi, T.; Kitayama, T. "Woody fragrance made from a wild ginger: the chemistry of zerumbone" *Aroma Res.*, **2002**, *9*, 34–39, and the references therein.
- Shi, Z.; Zhang, C.; Tanga, C.; Jiao, N. "Recent advances in transition-metal catalyzed reactions using molecular oxygen as the oxidant" *Chem. Soc. Rev.*, **2012**, *41*, 3381–3430.
- Singh, C. B.; Nongalleima, Kh.; Brojendrosingh, S.; Ningombam, S.; Lokendrajit, N.; Singh, L. W. "Biological and chemical properties of Zingiber zerumbet Smith: a review" *Phytochem Rev*, **2012**, *11*, 113–125.
- Singhal, N.; Sharma, P. K.; Dudhe, R.; Kumar, N. "Recent advancement of triazole derivatives and their biological significance" *J. Chem. Pharm. Res.*, **2011**, *3*, 126-133.
- Song, Z.; He, X. P.; Li, C.; Gao, L. X.; Wang, Z. X.; Tang, Y.; Xie, J.; Li, J.; Chen, G. R. "Preparation of triazole-linked glycosylated  $\alpha$ -ketocarboxylic acid derivatives as new PTP1B inhibitors" *Carbohydrate Research*, **2011**, *346*, 140-145.
- Spande, T. F.; Garraffo, H. M.; Edwards, M. W.; Yeh, H. J. C.; Pannell, L.; Daly, J. W. "Epibatidine- A novel (chloropyridyl) Azabicycloheptane with potent analgesic activity from an Ecuadorian poison frog" *J. Am. Chem. Soc.*, **1992**, *114*, 3475–3478.
- Springer, T. A. "Adhesion receptors of the immune system" *Nature*, **1990**, *346*, 425-434.
- Sulaiman, M. R.; Perimal, E. K.; Akhtar, M. N.; Mohamad, A. S.; Khalid, M. H.; Tasrip, N. A.; Mokhtar, F.; Zakaria, Z. A.; Lajis, N. H.; Israf, D. A. "Anti-inflammatory effect of zerumbone on acute and chronic inflammation models in mice" *Fitoterapia*, **2010**, *81*, 855-858.
- Sung, B.; Prasad, S.; Yadav, V. R.; Aggarwal, B. B. "Cancer cell signaling pathways targeted by spice-derived nutraceuticals" *Nutr. Cancer*, **2012**, *64*, 173-197.

- Szabolcs, A.; Tizslavicz, L.; Kaszaki, J.; Pósa, A.; Berkó, A.; Varga, I. S.; Boros, I.; Szüts, V.; Lonovics, J.; Takács, T. "Zerumbone exerts a beneficial effect on inflammatory parameters of cholecystokinin octapeptide-induced experimental pancreatitis but fails to improve histology" *Pancreas*, **2007**, *35*, 249-255.
- Taha, M. M.; Abdul, A. B.; Abdullah, R.; Ibrahim, T. A.; Abdelwahab, S. I.; Mohan, S. "Potential chemoprevention of diethylnitrosamine-initiated and 2-acetylaminofluorene-promoted hepatocarcinogenesis by zerumbone from the rhizomes of the subtropical ginger (*Zingiber zerumbet*)" *Chem Biol Interact.*, **2010**, *186*, 295-305.
- Takaya, Y.; Ogasawara, M.; Hayashi, T.; Sakai, M.; Miyaura, N. "Rhodium-Catalyzed Asymmetric 1,4-Addition of Aryl- and Alkenylboronic Acids to Enones" *J. Am. Chem. Soc.*, **1998**, *120*, 5579-5580.
- Tanaka, D.; Myers, A. G. "Heck-Type Arylation of 2-Cycloalken-1-ones with Arylpalladium Intermediates Formed by Decarboxylative Palladation and by Aryl Iodide Insertion" *Org. Lett.*, **2004**, *6*, 433-436.
- Tanaka, D.; Romeril, S. P.; Myers, A. G. "On the Mechanism of the Palladium(II)-Catalyzed Decarboxylative Olefination of Arene Carboxylic Acids. Crystallographic Characterization of Non-Phosphine Palladium(II) Intermediates and Observation of Their Stepwise Transformation in Heck-like Processes" *J. Am. Chem. Soc.* **2005**, *127*, 10323-10333.
- Takada, Y.; Murakami, A.; Aggarwal, B. B. "Zerumbone abolishes NF- $\kappa$ B and I $\kappa$ B $\alpha$  kinase activation leading to suppression of antiapoptotic and metastatic gene expression, upregulation of apoptosis, and downregulation of invasion" *Oncogene*, **2005**, *24*, 6957-6969.
- Toshima, K.; Tatsuta, K. "Recent progress in O-glycosylation methods and its application to natural products synthesis" *Chem. Rev.*, **1993**, *93*, 1503-1531.
- Tsubomura, T.; Ogawa, M.; Yano, S.; Kobayashi, K.; Sakurai, T.; Yoshikawa, S. "Highly active antitumor platinum(II) complexes of amino sugars" *Inorg. Chem.*, **1990**, *14*, 2622-2626.
- "Traditional medicine strategy launched" WHO News, **2002**, *80*, 610.

- Vinay, K.; Nelson, F.; Abul, K. A.; Ramzi, S. C.; Stanley, L. R. (2005). "Robbins and Cotran Pathologic Basis of Disease (7th ed.)" **2005**, Philadelphia, Pa. Saunders, ISBN 0-7216-0187-1, 1194–1195.
- Wall, M. E.; Wani, M. C.; Cook, C. E.; Palmer, K. H.; McPhail, A. I.; Sim, G. A. "Plant antitumor agents. I. The isolation and structure of camptothecin, a novel alkaloidal leukemia and tumor inhibitor from camptotheca acuminata" *J. Am. Chem. Soc* **1966**, *88*, 3888–3890.
- Xian, M.; Ito, K.; Nakazato, T.; Shimizu, T.; Chen, C-K.; Yamato, K.; Murakami, A.; Ohigashi, H.; Ikeda, Y.; Kizaki, M. Blackwell Publishing Asia "Zerumbone, a bioactive sesquiterpene, induces G2/M cell cycle arrest and apoptosis in leukemia cells via a Fas- and mitochondria-mediated pathway" *Cancer Sci* **2007**, *98*, 118–126.
- Xiang, S.; Cai, S.; Zeng, J.; Liu, X-W. "Regio- and Stereoselective Synthesis of 2-Deoxy-C-aryl Glycosides via Palladium Catalyzed Decarboxylative Reactions" *Org. Lett.*, **2011**, *13*, 4608-4611.
- Yang, J.; Hoffmeister, D.; Liu, L.; Fu, X.; Thorson, J. S. "Natural product glycorandomization" *Bioorg. Med. Chem.*, **2004**, *12*, 1577-1584.
- Yob, N. J.; Jofry, S. M.; Affandi, M. M. R. M. M.; Teh, L. K.; M. Z. Salleh, M. Z.; Zakaria, Z. A. "Zingiber zerumbet (L.) Smith: A Review of Its Ethnomedicinal, Chemical, and Pharmacological" Uses *Evidence-Based Complementary and Alternative Medicine*, **2011**, *2011*, 1-12.
- You, Y. "Podophyllotoxin derivatives: current synthetic approaches for new anticancer agents" *Current Pharmaceutical Design* **2005**, *11*, 1695–1717
- Zunino, F.; S. Dallavalle, S.; Laccabue, D.; Beretta, G.; Merlini, L.; Pratesi, G. "Current status and perspectives in the Development of Camptothecins" *Current Pharmaceutical Design* **2002**, *8*, 2505–2520.

## SUMMARY

The thesis entitled “**SYNTHETIC TRANSFORMATIONS OF PHYTOCHEMICALS FROM *ZINGIBER ZERUMBET* (L.) SMITH AND SYNTHESIS OF CARBOHYDRATE APPENDED ALKYLIDENE CYCLOPENTENES AS BIOACTIVE ANALOGUES**” embodies the results of the phytochemical investigation of *Zingiber zerumbet* (L.) Smith and transition metal catalyzed synthetic modifications of its bioactive lead molecule. Thesis also describes an efficient methodology for the synthesis of novel and bioactive alkylidene cyclopentene appended neoglycoconjugates. Moreover, nearly all the synthetic and natural molecules were subjected to biological evaluation with focus on the targets of diabetes mellitus type II, a life threatening disease.

The importance of natural products and its synthetic analogues in the modern drug design and discovery is clearly portrayed in the introductory chapter. It starts with the definition and classifications of natural products and progresses through their pharmaceutical value in treating various diseases. The unavoidable role of synthetic methodologies is also highlighted at the end of the chapter.

The isolation, characterization, and biological evaluation of phytochemicals from an Asian ginger, *Zingiber zerumbet* (L.) Smith is the subject matter of second chapter. Seven known phytochemicals are isolated from the dried rhizomes of *Zingiber zerumbet* and one natural product is synthesized from an isolated compound by alkaline hydrolysis. All the eight compounds were screened for  $\alpha$ -glucosidase enzyme, aldose reductase enzyme and protein glycation reaction. Kaempferol and kaempferol-3-*O*-methyl ether were found to be potent  $\alpha$ -glucosidase, aldose reductase as well as protein glycation inhibitors.

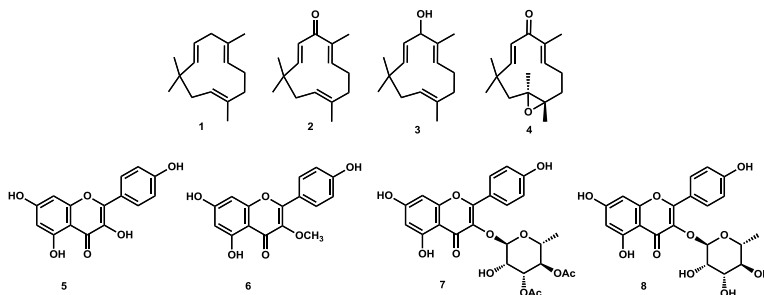
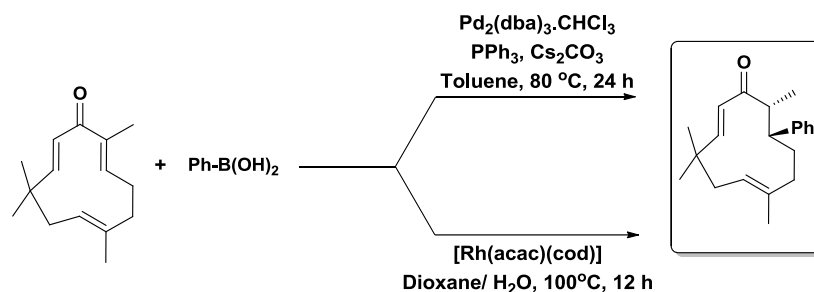


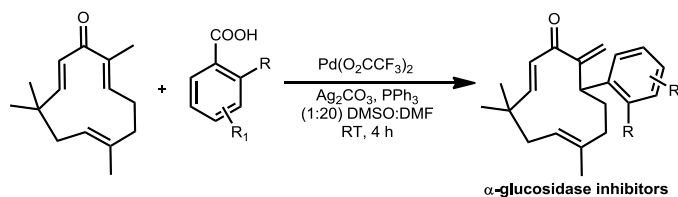
**Figure 1.** Structures of compounds 1-8

The third chapter comprises of two parts *viz* part A and part B. Both the parts explain our efforts towards the synthetic transformations of bioactive zerumbone by transition metal catalyzed reactions. An efficient method for the synthesis of novel zerumbone derivatives *via* palladium and rhodium catalyzed regio- and diastereoselective 1,4-conjugate addition using boronic acids is described in part A. The reaction is general with aryl boronic acids containing both electron donating as well as electron withdrawing groups (Scheme 1).



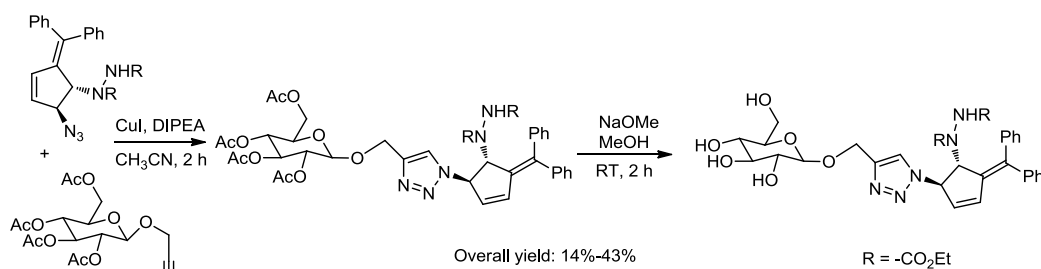
**Scheme 1**

Part B of chapter 3 deals with the synthesis of novel zerumbone derivatives *via* a regioselective palladium catalyzed decarboxylative coupling reaction using arene carboxylic acids (Scheme 2). The current methodology involves the repositioning of endocyclic double bond to exocyclic double bond of zerumbone. Preliminary *in vitro* analysis revealed that most of the newly synthesised derivatives are potent  $\alpha$ -glucosidase enzyme inhibitors.



**Scheme 2**

The final chapter of the thesis explains a new and efficient route towards the synthesis of glycohydrids having an alkylidene cyclopentene moiety with triazole ring as a linker. The protocol involves a palladium catalyzed ring opening reaction and click chemistry as the key steps. The sugars used in the synthesis glycohydrids are glucose, mannose and galactose. An illustrative example is presented in scheme 3.



### Scheme 3

Out of the six synthesized compounds, four were screened against  $\alpha$ -glucosidase,  $\alpha$ -amylase and protein glycation reaction inhibition assays. From the results, it is found that the compound **22f** with a galactose appendage is a good  $\alpha$ -glucosidase inhibitor and a potent anti-glycating agent (Figure 2). Moreover, the four compounds were found to be non-cytotoxic against H9c2 cardiac myoblast cell lines by MTT assay.

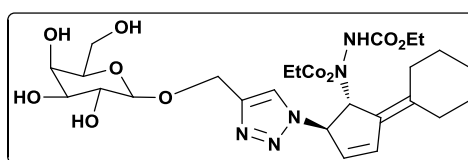


**Figure 2.** Compound **22f**

In conclusion, we have screened eight known phytochemicals of *Zingiber zerumbet* (L.) Smith for  $\alpha$ -glucosidase enzyme, aldose reductase enzyme and protein glycation reaction. From the studies we found that kaempferol and kaempferol-3-*O*-methylether are potent  $\alpha$ -glucosidase, aldose reductase as well as protein glycation inhibitors. Moreover, we have developed two synthetic strategies for the derivatization of bioactive zerumbone. Among the two, the first one was palladium and rhodium catalyzed regio- and diastereoselective 1,4-conjugate addition using boronic acids and the second one was regioselective palladium catalyzed decarboxylative coupling reaction using arene carboxylic acids. An efficient protocol for the synthesis of carbohydrate appended alkyldiene cyclopentenes as the main core is also developed.

## **List of publications**

1. Transition-metal-catalyzed regio- and diastereoselective 1,4-conjugate addition of zerumbone using boronic acids: A simple route toward novel zerumbone derivatives. **K. R. Ajish**, Nayana Joseph, K. V. Radhakrishnan *Synthesis* **2013**, *45*, 2316-2322.
2. Synthesis and biological evaluation of carbohydrate appended hydrazinocyclopentenes with potent glycation and  $\alpha$ -glucosidase inhibition activities. **K. R. Ajish**, Nayana Joseph, M. Priya Rani, K. G. Raghu, V. P. Vineetha, K. V. Radhakrishnan. *Tetrahedron lett.* **2013**, *54*, 5682-5685.
3. Synthesis of novel zerumbone derivatives *via* regioselective palladium catalyzed decarboxylative coupling reaction: A new class of  $\alpha$ -glucosidase inhibitors. **K. R. Ajish**, B.P. Dhanya, Nayana Joseph, M. Priya Rani, K. G. Raghu, V. P. Vineetha and K. V. Radhakrishnan. *Tetrahedron lett.* **2014**, *55*, 665-670.

### **Manuscripts submitted**

1. Studies on  $\alpha$ -glucosidase, aldose reductase and glycation inhibitory properties of sesquiterpenes and flavonoids of *Zingiber zerumbet* Smith. **K. R. Ajish**, K. A. Antu, M. P. Riya, M. R. Preetharani, K. G. Raghu, B. P. Dhanya K. V. Radhakrishnan. (**Submitted to *Planta Medica***)
2. Inhibitory activity of sesquiterpenes and flavonoids from *Zingiber zerumbet* Smith on angiotensin converting enzyme (ACE) and hyaluronidase enzyme. K. R. Ajish, Saumini Mathew, K. V. Radhakrishnan. (**Submitted to *Natural product research***)

### **Papers Presented at National and International Conferences**

#### **Oral presentations:**

1. Isolation, characterization and biological evaluation of phytochemicals from the rhizomes of *Zingiber zerumbet* Smith, **Ajish K. R.**, M. Priya Rani, K. G. Raghu and K. V. Radhakrishnan, an oral presentation at National Seminar on Emerging Trends in Chemical Sciences (ETCS-2013), held at University of Kerala, Kariavattom, May, **2013** [**Best Paper Award**].

2. Value Addition to herbal plants: Synthetic transformation & biological evaluation of phytochemical from *Zingiber Zerumbet*. **K. R. Ajish**, K.V. Radhakrishnan. *International Seminar on "Molecular Secrets of Plant Medicines (MSPM 2013)* CMS College, Kottayam, October, **2013 [Best Paper Award]**.
3. Isolation, synthetic transformation and biological evaluation of phytochemicals from zingiber zerumbet smith (malayinji). **K. R. Ajish**, K.V. Radhakrishnan. *23<sup>rd</sup> Swadeshi Science Congress (SSC-2013)*, M. G. University, Kottayam, November, **2013 [Best Paper Award]**.
4. Synthesis of carbohydrate appended hydrazinocyclopentenes with potent glycation and  $\alpha$ -glucosidase inhibition activities. **K. R. Ajish**, M. Priya Rani, V. P. Vineetha, K. G. Raghu, K. V. Radhakrishnan. *National Seminar on Current Trends in Chemistry (CTriC 2014)*, Department of Applied Chemistry, Cochin University of Science and Technology (CUSAT), January, **2014**.
5. Value addition to traditional knowledge: isolation, synthetic transformation and evaluation of bioactives from *zingiber zerumbet* (malayinji). **K.R. Ajish**, K. V. Radhakrishnan. *26<sup>th</sup> Kerala Science Congress*, KVASU, Wayanad, January, **2014**.

**Posters presented :**

6. Efforts towards the Synthesis and Lanthanide Binding Studies of mannose Based Neoglycoconjugates. **K. R. Ajish**, V. S. Sajisha, K. V. Radhakrishnan. *National Conference on Recent Trends in Organic Synthesis (RTOS 2011)*, Bharathidasan University, Tiruchirappalli, February, **2011**.
7. An efficient strategy to functionalized cyclopentenes via palladium catalyzed ring opening of bicyclic hydrazines with catechol and resorcinol. **K. R. Ajish**, S. Saranya, K. Ramesh Babu, K. V. Radhakrishnan. *International Symposium on Drug Development for Orphan/Neglected Diseases (CTDDR 2013)*, CDRI, Lucknow, February, **2013**.
8. Design and Synthesis of carbohydrate appended hydrazino cyclopentenes with triazole linker: A new class of neoglycoconjugates with anti-glycation properties. **K. R. Ajish**, M. Priya Rani, K. G. Raghu, K. V. Radhakrishnan. *National Seminar*



- 
- on Emerging Trends in Chemical Sciences (ETCS-2013)*, University of Kerala, Kariavattom, May, **2013**.
9. Transition metal catalyzed regio- and stereoselective 1,4-conjugate addition of boronic acids to zerumbone: A facile route towards novel zerumbone derivatives. **K. R. Ajish**, B. P. Dhanya, K. V. Radhakrishnan. *National Seminar on Emerging Trends in Chemical Sciences (ETCS-2013)*, University of Kerala, Kariavattom, May, **2013**.
10. Synthesis of novel zerumbone derivatives *via* transition metal catalyzed regio- and diastereoselective 1,4-conjugate addition using boronic acids. **K. R. Ajish**, K. V. Radhakrishnan. *9<sup>th</sup> Junior National Organic Symposium Trust (J-NOST) Conference*, IISER, Bhopal, December, **2013**.